Quarterly Publication

ISSN 2383 - 3572

Global Journal of Environmental Science and Management

Volume 9, Number 2, Spring 2023

Global Journal of Environmental Science and Management (GJESM)

(QUARTERLY PUBLICATION)

OPEN ACCESS

Publication authorization is certified by the Ministry of Culture and Islamic Guidance; No. 93/3629; 14 May 2014
Scientific-Research grade is accredited by the Ministry of Science, Research and Technology; No. 3/18/59975; 20 June 2015

Global
Journal of Environmental Science and Management (GJESM)

Editor-in-Chief
Professor J. Nouri

pISSN 2383 - 3572
eISSN 2383 - 3866

QUARTERLY FULL OPEN ACCESS PEER REVIEWED PUBLICATION

Journal Abbreviation: Global J. Environ. Sci. Manage.

CALL FOR PAPERS

Publication benefits in
Global Journal of Environmental
Science and Management

- *Quarterly Publication journal*
- *Online submission and reviewing*
- *Online status inquiry*
- *Double blind peer reviewing*
- *Rapid evaluation and publication*
- *Immediate publication on the net*
- *Open access to all PDF full text of published articles*
- *No pay charge for publication*
- *Indexed and cited in well-known databases;*
  particularly Web of Science and Scopus

www.gjesm.net
www.gjesm.org

editor@gjesm.net
global.jesm@gmail.com
gjesm.publication@gmail.com

Tel.: +9821 2610 5110
Fax: +9821 2610 5111

CONTENTS

Volume 9, Number 2, Spring 2023

1. Sediment organic carbon stocks in tropical lakes and its implication for sustainable lake management 173

T.R. Soeprobowati, N.D. Takarina, P.S. Komala, L. Subehi, M. Wojewódka-Przybył, J. Jumari, R. Nastuti (INDONESIA/ POLAND)

2. Application of microbially induced calcite precipitation to mitigate soil frost heave 193

M.F. Nikshoar, M.A. Rowshanzamir, S.M. Abtahi, S. Soleimanian-Zad (IRAN)

3. Environmental vulnerability characteristics in an active swarm region 211

A.V.H. Simanjuntak, U. Muksin, A. Arifullah, K. Lythgoe, Y. Asnawi, M. Sinambela, S. Rizal, S. Wei (INDONESIA/ SINGAPORE)

4. Municipal solid wastes quantification and model forecasting 227

Y.M. Teshome, N.G.Habtu, M.B. Molla, M.D. Ulsido (ETHIOPEA)

5. Components and predictability of pollutants emission intensity 241

Z. Farajzadeh , M.A. Nematollahi (IRAN)

6. Ecological and human health implications of mercury contamination in the coastal water 261

A. Mallongi, A.U. Rauf, R.D.P. Astuti, S. Palutturi, H. Ishak (INDONESIA)

7. Environmental assessment of river water quality near oil and gas fields 275

A.S. Patimah, A. Prasetya, S.H.M.B. Santosa (INDONESIA)

8. Drought stress tolerance based on selection indices of resistant crops variety 287

R. Daneshvar Rad, H. Heidari Sharifabad, M. Torabi, R. Azizinejad, H. Salemi, M. Heidari Soltanabadi (IRAN)

9. Microplastics contamination in two peripheral fish species harvested from a downstream river 299

M.R. Maulana, S. Saiful, Z.A. Muchlisin (INDONESIA)

10. Geospatial visualization and seasonal variation of heavy metals in river sediments 309

D. Justus Reymond, K. Sudalaimuthu (INDIA)

11. Heavy metals concentration in the sediment of the aquatic environment caused by the leachate discharge from a landfill 323

L. Sulistyowati, N. Nurhasanah, E. Riani, M.R. Cordova (INDONESIA)

12. Characterization and quantification of solid waste in rural regions 337

S. Syafrudin, J.M. Masjhoer, M. Maryono (INDONESIA)

COVERING LETTER

Subject: **Submission of manuscript**

Dear Editor,

I would like to submit the following manuscript for possible evaluation

Manuscript Title:

Running Title (Short title):

Main Subjects:

Name and address of corresponding author:

Telephone #

Fax #

Email:

I affirm that the manuscript has been prepared in accordance with Global Journal of Environmental Science and Management guide for authors.

I have read the manuscript and I hereby affirm that the content of this manuscript or a major portion thereof has not been published in a refereed journal, and it is not being submitted fully or partially for publication elsewhere. The manuscript has been read and approved by all listed authors.

The source(s) of financial support of study (if any):

Type of Manuscript (check one):

- ☐ Original research paper
- ☐ Case report
- ☐ Research note
- ☐ Short communication
- ☐ Review paper

Name:

Corresponding Author Signature:

Date:

Global J. Environ. Sci. Manage. 9(2): 173-192, Spring 2023, Serial #34

Global Journal of Environmental Science and Management
(GJESM)

Homepage: https://www.gjesm.net/

ORIGINAL RESEARCH PAPER

Sediment organic carbon stocks in tropical lakes and its implication for sustainable lake management

T.R. Soeprobowati[1,6,7,*], N.D. Takarina[2], P.S. Komala[3], L. Subehi[4], M. Wojewódka-Przybył[5], J. Jumari[6], R. Nastuti[7]

[1] *Center for Paleolimnology (CPalim), Universitas Diponegoro, Semarang, Indonesia*

[2] *Department Biology, Faculty Mathematics and Natural Sciences, Universitas Indonesia, Depok, Indonesia*

[3] *Department of Environmental Engineering, Faculty of Engineering, Universitas Andalas, Padang, Indonesia*

[4] *Research Center for Limnology and Water Resources, National Research and Innovation Agency, Cibinong, Indonesia*

[5] *Institute of Geological Sciences, Polish Academy of Sciences, Warsaw, Poland*

[6] *Department Biology, Faculty Science and Mathematics, Universitas Diponegoro, Semarang, Indonesia*

[7] *School of Postgraduate Studies, Universitas Diponegoro, Semarang, Indonesia*

ARTICLE INFO

Article History:
Received 05 June 2022
Revised 11 September 2022
Accepted 20 October 2022

Keywords:
Carbon stock
Lakeside
Sediment
Maninjau Lake
Sustainable management

DOI: 10.22034/gjesm.2023.02.01

ABSTRACT

BACKGROUND AND OBJECTIVES: The lakeside has an enormous sediment carbon storage potential; however, it is susceptible to various environmental changes and can easily become a source of carbon emissions. Understanding the amount of carbon storage in lakeside sediments and organic matter sources may provide information about the potential of lakeside zones in climate change mitigation, particularly for sustainable lake management. This study aims to estimate sediment organic carbon stock and the sources of organic matter in the Maninjau Lakeside-West Sumatera, Indonesia.

METHODS: Sediment sampling was performed at five research sites, with a depth of 0–100 centimeters. Sediment samples were divided into 4 subsamples: 0–15; 15–30; 30–50; and 50–100 centimeters. Bulk density and total nitrogen content were analyzed, and the percentage of organic carbon was calculated from the loss of ignition. The sediment organic carbon stock was calculated based on the bulk density and organic carbon content. Carbon per nitrogen ratio was also calculated to determine temporal changes in the sources of organic matter in the lake.

FINDINGS: This study demonstrated that Maninjau Lakeside has an enormous potential sedimentary organic carbon stock range between 284.23–442.59 megagrams per carbon per hectare. The highest total sediment carbon stock was found in Duo Koto (442.59 megagrams per carbon per hectare), with the lowest in Koto Kaciak (284.23 megagrams per carbon per hectare). In addition, the study's results also exhibited significant differences in sediment organic carbon stocks at each location with different land use and cover; in this case, the forest area has a higher carbon stock value than the agricultural and settlement areas. Therefore, it is essential to take initiatives for the restoration and conservation of lakeside areas because of their essential role in mitigating the climate change. The mean ratio of organic carbon and total nitrogen was between 9.96 to 16.91, indicating that phytoplankton, a mixture of floating macrophytes, and submerged vegetation were the sources of organic matter.

CONCLUSION: In general, the value of sediment organic carbon stocks tends to be lower in locations with intensive agricultural settlements than in forest areas. This study emphasizes that restoring lakeside wetland is vital in increasing sediment organic carbon stocks and maintaining lake sustainability.

NUMBER OF REFERENCES	NUMBER OF FIGURES	NUMBER OF TABLES
97	10	7

*Corresponding Author:
Email: *trsoeprobowati@live.undip.ac.id*
Phone: +6224 8442990
ORCID: 0000-0001-7525-7028

Note: Discussion period for this manuscript open until July 1, 2023 on GJESM website at the "Show Article".

INTRODUCTION

Carbon dioxide (CO_2) emissions are a significant contributor to greenhouse gas (GHG) emissions (accounting for around 74 percent of all GHG), making them the primary driver of global warming and climate change (UNFCCC, 2008). As an impact, global temperature has increased by almost a degree centigrade (°C) from the pre-industrial levels; the current increase is 1.1 °C specifically, and if the current emission rates remain high without any mitigation, the temperature rise is likely to increase by 1.5 °C from 2021 to 2040 (IPCC, 2021). Therefore, burning of fossil fuels, deforestation, and land use changes are some of the primary sources of CO_2 emissions in the atmosphere (Donato *et al*., 2011). Wetlands, rainforests, and oceans, are among the most productive ecosystem types in the world (Balwan and Kour, 2021). Wetlands develop between the land and water bodies (such as peatlands and swamps), rivers, and lakes, and their capacity for carbon sequestration, particularly that of carbon deposited in sediments, can significantly contribute to climate change mitigation (Comer-Warner *et al*., 2022). The biogeochemical process in the wetlands sediments affects carbon (C) and nitrogen (N) cycling and may lower the GHG in the atmosphere (Adame *et al*., 2018). Sediment organic carbon (SOC) stocks in wetlands represent one-third of earth's SOC (500–700 Petagram Carbon, Pg C) despite covering only about 3% of global land (Page and Baird, 2016). However, despite having a high potential for carbon storage, wetland ecosystems are vulnerable to degradation due to various anthropogenic activities. Lakeside is one of the wetland ecosystems that have significant carbon storage potential. However, its sensitivity to environmental changes triggered by land conversion activities, may reverse its function as a source of carbon emissions (Minnick *et al*., 2021; Lei *et al*., 2022). Wetland disruption significantly impacts the organic carbon content of sediments, and it is estimated to have increased carbon emissions by 37.5% (Liu *et al*., 2020). In the last few decades, widespread deforestation and massive land conversion for agriculture, aquaculture, and settlements have significantly threatened the wetland ecosystem and likely exacerbated the impacts of global climate change (Alongi, 2002; Adame *et al*., 2018). Previous studies have indicated that the conversion of wetlands to other land uses may decrease the SOC stocks (Sakin and Sakin (2011) found a lower SOC value for the agricultural land than the forest land. These findings were supported by Dayathilake *et al.* (2021), who also discovered a significantly higher percentage value of SOC in wetlands with high vegetation cover (Kolonawa wetlands) than those with lower vegetation cover (Thalawathugoda wetland park). The highest SOC was found in the natural forest zone (147,000 kilogram per hectare (kg/ha), while the lowest SOC was found in the grasslands surrounding the lake Victoria Crescent Agro-Ecological Zone, Uganda (65,000 kg/ha) (Akodi *et al*., 2016). Lei *et al*., (2022) also reported different SOC values for different land uses, where the restoration zone (20.59 kg/m^2) and the mesophytic farmland rewetting zone (19.51 kilogram per square meter (kg/m^2) have a higher SOC than the lakeside zone without vegetation (3.63 kg/m^2). Meanwhile, wetlands can store carbon stock; therefore, it is essential to conduct research related to the quantification of carbon stocks in such ecosystems. Thus, understanding the SOC stock distribution across the different types of land uses and sediment depths offers a framework for assessing the vulnerability of SOC to disturbances (Uhran *et al*., 2021). Indonesia has enormous potential for wetlands, with an area of 30.3 million hectare (ha), with various habitats, such as swamps, peatlands, wetlands, rivers, lakes, peatlands, and mangrove forests (Amin, 2016). Therefore, wetlands in Indonesia can play an essential role in mitigating climate change by storing significant carbon amount, especially underground. Despite the importance of wetlands in carbon sequestration, the level of wetland degradation in Indonesia is substantial, mainly due to land conversion, peatland burning, and illegal logging to expand plantations, agriculture, and settlements, contributing up to 50% carbon emissions in Indonesia's total national emissions (Margono *et al.*, 2014). Research on carbon storage estimation in Indonesian wetlands is critical, particularly to establish a database that can be utilized as a reference in wetland management strategies. There has been much research on estimating the carbon stocks in the wetlands of Indonesia, but most studies have only focused on the carbon stocks in peatlands (Basuki *et al.*, 2021; Siregar and Narendra, 2021; Silviana *et al.*, 2021), swamps (Novita *et al.*, 2021; Sufrayogi and Mardiatmoko, 2022; Purwanto *et al.*, 2020), and mangrove forests (Murdiyarso *et*

al., 2015; Arifanti *et al.,* 2019; Kusumanigtyas *et al.,* 2019). Meanwhile, research on estimating carbon stocks in lakeside wetland areas is still limited (Sujarwo and Darma, 2011; Priyadi *et al.,* 2014), despite its enormous potential to store carbon and vulnerability to degradation due to land use change and deforestation. Furthermore, knowledge regarding the effect of land use/cover on organic carbon stocks stored in soil or sediments also remains relatively unclear. Meanwhile, the land conversion rate of forest area into plantations and agricultural land continues to expand in Indonesia. This led to the establishment of this research, specifically conducted to determine the potential of SOC stocks in the lakeside wetlands and compare the amount of SOC stocks between locations with different land uses/covers. This study employed Maninjau Lake, a big lake in Indonesia, as the case study location. Lake Maninjau is one of the largest lakes in the West Sumatra Province, Indonesia, which plays a vital role in the local community's economy, including tourist destinations, aquaculture, and agriculture (Syandri *et al.,* 2014). Maninjau Lake has faced heavy eutrophication exacerbated by anthropogenic nutrient inputs regarding the aquaculture and agricultural expansion since 1990. Aside from contributing to water contamination, excessive use of chemical fertilizers in agriculture and feed aquaculture in Lake Maninjau has also seriously harmed the local economy and public health (Tasri *et al.,* 2021). This study particularly aims to determine the SOC stock and composition of sediment variables, including organic carbon concentration (OC), total nitrogen (TN), and bulk density (Bd), as well as compare the SOC stock at each research site with different land uses/covers. This study also aims to determine the source of organic matter in the northern part of Maninjau Lake. This study is essential for the sustainable management of Lake Maninjau and climate change mitigation. This study was conducted at Maninjau Lake, West Sumatra, Indonesia, in 2022.

MATERIALS AND METHODS

Study area description

This research was conducted at Lake Maninjau (0° 19' S 100° 12' E) in Tanjung Raya District, Agam Regency, West Sumatra Province, Indonesia, which lies at an elevation of 461.50 meters (m) above sea level. Maninjau Lake has an elongated shape with an approximate dimension a length of 17 kilometers (km) and a width of 8 km extending from north to south, along with a surface area and volume of 9,737.50 ha and 10,226 x 10^6 cubic meters (m^3), respectively. This lake has a natural outlet, namely the Batang Antokan River, which flows towards the west. The depth of Maninjau Lake increases in the southern part, and the maximum depth reaches ± 165 m. The study area has a wet tropical climate with an average rainfall of 345.58 millimeters (mm) per month and the average humidity of 95.20%. The average temperature of Maninjau Lake is 22.66 °C-31.27 °C (MERI, 2011). Maninjau Lake is located within the physiographical area of the Bukit Barisan Mountains and was formed from the eruption of ancient volcanoes embodying a strato morphology of the surrounding landscape. Topography classes of Maninjau Lake consist of flat (0–8% slope), mild (8–15%), fairly steep (15–25%), steep (25–40%), and very steep (> 40%) areas, with the southern part being steeper than the north-west. The lake's sediment can record the frequency and magnitude of volcanic eruptions, given its proximity to several active volcanoes, namely Mount Marapi, Singgalang, and Talang (De Maisonneuve *et al.*, 2019). Maninjau Lake is an important tourist destination, with a hydroelectric power plant with a capacity of 64 Mega Watts (MW), capturing fisheries, floating net cages, and agriculture (Junaidi *et al.,* 2014). Lake Maninjau is included in the list of National Priority Lakes together with 15 other lakes in Indonesia because of its strategic economic, ecological, socio–cultural, scientific values, and an experience of significant pressure and degradation (Presidential Regulation of the Republic of Indonesia No. 60 of 2021). The catchment area's primary land uses are rice farming, arid land, plantation, settlements, and forest. The water surface of Maninjau Lake covers a sizable portion (75.38%) of the catchment area (24,800 ha). Maninjau Lake is in a heavy eutrophic state due to the rapid expansion of floating net cage-based carp and tilapia, resulting from an influx of nutrients, including N and phosphorus (Syandri *et al.*, 2014).

Field sampling designs

The field sampling was conducted in June 2022. The research sites were determined based on random judgemental sampling, a method that identifies distinct characteristics relevant to the study goals

(Bhardwaj, 2019). The sampling point in this study was determined based on the representativeness and accessibility of the sampling locations. Sediment sampling was limited to five sites in the northern part of the Lake, which is more accessible and sloped than the southern part. The five sampling sites included Koto Malintang (M1), Koto Gadang (M2), Koto Kaciak (M3), Duo Koto (M4), and Koto Maninjau (M5) (Fig. 1 and Table 1). Several sediment variables were measured, including depth, Bd, OC concentration, and TN. Sediment sampling was performed at each site using a D'Section corer, a cylindrical stainless steel tube 50 centimeters (cm) long and 2.5 inches in diameter. The depth of sediment coring at all research sites reached 100 cm. The sediment samples were then divided into several layers according to the depth intervals of 0–15 cm, 15–30 cm, 30–50 cm, and 50–100 cm. A total of 20 sediment samples were obtained from the five research sites.

Laboratory analysis

Analyses of Bd, percentage of SOC content, and TN were performed at the Environmental Engineering Laboratory, Diponegoro University, and the CNH Laboratory, Semarang.

Sediment organic carbon stock (SOC)

Bd (gram per cubic centimeter: g/cm^3) was determined by calculating the ratio of the dry weight and volume of the sample. The sediment sample was oven-dried at 60 °C for at least 48 hours and later weighted. Dry Bd was calculated using Eq. 1 (Kauffman and Donato, 2012).

Bd (g/cm^3) = Oven-dry sample mass (g) / Volume of the sample (m^3) (1)

The Loss on ignition (LOI) method was used to calculate the percentage of OC content (%OC) (Nelson

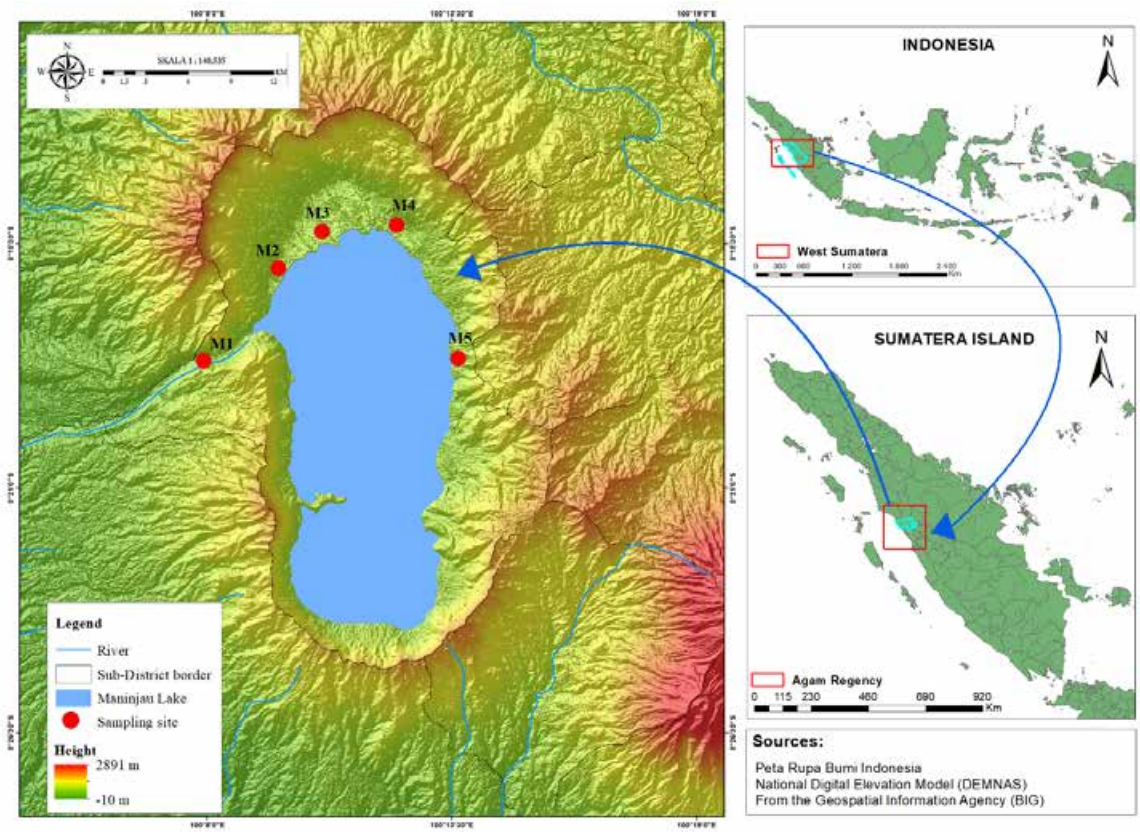

Fig. 1: Geographic location of the study area in the north part of Maninjau Lakeside in Indonesia

Table 1: Description of the study sites

Site	Location	Geographical position	Description
M1	Koto Malintang	-1° 42' 25.6''S 100° 8' 56.5''E	The lake outlet with conservation and tourism areas with sandy substrate types.
M2	Koto Gadang	-1° 44' 18.5''S 100° 10' 26.2''E	An inlet of the lake, with overgrown water hyacinth and sandy-mud substrate type
M3	Koto Kaciak	-1° 44' 41.4''S 100° 10' 59''E	Sloping lakeside, floating net cage, and riparian areas are dominated by agricultural land with muddy substrate types.
M4	Duo Koto	-1° 44' 54.3'' S 100° 11' 40.4''E	Dominated by forest areas with the sandy-mud substrate
M5	Maninjau	-1° 41' 50.2'' S 100° 13' 33.4''E	Near dense settlements with minimal vegetation cover, with several aquaculture activities in the lake's water bodies with a sandy substrate type.

et al., 1996). A total of 20 collected sediment samples were placed in weighted crucibles and oven-dried at 105 °C for 12-24 hours to determine the water loss. After oven-drying, the sample was burned in a furnace at 550 °C for 4 hours, then weighed to define the organic matter. The LOI is calculated using Eq. 2 (Heiri *et al.*, 2001).

$$LOI_{550}(\%) = ((DW_{105} - DW_{550})/ DW_{105})*100 \quad (2)$$

Where;
LOI_{550} : percentage of LOI at 550°C
DW_{105} : dry sample weight before combustion
DW_{550} : dry sample weight after combustion (heating at 550 °C)

The total OC content percentage was estimated through LOI at 550 °C (LOI_{550}), which is then transformed by a factor of 0.55 as in Eg. 3 (Hoogsteen *et al.*, 2015), while, the SOC stock was calculated using Eq. 4 (Howard *et al.*, 2014).

$$OC = LOI_{550}*0.55 \quad (3)$$

$$SOC\ (Mg/C/ha) = Bd \times H \times OC \quad (4)$$

Where;
SOC : Sediment organic carbon stock (Mg/C/ha)
OC : organic carbon concentration (%)
Bd : bulk density (g/cm^3)
H : sediment thickness (cm)

Total nitrogen and carbon/nitrogen (C/N) ratio

TN was determined by indophenol-blue methods, followed by Kai *et al.* (2016). TN analysis commenced with the destruction of the sediment samples. Sediment samples (0.5 g) were digested using 10 mL sulfuric acid (H_2SO_4) and 10 mL hydrogen peroxide (H_2O_2) at 420 °C for 1.5 hours using Kjeldahl. 0.5 g of copper (II) sulfate ($CuSO_4$) catalyst was used to accelerate the destruction reaction. Furthermore, the crude extract was filtered using ADVANTEC Filter Paper number 6. TN content was measured by mixing 1 mL of the extract with 0.6 mL of indophenol solution and 0.4 mL of sodium hypochlorite (NaOCl) solution. The mixture was then incubated at room temperature for 45 min until the solution color changed. The solution absorbance was then measured using a UV-Vis spectrophotometer at a wavelength of 635 nanometers (nm) (Santoni *et al.*, 2001). The C/N ratio was also calculated to determine the temporal changes in the sources of organic matter in the lake. The C/N ratio was calculated based on the OC (%) and TN (%) concentration and then multiplied by 1.167 to obtain the yield atomic mass ratios using Eq. 5 (Fan *et al.*, 2017).

$$C/N\ ratio = (OC/TN)*1.167 \quad (5)$$

Where;
OC : organic carbon (%)
TN : total nitrogen (%)
1.167 : yield atomic mass ratios

The C/N ratio of fresh algae in lacustrine sediment generally ranges between 3–8, and the C/N ratio of terrestrial vegetation ranges from 14–23 or may reach up to 45–50 (Mayers, 1997).

Statistical analysis

Statistical analysis was performed to determine the difference in the OC and TN between Bd. Sediment carbon concentrations between the research sites and depths were tested with analysis of variance (ANOVA). The relationships between OC and TN (dependent variables) and Bd (independent variables) were examined using linear regression. The Shapiro–Wilk test assessed data normality, and all statistical tests used a significance level of 0.05.

RESULT AND DISCUSSION

Sediment organic carbon stocks

The SOC in the different depth intervals is presented in Fig. 2, and it can be seen that SOC increased with depth. The SOC stock in each depth interval differs significantly with the probability (p= 0.000 <0.05) (Table 2). A remarkable difference was observed between SOCs in the surface and deeper layer (p= 0.000 <0.05). The highest SOC stock of 267.56 Mg/C/ha was noted for the deepest layer of (50–100 cm), and the lowest stock was 43.47 Mg/C/ha at the depth of 15–30 cm.

The findings of this research are in agreement with Wei *et al.* (2022), who found that SOC stocks of 25% at the surface layer and 53% in the deeper sediment layer. A similar pattern was observed by Wang *et al.* (2018) and Jiang *et al.* (2019). They reported the highest SOC at the deepest layer (300 cm). The SOC stocks at five research sites are shown in Fig. 3. The SOC in the Maninjau lakeside ranged between 284.23 (M3)–442.59 Mg/C/ha (M4). The average stock at the Maninjau lakeside (365.54 Mg/C/ha) was lower than that in the urban freshwater wetlands at Kolonawa and Thalawathugoda, Colombo (504 ± 14 and 550 ± 23 Mg/C/ha) (Dayathilake *et al.*, 2021), but higher than the highest SOC stocks in the lakeside of West Mauri Lake, China (313.16 Mg/C/ha) (Lei *et al.*, 2022) and the Lake Victoria, Uganda (147 Mg/C/ha) (Akodi

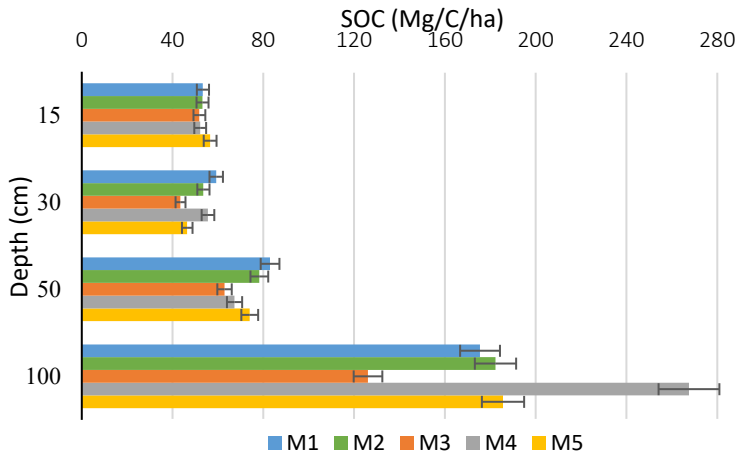

Fig. 2: SOC stock at different sites in various depth intervals

Table 2: Anova test of SOC at each site

Source of variation	SS	df	MS	F	P-value	F crit
Between groups	60349.58	3	20116.53	30.70605	7.16E-07	3.238872
Within groups	10482.12	16	655.1324	—	—	—
Total	70831.7	19	—	—	—	—

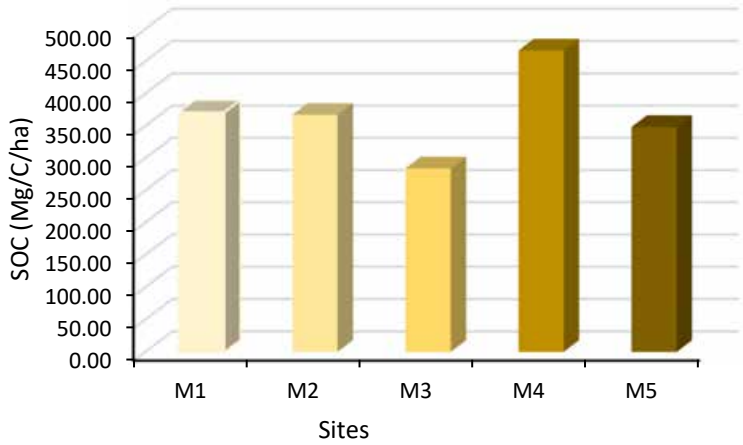

Fig. 3: SOC stocks at five different research sites

Table 3: The type of land use in the catchment area of Maninjau Lake (BPS-SAR, 2015)

No	Village (Nagari)	Forest (ha)	Built-up area (ha)	Plantation (ha)	Rice -field (ha)
1	Tanjung Sani	2,421	154	1773	126
2	Sungai Batang	720	180	279	389
3	Maninjau	560	110	426	205
4	Bayua	692	140	140	524
5	Duo Koto	2,037	75	159	275
6	Paninjauan	58	60	99	145
7	Koto Kaciak	369	110	236	458
8	Koto Gadang	606	64	101	216
9	Koto Malintang	1,431	80	98	174

et al., 2016). The highest SOC was observed at M4 (442.59 Mg/C/ha), with the highest forest area cover, whereas the lowest was noted at M3 (284.23 Mg/C/ha). Based on the data from Syandri *et al.* (2014), the forest area in M4 reaches 2,037 ha. In contrast, the forest area around the M3 constitutes only 369 ha, and land use is dominated by rice fields, causing low SOC stock in comparison to other study sites (Table 3). The SOC and TN amounts in sediments was significantly influenced by land use or cover in the Maninjau Lake catchment area. This suggests that the presence and type of vegetation on the lakeside have a critical impact on the OC storage in sediments. It also emphasizes the importance of the restoration efforts in wetlands, considering that the land use type significantly affects the SOC stocks (Lei *et al*., 2022).

The land use in the Maninjau Lake area has undergone significant changes, especially in the forest areas. The forest area surrounding the lake has been declining from 1989 to 2020. In 1989, the forest area was 8,228.25 ha; it has declined considerably to 5,190.21 ha in 2020, and it is predicted to continue declining until 3,607.83 ha in 2050 (Antoni *et al.,* 2016). Meanwhile, agriculture, plantations, and built-up area have increased sharply due to the economic and population growth. Land use in the catchment area affects the quality of the environment and water quality. The use of chemical fertilizers on the agricultural and plantation land affected the TN sediment. Meanwhile, reduced forest area will directly reduce the organic inputs and SOC (Akodi *et al.,* 2016). The amount of SOC

and other organic elements are also influenced by the topography of the catchment area of Maninjau Lake, which mainly contains steep slopes and is prone to landslides. Landslides and erosion are closely related to the carbon cycle (C) and cause changes in physical, chemical, and biological properties (Shiels and Walker, 2013). Landslides can release carbon into the atmosphere (Lal, 2004). Soil experiencing landslides causes the loss of the topsoil and most of the soil's organic matter (Stalard, 2012). The presence of SOC in the eroded soil is highly dependent on the ecohydrological factors (Quijano *et al.,* 2013), topography, and land cover (Dialynas *et al.,* 2016a). One of the northern parts of the Maninjau catchment areas with a high landslide susceptibility is Koto Malintang (M1), with a slope of 30–45% (Ramanda *et al.,* 2019). Other areas in the northern part of Maninjau Lake are relatively sloping and not prone to landslides. M1 has a relatively large forest area, which can minimize the landslides and loss of SOC stock. This is in line with the results of Dialynas *et al.* (2016b), which showed that the land cover type dramatically affects the extent of SOC loss due to erosion, where the land with forest cover type loses lesser SOC when compared to oil palm plantation areas. Thus, the presence or absence of above-ground vegetation and the density and health of its growth regulate the organic matter input and SOC in the sediment (Zhao *et al*., 2018; Wei *et al*., 2022). Lakeside wetland areas with forest cover have a higher SOC stock than those with minimum vegetation cover; this indicates that vegetation restoration in the lakeside regions may substantially increase the SOC stock (Ji *et al.*, 2020). A similar conclusion was drawn by Adame *et al.* (2018), who found that the restoration of wetlands may help increase the OC stock of sediments in the long term. They found that the SOC stock increased from 1234±18 to 1309±270 Mg/C/ha from 5 to 70 years of restoration. Furthermore, Creed *et al.* (2022) also showed that wetlands from the agricultural land could restore the wetland carbon stock to that of intact wetlands within 40 years or less. Meanwhile, the conversion of forest areas on the lakeside and wetlands into settlements will significantly decrease the SOC stock and potentially contribute to carbon emissions.

Distribution of sediment organic carbon concentration and total nitrogen content

The distribution of OC concentration and TN at different depths and sites is presented in Fig. 4a and b. OC fluctuated significantly, with a trend towards the lower values at the deeper layers. However, an opposite pattern was reported at the M4 site, where high OC was found at the deepest layer (50–100 cm) (35.368%), whereas it was 22.29% in the surface sediment layer (0–15 cm). TN's vertical distribution showed a similar trend, except for sites M3 and

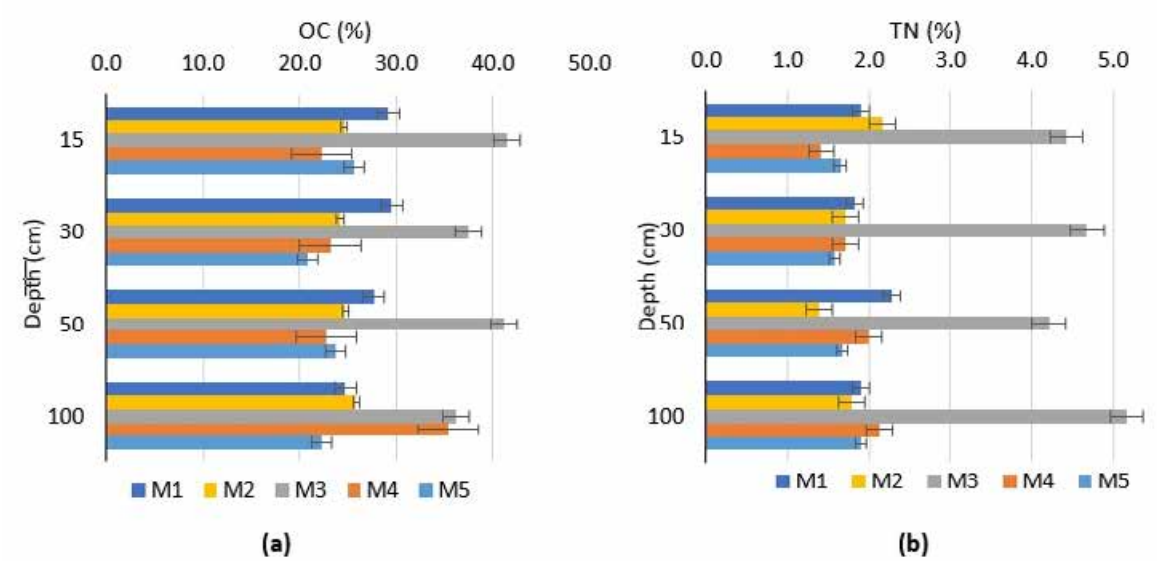

Fig. 4: Vertical distribution of (a) OC in the sediment and (b) TN

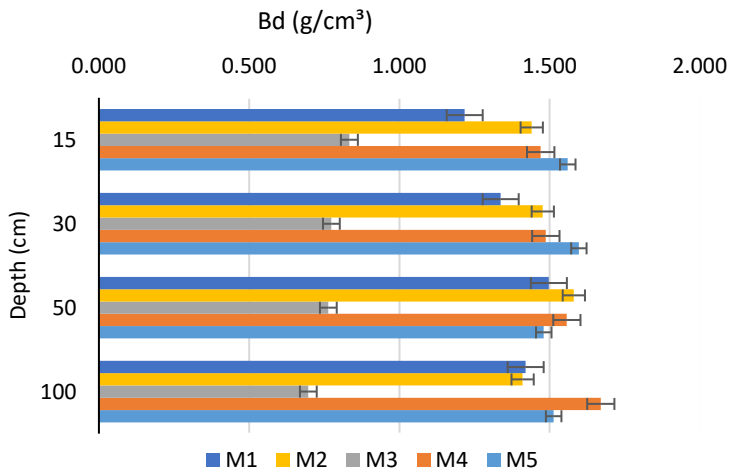

Fig. 5: Vertical distribution of Bd

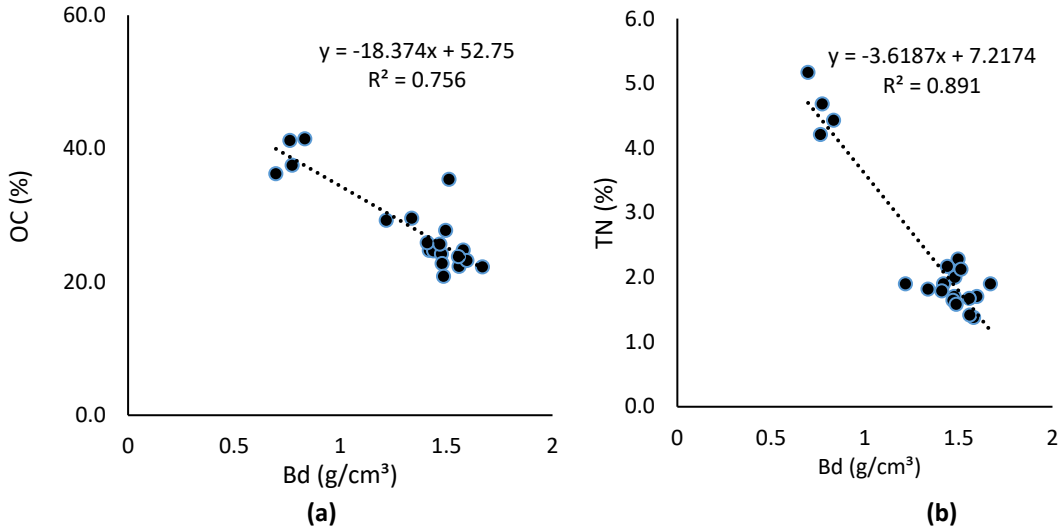

Fig. 6: Correlation between (a) OC and Bd; and (b) TN and Bd

M4, where TN was higher in the deepest layer than the surface layer. There was a significant positive correlation between OC and TN (y=0.1554x–2.003, R^2=0.7342), which indicated that most of the nitrogen was in the form of organic nitrogen (Yu *et al.,* 2018).

Generally, the vertical distributions of OC and TN varied among the different sediment depth intervals. Thus, the vertical variations in OC and TN were correlated with the Bd of the sediment. The Bd of a sediment increased with its depth. However, the opposite trend was observed in OC and TN at the M3 and M5 sites (Fig. 5), which showed that Bd positively correlates with sediment depth, in agreement with previous studies (Twum and Nii-Annang 2015; Gnanamoorthy *et al.,* 2019). It was also found that sediment Bd has a significant negative correlation with OC and TN (y= −18.374x + 52.75, R^2= 0.756; and y= −3.6187 + 7.2174, R^2 = 0.891, respectively) (Fig. 6a and b). Thus, high Bd may indicate lower OC and TN in the sediment. The biological cycles and microbial decomposition restricted to the deeper sediment layers are two complex processes contributing to the declining trend in OC correlated with the increase in the sediment depth (Bhomia *et al.,* 2016; Sasmito *et al.,* 2020).

The mean of OC, TN, and Bd in the sediments differed significantly (p=0.000; p=0.000; p=0.000<0.05, respectively) (Tables 4 to 6) among the research sites. The highest average of %OC was found at M3 (39.07%), while the lowest was noted for site M5 (23.11%) (Fig. 7a). Likewise, the highest average value of TN was also found at M3 (4.62%), with the lowest in M5 (1.69%) (Fig. 7b). A previous study reported that the TN and OC in the sediment of Maninjau Lake ranged from 1.10% to 2.10% and 48.81% to 62.35%, respectively, and the highest values were also found at M3 (Junaidi *et al*. 2014). In this case, the dynamics of TN and OC in sediments are influenced by various biota activities at the lake bottom, which correlated with water quality parameters, including temperature, DO, pH, and others. The waste from the floating net cages strongly influences the quality of the lake waters. There is massive sediment waste at M3 since its topography is relatively sloping compared to other locations and thus, supports waste accumulation. The extensive deposition of organic matter has resulted in water hyacinth blooms in that area (Syandri *et al*., 2014).

Anthropogenic sources, including the use of fertilizers in agricultural activities and runoff from the settlement can also increase the input of organic matter in the lake (Avarimidis *et al*., 2015). Fishery production in Maninjau Lake showed an increasing trend from 2018 to 2019 (from 187.87 to 593.86 tons). Concurrently, agricultural production, especially in the rice field, increased from 35,506 to 38,303 tons (BPS-SAR, 2020). The trend of increasing fishery and agricultural production due to the use of fertilizers also increased the input of organic matter in Maninjau Lake. The highest and lowest Bd were found in M5 (1.546 g/cm^3) and M3 (0.7665 g/cm^3), respectively (Fig. 7c). Bd concentration depends upon the vegetation's roots, which in turn, influences the biological activity, increases water permeability, and decreases sediment compaction (Bhomia *et al*., 2016; Arifanti *et al*., 2019). This condition probably originates from the differences in land use and vegetation density among the research sites. Site M5 is mostly an urbanized area with minimum vegetation coverage and a sandy substrate, while M3 is dominated by agricultural land with a muddy substrate. In addition, sediment texture also significantly affects the OC content. For instance, the finer sediments, such as mud, generally have a higher content of OC than sandy substrates (Musale *et al*., 2015).

Table 4: Anova test of the OC concentration at each site

Source of variation	SS	df	MS	F	P-value	F crit
Between groups	642.9768	4	160.7442	14.19317	5.52E-05	3.055568
Within groups	169.8819	15	11.32546	—	—	—
Total	812.8587	19	—	—	—	—

Tabel 5: Anova test of TN at each site

Source of variation	SS	df	MS	F	P-value	F crit
Between groups	25.43542	4	6.358854	72.51939	1.25E-09	3.055568
Within groups	1.315273	15	0.087685	—	—	—
Total	26.75069	19	—	—	—	—

Tabel 6: Anova test of Bd at each site

Source of Variation	SS	df	MS	F	P-value	F crit
Between groups	1.718473	4	0.429618	63.37768	3.24E-09	3.055568
Within groups	0.101681	15	0.006779	—	—	—
Total	1.820154	19	—	—	—	—

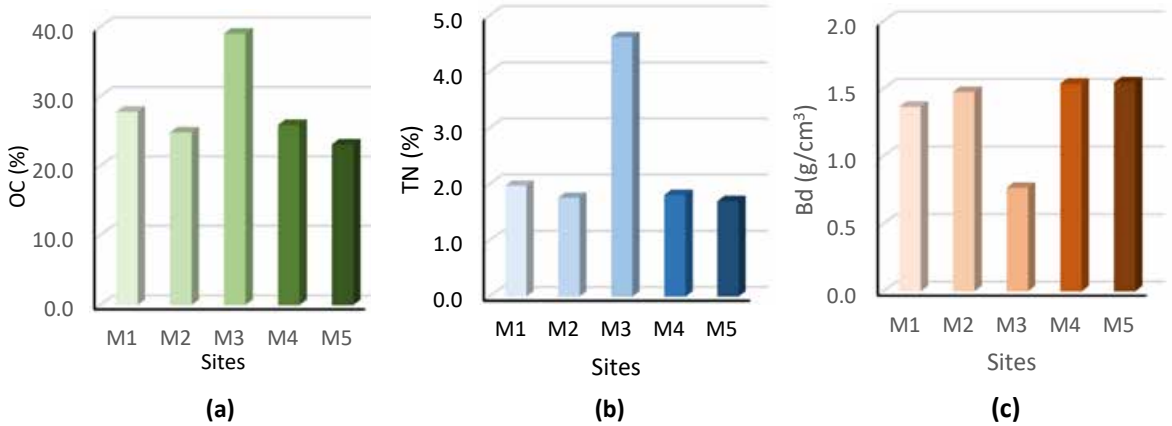

Fig. 7: The differences among (a) OC, (b) TN, and (c) Bd at each site

Table 7: OC and TN concentration in the lake sediments in several countries

Lake	Characteristic	OC (%)	N (%)	References
Maninjau, Indonesia	heavy eutrophic	20.82–41.44	1.37–5.16	This study
Chaohu, China	oligotrophic	0.59–1.02	0.07–0.15	Yu *et al.*, 2018
Balkhash, Kazakhstan	oligotrophic	1.13–1.69	0.16–0.21	Liu *et al.*, 2021
Dali, Mongolia	mesotrophic	1.0–7.3	0.13–0.56	Fan *et al.*, 2017
El Sol, Mexico	oligotrophic	4.6–7.9	—	Alcocer *et al.*, 2020
Towuti, Indonesia	mesotrophic	0.4–4	—	Friese *et al.*, 2021
Sentani, Indonesia	oligotrophic	8.0–16.0	0.33–1.91	Nomosatryo *et al.*, 2021
Tempe, Indonesia	mesotrophic	4.7–5.8	0.30–0.50	Yustiawati *et al.*, 2021
Qinghai, China	mesotrophic	1.4–4.8	0.14–0.72	Chen *et al.*, 2021
Halai, China	—	13.2	—	Xu *et al.*, 2019
Dahu, China	—	48.76	—	Xu *et al.*, 2019
Chapala, Mexico	oligothropic	15–22	—	Xu *et al.*, 2019
Great Ghost, Taiwan	oligotrophic	7.1–22.2	—	Kandasamy *et al.*, 2018
Ovre Bjorntjarn, Sweden	eutrophic	39.9–40.0	—	Gudasz *et al.*, 2017
Solbacka, Sweden	eutrophic	31.5–34.4	—	Gudasz *et al.*, 2017

The concentrations of OC and TN in Lake Maninjau (20.82–41.44% and 1.37–5.16%, respectively) are significantly higher than in several lakes in Indonesia, such as Lake Towuti (0.4–4 %) (Friese *et al.*, 2021), Lake Sentani (8–16%) (Nomosatryo *et al.*, 2021), and Lake Tempe (4.7–5.8 %) (Yustiawati *et al.*, 2021). This is closely related to the trophic level of the lake, where a lake with a trophic level of heavy eutrophic such as Maninjau Lake, will have a higher OC concentration. The result of sediment OC concentration and TN in this study were comparable to the average value reported for eutrophic lakes and significantly higher than the mesotrophic and oligotrophic lakes in several countries (Table 7). The heavy eutrophic status of Lake Maninjau was established in 2013 due to high nutrient inputs, such as nitrogen and phosphorus from aquaculture waste (floating nets cages) and agriculture activities on the lakeside. The number of floating net cages in Lake Maninjau shows an increasing yearly trend (Fig. 8), for instance, from 16 units in 1992the number increased to 17,226 units in 2014 (MERI, 2015). The newest 2021 data displayed

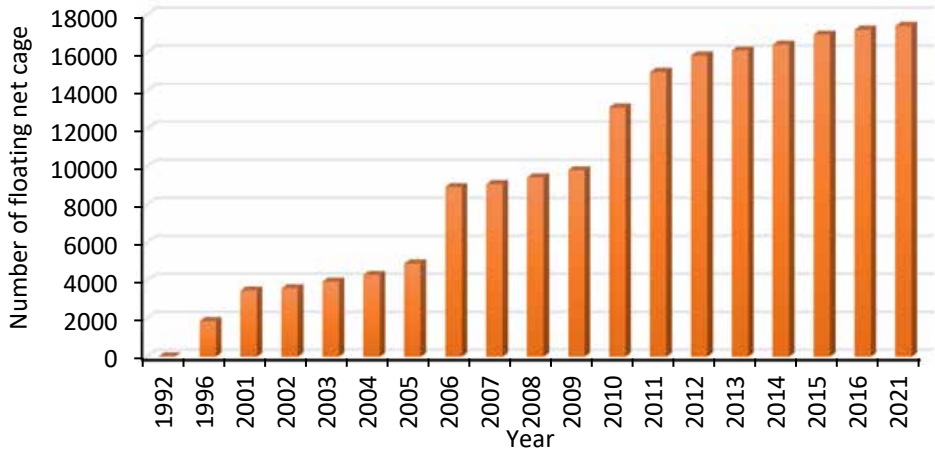

Fig. 8: The number of floating net cages in Lake Maninjau in 1992–2021 (MERI, 2011; Junaidi *et al.*, 2014; MERI, 2015; Soejarwo *et al.*, 2022)

17,441 units of floating net cages in Lake Maninjau (Soejarwo *et al*., 2022).

The additional source of nutrient pollution in Maninjau Lake is associated with the widespread land use transformation in the lakeside area for settlements, rice fields, and other uses. This has led to the occurrence of blue-green algae blooms and the dominance of phytoplanktons, such as the genera Gloeocapsa, Oscillatoria, and Mycrocystis (Sulastri, 2019). Syakti *et al.* (2019) reported that hazardous algae blooms (HABs), and generated by the dynamics of various phytoplankton species, emanated from increased human activity.

Sources of organic matter in lakeside sediment

The organic matter in lake sediments originate from the internal primary production (autochthonous) and terrestrial materials introduced into the lake (allochthonous) (Lin *et al.,* 2022). The source of organic matter in the lake sediment is commonly determined by the ratio of OC and TN (C/N ratio) (Mayers, 2003; Barus *et al.*, 2019). The vertical distribution of C/N atomic ratios at each site is presented in Fig. 8. The general trend in C/N atomic ratios decreased from the surface towards the deeper sediment layers. The exceptions constitute sites M2 and M4, where the C/N atomic ratios increased with the sediment depth. The C/N atomic ratio varies depending on the organic matter source. Values between 3 and 8 are typically noted when the allochthonous sources dominate. A C/N ratio greater than 20 indicates that allochthonous material is the main source of organic matter. Considering this, a decreasing trend in the C/N ratio with the sediment depth may indicate an increasing share of autochthonous sources. In contrast, an increasing trend in the C/N ratio may relate with a higher allochthonous proportion (Yu *et al*., 2018). The result of the C/N atomic ratio in this research showed that at the sites M1, M3, and M5, the organic matter mainly originates from autochthonous sources, while allochthonous sources and terrestrial input dominate at sites M2 and M4. These results indicate that the organic matter in Maninjau Lake sediments is dominated by autochthonous material, especially from the floating net cage waste. The average C/N atomic ratio of all research sites (M1–M5) ranged from 9.96 to 16.75 (Fig. 9), with the lowest and highest ratios found at M3 and M4, respectively. These values were in the range typically noted for phytoplanktons (4–10) and were close to the range reported for submerged and floating macrophytes (10–20), but were significantly less than those of terrestrial plants (greater than 20) (Tyson, 1995; Sasmito, 2020). The average value of the C/N ratio at M3 was below 10 (9.96) (Fig. 10), indicating that the main source of the organic matter is phytoplankton or endogenous aquatic organism. The C/N value is inversely proportional to the intensity of land use by humans. (Enters *et al*., 2006). M3 is located in Koto Kaciak and is the most polluted site by organic matter—reflected by the high concentration of OC and TN in the sediment of the

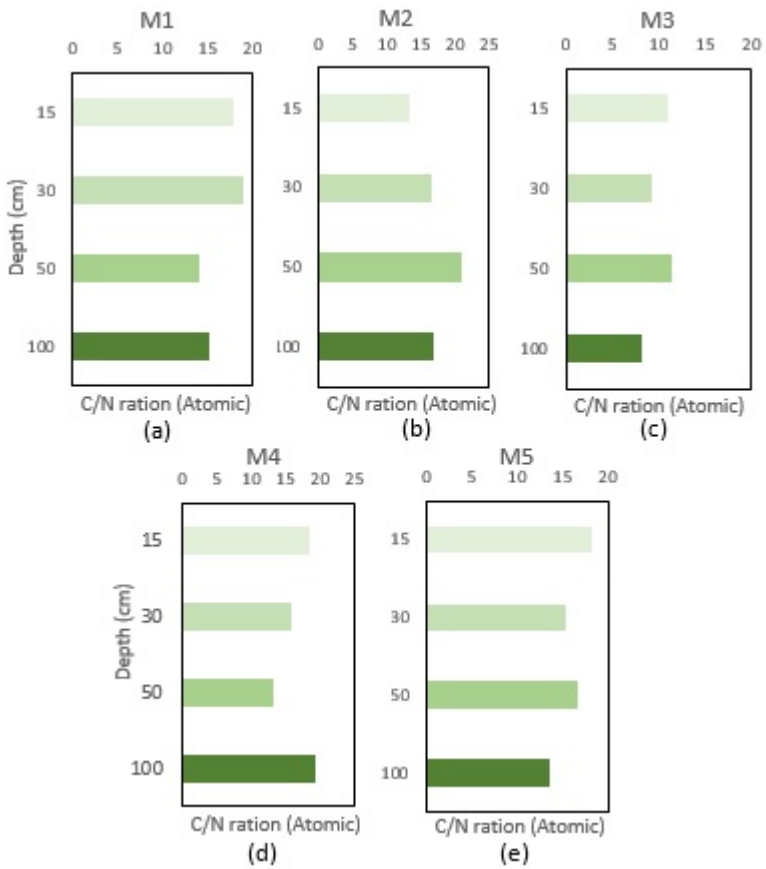

Fig. 9: The vertical variation of C/N atomic ratios at each site

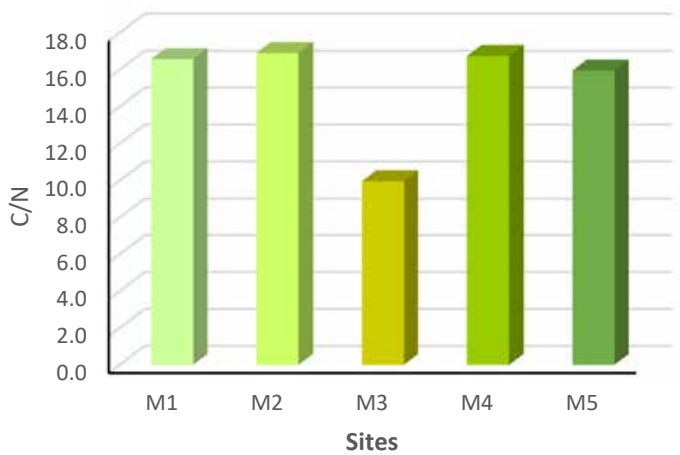

Fig. 10: The average C/N atomic ratio at each site

Maninjau Lakeside. The relatively sloping topography of M3 causes a significant waste accumulation in the surface sediments. The high expansion of organic matter has caused a phytoplankton bloom in that area (Barus *et al*., 2019). Consequently, a low C/N ratio was reported for Koto Kaciak. The mean atomic C/N ratios at the remaining sites, including M1, M2, M4, and M5, ranged from 15.95 to 16.91, indicating that the primary source of organic matter in these locations is a mixture of floating macrophyte derivatives and submerged vegetation. Furthermore, these results also illustrate that the high OC value in these locations mainly results from terrestrial plant material (forest litter) from the forested catchment and the impact of anthropogenic terrestrial activities (Mahapatra *et al.,* 2012). This is in agreement with the characteristics of each site: site M1 (Koto Gadang) is an outlet area and a conservation forest; M2 (Koto Malintang) is an inlet area overgrown by water hyacinth; M4 (Duo Koto) is dominated by forest; M5 (Koto Maninjau) is a settlement area. The mean atomic C/N ratios at the remaining sites, including M1, M2, M4, and M5, ranged from 15.95 to 16.91, indicating that the primary source of organic matter in these locations is a mixture of floating macrophyte derivatives and submerged vegetation.

Implication for sustainable management of lake

The lakeside area is a type of wetland ecosystem vulnerable to environmental changes, mainly caused by human interference. The significant land use change in the lakeside, primarily for agriculture, plantations, and settlements, has transformed this area into a carbon source because of its sensitivity to changes in the nutrient content, temperature, pH, etc (Mitra *et al*., 2005). The findings of this study have demonstrated that SOC stocks are higher in the lakeside area with a dense vegetation cover, such as conservation forest areas, than within agricultural land and settlements with a sparse vegetation cover. This suggests that restoration and conservation efforts of lakeside wetlands may enhance the SOC stock. SOC stock has continued to rise as the lakeside vegetation succession stage has been developed (Li *et al*., 2018). The presence of land vegetation in the lakeside area essentially reduces the erosion susceptibility of environments within sandy soils, such as in M1. Restoration initiatives in the lakeside area, such as converting agricultural land to wetlands may thereby reduce human disturbance, which is beneficial for ecosystem recovery and SOC accumulation (Lei *et al*., 2022). In addition, the condition of the catchment area along the lakeside significantly affects the state of Maninjau Lake. Agricultural activity contributes to sewage ingress and nutrient input into the lake, thus contaminating lake waters and settling as sludge sediment (Mahapatra, 2012). The high nutrient load released from floating net cage waste further pollutes the waters of Maninjau Lake. Additionally, it is generally recognized that anthropogenic activities increase the nutrient inputs into the lakes and affect their trophic state (May *et al*., 2021). Lake Maninjau is characterized as being heavily eutrophic, thus substantially influencing ecological degradation (Syandri *et al*., 2014). Therefore, a proper management strategy is required to reduce the pollution load in Maninjau Lake. The potential management actions to improve the lake water quality encompass the following: developing sewage treatment plants, raising industrial waste disposal standards, limiting industrial and domestic sewage disposal, preventing regional sources of pollution from agricultural irrigation, and lowering fertilizer and pesticide usage in the lakeside area (Qing *et al*., 2007; Yu *et al*., 2020). Additionally, the self-purification of water bodies may be significantly boosted with sufficient restoration efforts in the riparian zone along the lakeside. These initiatives may also enhance the biodiversity, protect soil quality, and limit eutrophication (Chen *et al.,* 2019). Hence, to improve the sustainability of the water and lakeside environment of Maninjau Lake, it is essential to invest restoration efforts by considering the suitable type of vegetation in the lakeside area. Following this, the ecosystem's total carbon stock could be significantly increased by planting local plant species and maintaining plant biodiversity. Moreover, the water balance must be considered to ensure the effectiveness and sustainability of the ecological restoration efforts in the lakeside area (Jiang *et al.,* 2019). Regarding the global climate change mitigation, restoring and protecting the sustainability of Maninjau lakeside may significantly reduce carbon emissions, increase carbon storage capacity in sediments, and improve the local community's livelihoods. It is also necessary to have early detection of pollutants dissolved in Maninjau Lake; referring to the research of Kamyab *et al.,* (2022), carbon-based molecularly-imprinted polymers

(MIPs) can be effectively used to detect harmful pollutants. Since carbon-based nanomaterials are sensitive to molecular identification, they are widely used to assess the environmental quality. Agricultural waste, aquaculture, and water pollution in Maninjau Lake are also caused by household waste, which is generally discharged into rivers before eventually entering the lake. To overcome those problems, initiatives are needed in managing household waste, such as converting waste into compost that can be reused by the community. Based on the research study by Kamyab *et al.,* (2015), the management of waste into compost can provide considerable benefits from an economic perspective and help reduce the greenhouse gas emissions by 90%.

CONCLUSION

This study has indicated that the lakeside wetlands have a relatively large capacity to store carbon stocks, especially in sediments. In general, SOC stocks show an increasing trend with the increasing sediment depth, which confirms the findings of previous studies. The estimated SOC stocks in the lakeside also significantly differ among the research sites, indicating that environmental conditions, land use, and land cover can affect the SOC stock. The highest SOC stock (442.59 Mg/C/ha) was found at site M4, a lakeside area dominated by forest cover. In contrast, the lowest stock (284.23 Mg/C/ha) was found at site M3, dominated by the agricultural land. Our results support the assertion that vegetation cover plays an essential role in the SOC stock. Furthermore, the land use differences also affect the distribution of OC, TN, and Bd. The spatial variations in the OC and TN content display a tendency towards higher values in locations close to the agricultural land. In contrast, Bd tends to be high in areas with minimal vegetation, such as settlements. Moreover, Maninjau Lake has a heavy eutrophic state with a much higher OC and TN contents compared to several other Indonesian lakes and eutrophic lakes in other countries. The primary source of organic matter in the sediments of Maninjau Lakeside is phytoplankton, a mixture of floating macrophyte and submerged vegetation. The unregulated increase of floating net cages and widespread change of land use into extensive agricultural and settlements are the main contributors to water pollution and ecological degradation in Maninjau Lake. This study's results confirm the relationship among the anthropogenic activities (land use), SOC stocks, and the lake's trophic state. It was also found that the restoration efforts of the lakeside wetlands are important for maintaining the sustainability of the water and lakeside environment. The preserving and protecting lakeside wetlands may support global climate change mitigation through sequestration processes that can reduce carbon emissions in the atmosphere.

AUTHOR CONTRIBUTIONS

T.R. Soeprobowati, the corresponding author, has contributed to the sediment carbon stock analysis, interpreted the results, and prepared the manuscript. N.D. Takarina performed sediment analysis. P.S. Komala designed the field experiment, L. Subehi prepared all the maps and figures; M. Wojewódka-Przybył participated in the interpretation of the results and manuscript preparation, J. Jumari prepared related text and R. Nastuti conducted field data acquisition and contributed to the data analysis.

ACKNOWLEDGEMENT

The study was conducted in Lake Maninjau, funded by Riset Kolaborasi Indonesia, a with the contract number [434-05/UN7.D2/PP/VI/2022]. Thanks to the World Class University Program of Diponegoro University which supported the involvement of Wojewódka-Przybył in the fieldwork. Thanks to, Mirza Hanif Al Fallah and Muhammad Ilham Jasir, and Aulia Rahim for their help in the preparation of equipment.

CONFLICT OF INTEREST

The author declares that there is no conflict of interest regarding the publication of this manuscript. In addition, the ethical issues, including plagiarism, informed consent, misconduct, data fabrication and falsification, double publication and submission, and redundancy, have been ultimately observed by the authors.

PUBLISHER'S NOTE

ABBREVIATIONS

%	percent
°C	centigrade
ANOVA	Analysis of variation
Bd	Bulk density
C	carbon
C/N	Organic carbon and total nitrogen ratio
cm	Centimeter
CO_2	Carbon dioxide
$CuSO_4$	Copper (II) sulfate
df	degree of freedom
DW_{105}	A dry weight of the sample before combustion
DW_{550}	dry weight of the sample after combustion
E	East
Eq.	Equation
F	Freedom
F crit	Freedom critical
Fig.	Figure
g	Gram
g/cm^3	Gram per cubic centimeter
GHG	Greenhouse Gas
H	The thickness of sediment
H_2O_2	Hydrogen peroxide
H_2SO_4	Sulfuric acid
ha	Hectare
HABS	Hazardous algae blooms
kg/m^2	Kilogram per square meter
Km	Kilometer
LOI	Loss of ignition
LOI_{550}	percentage of LOI at 550°C
M1	Koto Malintang
M2	Koto Gadang
M3	Koto Kaciak
M4	Duo Koto
M5	Koto Maninjau
m.a.s.l	Meter above sea level
mm	millimeter
m	meter
mL	Milliliter
m^3	Cubic meter
Mg/C/ha	Mega gram per carbon per hectare
MIPs	molecularly-imprinted polymers
MS	Mean square
nm	nanometer
OC	Organic carbon
pH	Power of Hydrogen
p	probability
Pg C	Petagram Carbon
R^2	Determination coefficient
S	South
SOC	Sediment organic carbon
SS	Sum of square
TN	Total nitrogen
y	Dependent variable

REFERENCES

Adame, M.F.; Zakaria, R.M.; Fry, B.; Chong, V.C.; Then, Y.H.A.; Brown, C.J.; Lee, S.Y., (2018). Loss and recovery of carbon and nitrogen after mangrove clearing. Ocean Coastal Manage., 161: 117–126 **(10 pages)**.

Akodi, D.; Komutunga, E.; Agaba,C.; Oratungye, K.J.; Ahumuza, E., (2016). The effect of land use on soil organic carbon stocks in Lake Victoria Crescent Agro-Ecological Zone, Uganda. J. Agric. Sci. Technol. A, 6(3): 154–160 **(7 pages)**.

Alcocer, J.; Ruiz-Fernández, A.C.; Oseguera, L.A.; Caballero, M.; Sanchez-Cabeza, J.A.; Pérez-Bernal, L.H.; Hernández-Rivera, D.M., (2020). Sediment carbon storage increases in tropical, oligotrophic, high mountain lakes. Anthropocene. 32: 1–12 **(12**

pages).
Alongi, D.M., (2002). Present state and future of the world's mangrove forests. Environ. Conserv., 29(3): 331–349 **(19 pages).**
Amin, M., (2016). Potensi, eksploitasi, dan konservasi lahan basah Indonesia berkelanjutan. Prod. Semnas. Lahan Basah, 1: 14–22 **(9 pages).** (In Bahasa).
Antoni, Y.; Hartono, D.M.; Suparmoko, M.; Koestoer, R.H., (2016). Water Quality Index in Lake Maninjau as a Parameter to Determine the Optimum Economic Growth of Floating Net Cages and Land-based Livelihood. OIDA Int. J. Sustainable Dev., 9(2): 51–61 **(11 pages)**.
Arifanti, V.B.; Kauffman, J.B.; Hadriyanto, D.; Murdiyarso, D.; Diana, R., (2019). Carbon dynamics and land use carbon footprints in mangrove-converted aquaculture: The case of the Mahakam Delta, Indonesia. For. Ecol. Manage, 432: 17–29 **(13 pages).**
Avramidis, P.; Nikolaou, K.; Bekiari, V., (2015). Total organic carbon and total nitrogen in sediments and soils: a comparison of the wet oxidation – titration method with the combustion-infrared method. Agric. Agric. Sci. Proc., 4: 425–430 **(6 pages).**
Balwan, W.K.; Kour, S., (2021). Wetland-an ecological boon for the environment East African scholars journal of agriculture and life sciences wetland- an ecological boon for the environment. East African Scholars J. Agri. Life Sci., 4(3): 38–48 **(11 pages).**
Barus, B. S.; Aryawati, R.; Putri, W. A. E.; Nurjuliasti, E.; Diansyah, G.; Sitorus, E., (2019). Relationship of N-total and C-organic sediments with macrozoobenthos in Payung Island, Banyuasin, South Sumatera. Jurnal Kelautan Tropis, 22(2): 147–156 **(10 pages)**. (In Bahasa).
Basuki, I.; Kauffman, J.B.; Peterson, J.T.; Anshari, G.Z.; Murdiyarso, D., (2021). Land Cover and Land Use Change Decreases Net Ecosystem Production in Tropical Peatlands of West Kalimantan, Indonesia. Forest, 12: 1–15 **(15 pages).**
Bhardwaj, P., (2019). Types of Sampling in Research. J. Pract. Cardiovascular Sci., 5: 157–163 **(7 pages).**
Bhomia, R.K.; Mackenzie, R.A.; Murdiyarso, D.; Sasmito, S.D.; Purbopuspito, J., (2016). Impacts of land use on Indian mangrove forest carbon stocks: implications for conservation and management. Ecol. Appl., 26(5): 1396–1408 **(13 pages).**
BPS-SAR, (2020). Tanjung Raya Subdistrict In Figures. **(119 pages)**.
BPS-SAR, (2015). Tanjung Raya Subdistrict In Figures. **(148 pages)**.
Chen, F.; Lu, S.; Hu, X.; He, Q.; Feng, C.; Xu, Q.; Chen, N.; Ngo, H.H.; Guo, H. Multi-dimensional habitat vegetation restoration mode for lake riparian zone, Taihu, China. Ecol. Eng., 134: 56–64 **(9 pages)**.
Chen, X.; Meng, X.; Song, Y.; Zhang, B.; Wan, Z.; Zhou, B.; Zhang, E., (2021). Spatial Patterns of Organic and inorganic carbon in Lake Qinghai surficial sediments and carbon burial estimation. Fron. Earth Sci., 9: 1–11 **(11 pages)**.
Comer-Warner, S.A.; Nguyen, A.T.Q.; Nguyen, M.N.; Wang, M.; Turner, A.; Le, H.; Sgouridis, F.; Krause, S.; Kentridge, N.; Nguyen, N.; Hamilton, R.L.; Ullah, S., (2022). Restoration impacts on rates of denitrification and greenhouse gas fluxes from tropical coastal wetlands. Sci. Tot. Environ., 803: 1–13 **(13 pages)**.
Creed, I. F.; Badiou, P.; Enanga, E.; Lobb, D.A.; Pattison-Williams, J.K.; Lloyd-Smith, P.; Gloutney, M., (2022). Can Restoration of freshwater mineral soil wetlands deliver nature-based climate solutions to Agricultural Landscapes? Fron. Ecol. Evol., 10: 1–12 **(12 pages).**
Dayathilake, D.D.T.L.; Lokupitiya, E.; Wijeratne, V.P.I.S., (2021). Estimating soil carbon stocks of urban freshwater wetlands in the Colombo Ramsar Wetland City and their otential role in climate change mitigation. Wetlands, 41(2): 1–10 **(10 pages)**.
De Maisonneuve, C. B.; Eisele, S.; Forni, F.; Hamdi; Park, E.; Phua, M.; Putra, R., (2019). Bathymetric survey of lakes Maninjau and Diatas (West Sumatra), and Lake Kerinci (Jambi). J. Phys. Conf. Ser., 1185(1): 1–9 **(9 pages)**.
Dialynas, Y.G.; Bastola, S.; Bras, R.L.; Billings, S.A.; Markewitz, D.; Ritcher, D.D., (2016a). Topographic variability and the influence of soil erosion on the carbon cycle. Global Biogeochem. Cycles, 30(5): 644–660 **(16 pages).**
Dialynas, Y.G.; Bastola, S.; Bras, R.L.; Spiotta, E.M.; Silver, W.L.; Arnone, E.; Noto, L.V., (2016b). Impact of hydrologically driven hillslope erosion and landslide occurrence on soil organic carbon dynamics in tropical watersheds. Water Resour.Res., 52: 8895–8919 **(24 pages).**
Donato, D.C.; Kauffman, J.B.; Murdiyarso, D.; Kurnianto, S.; Stidham, M.; Kanninen, M., (2011). Mangroves among the most carbon-rich forests in the tropics. Nat. Geosci., 4(5): 293–297 **(5 pages)**.
Enters, D.; Lücke, A.; Zolitschka, B., (2006). Effects of land-use change on deposition and composition of organic matter in Frickenhauser See, northern Bavaria, Germany. Sci. Total Environ., 369(1–3): 178–187 **(10 pages).**
Fan, J.; Xiao, J.; Wen, R.; Zhang, S.; Wang, X.; Cui, L.; Yamagata, H., (2017). Carbon and nitrogen signatures of sedimentary organic matter from Dali Lake in Inner Mongolia: Implications for Holocene hydrological and ecological variations in the East Asian summer monsoon margin. Quat. Int., 452: 65–78 **(14 pages).**
Friese, A.; Bauer, K.; Glombitza, C.; Ordoñez, L.; Ariztegui, D.; Heuer, V.B.; Vuillemin, A.; Henny, C.; Nomosatryo, S.; Simister, R.; Wagner, D.; Bijaksana, S.; Vogel, H.; Melles, M.; Russell, J.M.; Crowe, S.A.; Kallmeyer, J., (2021). Organic matter mineralization in modern and ancient ferruginous sediments. Nat. Commun., 12(1): 1–9 **(9 pages).**
Gnanamoorthy, P.; Selvam, V.; Ramasubramanian, R.; Chakraborty, S.; Pramit, D.; Karipot, A., (2019). Soil organic carbon stock in natural and restored mangrove forests in pichavaram south-east coast of india. Indian J. Geo. Mar. Sci., 48(5): 801–808 **(8 pages).**
Gudasz, C.; Ruppenthal, M.; Kalbitz, K.; Cerli, C.; Fiedler, S.; Oelmann, Y.; Andersson, A.; Karlsson, J., (2017). Contributions of terrestrial organic carbon to northern lake sediments. Limnol. Oceanogr. Lett., 2(6): 218–227 **(10 pages).**
Heiri, O.; Lotter, A.F.; Lemcke, G., (2001). Loss on ignition as a method for estimating organic and carbonate content in sediments: reproducibility and comparability of results. J. Paleolimnol., 25: 101–110 **(10 pages)**.
Hoogsteen, M.J.J.; Lantinga, E.A.; Bakker, E.J.; Groot, J.C.J.; Tittonell, P.A., (2015). Estimating soil organic carbon through loss on ignition: Effects of ignition conditions and structural water loss. Eur. J. Soil Sci., 66(2): 320–328 **(9 pages)**.
Howard, J.; Hoyt, S.; Isensee, K.; Telszewski, M.; Pidgeon, E., (2014). Coastal blue Carbon: Methods for assessing carbon stocks and emissions factors in mangroves, tidal salt marshes, and seagrasses. Conservation International, Intergovernmental Oceanographic Commission of UNESCO, International Union for Conservation of Nature: Arlington, Virginia, USA. **(163 pages)**.
IPCC, (2021). Summary for Policymakers. In: Climate Change 2021: The Physical Science Basis. Contribution of Working Group I to

the Sixth Assessment Report of the Intergovernmental Panel on Climate Change. [Masson-Delmotte, V.; Zhai, P.; Pirani, A.; Connors, C.; Pean, S.; Berger, N.; Caud, Y.; Chen, L.; Goldfarb, M.I.; Gomis, M.; Huang, K.; Leitzell, K.; Leitzell, E.; Lonnoy, J.B.R.; Matthews, T.K.; Maycock, T.; Waterfield, O.; Yelekci, R.; Yu; Zhou, B (eds)]. In Press, 1–40 **(40 pages).**

Ji, H.; Han, J.; Xue, J.; Hatten, J.A.; Wang, M.; Guo, Y.; Li, P., (2020). Soil organic carbon pool and chemical composition under different types of land use in a wetland: Implication for carbon sequestration in wetlands. Sci. Total Environ., 716: 136996: 1–9 **(9 pages)**.

Jiang, C.; Zhang, H.; Wang, X.; Feng, Y.; Labzovskii, L., (2019). Challenging the land degradation in China's Loess Plateau: Benefits, limitations, sustainability, and adaptive strategies of soil and water conservation. Ecol. Eng., 127: 135–150 **(16 pages)**.

Junaidi; Syandri, H.; Azrita, (2014). Loading and Distribution of Organic Materials in Maninjau Lake West Sumatra Province-Indonesia. J. Aquac. Res. Dev., 5(7): 1–4 **(4 pages)**.

Kai, T.; Mukai, M.; Araki, K.S.; Adhikari, D.; Kubo, M., (2016). Analysis of Chemical and Biological Soil Properties in Organically and Conventionally Fertilized Apple Orchards. J. Agric. Chem. Environ., 5(2): 92–99 **(8 pages)**.

Kandasamy, S.; Lin, B.; Lou, J-Y.; Kao, S-J.; Chen, C-T.A; Mayer, L.M., (2018). estimation of marine versus terrigenous organic carbon in sediments off Southwestern Taiwan using the bromine to total organic carbon ratio as a proxy. J. Geophys. Res.: Biogeosciences, 123: 3387–3402 **(16 pages)**.

Kamyab, H.; Goh, R.K.Y.; Wong, J.H.; Lim, J.S.; Khademi, T.; Ho, W.S.; Ahmad, R.B.; Hashim, H.; Ho, C.S.; Lee, C.T., (2015). Cost-Benefit and Greenhouse-Gases Mitigation of Food Waste Composting: A Case Study in Malaysia. Chem. Eng. Trans., 45: 577–582 **(6 pages)**.

Kamyab, H.; Chelliapan, S.; Tavakkoli, O.; Mesbah, M.; Bhutto, J.K.; Khademi, T.; Kirpichnikova, I.; Ahmad, A.; Aljohani, A.A., (2022). A review on carbon-based molecularly-imprinted polymers (CBMIP) for detection of hazardous pollutants in aqueous solutions. Chemosphere, 308: 1–11 **(11 pages)**.

Kauffman, J.B.; Donato, D.C., (2012). Protocols for the measurement, monitoring and reporting of structure, biomass, and carbon stocks in mangrove forests. Working Paper 86, CIFOR, Bogor, Indonesia, 1–37 **(37 pages)**.

Kusumaningtyas, M.A.; Hutahaean, A.A.; Fischer, H.W.; Perez-Mayo, M.; Ransby, D.; Jennerjahn, T.C., (2019). Variability in the organic carbon stocks, sources, and accumulation rates of Indonesian mangrove ecosystems. Estuarine Coastal Shelf Sci., 218: 310–323 **(13 pages).**

Lal, R., (2004). Soil carbon sequestration to mitigate climate change. Geoderma, 123: 1–22 **(22 pages).**

Lei, D.; Jiang, L.; Wu, X.; Liu, W.; Huang, R., (2022). Soil organic carbon and its controlling factors in the lakeside of West Mauri Lake along the wetland vegetation types. Processes, 10(4): 1–10 **(10 pages)**.

Li, N.; Shao, T.; Zhu, T.; Long, X.; Gao, X.; Liu, Z.; Shao, H.; Rengel, Z., (2018). Vegetation succession infuences soil carbon sequestration in coastal alkali-saline soils in southeast China. Sci. Rep., 8: 1-13 **(13 pages)**.

Lin, Q.; Liu, E.; Zhang, E.; Bindler, R.; Nath, B.; Zhang, K.; Shen, J., (2022). Spatial variation of organic carbon sequestration in large lakes and implications for carbon stock quantification. Catena, 208: 105768 **(11 pages)**.

Liu, W.; Ma, L.; Abuduwaili, J.; Issanova, G.; Saparov, G., (2021). Sediment organic carbon sequestration of Balkhash Lake in central Asia. Sustainability. 13(17): 1–12 **(12 pages)**.

Mahapatra, D.M.; Chanakya, H.N.; Ramachandra, T.V., (2012). Role of macrophytes in a sewage fed urban lake. IIOAB J., 2(8): 1–9 **(9 pages)**.

Margono, B.A.; Bwangoy, J.R.B.; Potapov, P.V.; Hansen, M.C., (2014). Mapping wetlands in Indonesia using Landsat and PALSAR data-sets and derived topographical indices. Geo-spatial Inf. Sci., 17(1): 60–71 **(12 pages).**

May, L.; Aura, C.M.; Becker, V.; Briddon, C.L.; Carvalho, L.R.; Dobel, A.J.; Jamwal, P.; Kamphuis, B.; Marinho, M.M.; McGowan, S.; Nandini, S.; Nyamweya, C.; Ongore, C.; Sarma, S.S.S.; Wishart, M.J., (2021). Getting into hot water: Water quality in tropical lakes in relation to their utilization. IOP Conference Series: Earth and Environmental Science, 789 (1): 1–22 **(22 pages)**.

Mayer, L.M., (1994). Relationships between mineral surfaces and organic carbon concentrations in soils and sediments. Chem. Geol., 114(3–4): 347–363 **(17 pages)**.

Meyers, P.A., (1997). Organic geochemical proxies of paleoceanographic. Org. Geochem., 27(5): 213–250 **(38 pages).**

Meyers, P.A., (2003). Application of organic geochemistry to paleolimnological reconstruction: a summary of examples from the Laurentian Great Lakes. Org. Geochem., 34(2): 261–289 **(29 pages)**.

Minick, K.J.; Mitra, B.; Li, X.; Fischer, M.; Aguilos, M.; Prajapati, P.; Noormets, A.; King, J.S., (2021). Wetland microtopography alters response of potential net CO_2 and CH_4 production to temperature and moisture: Evidence from a laboratory experiment. Geoderma, 402: 1–13 **(13 pages)**.

MERI, (2011). Profile of 15 national priority lakes. Kementerian Lingkungan Hidup Republik Indonesia. Ministry of Environmental, Republic Indonesia. Jakarta **(154 pages).** (In Bahasa).

MERI, (2015). Movement for save Lake Maninjau (Gerakan Penyelamatan Danau Maninjau), Ministry of Environment Republic of Indonesia, Jakarta. 1–63 **(63 pages)**. (In Bahasa).

Mitra, S.; Wassmann, R.; Vlek, P.L.G.V., (2005). An appraisal of global wetland area and its organic carbon stock Sudip. Curr. Sci., 88(1): 25–35 **(11 pages).**

Murdiyarso, D.; Purbopuspito, J.; Kauffman, J.B.; Warren, M.W.; Sasmito, S.D.; Donato, D.C.; Manuri, S.; Krisnawati, H.; Taberima, S.; Kurnianto, S., (2015). The potential of Indonesian mangrove forests for global climate change mitigation. Nat. Clim. Change, 5: 1089–1092 **(4 pages).**

Musale, A.S.; Desai, D.V.; Sawant, S.S.; Venkat, K.; Anil, A.C., (2015). Distribution and abundance of benthic macroorganisms in and around Visakhapatnam Harbour on the east coast of India. J. Mar. Biol. Assoc., 95(2): 215–231 **(17 pages)**.

Nelson, D.W.; Sommers, L.E., (1996). Total carbon, organic carbon, and organic matter. Methods of Soil Analysis, Part 3: Chem. Methods, 5: 961–1010 **(50 pages)**.

Nomosatryo, S.; Tjallingii, R.; Schleicher, A.M.; Boli, P.; Henny, C.; Wagner, D.; Kallmeyer, J., (2021). Geochemical characteristics of sediment in tropical Lake Sentani, Indonesia, are influenced by spatial differences in catchment geology and water column stratification. Earth Sci., 9: 1–16 **(16 pages)**.

Novita, N.; Kauffman, J.B.; Hergoualc'h, K.; Murdiyarso, D.; Tryanto, D.H.; Jupesta, J., (2021). Carbon Stocks from Peat Swamp Forest

and Oil Palm Plantation in Central Kalimantan, Indonesia. In Djalante, R.; Jupesta, J.; Aldrian, E. (eds) Climate Change Research, Policy and Actions in Indonesia. Springer Clim., 203–227 **(24 pages).**

Page, S.E.; Baird, A.J., (2016). Peatlands and global change: response and resilience. Annu. Rev. Environ. Resour., 41: 35–57 **(23 pages)**.

Presidential Regulation of the Republic of Indonesia No. 60 of 2021 concerning Saving National Priority Lakes (Peraturan Presiden Republik Indonesia No. 60 Tahun 2021 Tentang Penyelamatan Danau Prioritas Nasional). In Bahasa **(243 pages)**. (In Bahasa).

Priyadi, A.; Sutomo; Darma, I.D.P.; Arisana, I.B.K., (2014). Selecting Tree Species with High Carbon Stock Potency from Tropical Upland Forest of Bedugul-Bali, Indonesia. J. Trop. Life Sci., 4(3): 201–205 **(5 pages)**.

Purwanto E.; Wibisono, I.T.C.; Dipa, S.R.; Kurniasari, T.; Wijaya, K.; Jelsma, I., (2020). Assessing potential of - and challenges in - developing a REDD+ Result Based Payment scheme: Insights from the Pematang Gadung Peat Swamp Forest in West Kalimantan. Info. Brief., 1-6 **(6 pages).**

Qing, B.; Liu, Z.; Havens, K., (2007). Environmental issues of Lake Taihu, China. Hydrobiologia, 581: 3–14 **(12 pages).**

Quijano, J.C.; Kumar, P.; Drewry, D.T., (2013). Passive regulation of soil biogeochemical cycling by root water transport. Water Resour. Res., 49(6): 3729–2746 **(17 pages)**.

Ramanda, R.A.; Noor, D.; Ridwansyah, I., (2019). The potential of landslide in Lake Maninjau Catchment Area, West Sumatra. IOP Conference Series: Earth and Environmental Science, 311: 1–6 **(6 pages)**.

Ridwansyah, I.; Rustini, H.A.; Yulianti, M.; Apip; Harsono, E., (2019). Water balance of Maninjau watershed with SWAT hydrological model. IOP Conference Series: Earth and Environmental Science, 535: 1–11 **(11 pages).**

Sakin, E.; Sakin, E.D., (2011). Soil organic carbon stocks of East Anatolia Region in Turkey. American-Eurasian J. Agric. Environ. Sci., 10(5): 776–780 **(5 pages)**.

Santoni, S.; Bonifacio, E.; Zanini, E., (2001). Indophenol blue colorimetric method for measuring cation exchange capacity in sandy soils. Commun. Soil Sci. Plant Anal., 32 (15): 2519–2530 **(12 pages)**.

Sasmito, S.D.; Kuzyakov, Y.; Lubis, A.A.; Murdiyarso, D.; Hutley, L.B.; Bachri, S.; Friess, D.A.; Martius, C.; Borchard, N., (2020). Organic carbon burial and sources in soils of coastal mudflat and mangrove ecosystems. Catena. 187: 1–11 **(11 pages)**.

Shiels, A.B.; Walker, L.R., (2013). Landslides cause spatial and temporal gradients at multiple scales in the Luquillo Mountains of Puerto Rico. Ecol. Bull., 54: 211–221 **(11 pages).**

Silviana, S.H.; Saharjo, B.H.; Sutikno, S., (2021). Distribution of carbon stocks in drainage areas on peatlands of Sungai Tohor Village, Meranti Islands District, Indonesia. Biodiversitas, 22(11): 5106–5114 **(8 pages).**

Siregar, C.A.; Narendra, B.H., (2021). Assessment of soil carbon stocks in several peatland covers in Central Kalimantan, Indonesia. IOP Conference Series: Earth and Environmental Science, 914: 1–8 **(8 pages).**

Sufrayogi, D.; Mardiatmoko, G., (2022). Carbon Storage Expectations on Swamp Jelutung (Dyera polyphylla Miq. Steenis.) on Peatland for Tackling Climate Change. Forest, 13: 1–15 **(15 pages).**

Sujarwo, W.; Darma, I.D.P., (2011). Analisis Vegetasi Dan Pendugaan Karbon Tersimpan Pada Pohon Di Kawasan Sekitar Gunung Dan Danau Batur Kintamani Bali. J. Bumi Lestari, 11(1): 85–92 **(8 pages).** (In bahasa).

Soejarwo, P.A.; Koeshendrajana, S.; Apriliani, T.; Yuliaty, C.; Deswati, R.H.; Sari, Y.D.; Sunoko, R.; Sirait, J., (2022). Management of floating net cages (KJA) aquaculture in an effort to save Maninjau Lake. J. Kebijakan Sosek KP., 12 (1): 79–87 **(9 pages)**. (In Bahasa).

Stallard, R.F., (2012). Weathering, landscape equilibrium, and carbon in four watersheds in Eastern Puerto Rico, in Water Quality and Landscape Processes of Four Watersheds in Eastern Puerto Rico, edited by S. F. Murphy and R. F. Stallard. U.S. Geological Survy Professional paper. 1789: 199-247 **(48 pages)**.

Sulastri; Henny, C.; Santoso, A.B., (2019). Phytoplankton composition and the occurrence of cyanobacterial bloom in Lake Maninjau, Indonesia. IOP Conference Series: Earth and Environmental Science, 380(1): 1–13 **(13 pages)**.

Syakti, A.D.; Idris, F.; Koenawan, C.J.; Asyhar, R.; Apriadi, T., (2019). Biological pollution potential in the water of Bintan-Riau Islands Province, Indonesia: first appearance of harmful algal bloom species. Egypt. J. Aquat. Res., 45(2): 117–122 **(6 pages)**.

Syandri, H.; Junaidi; Azrita; Yunus,T., (2014). State of aquatic resources Maninjau Lake West Sumatra Province, Indonesia. Int. J. Ecol. Environ. Sci., 5(1): 109–113 **(5 pages).**

Tasri, E.S.; Karimi, K.; Muslim, I., (2021). The study of the impact of Maninjau lake pollution on economic and public health. IOP Conference Series: Earth and Environmental Science, 747(1): 1–7 **(7 pages)**.

Twum, E.K.A.; Nii-Annang, S., (2015). Impact of soil compaction on bulk density and root biomass of quercus petraea l. at reclaimed post-lignite mining site in Lusatia, Germany. Appl. Environ. Soil Sci., 2015: 1–5 **(5 pages)**.

Tyson, R.V., (1995). Sedimentary organic matter (First). Springer Netherlands **(633 pages)**.

Uhran, B.; Windham-Myers, L.; Bliss, N.; Nahlik, A.M.; Sundquist, E.T.; Stagg, C.L., (2021). Improved wetland soil organic carbon stocks of the Conterminous U.S. through data harmonization. Frontiers in Soil Sci., 1: 1–16 **(16 pages**).

UNFCCC., (2008). Kyoto protocol reference manual on accounting of emissions and assigned amount **(122 pages)**.

Virni, B.A.; Kauffman, J.B.; Hadriyanto, D.; Murdiyarso, D.; Diana, R., (2019). Carbon dynamics and land use carbon footprints in mangrove-converted aquaculture: The case of the Mahakam Delta, Indonesia. For. Ecol. Manage., 432: 17–29 **(12 pages).**

Wang, B.; Waters, C.; Orgill, S.; Cowie, A.; Clark, A.; Li Liu, D.; Simpson, M.; McGowen, I.; Sides, T., (2018). Estimating soil organic carbon stocks using different modeling techniques in the semi-arid rangelands of eastern Australia. Ecol. Indic., 88: 425–438 **(14 pages)**.

Wang, M.; Houlton, B.Z.; Wang, S.; Ren, C.; van Grinsven, H.J.M.; Chen, D.; Xu, J.; Gu, B., (2021). Human-caused increases in reactive nitrogen burial in sediment of global lakes. Innovation. 2(4): 1–7 **(7 pages)**.

Wei, Z.; Du, Z.; Wang, L.; Zhong, W.; Lin, J.; Xu, Q.; Xiao, C., (2022). Sedimentary organic carbon storage of thermokarst lakes and ponds across Tibetan permafrost region. Sci. Total Environ, 831: 1–13 **(13 pages)**.

Xu, L.; Li, Y.; Ye, W.; Zhang, X., (2019). Terrestrial organic carbon storage modes based on relationship between soil and lake carbon, China. J. Environ. Manage., 250: 1–9 **(9 pages)**.

Yu, C.; Li, Z.; Xu, Z.; Yang, Z., (2020). Lake recovery from eutrophication: Quantitative response of trophic states to anthropogenic influences. Ecol. Eng., 143: 1–10 (**10 pages**).

Yu, Q.; Wang, F.; Yan, W.; Zhang, F.; Lv, S.; Li, Y., (2018). Carbon and nitrogen burial and response to climate change and anthropogenic disturbance in Chaohu Lake, China. Int. J. Environ. Res. Public Health. 15(12): 1–18 (**18 pages**).

Yustiawati; Syawal, M.S.; Rosidah., (2021). Carbon, Nitrogen and C/N ratio of sediment in a floodplain lake: Lake Tempe, South Sulawesi. IOP Conference Series: Earth and Environmental Science, 1062: 1–7 (**7 pages**).

Zhao, L.; Wu, X.; Wang, Z.; Sheng, Y.; Fang, H.; Zhao, Y.; Hu, G.; Li, W.; Pang, Q.; Shi, J.; Mo, B.; Wang, Q.; Ruan, X.; Li, X.; Ding, Y., (2018). Soil organic carbon and total nitrogen pools in permafrost zones of the Qinghai-Tibetan Plateau. Sci., 8(1): 1–9 (**9 pages**).

AUTHOR (S) BIOSKETCHES

Soeprobowati, T.R., Ph.D., Professor, Center for Paleolimnology (CPalim), Universitas Diponegoro, Semarang, Indonesia.
- Email: *trsoeprobowati@live.undip.ac.id*
- ORCID: 0000-0001-7525-7028
- Web of Science ResearcherID: AAU-1719-2020
- Scopus Author ID: 55339731500
- Homepage: https://pasca.undip.ac.id/struktur/#pasca

Takarina, N.D., Ph.D., Associate Professor, Department Biology, Faculty Mathematics and Natural Sciences, Universitas Indonesia, Depok, Indonesia.
- Email: *noverita.dian@sci.ui.ac.id*
- ORCID: 0000-0003-1766-7445
- Web of Science ResearcherID: ABD-9794-2021
- Scopus Author ID: 6505460222
- Homepage: https://www.sci.ui.ac.id/staff-members/noverita-dian-t-msc/

Komala, P.S., Ph.D., Associate Professor, Department of Environmental Engineering, Faculty of Engineering,Universitas Andalas, Padang, Indonesia
- Email: *putisrikomala@eng.unand.ac.id*
- ORCID: 0000-0002-5048-6518
- Web of Science ResearcherID: GLQ-7067-2022
- Scopus Author ID: 55836021500
- Homepage: http://lingkungan.ft.unand.ac.id/id/component/k2/item/330-puti-sri-komala

Subehi, L., Ph.D. Assistant Professor, Research Center for Limnology and Water Resources – National Research and Innovation Agency, Cibinong, Indonesia.
- Email: *luki001@brin.go.id*
- ORCID: 0000-0001-9741-0249
- Web of Science ResearcherID: W-4045-2019
- Scopus Author ID: 25958454100
- Homepage: https://lukisubehi.wordpress.com

Wojewódka-Przybył, M., Ph.D., Institute of Geological Sciences, Polish Academy of Sciences, Warsaw, Poland.
- Email: *m.wojed@twarda.pan.pl*
- ORCID: 0000-0002-2880-3185
- Web of Science ResearcherID: EDZ-9622-2022
- Scopus Author ID: 57004761400
- Homepage: https://www.researchgate.net/profile/Marta-Wojewodka-Przybyl

Jumari, J., Ph.D., Assistant Professor, Department Biology, Faculty Science and Mathematics, Universitas Diponegoro, Sematang, Indonesia.
- Email: *jumari@live.undip.ac.id*
- ORCID: 0000-0002-3150-5293
- Web of Science ResearcherID: GWC-4962-2022
- Scopus Author ID: 57204068212
- Homepage: https://bio.fsm.undip.ac.id/v1/staf-dosen/

Nastuti, R., Ph.D. Candidate, School of Postgraduate Studies, Universitas Diponegoro, Semarang, Indonesia.
- Email: *reni.nastuti@gmail.com*
- ORCID: 0000-0001-8564-9615
- Web of Science ResearcherID: GWC-5075-2022
- Scopus Author ID: 55339731500
- Homepage: https://stkipydb.ac.id/hal-dosen1.html

HOW TO CITE THIS ARTICLE

Soeprobowati, T.R.; Takarina, N.D.; Komala, P.S.; Subehi, L.; Wojewódka-Przybył, M.; Jumari, J.; Nastuti, R., (2023). Sediment organic carbon stocks in tropical lakes and its implication for sustainable lake management. Global J. Environ. Sci Manage., 9(2): 173-192.

DOI: 10.22034/gjesm.2023.02.01

url: https://www.gjesm.net/article_696620.html

Global J. Environ. Sci. Manage. 9(2): 193-210, Spring 2023, Serial #34

Global Journal of Environmental Science and Management
(GJESM)

Homepage: https://www.gjesm.net/

ORIGINAL RESEARCH ARTICLE

Application of microbially induced calcite precipitation to mitigate soil frost heave

M.F. Nikshoar[1], M.A. Rowshanzamir[1], S.M. Abtahi[1,*], S. Soleimanian-Zad[2]

[1]*Department of Civil Engineering, Isfahan University of Technology, Isfahan, Iran*

[2]*Department of Food Science and Technology, College of Agriculture, Isfahan University of Technology, Isfahan, Iran*

ARTICLE INFO

Article History:
Received 21 May 2022
Revised 29 July 2022
Accepted 22 August 2022

Keywords:
Microbially induced calcite precipitation (MICP)
Soil frost heave
Soil improvement
Sporosarcina pasteurii

DOI: 10.22034/gjesm.2023.02.02

ABSTRACT

BACKGROUND AND OBJECTIVES: Soil frost heaving causes significant destruction to road pavements, railways, pipelines, and other lifeline infrastructures. The conventional methods for dealing with the soil frost heave are primarily based on using the materials whose production and use are harmful to the environment. Due to the recent ecological concerns, developing novel alternative methods has received much attention. This study aims to investigate the possibility of using the microbially induced calcite precipitation method to control soil frost heave for less pollution introduction to the soil.

METHODS: In this study, the *Sporosarcina Pasteurii* bacterium was used for calcite precipitation. The influence of three factors in four levels, including bacteria concentration, cementing solution concentration, and curing time, was investigated based on a plan set by Taguchi design of experiment method. The results were obtained by analysis of means and analysis of variance statistical methods and compared with the conventional frost heave reduction methods.

FINDINGS: The results were presented in terms of heave ratio. Based on the testing results, the heave ratios (frost heave ratios of the treated to untreated samples) were obtained to be in the range of 0.21 to 0.42. The results showed that bacteria concentration was the most influential factor in the total frost heave of the treated soil. The influence of curing time was in second place, and the effect of cementing solution concentration was relatively less. The minimum frost heave was achieved in 10^8 colony-forming units per milliliter bacteria concentration, 0.6 mole per litre cementing solution concentration, and 21 days of curing.

CONCLUSION: The findings indicated that the used method could be efficiently used to reach the desired objective. The heave ratios obtained by this method were promising to a great extent compared to the conventional methods. The reduction of frost heave due to the application of this method was attributed to the precipitated calcite within the soil voids and was justified by the scanning electron microscopy images of the treated soil samples. This study proved that the proposed method might be utilized as a potential ecological-friendly approach in the future researches.

NUMBER OF REFERENCES	NUMBER OF FIGURES	NUMBER OF TABLES
50	9	6

*Corresponding Author:
Email: *mabtahi@iut.ac.ir*
Phone: +98311 3913813
ORCID: 0000-0001-8118-2456

Note: Discussion period for this manuscript open until July 1, 2023 on GJESM website at the "Show Article".

INTRODUCTION

Soil frost heaving occurs when several factors, including water and frigid weather, are simultaneously available in the presence of susceptible soils in civil engineering projects. The most influential factors in frost heave are soil particle size distribution (Qi *et al.,* 2022), dry density (Zhao et al., 2019), plasticity index (Isik *et al.,* 2013), fines percent (Wu *et al.,* 2018), groundwater level (Lin et al., 2018), moisture content (Mao and Zhang, 2018), and water solutes (Shah and Mir, 2022). When the water is under significant forces from soil particles, it will freeze at lower temperatures than normal freezing water temperatures. The excess water would be absorbed from other zones due to the capillary effect and via heat flow simultaneously, and the ice lens grows, leading to soil swelling (Bai *et al.,* 2020). In this condition, the soil frost heave happens and develops with the connection of the freezing zone to the external water sources (Fig. 7a). This detrimental phenomenon causes a significant damage occurring seasonally and periodically to roads, pavements, railways, buildings, and other lifeline infrastructures such as pipelines. Dealing with this phenomenon in susceptible areas is vital, and the solution must be both economically justifiable and eco-friendly. Thus, using novel methods to deal with this problem can be important for geotechnical engineers. Some studies and many real-life projects have been done to control and mitigate the soil frost heave and its effects. Frost heave mitigation can be met through bounding soil particles, filling the voids among particles, disbanding soil particles, and changing the fluid characteristics among particles (Lambe, 1956) (Fig. 7b). In one of the most comprehensive and early studies, Lambe, (1956) introduced 40 different additives to the sample soils and presented the treatment effect in terms of heave ratio. He also evaluated resin-type additives, portland cement, cations, dispersants, and water proofers on the frost heave of three soil samples. Kettle and McCabe, (1985) investigated the effect of mechanical stabilization using slag, basalt, and limestone as stabilizing agents, which were divided into two particle groups for their gradation to control frost heave. They reported that the slag aggregate led to the highest heave reduction and the increased coarse-aggregate content was directly related to the performance of the used method. Zieba *et al.* (2019) applied micro-silica and nano-silica to sandy clayey silt (saclSi) which is frost-susceptible soil. They showed that adding 5% nano-silica could lead to an almost complete reduction in frost heave. They also reported that mixing the same amount of micro-silica reduced the frost heave by 21%. Liu *et al.* (2022) indicated that the frost heave amount can be mitigated by electro-osmosis dewatering. A growing trend is forming to limit the application of conventional additives, such as chemical grouts, lime, and cement, for ground improvement purposes, including frost heaving control. This limitation stems from the fact that materials production and use have been proven to be harmful to the environment. According to Karol, (2003), almost all chemical grouts are toxic and hazardous to nature. Thus, many researchers have pursued the growing prospect of developing new safe ground improvement methods. Among the new ground improvement techniques in some fields of civil engineering, such as self-healing concretes (Muhammad *et al.,* 2016) in structural engineering and soil improvement in geotechnical engineering (Shahrokhi-Shahraki *et al.,* 2015), microbially induced calcite precipitation (MICP) seems to be a promising method, particularly from an environmental point of view. This method, however, faces some challenges including ammonia by product (Lee *et al.,* 2019). In this context, some soil native microbes are triggered to procure rapidly and create calcite cement within the soil matrix, which enhances the soil's hydro-mechanical properties. Several bacteria, such as *Proteus mirabilis* and *Proteus vulgaris mixture* (Talaiekhozani *et al.,* 2014), *Bacillus sphaericus* (Hataf and Baharifard, 2020), *Sporosarcina pasteurii* (Han *et al.,* 2016), and *Bacillus subtilis* (Wath and Pusadkar, 2021) have been used in the MICP procedures. Among these bacteria, *Sporosarcina pasteurii* has been suggested as the most efficient bacteria for the MICP process in soil (Rahman *et al.,* 2020). *Sporosarcina pasteurii* is a non-pathogenic bacterium capable of producing high amounts of enzyme urease (Henze and Randall, 2018). These rod-shaped, gram-positive bacteria precipitate calcite if suitable conditions are provided. In the most common procedure, calcite needs to precipitate within soil pores, cementite the soil, and bound its particles together. This calcite is produced by hydrolysis of urea via urease enzyme, which occurs in a calcium-rich environment (Castanier *et al.,* 1999). The reactions in which this process occurs using Eqs.

1, 2, 3 and 4 (Deng *et al.*, 2021).

$$(NH_2)_2CO + H_2O \rightarrow 2NH_3 + CO_2 \quad (1)$$

$$2NH_3 + 2H_2O \rightarrow 2NH_4^+ + 2OH^- \quad (2)$$

$$CO_2 + OH^- \rightarrow HCO_3^- \quad (3)$$

$$Ca^{2+} + HCO_3^- + OH^- \rightarrow H_2O + CaCO_3 \quad (4)$$

Many studies have been performed on improving soil properties using the MICP approach. Modification of soil compressive strength (Xiao *et al.*, 2021), increasing the soil shear strength (Zamani and Montoya, 2017), reducing soil permeability (Roth and Caslake, 2019), creating waste containment barriers (Etim *et al.*, 2022), mitigating liquefaction (Zamani *et al.*, 2021), and increasing the shear capacity of the soil-steel interface (Bak *et al.*, 2021) are among these studies. In general, application of the biological soil improvement technique is a very promising method. It can also be considered as a suitable alternative to conventional methods and reduce the harmful environmental effects. Some studies have shown the significant ability of calcite precipitation in various aspects of soil improvement as it increases the bounding of soil particles and reduces the voids among them. Various applications of the MICP method have attracted the attention of many researchers till now, and different aspects of this approach are becoming more apparent. The aim of this study was to evaluate the possibility of using this approach to improve, control, and mitigate the soil frost heave for the first time. It was also attempted to assess the Influence of three essential factors, including bacteria concentration, cementing solution concentration (CSC), and curing time, which could affect this phenomenon. For this purpose, a research testing program was developed by Taguchi design of experiment method. A frost heave testing apparatus was designed and built to assess the frost heave in the soil samples. The *Sporosarcina pasteurii* bacterium was selected to proceed with the MICP procedure as approved in the previous studies. The results were analyzed for the influence of each factor and their optimum level tested by ANOVA and ANOM statistical methods. The findings approved the efficiency of the adopted method as the frost heave in the soil treated with optimal bacterial culture was reduced to nearly one-fifth of the untreated soil. The novelty of this study lies behind successful application of the MICP approach to control soil frost heave for the first time. This revealed the MICP's capacity for development and industrialization in the future. This study was performed in Isfahan, Iran, during 2020-2022.

MATERIALS AND METHODS

Microorganism and cultivation

Sporosarcina pasteurii American Type Culture Collection (ATCC) 6453 was used to accomplish the MICP procedures on a silty soil identified as soil with frost heave potential. All the culture mediums used for bacterial cultivation were the same. To prepare the culture medium for bacteria cultivation, 13 g of nutrient broth powder was mixed in 1 L distilled water and autoclaved for 20 minutes (min) at 121 °C. After cooling the medium, 20 g/L urea sterilized by a Polytetrafluoroethylene (PTFE) filter was added to it. The bacteria strains were provided in a lyophilized form. The lyophilized powder was solved in 40 milliliter (mL) of the above medium, cultivated overnight in a shaking incubator at 30 °C, and centrifuged at 120 rpm to activate the bacteria. Then the solution was subcultured two more times with the same culture medium. To safely store the bacteria, 900 mL of cultivated bacteria and 600 mL of glycerol solution were mixed in some vials, and the obtained bacterial stocks were kept in a -80 °C freezer.

Bacterial transfer solution

As suggested by Stocks-Fischer *et al.*, (1999), a solution was made containing 3 g/L nutrient broth, 10 g/L of ammonium chloride (NH_4Cl), and 2.12 g/L sodium bicarbonate ($NaHCO_3$) autoclaved for 20 min in 121 °C. Using syringe PTFE filters, 20 g/L sterilized urea was added to the solution while its pH was adjusted at 6. The prepared solution was called bacterial transfer solution. For the primary cultivation of bacteria, a sample subcultured three times from the bacterial glycerol stocks was poured into a culture medium comprising sterilized nutrient broth and 20 g/L sterilized urea using syringe PTFE filters and was cultivated overnight. The outcome was fresh bacteria mixed with metabolic supernatants. The obtained solution was centrifuged for 25 min at 4000 rpm to harvest the bacteria. After removing the supernatant, the sedimented bacteria was mixed with sterilized physiological saline made of distilled water and NaCl.

The solution was re-centrifuged with the same profile to remove all impurities. This step was repeated two times, and the pure bacteria was then mixed with an appropriate amount of the injection solution to reach the desired bacteria concentration. The bacteria concentration was adjusted by a spectrophotometer, which measured the absorbed light of solution in a specific wavelength, in order to calculate the concentration of the bacteria. For the wavelength of 600 nm, the bacteria concentration was calculated using Eq. 5 (Okwadha and Li, 2010).

$$\mathrm{CFU/mL} = 8.59 \times 10^{7} \times \mathrm{OD}_{600}^{1.3627} \quad (5)$$

To determine the viable bacteria count and verify the spectrophotometer data, some samples were taken from the final solutions and cultivated on a petri dish filled with a culture medium consisting of sterilized nutrient agar and 20 g/L sterilized urea using syringe PTFE filters. The bacteria concentration was later estimated using the Miles method (Miles *et al.*, 1938).

Cementing solution

To trigger and maintain the MICP process at an adequate rate, a calcium-rich environment and a sufficient amount of urea are necessary for continuous urea hydrolysis. These substances are usually provided continuously to prohibit the termination of the MICP processes and end their reactions. The referred substances are provided in different forms and concentrations. In this study, the cementing solution consisted of anhydrous calcium chloride (110.98 g/M) sterilized by 20 min autoclaving at 121 °C and urea (60.06 g/M) sterilized by PTFE filters. According to previous studies (Whiffin *et al.*, 2007), the calcium chloride and urea concentrations were considered equimolar for all the cementing solutions.

Table 1: Specifications of the testing soil

Composition	Amount
G_S	2.69
D_{50}	0.1 (mm)
$\gamma_{d\,max}$	17.4 (kN/m^3)*
$\gamma_{d\,min}$	14.9 (kN/m^3)
C_u	2.2
C_c	1.16

*Kilonewton per cubic meter

Testing soil

Frost heave susceptible soils contain fine particles, especially silt, and the probability of frost heave occurrence increases with the increase of silt percentage. The soil particle size analysis was performed according to the ASTM D2487-17 standard and categorized using the Unified Soil Classification System. The sieve analysis testing results related to the selected soil are presented as a grading curve in Fig. 1. The soil sample was classified as SM in the unified soil classification system. The sample soil contained 24% cohesionless fines. Such soil was prone to frost heave occurrence. Some of the soil specifications are summarized in Table 1.

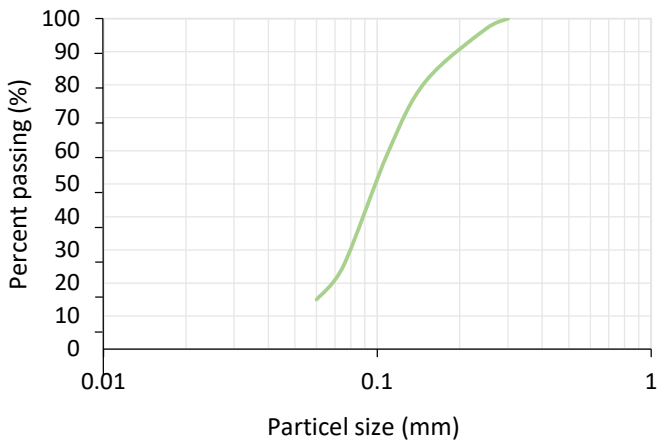

Fig. 1: Particle size distribution of the testing soil

Frost heave testing apparatus

A set-up of frost heave testing apparatus was designed and built considering the characteristics required to measure the amount of soil frost heave and also the data needed to proceed. The apparatus consisted of some main parts, including a specimen cylinder, top and bottom caps, top cap cooling and bottom cap heating parts, a saturation tank, and a processor that controlled the specimen cylinder's temperature gradient and recorded the data from sensors. The sections of the testing apparatus are shown in Fig. 2. The specimens were prepared in an acrylic cylinder with 120 mm diameter and 350 mm height. The bottom and top caps were made of copper plates for rapid and better heat exchange. Thermoelectric coolers were mounted at the top cap of the apparatus, Thus, controlling the temperature of the top cap could be made more precisely as compared to traditional methods. These thermoelectric coolers could quickly reduce the temperature of the top cap as low as -25 °C. The movement of the upper cap was restricted to move only in the vertical direction by two shafts connected to the main frame using a restricting bearing system. The bottom of the cylinder was closed with the bottom cap, sealed, and fixed in its place. A heating element controlled by an appropriate processor was used for heating the bottom cap in order to achieve the desired temperature. The processor got its data from three sealed digital temperature sensors placed at the specimen's top, middle, and bottom (with 10 cm spacing intervals). These sensors controlled the temperature of the top and bottom caps by two separate control systems to attain the temperature gradient set by the user. The processor recorded the data of the displacement sensor, time, and the step number in each step on a memory card with two-second steps. It also sent this data to the computer through its USB port connector. Strong insulation was employed to cover the acrylic cylinder in order to prevent the heat exchange of the perimeter of the cylinder with open air. The saturation tank was connected to the lower cap, and the water intake of the frost heave was supplied from the water of this tank.

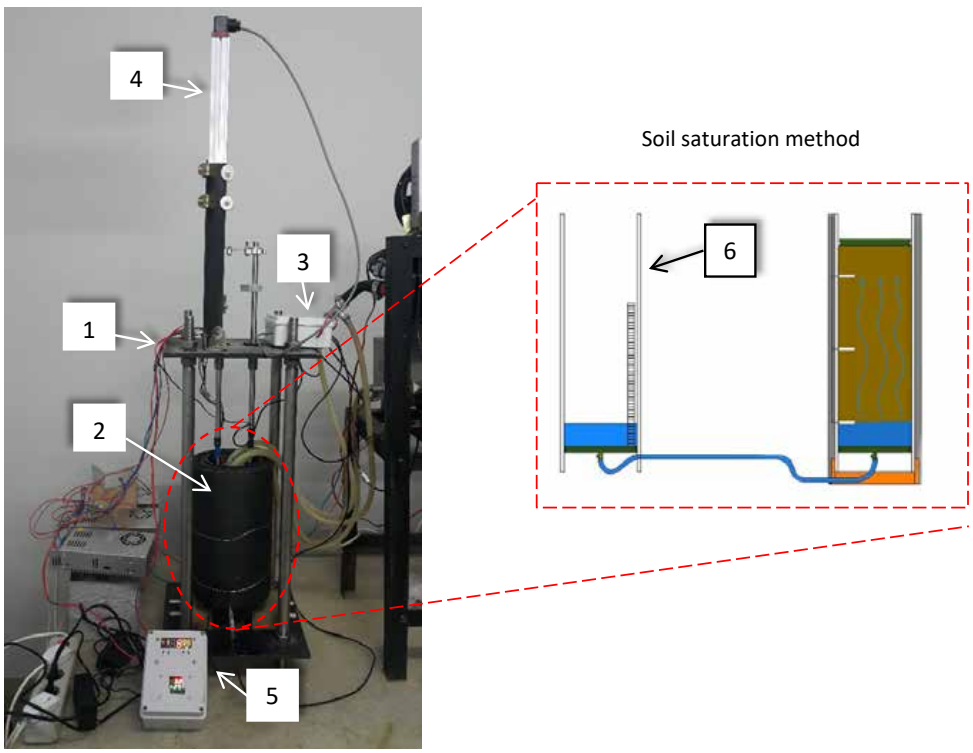

Fig. 2: Frost heave testing apparatus: main frame (1), insulated specimen cylinder (2), data processor and recorder (3), displacement sensor (4), temperature control panel (5), and water tank (6)

Experimental procedure

Specimen preparation

The first step for sample preparation was to clear the soil from any likely available bacteria that could affect the test conditions. For this purpose, the required amount of the testing soil (3000 g) was poured into an appropriate container and put in an oven at 120 °C for 24 hours. After cooling to the laboratory temperature, 600 mL of the transfer solution containing bacteria was mixed well with the soil sample. To prevent fine particles from washing out of the soil sample, a suitable filter was placed on the bottom cap of the cylinder. Moreover, the inner side of the acrylic cylinder was lubricated with silicone grease to prevent the adhesion of ice lenses to the wall and guarantee the free vertical movement of the soil sample. The prepared soil was then poured into the cylinder and compacted into five equal lifts with a thickness of 4 cm for each layer to obtain the same density of 1.63 g/cm^3 for all the specimens. After placing a filter at the top of the sample, the first cycle of injecting cementation solution into the sample was carried out from the top of the cylinder using 600 mL of the solution at a rate of 0.8 mL/min. The second injection cycle was started 12 hours after the end of the first cycle, using another 600 mL of cementation solution at the same rate. Based on previous studies, the specimens were cured under a constant temperature of 28 °C for all considered curing times (Khaleghi and Rowshanzamir, 2019). To explore the effects of the curing time on the performance of treated samples, the specimens were cured for various periods of 0, 7, 14, and 21 days before being subjected to frost heave testing. After curing, the testing specimen was washed with sterilized water injection to stop all the metabolic processes and then dried thoroughly.

Testing method

The prepared specimen was then placed into the frost heave test apparatus, and the saturation tank was connected to the valve of the bottom cap of the testing cylinder. The water level at the lower part of the testing sample played an essential role in the soil frost heaving procedure, as reported in previous studies (Hermansson and Guthrie, 2005). The water level within the testing sample was maintained at a height of 5 cm relative to the bottom cap for all the considered specimens. To simulate ambient natural conditions, no extra saturation was imposed to the specimens. The moisture within the specimen was achieved through capillary water rise from the bottom connection to the water tank with an adjusted stable water level. The hydrostatic water pressure constantly maintained a water level with 5 cm height within the sample through the connected saturation tank until there was no change in the water level in the tank. To conduct the frost heave test, the temperature of the top cap was adjusted to -25 °C, and the bottom cap was kept at 4 °C. This temperature condition provided a 1.05 °C/cm temperature gradient for the testing specimen. The test run for 35 hours to allow the testing specimen to reach a steady state.

Design of experiment

Various factors affect the frost heave phenomenon and the MICP treatment procedure. Nevertheless, some factors have more influence on the final result and must be considered more precisely. Considering the previous studies (Khaleghi and Rowshanzamir, 2019), bacteria concentration, CSC, and curing time were selected as most influential factors to be used in the present study. All the three factors were considered at four different levels in the designed tests (Table 2). However, other factors and parameters of the experiments were kept constant for all tests.

Taguchi's design of experiment (TDOE) (Taguchi *et al.*, 2005) was chosen to be used for planning the tests, due to its efficiency in reducing the number of required tests and its precise and reliable results. Each test ran within the given factor and level until achieving three logical repetitions. If an ambiguous result was obtained, the same experiment would be repeated until reaching a trustworthy outcome. The

Table 2: Different levels of the studied factors

Variable Factor	Level 1	Level 2	Level 3	Level 4
Curing period (day)	0	7	14	21
CSC (M)	0.3	0.6	0.9	1.2
Bacteria concentration (CFU/mL)	10^5	10^6	10^7	10^8

Table 3: MICP treatment test program designed by Taguchi method

Input factors			
Test No	Curing times (day)	CSC (M)	Bacteria concentration (CFU/mL)
T1	0	0.3	10^5
T2	0	0.6	10^6
T3	0	0.9	10^7
T4	0	1.2	10^8
T5	7	0.3	10^6
T6	7	0.6	10^5
T7	7	0.9	10^8
T8	7	1.2	10^7
T9	14	0.3	10^7
T10	14	0.6	10^8
T11	14	0.9	10^5
T12	14	1.2	10^6
T13	21	0.3	10^8
T14	21	0.6	10^7
T15	21	0.9	10^6
T16	21	1.2	10^5

experiment was designed using Minitab statistical software (20.4 version) in Taguchi's L16 orthogonal array framework. The developed testing program is provided in Table 3.

Data analysis

To further analyze the tests results, first the signal-to-noise ratio (SNR) were calculated via the less is better assumption. The SNR equation can be presented as Eq. 6 (Mortazavi Bak *et al.*, 2021).

$$SNR = -10 \times \log\left(\sum_{i=1}^{n}\left(FH_i\right)^2 \Big/ n\right) \quad (6)$$

Where, n is equal to three as each test was repeated for three times. After calculating the SNRs, the obtained data were put under the analysis of means (ANOM) to identify the optimum level of each factor for achieving the minimum frost heave amount. For this purpose, the mean SNR ratio was calculated according to Eq. 7 (Mortazavi Bak *et al.*, 2021).

$$\text{Mean SNR} = \frac{1}{z}\sum_{t=1}^{z}\left(\text{SNR}\right)_t \quad (7)$$

Where, z is the selected to be four earlier. To determine the mean SNR for each factor level, the obtained SNRs for that level were inserted in Eq. 7. The analysis of variance (ANOVA) was also performed to determine contribution percent (CP) of each factor and p-value (Frossard and Renaud, 2021). The CP of each factor is calculated based on Eq. 8-12 (Bak *et al.*, 2021).

$$\text{CP} = \frac{\text{SS} - \left(\text{DOF} \times \text{V}_{er}\right)}{\text{SS}_T} \times 100 \quad (8)$$

$$SS = \frac{mn}{Z}\sum_{z=1}^{Z}\left(\bar{X}_z^{\,f} - \bar{X}_T\right)^2 \quad (9)$$

$$\text{SS}_T = \sum_{j=1}^{m}\left(\sum_{i=1}^{n}X_i^2\right)_j - mn(\bar{X}_T)^2 \quad (10)$$

$$\bar{X}_T = \sum_{j=1}^{m}\left(\sum_{i=1}^{n}X_i\right)/(mn) \quad (11)$$

$$V_{er} = \frac{SS_T - \sum_{f=1}^{F}SS}{m(n-1)} \quad (12)$$

The test results in a set of data revealed that the sample heave magnitude with time was the most important case. Typical diagrams, including the one shown in Fig. 3, were plotted for each tested sample based on the acquired data. These diagrams

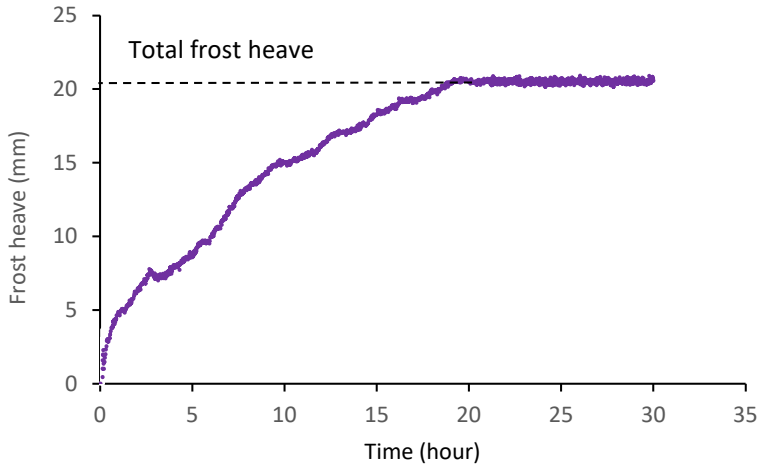

Fig. 3: Diagram of time and frost heave for the untreated soil sample

illustrated the frost heave magnitudes versus time and provided the required knowledge to investigate the process of frost heaving for each sample. During the testing period, each specimen reached a steady state in which the frost heave tended to a constant limiting value with no more change with time. This maximum limiting value of heaving was considered as the total frost heave value for the testing sample based on which the frost heave performance of the sample was processed to analyze the experimental results.

RESULTS AND DISCUSSION

The first test was conducted on an untreated soil specimen without performing any stabilization measure. This test was performed for two more times to assess the precision of the measured frost heave. The recorded heaves from these repetitions were 20.48, 20.51, and 20.60 mm, indicating high precision in the measured data. Moreover, the mean total frost heave for the untreated soil was obtained as 20.5 mm. Subsequently, the frost heave tests were conducted on the microbially treated soil samples (Table 3). The testing results are summarized in Table 4, which introduces the results from the defined tests derived from three repetitions (columns 5-7). Column (8) of Table 4 gives the mean value of the soil sample frost heave which is obtained from three repetitions for each testing case. These mean values were used to determine Taguchi predictions for all the designed testing cases presented in column (9) of Table 4. Column (10) gives the values for Taguchi predictions in column (9), divided into the frost heave value of the untreated samples. Finally, column (11) of Table 4 presents the SNR values calculated from Eq. 6.

Table 5 presents the data derived from Table 4 and Eq. 7. Table 5 includes the amounts of mean SNRs for all the factors considered in the experiment program. The SOP was obtained by subtraction of the maximum and minimum levels of each parameter.

The smaller mean SNR of a level for a test factor of the experiment implied that the factor level had a higher influence on the obtained result. Moreover, the significance of the parameters for each factor demonstrated the impact of the parameters on the measured frost heave. For more clarification, the data in Table 5 were plotted in Fig. 4. Obviously, the optimum conditions occurred within the 4th level (21 days) of curing time, 2nd level (0.6 M) of CSC, and 4th level (10^8 CFU/mL) of bacteria concentration leading to the lowest possible frost heave.

The ANOVA statistical analysis was performed using Eq. 8-13 to determine the contribution percent of each factor (Table 6).

The ANOVA results in Table 6 also demonstrated that bacteria concentration had the most significant effect (41.69%) on frost heave control. The curing times was in the second rank, with nearly the same influence (40.75%) on the test outcome as bacteria concentration. The CSC had the least effect (12.90%) on the frost heave reduction. The obtained

Table 4: **Frost heave test results and Taguchi predictions of MICP treated soil samples**

Test No.	Parameter level			Frost heave (mm)						
	Curing time	CSC	Bacteria concentration	First repetition	Second repetition	Third repetition	Mean $(\overline{FH})$	Taguchi prediction	Heave ratio	SNR
(1)	(2)	(3)	(4)	(5)	(6)	(7)	(8)	(9)	(10)	(11)
T1	1	1	1	8.36	8.4	8.47	8.41	8.61	0.42	18.50
T2	1	2	2	7.1	7.04	7.07	7.07	7.12	0.35	16.99
T3	1	3	3	6.79	6.82	6.70	6.77	6.79	0.33	16.61
T4	1	4	4	7.03	6.99	6.98	7.00	6.74	0.33	16.90
T5	2	1	2	7.40	7.39	7.35	7.38	7.43	0.36	17.36
T6	2	2	1	7.55	7.56	7.6	7.57	7.28	0.36	17.58
T7	2	3	4	5.51	5.56	5.55	5.54	5.82	0.28	14.87
T8	2	4	3	6.69	6.75	6.75	6.73	6.70	0.33	16.56
T9	3	1	3	6.13	6.08	6.09	6.10	6.06	0.30	15.71
T10	3	2	4	4.57	4.59	4.64	4.60	4.78	0.23	13.26
T11	3	3	1	6.85	6.79	6.82	6.82	6.65	0.32	16.68
T12	3	4	2	6.38	6.35	6.38	6.37	6.40	0.31	16.08
T13	4	1	4	5.59	5.60	5.61	5.60	5.40	0.26	14.96
T14	4	2	3	5.02	4.97	4.98	4.99	5.05	0.25	13.96
T15	4	3	2	5.91	5.87	5.92	5.90	5.78	0.28	15.42
T16	4	4	1	6.59	6.63	6.61	6.61	6.87	0.34	16.40

Table 5: Mean SNRs of the parameters at different levels

	Mean SNR				
Parameter	Level 1	Level 2	Level 3	Level 4	SOP
Curing time	17.27	16.64	15.52	15.33	1.94
CSC	16.69	15.57	15.91	16.58	1.12
Bacteria concentration	17.33	16.45	15.77	15.20	2.13

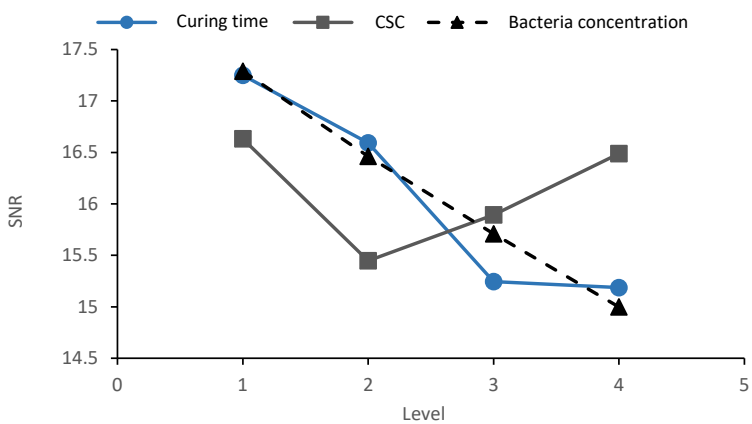

Fig. 4: Mean SNRs at different levels of each factor

p-values were less than 0.05, which rejected the null hypothesis (Andrade, 2019). The results of mean frost heave (column 8) and Taguchi predictions (column)) for T1 to T16 from Table 4 are plotted in Fig. 5. The R^2, which is calculated by Eq .13, is equal to 0.97, showing that the outcomes were firmly dependent on each other (Chicco *et al.*, 2021). The precision of the TDOE method was previously proved in previous studies (Lafifi *et al.*, 2019). This was in agreement with the results presented in the current study. Thus,

Table 6: ANOVA results

Factor	DOF	SS	MS	CP (%)	p-value
Curing time	3	11.39	3.80	40.75	0.002
CSC	3	3.60	1.20	12.90	0.037
Bacteria concentration	3	11.65	3.88	41.69	0.002
Residual Error	6	1.30	0.23	4.66**	
Total	15	27.94*		100.00	

*SS_T **V_{er}

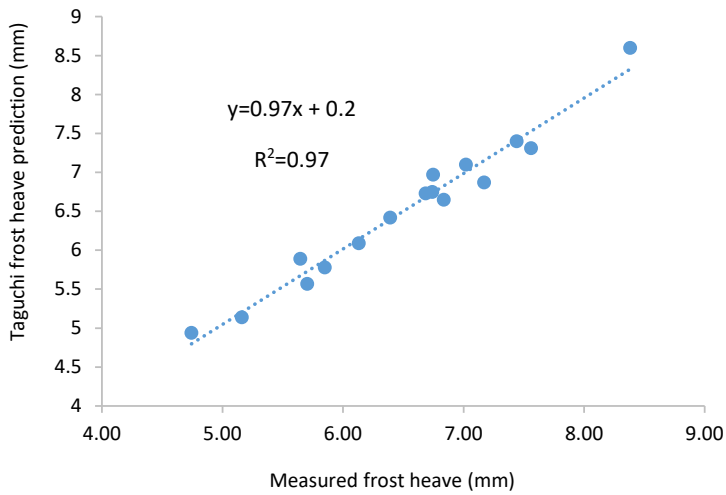

Fig. 5: Results of frost heaves measured versus Taguchi predictions

the Taguchi predictions were used afterward.

$$R = \frac{\Sigma\left[\left(X - X_m\right)\times\left(Y - Y_m\right)\right]}{\sqrt{\left[\Sigma\left(X - X_m\right)^2 \times \Sigma\left(Y - Y_m\right)^2\right]}} \quad (13)$$

A test was conducted for 10^8 CFU/mL bacteria concentration, 21 days of curing, and 0.6 CSC to justify the optimum predicted condition. Accordingly, the frost heave was found as 4.41 mm and the heave ratio was obtained as 0.21. These results were completely in agreement with the Taguchi predictions.

Heave ratio diagrams

Three diagrams for each input factor at its optimum level are shown in Fig. 6. The heave ratio of various bacteria concentrations and curing times were plotted for a CSC of 0.6 M (Fig. 6a). The same diagrams were delineated for 21 days of curing time and 10^8 CFU/mL of bacteria concentration (Figs. 6a and b). The heave ratio was in the range of 0.21-0.42, depending on the CSC, bacteria concentration, and curing time. This implied that the MICP treatment significantly decreased the amount of soil frost heave. Even the minimum treatment with no curing led to a 42% reduction in the soil frost heave. Therefore, the MICP treatment technique could be suggested as a viable alternative for the mitigation of the soil frost heave. As shown in Fig. 6, the amount of frost heave is changed with the variation of the CSC for the whole tests. However, the lowest frost heave was observed in the testing samples with 0.6 M CSC, after which the amount of the frost heave increased with the increase of CSC. Based on the testing results, the curing time of the treated soil samples had a significant role in their frost heave responses. The specimens with long curing periods presented less frost heave amounts in all the cases. The minimum frost heaves were observed in the samples treated with a CSC of

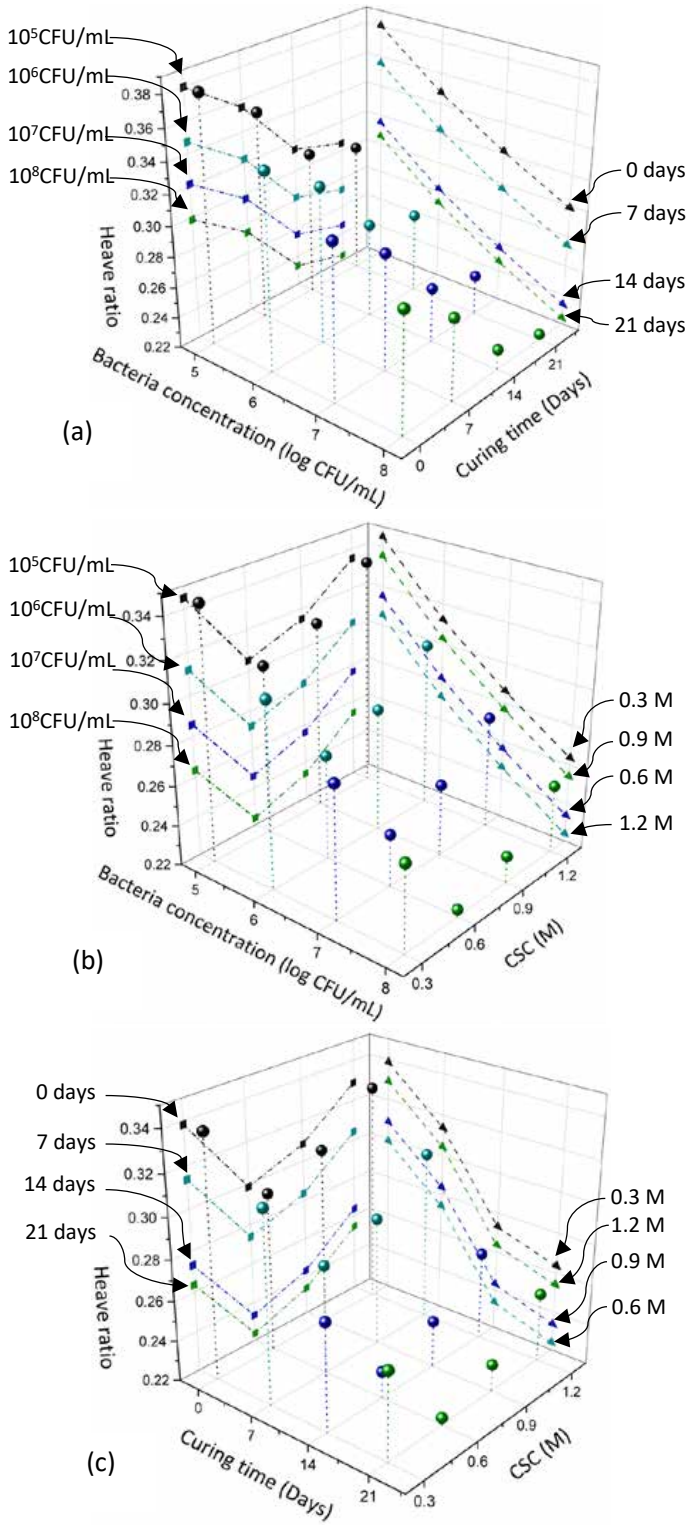

Fig. 6: Diagrams of heave ratios at 0.6 M CSC (a), 21 days curing time (b) and 10^8 CFU/mL bacteria concentration (c)

0.6 M and cured for 21 days for all testing bacteria concentrations.

Reduction of the MICP effect with the increment of CSC could be explained by the negative impact of a high salinity environment on the life and activity of the bacteria (Ng *et al.*, 2012). Higher carbonate precipitation causes lower soil frost heave due to the stronger bound among the particles and filling the voids among the soil particles, resulting in less water preservation within them (Lambe, 1956). As can be seen in Table 5, the bacteria concentration and curing time had a more significant role in the reduction of the soil frost heave compared to the cementation solution concentration. Notably, applying more bacteria concentrations imposed higher costs on the project, while curing the treated soil required very lesser expenses and attention.

Comparison of the MICP with previous methods

Numerous researchers have focused on the soil frost heave treatment. For instance, Lambe *et al.*, (1956) examined the effect of 40 additives in the reduction of frost heave. Kettle and McCabe, (1985) used the mechanical soil improvement method by mixing slag, basalt and limestone with soil. They reported 0.24 to 0.41 heave ratios for different materials in different sizes. Arabi and Wild, (1986) used lime to control the soil frost heave. They reported an increase in the frost heave level for using 2% or less lime, but the frost heave decreased as expected in higher percentages of lime and higher temperature and curing time. Guthrie *et al.* (2007) employed cement to control the frost heave, and reached higher amounts of frost heave for the soils treated with 2% or less cement rather than the untreated soil samples. They also demonstrated that the frost heave dramatically decreased when 3.5% or more cement additive was employed. Hu *et al.* (2018) used nano-silica to reduce the soil frost heave. They observed a slight reduction in frost heave (about 3.6%) when the nano-silica content was less than 1% or more than 2%. The claimed that the frost heave reduction was about 26% (0.74 heave ratio) when the applied nano-silica content was in the range of 1%-2%. Zieba *et al.* (2019) used 5% of nano-silica content to reduce the soil frost heave. They reported 97% (0.03 heave ratio) reduction in the frost heave for the treated sample. They also used 5% micro-silica which resulted in 21% (0.79 heave ratio) reduction in frost heave. Velsovskij *et al.* (2020) employed the anti-icing materials which resulted in 30% to 33% (0.67 to 0.70 heave ratios) reduction in frost heave. The results of a few previous studies are presented in Fig. 8 for comparison. These results are illustrated based on the heave ratios of the used soil (0 corresponds to a zero frost heave). Comparison of the results from Fig. 8

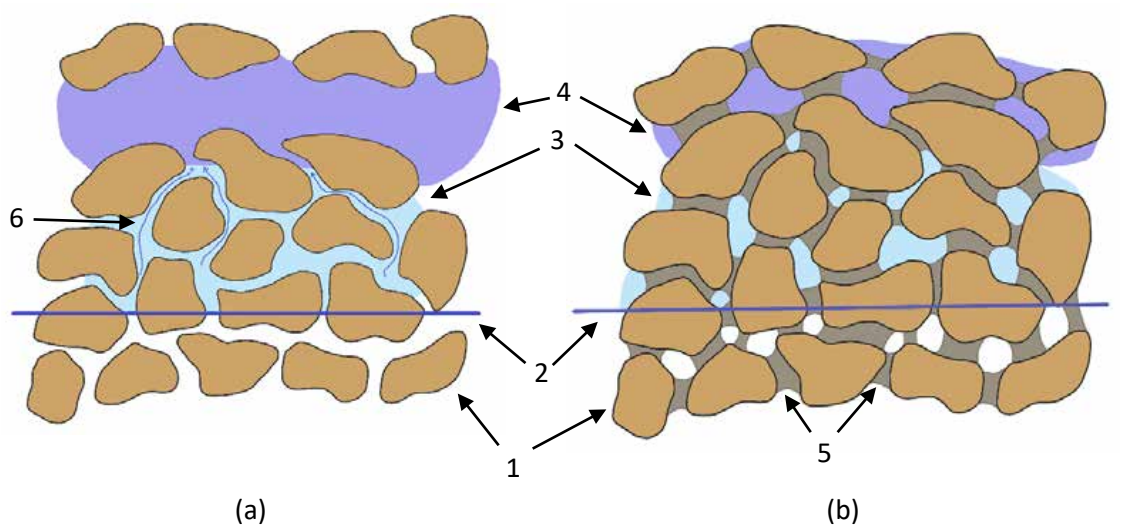

Fig. 7: Frost heave of untreated (a), and treated (b) soils: soil particles (1), freezing front (2), void ice (3), ice lens (4), precipitated calcite (5), and the path of water through ice lens (6)

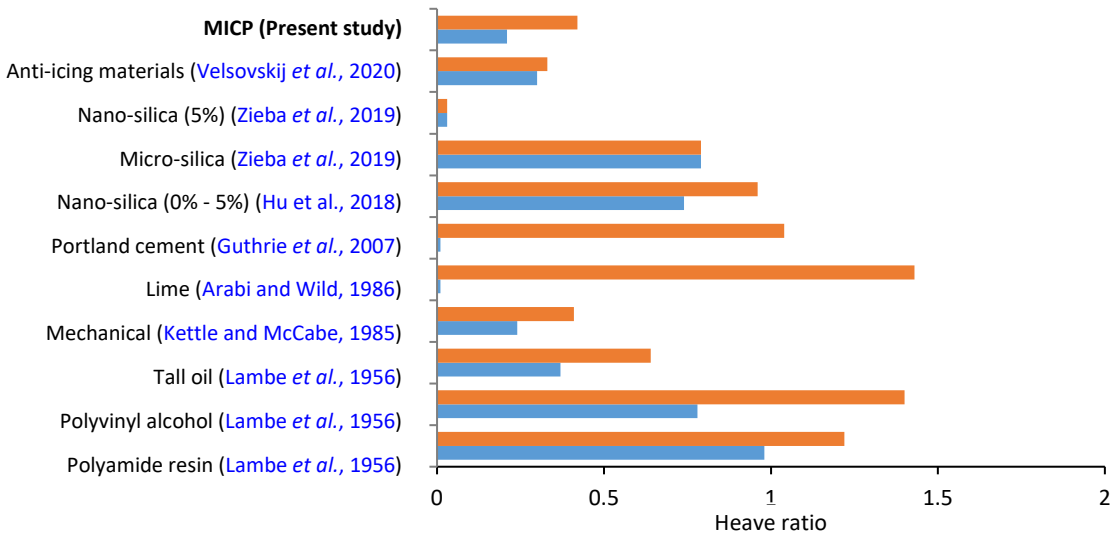

Fig. 8: Comparison of the different methods for the mitigation of frost heave

showed that the MICP used for controlling the soil frost heave let to a reasonable outcome compared to other methods. For example, higher amounts of lime or cement should be used to reach an acceptable outcome; otherwise, these additives would end up with adverse effects. Compared to other methods, the heave ratio of the samples treated with the MICP method was acceptable, showing the technical feasibility of the MICP method to confront the soil frost heave. This method can also eliminate the environmental pollution using the toxic synthetic materials.

The heave ratios of the MICP-treated samples were in the range of 0.21 to 0.42. The obtained heave ratios were smaller than the ratios of polyamide resin, polyvinyl alcohol, nano-silica (0%-5%), micro-silica, Portland cement (less than 2% content), and lime (less than 3.5 % content, or not cured at high temperatures). The Portland cement and lime (cured at 75 °C) showed a better function when utilized in more than 2% and 3.5% contents, respectively. The curing of lime at 75 °C was somehow impractical to some extent. Application of nano-silica (5%) mitigated the soil frost heave almost completely. Considering the debates over the possible health issues of nano-silica, some researchers believe that it causes chronic diseases like silicosis (Napierska *et al.*, 2010). Mechanical stabilization methods led to 0.24 to 0.41 heave ratios. This range was approximately the same as the range obtained in the MICP method. This method can be utilized for shallow soil improvement, while using it for deep layers is challenging, time-consuming, and costly. The MICP and other methods, which inject grouts to improve the soil characteristics, have the advantage of being employed in deeper layers with no necessity for removing upper levels. The obtained heave ratio for anti-icing materials was 0.3-0.33 which is nearly the same as the ratio obtained in the MICP method. The used materials were saline-based materials which reduced the water freezing point.

MICP efficiency justification through scanning electron microscopy (SEM) images

The images of both untreated and MICP-treated samples were provided by the SEM technique. For SEM imaging, a small specimen was carefully prepared with the given characteristics required for such imaging techniques. In this context, for both treated and untreated soils, a cubic representative specimen with a side length of 25 mm was separated from bulk samples with strict care. The SEM images of the treated specimen, from a typical testing case alongside those of the untreated soil specimens, are presented in Fig. 9. The quality and magnitude of calcite precipitation on the soil particle surfaces within the soil matrix can be evaluated by looking at the SEM, particularly at magnified spots of 1 and 2.

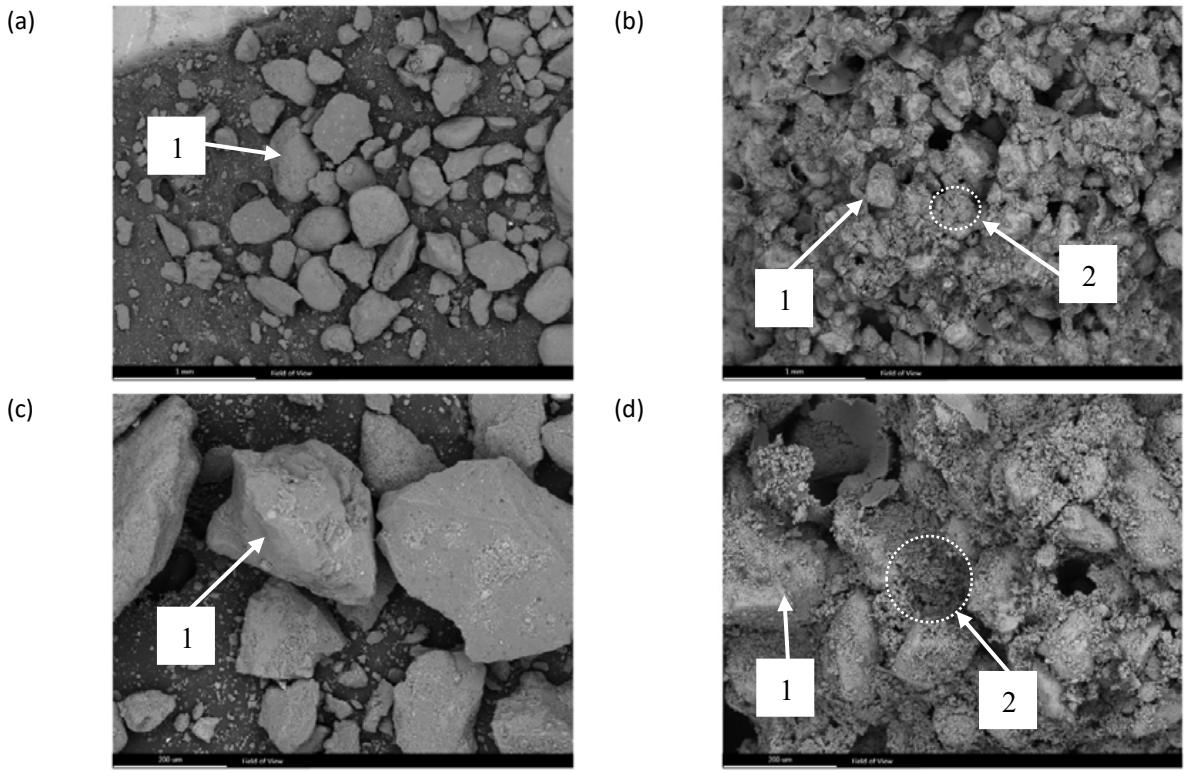

Fig. 9: SEM images of untreated (a,c), and treated T14 (b,d) soil samples (the magnification of each image is illustrated at its left bottom corner)

These images are similar to those illustrated in the previously reported studies on the MICP treated soils (DeJong *et al.*, 2006). Zamani and Montoya, (2018) illustrated the occurrence of calcite precipitation on the soil grains and the clear difference between the texture of the treated and untreated soils. As shown in Fig. 9b and d, the uniform formation of calcite crystals was observed on the surface of soil particles and also within the pores among the soil particles. Although the calcite formation was not too great to completely fulfill the soil pores, nonetheless properly bonded the soil particles and presented a robust and less permeable soil matrix. The partial fulfillment of pores with calcite led to a lower saturation degree in the capillarity zone which lowered the soil frost heave.

CONCLUSION

The soil frost heave is a common problem in cold regions and mainly destroys the infrastructures in the suburban areas such as roads, railways, and pavements. In this study, a novel approach was proposed to overcome this issue. For this purpose, a laboratory-scale experimental study was carried out to assess the efficiency of the MICP bacterial treatment to mitigate the frost heave of typical silty sand. An innovative frost heave testing apparatus was designed to meet the requirements of the soil frost heave measurement and control. The *Sporosarcina pasteurii* bacterium was employed to proceed with the MICP procedures for soil treatment. The MICP method was introduced as a viable and efficient alternative to conventional methods for treating the soil frost heave for the first time. According to the results, the *Sporosarcina Pasteurii* bacterial MICP treatment led to a reduction in the frost heave ratio to 0.21 in optimum treatment (i.e., lowering the soil frost heave to nearly one-fifth of the untreated soil). The minimum MICP treatment showed a heave ratio of 0.42. The ANOM and ANOVA analyses of data developed by the Taguchi-based experimental design showed that, among the three variables of the bacteria concentration, curing time, and CSC, the

bacteria concentration with 41.69% contribution to the results was the most influential factor. The curing time had a 40.75% contribution to the outcome, which was slightly less than the contribution of the bacteria concentration factor. The lowest contribution belonged to CSC, with 12.90% contribution. The P-values for all the three factors were less than 0.05, and thus the null hypothesis was rejected. The frost heave trend assessment revealed that increasing the bacteria concentration continuously decreased the soil frost heave. The analysis also defined the optimum (minimum) frost heave occurring at 10^8 CFU/mL bacteria concentration (the maximum level). The curing time factor also followed the same trend, and the minimum frost heave occurred at 21 days, (the highest curing time). The optimum CSC, leading to the lowest frost heave, was found to be 0.6 M. However, in contrast to the other two factors, the frost heave increased to higher levels of 0.9 M and 1.2 M. Except for using over 2% of cement, in application of 3.5% of lime cured at 75 °C, and 5% of nano-silica (which reduced the heave ratio to near zero), the heave ratios of the MICP-treated samples were lower. In a few cases, their range was the same in different methods. In contrast to other methods namely cement, lime, and nano-silica, one of the advantages of the used method was its effectiveness at any application level. The observational SEM imaging approved the formation of calcite precipitation, bonding soil particles, and filling soil pores. Therefore, the partial filling of soil pores, due to the MICP procedure, led to a lower saturation degree in the capillarity zone which lowered the soil frost heave. The MICP method faces some challenges, namely providing some undesirable by-products. This method may be used as an eco-friendly, cost-effective approach after development, modification, and industrialization in the future.

AUTHOR CONTRIBUTIONS

M.F. Nikshoar contributed to the literature review, experimental design, performing laboratory tests, data analysis, and writing the original draft. M.A. Rowshanzamir supervised the geotechnical laboratory tests, methodology, data analysis, writing review, and editing. S.M. Abtahi is the paper's corresponding author and performed conceptualization, methodology, and data compilation. S. Soleimanian-Zad supervised the biological laboratory tests and activities, performed biological methodology and biological investigation, writing reviews on biological aspects.

ACKNOWLEDGEMENT

The authors thank Mr. M. Haj Mostafa and other staff of Isfahan Research Institute for Biotechnology and Bioengineering. The authors also acknowledge the assistance of Isfahan University of Technology (IUT) personnel during the conduction of the experiment.

CONFLICT OF INTEREST

The author declares that there is no conflict of interests regarding the publication of this manuscript. In addition, the ethical issues, including plagiarism, informed consent, misconduct, data fabrication and/or falsification, double publication and/or submission, and redundancy have been completely observed by the authors.

ABBREVIATIONS

%	Percent
°C	Degree Celsius
ANOVA	Analysis of variance
ATCC	American Type Culture Collection

ANOM	Analysis of means
ASTM	American Society for Testing and Materials
BC	*Bacteria concentration*
Ca^{2+}	Calcium ion
$CaCO_3$	Calcium carbonate
Cc	The coefficient of gradation
CFU	Colony-forming unit
cm	Centimeter
cm^3	Cubic centimeter
CO_2	Carbon dioxide
CP	Contribution percent
CP_{er}	Contribution percent of errors
CSC	Cementing solution concentration
Cu	The uniformity coefficient
D_{50}	The median particle diameter
DOF	Degree of freedom
Eq.	Equation
Exp.	Experiment
FH	Frost heave test result
$\overline{FH}$	Mean frost heave
Fig.	Figure
g	Gram
g/L	Grams per liter
g/M	Grams per molar
G_S	The specific gravity of soil
H_2O	Water
HCO_3^-	Bicarbonate ion
Heave ratio	Average heave of treated soil divided by the average heave of untreated soil
hour	Hour
i	Number of the test repetition
IUT	Isfahan University of Technology
KN	Kilonewton
L	Liter
log	Logarithm
m	Number of experiments
M	One mole per litre
m^3	Cubic meter
MICP	Microbially induced calcium carbonate precipitation
min	Minute
mL	Milliliter
mm	Millimeter
MS	Mean of squares
n	Total number of repetitions for that factor
NaCl	Sodium chloride
$NaHCO_3$	Sodium bicarbonate
$(NH_2)_2CO$	Urea
NH_3	Ammonia
NH_4^+	Ammonia ion
NH_4Cl	Ammonium chloride
No.	Number
OD_{600}	Optical density of the biomass measured at 600 nm wavelength
OH^-	Hydroxide
p-value	Probability value
PTFE	Polytetrafluoroethylene
R^2	
rpm	
saclSi	Sandy clayey silt
SEM	Scanning Electron Microscopy
SM	Silty sand
SNR	Signal-to-noise ratio
SOP	Significance of the parameter
SS	
SS_T	
t	Level number if the test
TDOE	Taguchi's design of experiment
USB	Universal Serial Bus
X	Data points in the X data series
X_i	The i data point
V_{er}	Variance of error
$\overline{X}_T$	Total average of the data points
$\overline{X}_z^f$	Average value of the outputs for the parameter f
X_m	The mean of data points in the X data series
Y	Data points in the Y data series
Y_m	The mean of data points in the Y data series
$\gamma d\ min$	The minimum density of soil
$\gamma d\ max$	The maximum density of soil
Z	Number of levels for each input factor

REFERENCES

Andrade, C., (2019). The P Value and Statistical Significance: Misunderstandings, Explanations, Challenges, and Alternatives. Indian J. Psychol. Med. 41: 210-215 **(6 pages).**

Arabi, M.; Wild, S., (1986). Microstructural development in cured soil-lime composites. J. Mater. Sci., 21: 497-503 **(7 pages).**

Bai, R.; Lai, Y.: Pei, W.; Zhang, M., (2020). Investigation on frost heave of saturated–unsaturated soils. Acta Geotech., 15: 3295-3306 **(12 pages).**

Bak, H.M.; Halabian, A.M.; Hashemolhosseini, H.; Rowshanzamir, M., (2021). Axial response and material efficiency of tapered helical piles. J. Rock Mech. Geotech. Eng., 13: 176-187 **(12 pages).**

Bak, H.M.; Kariminia, T.; Shahbodagh, B.; Rowshanzamir, M.A.; Khoshghalb, A., (2021). Application of bio-cementation to enhance shear strength parameters of soil-steel interface. Constr. Build. Mater., 294: 123470 **(11 pages).**

Castanier, S.; Le Métayer-Levrel, G.; Perthuisot, J.-P., (1999). Ca-carbonates precipitation and limestone genesisthe microbiogeologist point of view. Sediment. Geol., 126: 9-23 **(13 pages).**

Chicco, D.; Warrens, M.J.; Jurman, G., (2021). The coefficient of determination R-squared is more informative than SMAPE, MAE, MAPE, MSE and RMSE in regression analysis evaluation. PeerJ Comput. Sci. 7, e623 **(24 pages).**

DeJong, J.T.; Fritzges, M.B.; Nüsslein, K., (2006). Microbially induced cementation to control sand response to undrained shear. J. Geotech. Geoenviron. Eng., 132: 1381-1392 **(12 pages).**

Deng, X.; Li, Y.; Liu, H.; Zhao, Y.; Yang, Y.; Xu, X.; Cheng, X.; Wit, B.d., (2021). Examining Energy Consumption and Carbon Emissions of Microbial Induced Carbonate Precipitation Using the Life Cycle Assessment Method. Sustainability.13: 4856 **(20 pages)**.

Etim, R.K.; Ijimdiya, T.S.; Eberemu, A.O.; Osinubi, K.J., (2022). Compatibility interaction of landfill leachate with lateritic soil bio-treated with Bacillus megaterium: Criterion for barrier material in municipal solid waste containment. CLNR. Mater. 5: 100110 **(14 pages).**

Frossard, J.; Renaud, O., (2021). Permutation Tests for Regression, ANOVA, and Comparison of Signals: The permuco Package. J. Stat. Softw. 99: 1- 32 **(32 pages).**

Guthrie, W.S.; Lay, R.D.; Birdsall, A.J., (2007). Effect of reduced cement contents on frost heave of silty soil: laboratory testing and numerical modeling. Transportation Research Board 86th Annual Meeting Compendium of Papers **(17 pages).**

Hataf, N.; Baharifard, A., (2020). Reducing Soil Permeability Using Microbial Induced Carbonate Precipitation (MICP) Method: A Case Study of Shiraz Landfill. Soil. Geomicrobiol. J., 37: 147-158 **(12 pages).**

Henze, J.; Randall, D.G., (2018). Microbial induced calcium carbonate precipitation at elevated pH values (> 11) using Sporosarcina pasteurii. J. Environ. Chem. Eng., 6: 5008-5013 **(6 pages).**

Hermansson, Å.; Guthrie, W.S., (2005). Frost heave and water uptake rates in silty soil subject to variable water table height during freezing. Cold Reg. Sci. Technol., 43: 128-139 **(12 pages).**

Hu, K.; Chen, X.; Chen, J.; Ren, X., (2018). Laboratory investigation of the effect of nano-silica on unconfined compressive strength and frost heaving characteristics of silty clay. Soil Mech. Found. Eng. 55: 352-357 **(6 pages).**

Isik, A.; Iyisan, R.; Çevikbilen, G.; Aysegul, B., (2013). Frost susceptiblity of fine grained soils related to consistency limits, 2nd International Balkans Conference on Challenges of Civil Engineering EPOKA University, Tirana, Albania **(7 pages).**

Karol, R.H., (2003). Chemical grouting and soil stabilization, revised and expanded. CRC Press **(584 pages).**

Kettle, R.; McCabe, E., (1985). Mechanical stabilization for the control of frost heave. Can. J. Civil Eng., 12: 899-905 **(7 pages).**

Khaleghi, M.; Rowshanzamir, M., (2019). Biologic improvement of a sandy soil using single and mixed cultures: a comparison study. Soil Tillage Res., 186: 112-119 **(6 pages).**

Lafifi, B.; Rouaiguia, A.; Boumazza, N., (2019). Optimization of Geotechnical parameters using Taguchi's design of experiment (DOE), RSM and desirability function. Innov. Infrastruct. Solut. 4: 1-12 **(12 pages).**

Lambe, T.W., (1956). Modification of frost-heaving of soils with additives. Highway Research Board Bulletin **(23 pages).**

Lee, M.; Gomez, M.G.; San Pablo, A.C.M.; Kolbus, C.M.; Graddy, C.M.R.; DeJong, J.T.; Nelson, D.C., (2019). Investigating Ammonium By-product Removal for Ureolytic Bio-cementation Using Meter-scale Experiments. Sci. Rep. 9: 18313 **(15 pages).**

Lin, Z.; Niu, F.; Li, X.; Li, A.; Liu, M.; Luo, J.; Shao, Z., (2018). Characteristics and controlling factors of frost heave in high-speed railway subgrade, Northwest China. Cold Reg. Sci. Technol., 153: 33-44 **(12 pages).**

Liu, D.; Yang, J.; Li, S.; Wang, X.; Xu, S., (2022). Experimental Study on the Electro-osmotic Treatment of Frost Boiling Damage of Cold-Region Subgrade. KSCE J. Civ. Eng. 26: 1579-1591 **(13 pages).**

Luo, J; Tang, L.; Ling, X.; Geng, L., (2018). Experimental and analytical investigation on frost heave characteristics of an unsaturated moderately expansive clay. Cold Reg. Sci. Technol., 155: 343-353 **(11 pages).**

Mao, X.-S.; Zhang, B.-l., (2018). Research on the Characteristics of Moisture, Temperature and Deformation in the Process of Frost Heaving and Thawing Settlement, 2018 3rd International Conference on Advances in Materials, Mechatronics and Civil Engineering (ICAMMCE 2018). Atlantis Press. 168-172 **(5 pages).**

Miles, A.A.; Misra, S.; Irwin, J., (1938). The estimation of the bactericidal power of the blood. Epidemiol. Infect., 38: 732-749 **(18 pages)**.

Mortazavi Bak; H., Noorbakhsh; M., Halabian; A.M., Rowshanzamir; M., Hashemolhosseini, H., (2021). Application of the Taguchi method to enhance bearing capacity in geotechnical engineering: Case studies. Int. J. Geomech., 21: 04021167 **(14 pages).**

Muhammad, N.Z.; Shafaghat, A.; Keyvanfar, A.; Abd. Majid, M.Z.; Ghoshal, S.K.; Mohammadyan Yasouj, S.E.; Ganiyu, A.A.; Samadi Kouchaksaraei, M.; Kamyab, H.; Taheri, M.M.; Rezazadeh Shirdar, M.; McCaffer, R., (2016). Tests and methods of evaluating the self-healing efficiency of concrete: A review. Constr. Build. Mater., 112: 1123-1132 **(10 pages).**

Ng, W.-S.; Lee, M.-L.; Hii, S.-L., (2012). An overview of the factors affecting microbial-induced calcite precipitation and its potential application in soil improvement. Int. J. Civil Environ. Eng., 6: 188-194 **(7 pages).**

Okwadha, G.D.; Li, J., (2010). Optimum conditions for microbial carbonate precipitation. Chemosphere, 81: 1143-1148 **(6 pages).**

Qi, J., Wang; F., Peng; L., Qu; Y., Zhao, J.; Liang, J., (2022). Model test on the development of thermal regime and frost heave of a gravelly soil under seepage during artificial freezing. Cold Reg. Sci. Technol., 196: 103495 **(10 pages).**

Rahman, M.M.; Hora, R.N.; Ahenkorah, I.; Beecham, S.; Karim, M.R.; Iqbal, A., (2020). State-of-the-art review of microbial-induced calcite precipitation and its sustainability in engineering applications. Sustainability. 12: 6281 **(41 pages).**

Roth, M.J.; Caslake, L.F., (2019). Reducing Soil Permeability Using In Situ Biofilm-Forming Bacteria: Overcoming Testing Apparatus Challenges, Geo-Congress 2019: Soil Improvement :187-195 **(9 pages).**

Shah, R.; Mir, B.A., (2022). Effect of varying pore water salinity on frost susceptibility behaviour of soils. Transp. Geotech., 35: 100776 **(10 pages).**

Shahrokhi-Shahraki, R.; Zomorodian, S.M.A.; Niazi, A.; O'Kelly, B.C., (2015). Improving sand with microbial-induced carbonate

precipitation. Proc. Inst. Civ. Eng.: Ground Improv., 168: 217-230 **(14 pages).**

Stocks-Fischer, S.; Galinat, J.K.; Bang, S.S., (1999). Microbiological precipitation of CaCO3. Soil Biol. Biochem. , 31: 1563-1571 **(9 pages).**

Taguchi, G.; Chowdhury, S.; Wu, Y.; Taguchi, S.; Yano, H., (2005). Taguchi's quality engineering handbook. Wiley-Intersci. Ser., **(1696 pages).**

Talaiekhozani, A.; Keyvanfar, A.; Andalib, R.; Samadi, M.; Shafaghat, A.; Kamyab, H.; Majid, M.Z.A.; Zin, R.M.; Fulazzaky, M.A.; Lee, C.T.; Hussin, M.W., (2014). Application of Proteus mirabilis and Proteus vulgaris mixture to design self-healing concrete. Desalination Water Treat., 52: 3623-3630 **(8 pages).**

Velsovskij, A.; Shorin, V.; Akhmetov, T., (2020). Study of the influence of chemical anti-icing materials on frost heaving of the roadbed soils, E3S Web of Conferences. EDP Sciences: 01064 **(4 pages).**

Wath, R.B.; Pusadkar, S.S., (2021). Influence of Bacteria on Physical Properties of Black Cotton Soil, In: Latha Gali, M., Raghuveer Rao, P. (Eds.), Problematic Soils and Geoenvironmental Concerns. Springer Singapore: 333-342 **(10 pages).**

Whiffin, V.S.; Van Paassen, L.A.; Harkes, M.P., (2007). Microbial carbonate precipitation as a soil improvement technique. Geomicrobiol. J., 24: 417-423 **(7 pages).**

Wu, X.; Niu, F.; Lin, Z.; Luo, J.; Zheng, H.; Shao, Z., (2018). Delamination frost heave in embankment of high speed railway in high altitude and seasonal frozen region. Cold Reg. Sci. Technol., 153: 25-32 **(8 pages).**

Xiao, Y.; Zhao, C.; Sun, Y.; Wang, S.; Wu, H.; Chen, H.; Liu, H., (2021). Compression behavior of MICP-treated sand with various gradations. Acta Geotech., 16: 1391-1400 **(10 pages).**

Zamani, A.; Montoya, B.M., (2017). Shearing and hydraulic behavior of MICP treated silty sand. Geotechnical Front., 2017: 290-299 **(10 pages).**

Zamani, A.; Montoya, B., (2018). Undrained monotonic shear response of MICP-treated silty sands. J. Geotech. Geoenviron. Eng., 144: 04018029 **(6 pages).**

Zamani, A.; Xiao, P.; Baumer, T.; Carey, T.J.; Sawyer, B.; DeJong, J.T.; Boulanger, R.W., (2021). Mitigation of liquefaction triggering and foundation settlement by MICP treatment. J. Geotech. Geoenviron. Eng., 147: 04021099 **(15 pages)**.

Zhao, Z.-K.; Wang, T.-H.; Jin, X.; Zhang, Y., (2019). Experimental Study on Normal Frost-Heave Force Generated from Loess upon Freezing considering Multiple Factors. Adv. Mater. Sci. Eng., 2019: 1237105 **(10 pages).**

Zieba, Z.; Witek, K.; Kilian, W.; Monka, J.; Swierzko, R., (2019). Influence of micro and nanosilica on the frost–heave process, IOP Conference Series: Materials Science and Engineering. 042020 **(10 pages).**

AUTHOR (S) BIOSKETCHES

Nikshoar, M.F., Ph.D. Candidate, Department of Civil Engineering, Isfahan University of Technology, Isfahan, 84156-83111, Iran.
- Email: *mf.nikshoar@cv.iut.ac.ir*
- ORCID: 0000-0002-5980-8691
- Web of Science ResearcherID: GPT-0587-2022
- Scopus Author ID: NA
- Homepage: https://iut.ac.ir/en

Rowshanzamir, M.A., Ph.D., Associate Professor, Department of Civil Engineering, Isfahan University of Technology, Isfahan, 84156-83111, Iran.
- Email: *mohamali@cc.iut.ac.ir*
- ORCID: 0000-0001-6242-179X
- Web of Science ResearcherID: GRJ-4754-2022
- Scopus Author ID: 36572580900
- Homepage: https://rowshanzamir.iut.ac.ir

Abtahi, S.M., Ph.D., Associate Professor, Department of Civil Engineering, Isfahan university of Technology, Isfahan, 84156-83111, Iran.
- Email: *mabtahi@iut.ac.ir*
- ORCID: 0000-0001-8118-2456
- Web of Science ResearcherID: GRJ-9626-2022
- Scopus Author ID: 24558620700
- Homepage: https://abtahi.iut.ac.ir

Soleimanian-Zad, S., Ph.D., Professor, Professor, Department of Food Science and Technology, College of Agriculture, Isfahan University of Technology, Isfahan, Iran.
- Email: *Soleiman@cc.iut.ac.ir*
- ORCID: 0000-0002-6956-8468
- Web of Science ResearcherID: AFM-6825-2022
- Scopus Author ID: 14022091000
- Homepage: https://soleimanian-zad.iut.ac.ir

HOW TO CITE THIS ARTICLE

Nikshoar, M.F., Rowshanzamir, M.A., Abtahi, S.M., Soleimanian-Zad, S., (2023). Application of microbially induced calcite precipitation to mitigate soil frost heave. Global J. Environ. Sci.Manage., 9(2): 193-210.

DOI: 10.22034/gjesm.2023.02.02

url: https://www.gjesm.net/article_254438.html

Global J. Environ. Sci. Manage. 9(2): 211-226, Spring 2023, Serial #34

Global Journal of Environmental Science and Management
(GJESM)

Homepage: https://www.gjesm.net/

ORIGINAL RESEARCH ARTICLE

Environmental vulnerability characteristics in an active swarm region

A.V.H. Simanjuntak[1,2,3], U. Muksin[3], A. Arifullah[3], K. Lythgoe[4], Y. Asnawi[5], M. Sinambela[6], S. Rizal[7], S. Wei[4,8]

[1] *Graduate School of Mathematics and Applied Sciences, Universitas Syiah Kuala, Banda Aceh, Indonesia*

[2] *Meteorological, Climatological, and Geophysical Agency, BMKG, Banda Aceh, Aceh, Indonesia*

[3] *Tsunami and Disaster Mitigation Research Center, Universitas Syiah Kuala, Gampong Pie, Indonesia*

[4] *Earth Observatory of Singapore, Nanyang Techonological of Singapore, Singapore*

[5] *Department of Science and Technology, Universitas Islam Negeri Ar-Raniry, Kopelma Darussalam, Banda Aceh, Indonesia*

[6] *Meteorological, Climatological, and Geophysical Agency, BMKG, Medan, Indonesia*

[7] *Graduate School of Mathematics and Applied Sciences, Universitas Syiah Kuala, Banda Aceh Indonesia*

[8] *Asian School of the Environment, Nanyang Technological University of Singapore*

ARTICLE INFO

Article History:
Received 28 June 2022
Revised 07 September 2022
Accepted 21 October 2022

Keywords:
Earthquake
Seismic
Spectral waveform
Swarm
Volcanic
Vulnerability

DOI: 10.22034/gjesm.2023.02.03

ABSTRACT

BACKGROUND AND OBJECTIVES: For the first time, an earthquake swarm occurred from April to August 2021 in Lake Toba (Indonesia), the world's largest caldera lake. Although the earthquakes were located in a volcanic environment, the swarm activities could also be related to tectonic activities on the Sumatran fault. The swarm activities occurred at shallow depths and may influence the ground surface condition in which soil or rock below the subsurface can amplify the shaking. The research objective was to investigate the characteristics of the earthquake swarm in the Toba Caldera from the spectrum of the earthquake waveforms, site frequency, and horizontal-to-vertical ratio of sites.

METHODS: The spectra of very closely located swarm and nonswarm earthquakes were analyzed to investigate the differences between both types of seismic events. The seismic spectral ratio of horizontal-over-vertical components was applied to calculate the spectrum in the active swarm region from all newly installed seismic sensors. The root mean square was applied to average the amplitude of the horizontal components. Then, the values of the horizontal-to-vertical ratios were obtained by comparing the average values of the horizontal and vertical components.

FINDINGS: The microtremor study showed a more complete spectrum waveform from the low-to-high frequency of a non swarm earthquake, while the swarm earthquakes generated high-frequency seismograms. From the combination values of natural site frequencies and the horizontal-to-vertical ratios, the Toba environment can be classified into five clusters: I) Samosir–Hasinggaan, II) Samosir–Parapat, III) Silimapuluh, IV) Balige–Paropo, and V) Panjaitan. Samosir Island located in the middle of the Toba Caldera has the highest frequency and amplification, which are divided into two clusters.

CONCLUSION: Cluster I, with high amplification corresponding to the earthquake intensity, was felt by people in northern Samosir. Cluster II is located in the southern part of Samosir Island. Cluster III features moderate values of amplification and seismic vulnerability and therefore needs attention before future infrastructure development. Cluster IV, located in the southern and northern regions with high amplification and vulnerability, is associated with the Quaternary eruption. Cluster V, situated in northeastern Toba, has the lowest amplification and vulnerability compared to other clusters. The microtremor results provide good correlation with the geology in the volcanic environment of the Toba region.

NUMBER OF REFERENCES	NUMBER OF FIGURES	NUMBER OF TABLES
49	7	0

*Corresponding Author:
Email: *muksin.umar@unsyiah.ac.id*
Phone: +6281 26328 9103
ORCID: 0000-0001-7297-8065

Note: Discussion period for this manuscript open until July 1, 2023 on GJESM website at the "Show Article".

INTRODUCTION

From April to August 2021, the local population was surprised by swarm activity that occurred in Lake Toba and its surrounding regions, as shown in Fig. 1. This swarm activity raises the question of its cause. Swarm activity can be either related to the movement of magma or hydrothermal fluids in a volcanic environment (Hayashi and Morita 2003) or continuous slips along preexisting faults caused by stress changes (Gualandi *et al.* 2017). The cause of the Toba earthquake swarm remains unclear. A simple method for understanding the cause of an earthquake swarm is assessing and comparing the waveform spectra of swarm and nonswarm earthquakes. Understanding the cause of swarm earthquakes is important so that a population or government can take appropriate mitigating action to reduce the future possible risks. Meanwhile, the strong shaking of 2–3 MMI caused by an earthquake swarm with magnitude of M ~3.0 created public concern about potential damage to Lake Toba and its surroundings. Shaking can be also caused by nonswarm earthquakes, such as the 2004 Indian Ocean earthquake with an M of 9.0 and the 2005 Nias earthquake with an M of 8.5 that were strongly felt at Toba Lake, while inland destructive earthquakes emanate from the Sumatra fault system.

The inland earthquakes are distributed along the Sumatra fault system (Sieh and Natawidjaja 2000), including the Renun fault and the Toru fault as the closest active faults to the Toba region (Muksin *et al.,* 2013, 2014). Both faults have generated major earthquakes near the Toba region accompanied by massive damage (Pasari *et al.,* 2021). Several major earthquakes occurred along the Renun segment in 1916 and 1921 with M~7, while the Toru fault has not generated a major earthquake larger than M 6.5 (Muksin *et al.,* 2014; Hurukawa 2014). The largest earthquake from the Toru fault occurred in 1984 (M 6.4) and caused serious damage and loss in the city of Tarutung (Ryberg *et al*., 2016; Pasari *et al.,* 2021). The most recent earthquakes on the Toru fault occurred along the Sarulla Basin in 2008 (M 6), 2011 (M 5.5) (Muksin *et al.,* 2013) and 2020 (M 5.4). Further, several major earthquakes were also felt in Toba, such as the doublet earthquake in 1926 (M 6.5 and M 6.8) and 2007 (M~6) that occurred on the Suliki and Sumani fault segments (Daryono *et al.,* 2012). In the last decade, no major events have been recorded near Toba, but the swarm activities suggest the potential for an unknown local tectonic system inside Toba that can generate a strong shaking. Among the swarm events, three earthquakes (M~3) with an MMI of 2–3 were strongly felt by the local population but without severe damage. Therefore, mitigation plans to anticipate either the volcanic or the tectonic impact in Toba should be prioritized because the region is highly populated and considered the most popular tourist destination in Sumatra. Several studies have been undertaken to highlight the environmental condition of Toba, involving geological modeling (Chesner *et al.,* 2008), tomography imaging (Koulakov *et al.,* 2010; Koulakov *et al.,* 2016), water pollution (Soeprobowati 2015), and the impact of climate change on the water level in Toba (Irwandi *et al.,* 2021). Although the Toba region is seismically active from tectonic and (possible) volcanic activities, no study has been conducted on its environmental vulnerability, particularly to seismic activities and microzonation. In May 2021, a seismic survey was conducted to assess the seismic amplification and the vulnerability level of Lake Toba. Seismic records can be used to study the horizontal-to-vertical spectral ratio (HVSR) and natural frequency based on microtremor data to derive the seismic vulnerability of the Toba region. Microtremor HVSR has been widely applied to assess the potential damage caused by earthquakes by using specific parameters such as seismic amplification and natural frequency that relate to the geological condition (Goda *et al.,* 2015; Parker *et al.,* 2015). Locations with possible damage during earthquakes are categorized as areas with low dominant frequencies (Nakamura 2009). Microtremor HVSR is one of the least expensive methods and is easy to operate where areas are inaccessible. The HVSR result is recommended for soon assessing a detailed soil cluster and its projected effect. Furthermore, the results can also be used to study the probabilistic seismic hazards to help diminish the potential losses in Toba. This study aims to investigate the vulnerability after swarm phenomena in a specific cluster in Toba. Another research objective is to define the possible cause of the swarm earthquake from different swarm and nonswarm earthquake spectra recorded by the same seismic stations. This seismic experiment was performed in Toba and its surroundings in Indonesia from April to May 2021.

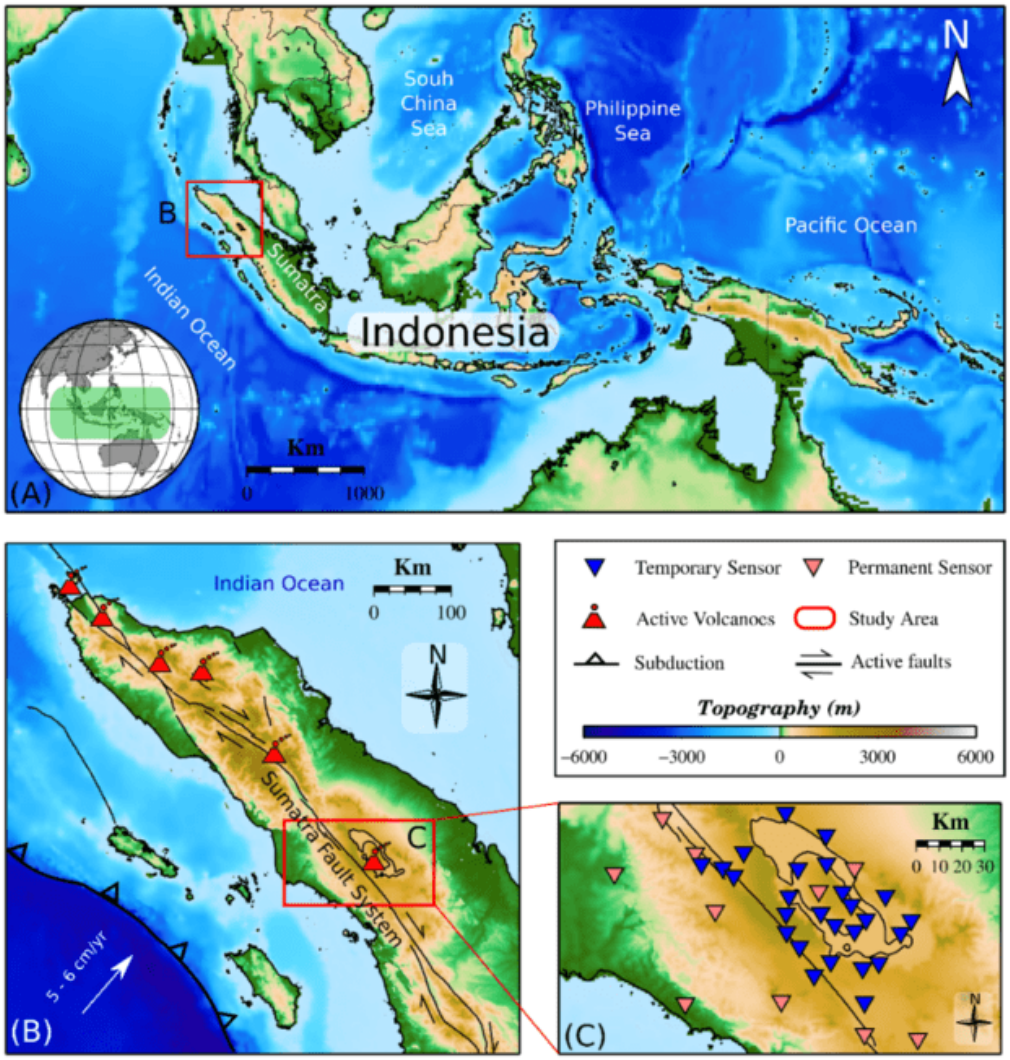

Fig. 1: (a) Geographical map of Indonesia and the study area in the northernmost part of Sumatra. (b) The tectonic map of the northernmost part of Sumatra features active subduction with a geodetic slip rate of 5–6 cm/yr and the Sumatra fault system with active volcanoes. The red square is the boundary area located in Lake Toba and its surroundings. (c) The study area in Lake Toba and its surroundings and the observation points from a temporary sensor (blue triangle) and a permanent sensor (red triangle).

Geology of the study area

Caused by a supereruption 74,000 yr B.P., the Toba caldera is one of Earth's many complex volcanic systems. The Toba volcano has erupted four times since the Quarternary, making a large depression area in northern Sumatra (Chesner *et al.,* 1991; Geethanjali *et al.,* 2019; Chesner *et al.,* 2020). As aforementioned, it is the largest of calderas, and the current condition of the complex volcanic system is influenced by the youngest Toba eruption that removed 2,800 km^3 of dense-rock-equivalent of rhyolitic magma at 74,000 yr B.P. (Chesner *et al.,* 2020; Pearce *et al.,* 2020). The young Toba tuff (YTT) (Fig. 2) was formed during the last eruption of the Toba volcano in the Late Pleistocene as a large area comprising pyroclastic material (Chesner and Luhr 2010; Chesner 2012). Eruption ash is detected at many locations in South Asia by paleoclimate studies, with

the results indicating an escalation of eruptions. The ash is composed of middle Toba tuff (MTT) (504 ka), old Toba tuff (OTT) (840 ka), and Haranggaol Dacite tuff (1.2 Ma) (Knight *et al.,* 1986; Chesner *et al.,* 1991) from previous eruptions. The YTT eruption removed a global mass of ash and various gases (Sarma *et al.,* 2018) that make a paleoclimate phenomenon with acid rain (Chesner and Luhr, 2010), resulting in the devastation of vegetation and living populations (Pearce *et al.,* 2020).

Geologically, the Toba tuff has special characteristics comprising the subsurface condition with low seismic velocity (Vs). Stankiewicz *et al.* (2010) found low Vs surrounding the Toba caldera. Low Vs can be associated with the presence of a magma chamber beneath the caldera, while at shallow depths, low Vs can be also interpreted as soft soil or rock (Asnawi et al., 2022) compared to the surrounding region. A low Vs value can also cause high seismic amplification and is subsequently classified as high seismic vulnerability. Therefore, an investigation of seismic amplification and vulnerability in the Toba region is considered essential.

MATERIALS AND METHODS

Microtremor acquisition

Microtremors were measured using two types of seismometers. The first type was a portable nodal seismic sensor used to record microtremors at 27 sites, and the second type was a broadband permanent seismic sensor used to record 9 sites (Fig. 2). The portable seismic sensor with a Magseis Fairfield nodal array was applied using three geographical components with a corner frequency of 5 Hz, a 24-bit ADC, and the ability to record with a 200 sps continuous reading. The observation location was set by a grid space of 10–30 km depending on the access to the site, with the recording time length at each site set at 45–60 min. The permanent station was equipped with a Nanometrics broadband seismometer with a sensitivity of 750 V/m ± 0.5% and operated by the Meteorology, Climatology, and Geophysics Agency (BMKG, Indonesia) to record the seismic activities in Sumatra. The sampling rate from the permanent seismic station was set to 40 sps with an effective resolution of 22 bits. The recording data of the portable and permanent seismic sensors were gathered at night to reduce the transient noise from human and machine activities. The seismic waveform was then used to calculate parameters such as the amplification and dominant frequency and subsequently to derive the seismic vulnerability.

HVSR microtremor processing

The HVSR is globally applied to assess the vulnerability level of a seismically active environment. Nakamura (2009) first developed the method with a single seismic sensor. The amplitude in the vertical shaking value is normally stable, while the amplitude in the horizontal direction is dominantly influenced by the soil subsurface condition that may receive a substantial amplification effect (Nakamura, 2009). Assuming the H/V as the frequency function that corresponds to the site characteristic, Nakamura (2009) found that the local effect can be measured using the spectral ratio of horizontal-over-vertical components using Eq. 1 (Nakamura, 2009).

$$\frac{H}{V} = \frac{\sqrt{NS^2 + EW^2}}{V} \quad (1)$$

The root mean square was applied to average the NS and EW as the representative of the horizontal components. The average of the horizontal amplitude was divided by the vertical amplitude to obtain the average H/V spectrum. From the H/V spectrum, the dominant frequency and period can be obtained at the H/V peak, which is associated with seismic amplification. The dominant frequency is closely related to the lithological conditions and thickness of the subsurface. The H/V spectrum is related to the rock density. The amplification value is large for areas composed of low-density rocks or soil. Seismic surface waves propagate slowly in soft sediments, and ground shaking can be amplified and thereby cause severe damage. The seismic vulnerability index (K_g) is calculated by dividing the square of the amplification with the dominant frequency using Eq. 2 (Nakamura, 2009).

$$K_g = \frac{A^2}{F} \quad (2)$$

The K_g value can be used to categorize the subsurface soil and qualitatively estimate possible damage areas (Tün *et al.,* 2016; Seivane *et al.,* 2022). Some studies have applied the result of K_g to assess an earthquake-prone area for earthquake mitigation

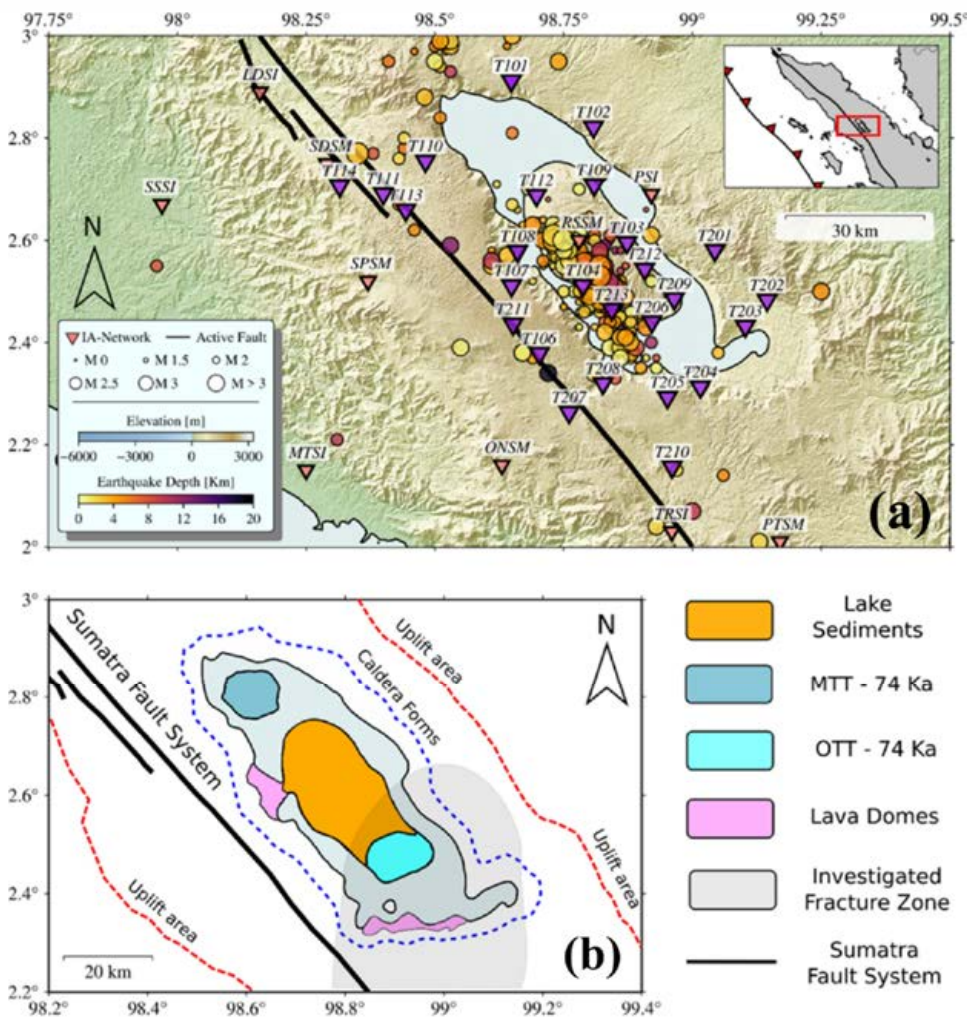

Fig. 2: (a) The seismicity map of the Toba area maps the swarm activities mostly located at Samosir Island and distributed in the NW–SE direction parallel with the Sumatra fault system (Chesner 2012). The seismometer for recording the seismic waveforms is divided into two types, temporary (purple triangle) and permanent (red triangle). (b) The local geological map of Toba features the lake sediments as the dominant geological unit. The three eruptions make a different rock age with old Toba tuffs (OTT)—840 ka, middle Toba tuffs (MTT)—500 ka, and young Toba tuffs (YTT)—74 ka.

plans (Boore 2004; Claprood *et al.,* 2014; Manzo *et al.,* 2022; Jiang *et al.,* 2022). This study is the first on seismic vulnerability based on swarm earthquakes in the Toba region.

RESULTS AND DISCUSSION

Example results of microtremor processing are shown in Fig. 3. A band pass filter with a range of 0.1–10 Hz was applied to the seismic waveform. The filtered waveform was segmented into several specific windows, as shown in Fig. 3a, and then a fast Fourier transform was applied to all accepted windows to transform the time domain data into the frequency domain (spectra). An STA/LTA antitriggering with a threshold range of 0.1–0.5 s was applied to exclude the transient noise from further analysis. After the transient effect was reduced, a 5% cosine taper was used to improve the spectrum quality of the frequency domain.

The examples of waveforms with spectrograms

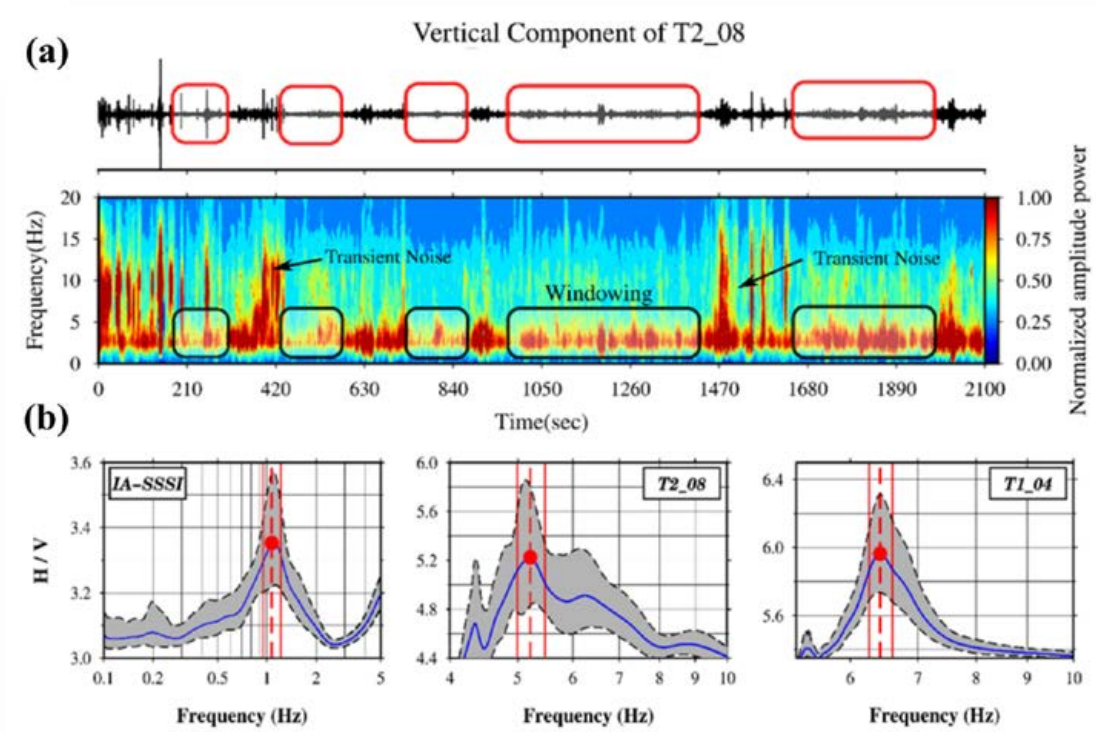

Fig. 3: (a) Example recording of the vertical component in 2100 s at site T208 and the spectrogram with a frequency range of 0–20 Hz. (b) The selected windowing is marked by a frequency of <5 Hz, while the transient noise is marked by a sudden peak. (b) Example of the H/V graph results from IA-SSSI as the permanent sensor and T2_08 and T1_04 as the temporary sensor.

(Fig. 3) show the quality of the seismic records. The selected waveform ranged from 1 to 5 Hz, while the transient noise shows a sudden peak in the high-frequency range. The three example results (IA-SSSI in the eastern part of the study area and T2_08 and T1_04 at Samosir Island) show different characters of subsurface soil response. The different H/V values for the three locations indicate variations in the site conditions depending on the rock properties of the area.

Analysis of swarm and non-swarm earthquakes

To propose the correct mitigation action, the cause of the earthquake swarm either by volcanic or tectonic activities must be investigated, which is undertaken by examining the spectra of swarm and nonswarm earthquake ash shown in Fig. 4. The chosen earthquakes occurred at different times but were located near each other. These swarm and nonswarm earthquakes were recorded by the same station and then the spectrum characteristics of the seismic waveforms from both earthquakes were analyzed.

The swarm recording shows high-frequency content larger than 10 Hz, which may be associated with possible hydrothermal fluid migration (Horton, 2012; Ross and Cochran, 2021). An earthquake swarm can also occur along the preexisting fault triggered by stress changes, caused by dike intrusion from the upper-crust layer. From the distinction of waveform frequencies, the cause of the intensity felt from the earthquake swarm in Toba was assumed to be a possible large sediment layer beneath the subsurface. A similar study determined the high-frequency content from a fluid-driven earthquake swarm in a Yellowstone caldera lake (Shelly *et al.*, 2013). Based on that study, the comparisons from some stations must be manually checked, as shown in Fig. 5.

The example recordings from different stations show the possible amplification effect beneath sensors T110 and T203. The waveforms from both

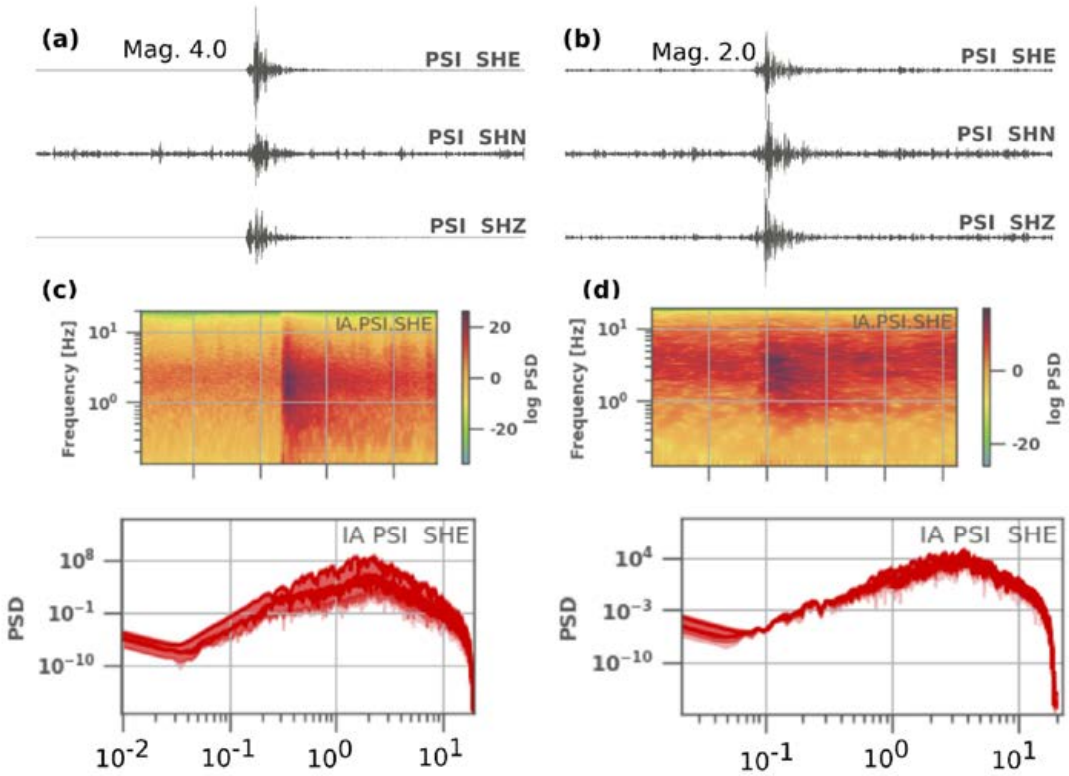

Fig. 4: (a) Example recordings of nonswarm and (b) swarm earthquakes. (c) Example spectrograms and power spectral densities (PSDs) of nonswarm (BOTTOM LEF and swarm (BOTTOM RIGHT) earthquakes. The spectrogram shows that the swarm earthquake has more high-frequency content than the nonswarm earthquake.

stations show a noise artifact that can be associated with the subsurface sediment. The spectrogram from four stations also shows T110 and T203 with saturated PSD influenced by the sediment subsurface. All sensors were manually inspected to assess the waveform quality that can be used to measure the possible site effect and support the separation of clusters based on the H/V value in the study area. The waveform spectrum of the swarm earthquake recorded by some stations in Fig. 5 follows the characteristics of the natural frequency recorded at each site. The natural frequency and H/V value at each measurement point having been obtained, the effect of the swarm earthquake in the study area can be investigated as the environmental conditions supporting soil or rock. In general, stations located in a region with high H/V will record high amplitude at the natural frequency.

Interpretation of HVSR results

After all results were collected, the microtremor parameters such as frequency and amplification were compiled to interpret the condition of the subsurface soil in the study area. The maps of the parameters of dominant frequency and period, the H/V values, and the vulnerability index are provided in Fig. 6. High dominant frequencies were recorded in Samosir Island, while low frequencies were located in the northern and southern parts outside Toba Lake (Fig. 6). In contrast to dominant frequencies, low dominant periods were observed along the Sumatra faults and outside Samosir Island (Fig. 6). The amplification obtained from the vertical axis of the peak of the H/V curve shows the highest amplification in Samosir Island, which can be related to the earthquake intensity felt by the local population (Maresca *et al.,* 2018; Alamri *et al.,* 2020).

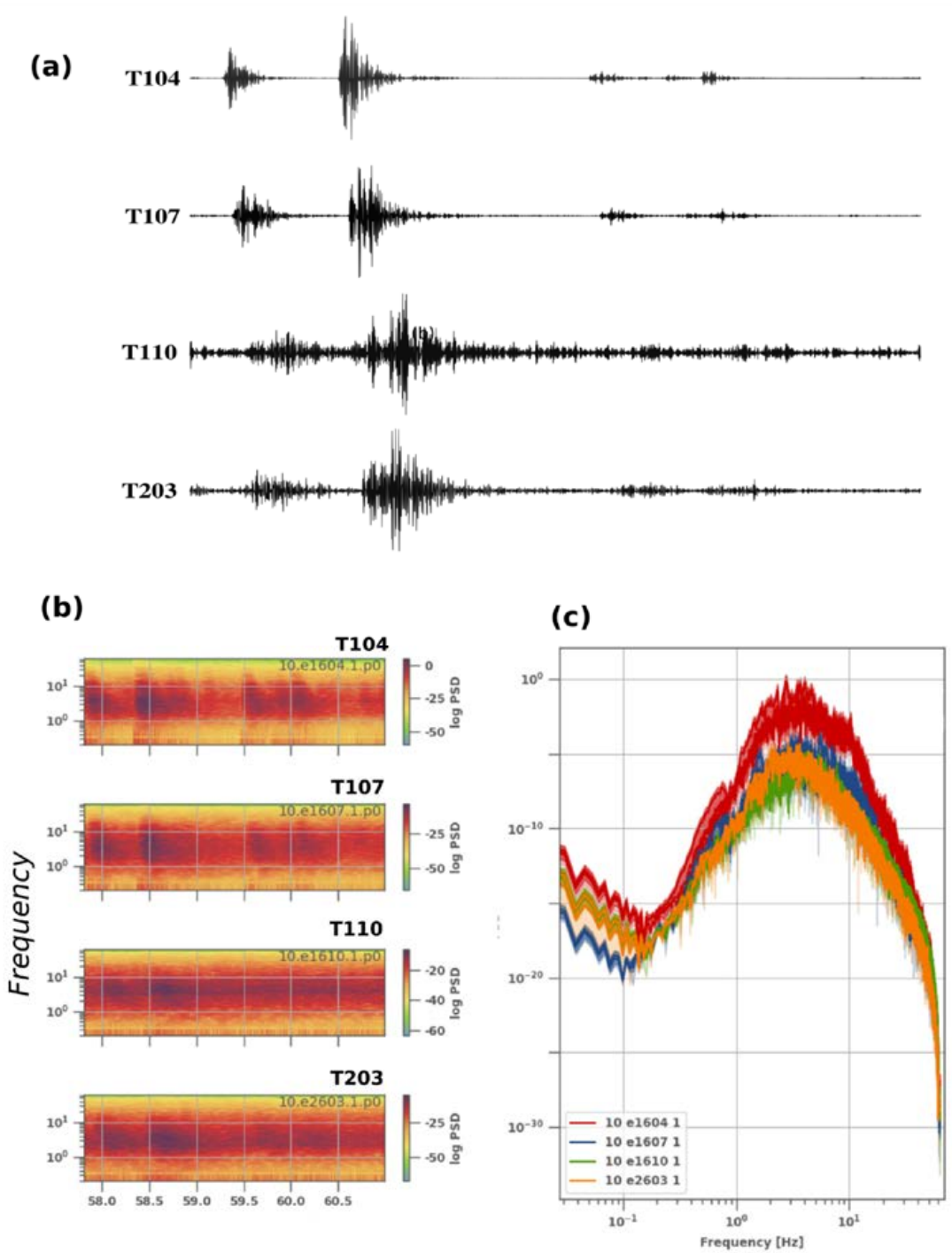

Fig. 5: (a) Example recording of two swarm events in the four sensors. The T110 and T203 stations show noise artifacts that can be associated with the subsurface condition. (b) The spectrogram from four stations also shows T110 and T203 with saturated PSD that can be related to the sediment subsurface. (c) The Fourier transform graph from all recordings highlights that T104 and T107 have higher amplitude factors than T110 and T203 (c).

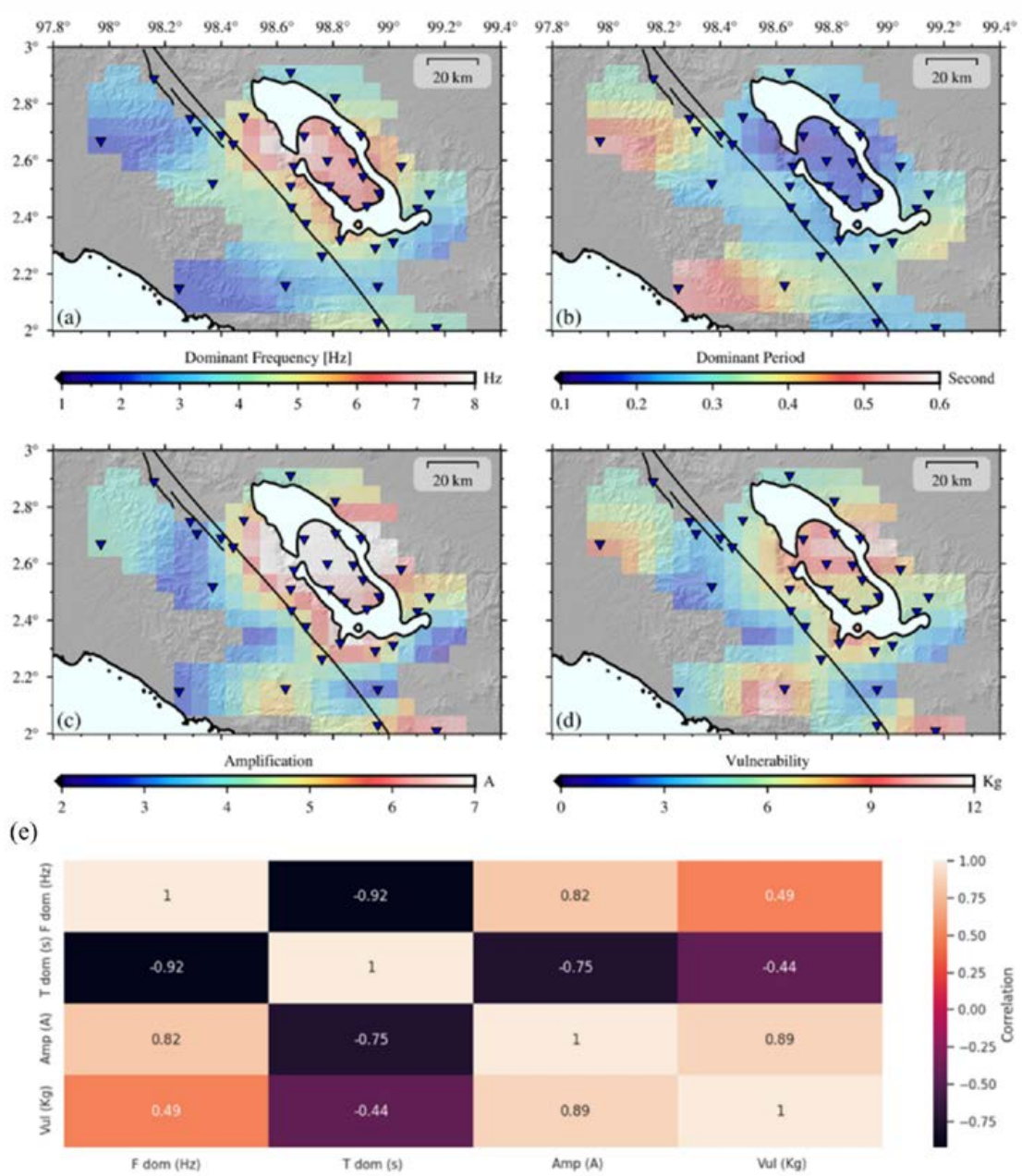

Fig. 6: (a) Spatial interpolation results of the HVSR result in dominant frequency, (b) dominant period, (c) amplification, and (d) vulnerability. (e) The heat map graphic explains the relationship between microtremor results and the correlation to all parameters.

Fig. 6(a – d) shows the map of dominant frequency and period as well as the seismic amplification and vulnerability. The seismic vulnerability K_g is highest mostly in the northern part of Samosir Island and lowest along the Renun segment of the Sumatra fault segmentation. Then, all seismic parameters, including dominant frequency, amplification, and seismic vulnerability, were spatially grouped into a specific

cluster. The relationship among all parameters (Fig. 6e) shows a linear correlation between amplification and vulnerability with a correlation value of 0.89 and amplification and frequency with a correlation value of 0.82. To examine the clusters, the seismic parameters were interpreted based on the geological condition and swarm zone mostly located in Samosir Island. Here, the low dominant frequency in the study area might be associated with the lithological condition that is composed of thick volcanic sediment layers in the upper subsurface, while the low frequency could be related to the solid rock structure. In general, the result of the dominant frequency due to the Rayleigh waves has a long period content that may connect with the lithological condition in which a thick layer lies beneath the sediments (Stanko *et al.* 2017; Forte *et al.* 2019). On the basis of the dominant frequency, the five clusters (Fig. 7) are Cluster I in northern Samosir Island and Hasinggaan, Cluster II in southern Samosir Island and Parapat, Cluster III in Silimapuluh, Cluster IV in Balige and Paropo, and Cluster V in Panjaitan.

Cluster I (Samosir Island - Hasinggaan)

Cluster I is located in northern Samosir Island and the Hasinggaan region (Fig. 7). Samosir Island is composed dominantly of lake sediment and therefore most stations recorded high amplification and frequency. The lake sediment may influence the amplification of the seismic waveform due to the

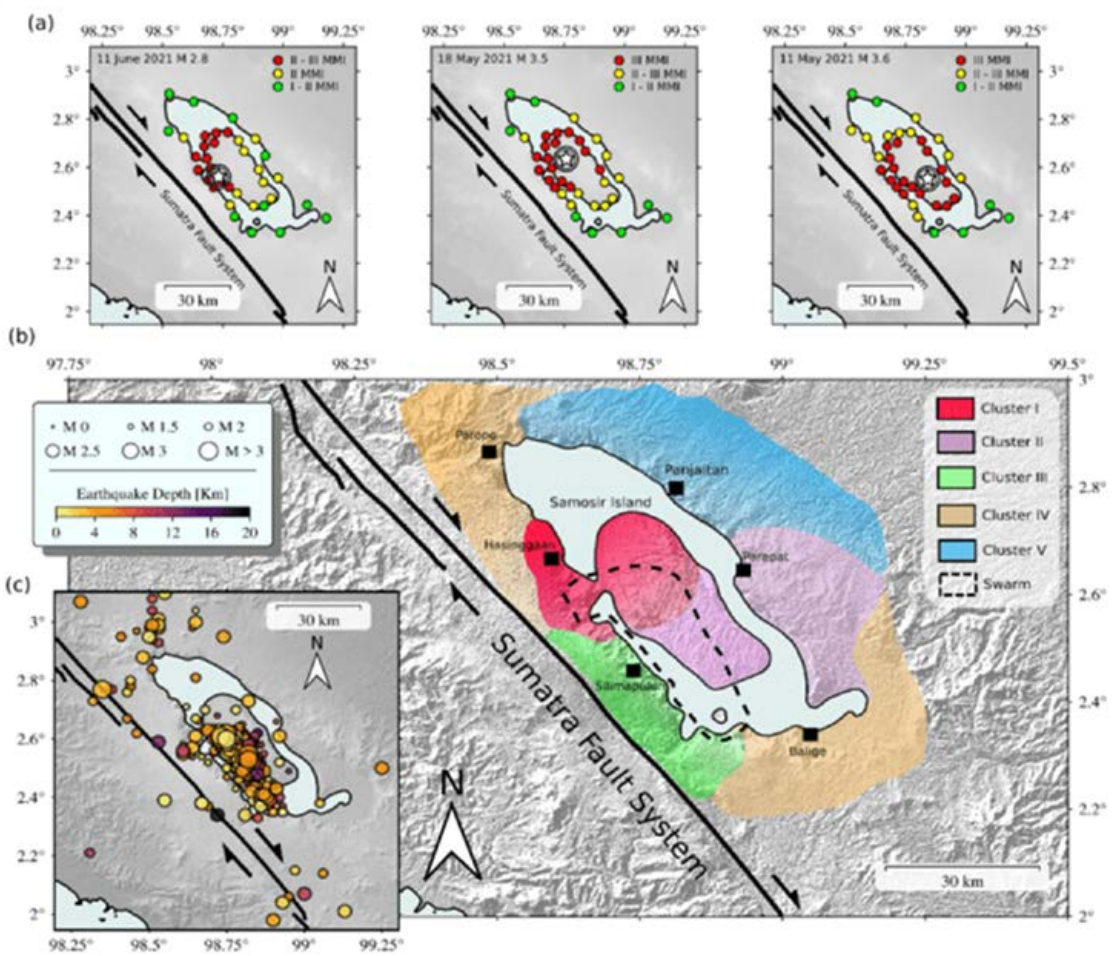

Fig. 7: (a) Clusters of zonation derived from the combination of dominant frequency and amplification (A) in the Toba area. (b) The area is divided into five clusters: Cluster I in northern Samosir Island and Hasinggaan, Cluster II in southern Samosir Island and Parapat, Cluster III in Silimapuluh, Cluster IV in Balige and Paropo, and Cluster V in Panjaitan. (c) Swarm earthquake location in the Toba area.

weak soil associated with volcanic deposits (Boore 2004; Claprood *et al.,* 2012). The amplification is relevant for the report on the earthquake felt by the local population in the central and northern parts of Samosir Island. Most people in the north of Samosir Island reported higher shaking compared with the southern part, as shown in Fig. 5(a). On the other hand, the dominant frequency ranges in Cluster I have the highest values, being between 7 and 8 Hz. The lake sediment is interpreted to have a thin layer, while the rock formation may have a thick layer below the subsurface. With the highest frequency and amplification parameters, Cluster I has a vulnerability value K_g of 9–12.

Cluster II (Samosir Island - Parapat)

Different subsurface soil characteristics divide Samosir Island into two clusters, Cluster I in the northern part and Cluster II in the southern part. The southern part of Samosir–Parapat has a slightly lower dominant frequency, with a range of 5–7 Hz. Geologically, the rock formation in the southern part of Lake Toba is older than that in the northern part, and it makes the sediment layer thicker. The OTT formation is the first quartz-bearing rock that was erupted, and this event created the Porsea caldera (Chesner *et al.* 2008). The deeper sediment layer makes a lower natural frequency range than the northern part. The Parapat region has lower seismic parameters, but both regions have similar values at the vulnerability level.

Cluster III (Silimapuluh)

The Silimapuluh region is categorized as Cluster III with a moderate amplification value and natural frequency. Cluster III is located in the southwestern part of YTT. The rock structure can be found along the Silimapuluh region. Cluster III has moderate parameters with a dominant frequency of 4–6 Hz, a dominant period of 0.2–0.3 s, an amplification of 5–6, and a seismic vulnerability K_g of 6–9. However, the moderate vulnerability level needs more attention due to the active fault in the western part. The right lateral Renun fault is suggested to have a slip rate of ~2 cm/yr. Furthermore, future studies must be conducted with more observation points in the western part of Cluster III and covering the Renun fault lineation to prepare a mitigation plan based on active faults near Toba.

Cluster IV (Paropo - Balige)

Cluster IV is located in the southern and northern parts of Lake Toba outside Samosir Island and is also constituted by OTT. The Quaternary eruption created the caldera in Balige. Cluster IV has a dominant frequency range of 3–4 Hz, the dominant period being ~0.3 s in Balige and ~0.4 s in Paropo, while the seismic amplification is less than 4 in Balige and greater than 4 in Paropo. The seismic vulnerability is classified as high with a seismic vulnerability K_g of 6–9 for the Balige and Paropo areas. Similar seismic parameters in the north and south indicate that the subsurface soil is mostly identical and the soil is formed by OTT from the Quaternary eruption. Cluster IV is located outside the swarm zone and Samosir Island, but it still needs a mitigation plan to reduce the effect of earthquake-derived shaking.

Cluster V (Panjaitan)

Cluster V is located in the northeastern part of Lake Toba, namely, in the Panjaitan region. Cluster V has a lower parameter than other clusters. The dominant frequency in the Panjaitan Cluster is 3–4 Hz, with an amplification of 5–6 and a seismic vulnerability K_g of 3–6. The population in the Panjaitan region did not report any shaking caused by the swarm earthquake because Panjaintan is far from the swarm center. The subsurface of Cluster V is mostly composed of YTT, as shown in the geological map (Fig. 2). On the basis of a lower frequency, the tuff deposit in Cluster V may indicate a larger layer in the upper subsurface compared to other clusters. However, Cluster V also needs a mitigation plan to anticipate the potential shaking derived from a swarm earthquake.

CONCLUSION

The swarm earthquake in the Toba region has changed the seismicity distribution that was distributed northwest–southeast in Samosir Island. The swarm earthquake can be considered an important event because of its shallow depth and repeated shaking duration of approximately 2–3 MMI. Therefore, a microtremor study was conducted to ascertain the previously unknown soil properties in Toba and the surrounding region. The novelty of five specific clusters was found based on the dominant frequency, seismic amplification, and vulnerability recorded by seismic temporary sensors. Cluster I is located in northern Samosir Island and in Hasinggaan

and is dominantly composed of lake sediment and characterized by high amplification and frequency. The amplification is relevant for the report about shaking felt by the local population in central and northern Samosir Island. The dominant frequency range in Cluster I has the highest values of 7–8 Hz from the lake sediment that may have a thin layer below the subsurface that produces the highest vulnerability index. The characteristics of Cluster II in southern Samosir Island are similar to those of Cluster I. The rock formation in the southern part of Lake Toba is older than that in the northern part, and it makes the sediment layer deeper. The range of the dominant frequency is lower in the southern part of Samosir Island than in the northern part, which correlates with the thicker sedimentary layer in the north. Cluster III (Silimapuluh) region has moderate amplification and vulnerability in the southwestern part of YTT and needs attention because of several major earthquakes in the last decade. Cluster IV is located in the southern and northern parts of Lake Toba and also the OTT location. The parameters in Cluster IV have a dominant frequency range of 3–4 Hz, a dominant period of ~0.3 s in Balige and ~0.4 s in Paropo, an amplification of <4 in Balige and >4 in Paropo, and K_g is 6–9 for both regions. Similar parameter values indicate the subsurface soil is mostly the same, which is formed by OTT from the Quaternary eruption. Cluster V is located in the northeastern part of Lake Toba, namely, in the Panjaitan region, and it has the lowest parameter. The dominant frequency is 3–4 Hz, the dominant period is <0.2 s, the amplification is 5–6, and K_g is 3–6. Cluster V is mostly composed of YTT as the subsurface soil, which has a lower frequency, indicating that the deposited layer may be larger in the upper subsurface. The clusters of the microtremor results provide a satisfactory spatial interpretation that is consistent with the recent geological condition and properties in the study area. A comprehensive study with more observation points with shear wave velocity must be conducted in the western part where the Sumatra fault is located. Further, this microtremor study in the swarm zone is the first research effort in the Toba region, which is important for reducing the environmental risk based on swarm earthquake disaster mitigation and policy.

AUTHOR CONTRIBUTIONS

A.V.H. Simanjuntak contributed by conducting the field experiments, HVSR data analysis, maps and figures production as well as interpreting the results, and drafting the manuscript. U. Muksin is the corresponding author and the leader of the project who provided funding for the project. A. Arifullah conducted the field experiments, and collected the seismic waveform data. Y. Asnawi was involved in data acquisition. K. Lythgoe supervised the field experiments, analyzed and interpreted the results. M. Sinambela conducted field experiments and the waveform data from BMKG. S. Rizal supervised the data processing and provided critical revision of the manuscript. S. Wei supervised the field experiments, analyzed and interpreted the results, and finalized the draft. All authors were involved in writing the manuscript.

ACKNOWLEDGEMENT

The microtremor experiment was conducted in Toba Lake, Northern Sumatra, Indonesia after swarm phenomena in 2021 by the team from Universitas Syiah Kuala (USK) and Meteorological, Climatological, and Geophysical Agency of Indonesia (BMKG). The seismic instruments were provided by Earth Observatory of Singapore of Nanyang Technological of Singapore (EOS – NTU). Authors thank to the additional waveform data from seismic station from Meteorological, Climatological, and Geophysical Agency of Indonesia (BMKG) in North Sumatra province. Authors also thank to the two anonymous reviewers for their fruitful comments and suggestions. The microtremor research was part of the World Class Research with the contract number [55/UN11.2.1/PT.01.03/DPRM2021].

CONFLICT OF INTEREST

The authors declare no potential conflict of interest regarding the publication of this work. In addition, the ethical issues including plagiarism, informed consent, misconduct, data fabrication and, or falsification, double publication and, or submission, and redundancy have been completely witnessed by the authors.

OPEN ACCESS

PUBLISHER'S NOTE

GJESM Publisher remains neutral with regard to jurisdictional claims in published maps and institutional affiliations.

ABBREVIATIONS

%	Percentage value
°C	Degree in Celsius
0°	Azimuth angle in 0 degree
1D	1-Dimension profile
A	Amplification
A	Amplitude
A^2	Square of the amplification
AB04	04th observation Point
AB05	05th observation Point
AB09	09th observation Point
AB13	13th observation Point
AB22	22th observation Point
AB23	23th observation Point
AB27	27th observation Point
b	Bandwidth coefficient
Bits	Bit per sample
B.P	Before Present
	Soil class for sediment – Rock
C-D	Line of cross section from C to D
cm	centimetre
cm/year	Centimetre over year
D	Soil class for sediment
E	Soil class for soft sediment
E-D	Soil class between soft sediment and hard soil
E-F	Line of cross section from E to F
e.g.	Latin phrase example gratia (for example)
Eq	Equation
EW	Spectrum amplitude in the horizontal east-west component
EW	East-west
f	Frequency
f	Dominant frequency
Fig.	Figure
H/V	The horizontal-to-vertical spectrum
H/V peak	Maximum peak of horizontal-to-vertical spectrum
HVSR	Horizontal to vertical spectral ratio
Hz	Hertz
i.e.	Latin phrase Id est (this is)
IA	Indonesia Seismic Network
IA-SSSI	Subulussalam Seismic Station Code
Idi	Idi Formation
Ka	Kilo annus (one thousand years)
K_g	Seismic vulnerability index
km	kilometre
km^3	cubic kilometre
log	logarithmic
m	meter
M	magnitude
m/s	meter per second
min.	minute
ms	millisecond
Ma	mega annum (5 million years from the present)
MMI	Modifie mercalli intensity

MTT	Middle Toba Tuff
NEHRP	National Earthquake Hazards Reduction Program
N	North Geographic
NS	Spectrum amplitude in the horizontal north–south component
NS	North-South
NW	North-West
OTT	Oldest Toba Tuff
PSD	Power Spectral Density
s	second
sps	Sampling per second
STA/LTA	Ratio between the amplitude
SW	South-West
T	Period
T1_06	Observation Point at T1_06
T1_09	Observation Point at T1_09
T2_08	Observation Point at T2_08
USD	United State Dollar
V	Spectrum amplitude in the vertical component of seismic waveform
V/m	Seismometer sensitivity (volt/meter)
Vp	Velocity of pressure
Vs	Shear Velocity
WCP	World Class Professor
Z	Vertical Component
YTT	Young Toba Tuff
π	Pi is a mathematical constant (3,14159)

REFERENCES

Alamri, A.M.; Bankher, A.; Abdelrahman, K.; El-Hadidy, M.; Zahran, H. (2020). Soil site characterization of Rabigh city, western Saudi Arabia coastal plain, using HVSR and HVSR inversion techniques. Arabian J. Geosci., 13(1): 1-16 **(16 pages).**

Asnawi, Y.; Simanjuntak, A.; Muksin, U.; Rizal, S.; Syukri, M.; Maisura, M., Rahmati, R. (2022). Analysis of Microtremor H/V Spectral Ratio and Public Perception for Disaster Mitigation. Geomate J., 23(97): 123-130 (**8 pages**).

Boore, D.M., (2004). Estimatings (30) (or NEHRP site classes) from Shallow Velocity Models (Depths < 30 m). Bull. Seismol. Soc. Am., 94: 591–597 (**7 pages**).

Chesner, C.A.; Rose, W.I.; Deino, A.L.; Drake, R.; Westgate, J. A., (1991). Eruptive history of Earth's largest Quaternary caldera (Toba, Indonesia) clarified. Geology. 19(3): 200-203 (**4 pages**).

Chesner, C.A.; Luhr, J.F., (2010). A melt inclusion study of the Toba Tuffs, Sumatra, Indonesia. J. Volcanol. Geotherm. Res., 197(1-4): 259-278 (**20 pages)**.

Chesner, C.A., (2012). The Toba caldera complex. Q. Int., 258: 5-18 (**14 pages**).

Chesner, C.A.; Barbee, O.A.; McIntosh, W.C., (2020). The enigmatic origin and emplacement of the Samosir Island lava domes, Toba Caldera, Sumatra, Indonesia. Bull. Volcanol., 82(3): 1-20 (**20 pages**).

Claprood, M.; Asten, M.W.; Kristek, J., (2012). Combining HVSR microtremor observations with the SPAC method for site resonance study of the Tamar Valley in Launceston. Geophys. J. Int., 191(2): 765-780 (**16 pages**).

Daryono, M.R.; Natawidjaja, D.H.; Sieh, K., (2012). Twin-surface ruptures of the March 2007 M> 6 earthquake doublet on the Sumatran Fault. Bull. Seismol. Soc. Am., 102(6): 2356-2367 (**12 pages**).

Forte, G.; Chiocarelli, E.; De Falco, M; Cito, P.; Santo, A.; Lervolino, I., (2019). Seismic soil classification of Italy based on surface geology and shear-wave velocity measurements. Soil Dyn. Earthquake Eng., 122: 79-93 (**15 pages**).

Geethanjali, K.; Achyuthan, H.; Jaiswal, M., (2019). The Toba tephra as a late Quaternary stratigraphic marker: investigations in the Sagileru river basin, Andhra Pradesh, India. Q. Int., 513: 107-123 (**17 pages**).

Goda, K.; Kiota, T.; Fokhrel, R.M.; Chiaro, G.; Katagiri, T.; Sharma, K.; Wilkinson, S., (2015). The 2015 Gorkha Nepal earthquake: Insights from earthquake damage survey. Front. Built Environ., 1(8): (**15 pages**).

Gualandi, A.; Liu, Z.; Rollins, C. (2020). Post-large earthquake seismic activities mediated by aseismic deformation processes. Earth Planet. Sci. Lett., 530: 115870 (**12 pages**).

Hayashi, Y.; Morita, Y. (2003). An image of a magma intrusion process inferred from precise hypocentral migrations of the earthquake swarm east of the Izu Peninsula. Geophys. J. Int., 153(1): 159-174 (**16 pages**).

Horton, S. (2012). Disposal of hydrofracking waste fluid by injection into subsurface aquifers triggers earthquake swarm in central Arkansas with potential for damaging earthquake. Seismol. Res. Lett., 83(2): 250-260 (**11 pages**).

Hurukawa, N.; Wulandari, B. R.; Kasahara, M., (2014). Earthquake history of the Sumatran fault, Indonesia, since 1892, derived from relocation of large earthquakes. Bull. Seismol. Soc. Am., 104(4): 1750-1762 (**13 pages**).

Irwandi, H.; Rosid, M.S.; Mart, T., (2021). The effects of ENSO, climate change and human activities on the water level of Lake Toba, Indonesia: a critical literature review. Geosci. Lett., 8(1): 1-13 (**14 pages**).

Jiang, C.; Yahong, D.; Huangdong, M.; You, X.; Ge, C., (2022). A microtremor study to reveal the dynamic response of earth fissure site: the case study in Fenwei Basins, China. Environ. Earth Sci., 81(3): 1-15 (**15 pages**).

Knight, M.D.; Walker, G.P.; Ellwood, B.B.; Diehl, J.F., (1986). Stratigraphy, paleomagnetism, and magnetic fabric of the Toba Tuffs: constraints on the sources and eruptive styles. J. Geophys. Res.: Solid Earth. 91(B10): 10355-10382 (**28 pages)**.

Koulakov, I.; Yudistira, T.; Luehr, B.G., (2009). P, S velocity and VP/VS ratio beneath the Toba caldera complex (Northern Sumatra) from local earthquake tomography. Geophys. J. Int., 177(3): 1121-1139 (**19 pages)**.

Koulakov, I.; Kasatkina, E.; Shapiro, N.M.; Jaupart, C.; Vasilevsky, A.; El Khrepy, S.; Al-Arifi, N.; Smirnov, S., (2016). The feeder system of the Toba supervolcano from the slab to the shallow reservoir. Nat. Commun., 7(1): 1-12 (**12 pages**).

Manzo, R.; Nardone, L.; Gaudiosi, G.; Martino, C.; Galluzzo, D.; Bianco, F.; Di Maio, R., (2022). A first 3-D shear wave velocity model of the Ischia Island (Italy) by HVSR inversion. Geophys. J. Int., 230(3): 2056-2072 (**17 pages).**

Maresca, R.; Nardone, L.; Gizzi, F. T.; Potenza, M. R., (2018). Ambient noise HVSR measurements in the Avellino historical centre and surrounding area (southern Italy). Correlation with surface geology and damage caused by the 1980 Irpinia-Basilicata earthquake. Measurement. 130: 211–222 (**12 pages**).

Muksin, U.; Bauer, K.; Haberland, C., (2013). Seismic Vp and Vp/Vs structure of the geothermal area around Tarutung (North Sumatra, Indonesia) derived from local earthquake tomography. J. Volcanol. Geotherm. Res., 260: 27-42 (**17 pages**).

Muksin, U.; Haberland, C.; Nukman, M.; Bauer, K.; Weber, M., (2014). Detailed fault structure of the Tarutung Pull-Apart Basin in Sumatra, Indonesia, derived from local earthquake data. J. Asian Earth Sci, 96: 123-131 (**9 pages**).

Muksin, U.; Bauer, K.; Muzli, M.; Ryberg, T.; Nurdin, I.; Masturiyono, M.; Weber, M., (2019). AcehSeis project provides insights into the detailed seismicity distribution and relation to fault structures in Central Aceh, Northern Sumatra. J. Asian Earth Sci., 171: 20–27 (**8 pages**).

Nakamura, Y., (2009)**.** Basic structure of QTS (HVSR) and examples of applications. In increasing seismic safety by combining engineering technologies and seismological data. Springer, Dordrecht. 33–51 (**19 pages**).

Parker, R.N.; Hancox, G.T.; Petley, D.N.; Messey, C.I.; Densmore, A.L.; Rosser, J.N., (2015). Spatial distributions of earthquake-induced landslides and hillslope preconditioning in the northwest South Island, New Zealand. Earth Surf. Dyn., 3(4): 501–525 (**25 pages**).

Pasari, S.; Simanjuntak, A.V.; Mehta, A.; Sharma, Y., (2021). A synoptic view of the natural time distribution and contemporary earthquake hazards in Sumatra, Indonesia. Nat. Hazard., 108(1): 309-321 (**13 pages**).

Pearce, N.J.; Westgate, J.A.; Gualda, G.A.; Gatti, E.; Muhammad, R.F., (2020). Tephra glass chemistry provides storage and discharge details of five magma reservoirs which fed the 75 ka Youngest Toba Tuff eruption, northern Sumatra. J. Quat. Sci., 35(1-2): 256-271 (**16 pages**).

Ryberg, T.; Muksin, U.; Bauer, K., (2016). Ambient seismic noise tomography reveals a hidden caldera and its relation to the Tarutung pull-apart basin at the Sumatran Fault Zone, Indonesia. J. Volcanol. Geotherm. Res., 321: 73-84 (**17 pages**).

Ross, Z.E.; Cochran, E.S., (2021). Evidence for latent crustal fluid injection transients in Southern California from long-duration earthquake swarms. Geophys. Res. Lett., 48(12): e2021GL092465.

Sarma, N.S.; Kiran, R.; Rama Reddy, M.; Iyer, S.D.; Peketi, A.; Borole, D.V.; Krishna, M.S., (2018). Hydrothermal alteration promotes humic acid formation in sediments: a case study of the Central Indian Ocean Basin. J. Geophys. Res.: Oceans, 123(1): 110-130 (**21 pages**).

Seivane, H.; García-Jerez, A.; Navarro, M.; Molina, L.; Navarro-Martínez, F., (2022). On the use of the microtremor HVSR for tracking velocity changes: a case study in Campo de Dalías basin (SE Spain). Geophys. J. Int., 230(1): 542-564 (**23 pages**).

Shelly, D.R.; Hill, D. P.; Massin, F.; Farrell, J., Smith, R.B., Taira, T.A. (2013). A fluid-driven earthquake swarm on the margin of the Yellowstone caldera. J. Geophys. Res. Solid Earth. 118(9): 4872-4886 (**15 pages**).

Sieh, K.; Natawidjaja, D., (2000). Neotectonics of the Sumatran fault, Indonesia. J. Geophys. Res.: Solid Earth, 105(B12): 28295–28326 (**32 pages**).

Soeprobowati, T.R. (2015). Integrated lake basin management for save Indonesian lake movement. Procedia Environ. Sci., 23: 368-374 (**7 pages**).

Stankiewicz, J.; Ryberg, T.; Haberland, C.; Fauzi.; Natawidjaja, D. (2010). Lake Toba volcano magma chamber imaged by ambient seismic noise tomography. Geophys. Res. Lett., 37(17) (**5 pages**).

Stanko, D.; Markušić, S.; Strelec, S.; Gazdek, M. (2017). Equivalent-linear site response analysis on the site of the historical Trakošćan Castle, Croatia, using HVSR method. Environ. Earth Sci., 76(18): 1-21 (**21 pages**).

Tün, M.; Pekkan, E., Ozel, O.; Guney, Y., (2016). An investigation into the bedrock depth in the Eskisehir Quaternary Basin (Turkey) using the microtremor method. Geophys. J. Int., 207(1): 589–607 (**19 pages**).

AUTHOR (S) BIOSKETCHES

Simanjuntak, A.V.H., Ph.D. Candidate, [1]Graduate School of Mathematics and Applied Sciences, Universitas Syiah Kuala, Banda Aceh, Indonesia. [2]Meteorological, Climatological, and Geophysical Agency, BMKG, Banda Aceh, Aceh, Indonesia, Tsunami and Disaster Mitigation Research Center, Universitas Syiah Kuala, Gampong Pie, Indonesia.
- Email: *andrean.simanjuntak@bmkg.go.id*
- ORCID: 0000-0003-0623-0037
- Web of Science ResearcherID: NA
- Scopus Author ID: 57195483722
- Homepage: http://bmkg.go.id/

Muksin, U., Ph.D., Associate Professor, Tsunami and Disaster Mitigation Research Center, Universitas Syiah Kuala, Gampong Pie, Indonesia.
- Email: *muksin.umar@unsyiah.ac.id*
- ORCID: 0000-0001-7297-8065
- Web of Science ResearcherID: W-3934-2018
- Scopus Author ID: 55795600300
- Homepage: http://fsd.unsyiah.ac.id/muksinumar/

Arifullah, A., B.Sc. Master Student, Tsunami and Disaster Mitigation Research Center, Universitas Syiah Kuala, Gampong Pie, Indonesia.
- Email: *arifullah.abd@gmail.com*
- ORCID: 0000-0003-4432-1378
- Web of Science ResearcherID: NA
- Scopus Author ID: NA
- Homepage: http://tdmrc.unsyiah.ac.id/

Lythgoe, K., Ph.D. Presidential Post Doctoral, Earth Observatory of Singapore, Nanyang Techonological of Singapore, Singapore.
- Email: *karen.lythgoe@ntu.edu.sg*
- ORCID: 0000-0002-7642-6900
- Web of Science ResearcherID: NA
- Scopus Author ID: 55927374800
- Homepage: https://www.karenlythgoe.com/

Asnawi, Y., Ph.D. Associate Professor, Universitas Islam Negeri Ar-Raniry, Lorong Ibnu Sina, Syiah Kuala, Kota Banda Aceh, Aceh, Indonesia.
- Email: *yusran@ar-raniry.ac.id*
- ORCID: 0000-0003-0806-1716
- Web of Science ResearcherID: NA
- Scopus Author ID: 57217127838
- Homepage: https://uin.ar-raniry.ac.id/

Sinambela, M., Ph.D., Senior Researcher, Meteorological, Climatological, and Geophysical Agency, BMKG, Medan, Indonesia.
- Email: *marzuki.sinambela@bmkg.go.id*
- ORCID: 0000-0003-3363-4440
- Web of Science ResearcherID: NA
- Scopus Author ID: 57189232496
- Homepage: http://bmkg.go.id/

Rizal, S., Ph.D., Professor, Graduate School of Mathematics and Applied Sciences, Universitas Syiah Kuala, Banda Aceh Indonesia.
- Email: *srizal@unsyiah.ac.id*
- ORCID: 0000-0002-7691-9449
- Web of Science ResearcherID: V-7627-2017
- Scopus Author ID: 56950902200
- Homepage: http://fsd.unsyiah.ac.id/syamsul_rizal/

Wei, S., Ph.D., Professor, [1]Asian School of the Environment, Nanyang Technological University of Singapore. Singapore. [2]Earth Observatory of Singapore, Nanyang Technological of Singapore, Singapore.
- Email: *shjwei@ntu.edu.sg*
- ORCID: 0000-0002-0319-0714
- Web of Science ResearcherID: M-2137-2015
- Scopus Author ID: 25925537600
- Homepage: https://dr.ntu.edu.sg/cris/rp/rp00132

HOW TO CITE THIS ARTICLE

Simanjuntak, A.V.H.; Muksin, U.; Arifullah, A.; Lythgoe, K.; Asnawi, Y.; Sinambela, M.; Rizal, S.; Wei, S., (2023). Environmental vulnerability characteristics in active swarm region. Global J. Environ., Sci. Manage., 9(2): 211-226.

DOI: 10.22034/gjesm.2023.02.03

url: https://www.gjesm.net/article_696623.html

Global J. Environ. Sci. Manage. 9(2): 227-240, Spring 2023, Serial #34

Global Journal of Environmental Science and Management
(GJESM)

Homepage: https://www.gjesm.net/

ORIGINAL RESEARCH ARTICLE

Municipal solid wastes quantification and model forecasting

Y.M. Teshome[1,*], N.G. Habtu[2], M.B. Molla[3], M.D. Ulsido[4]

[1]*Climate Change and Bioenergy Development, Wondo Genet College of Forestry and Natural Resources, Hawassa University, Ethiopia*

[2]*Chemical, Environmental and Process Engineering, Institute of Technology, Bahir Dar University, Ethiopia*

[3]*GIS-Remote Sensing and Environmental Management, Wondo Genet College of Forestry and Natural Resources, Hawassa University, Ethiopia*

[4]*Water Supply and Environmental Engineering, Institute of Technology, Hawassa University, Ethiopia*

ARTICLE INFO

Article History:
Received 12 April 2022
Revised 17 June 2022
Accepted 25 August 2022

Keywords:
Income levels
Model development
Socioeconomic factors
Solid waste
Waste composition

DOI: 10.22034/gjesm.2023.02.04

ABSTRACT

BACKGROUND AND OBJECTIVES: The amount of solid waste produced and its impact on communities and the environment are becoming a global concern. This study aims to assess the amount, composition, and prediction models of solid waste generation in the study area.

METHODS: Solid waste data were collected from both residential and non-residential areas using stratified and systematic sampling approaches. Interviews and field measurements were used to obtain socioeconomic and solid waste data from 90 households and 69 samples from non-residential areas.

FINDINGS: The research area's mean household solid waste generation rate is 0.39kilograms per capita per day. Organic waste accounted for the majority of the waste generated in the study area (71.28 percent), followed by other waste (9.77 percent), paper (6.71 percent), and plastic waste (6.41 percent). The solid waste generation rate demonstrated a positive relationship ($p<0.05$) with monthly household income and educational level. However, there was a negative association between family size and age ($p > 0.05$). Based on a high regression coefficient determination value (0.72), low mean absolute error (0.094), sum square error (1.28), and standard error of the estimate (0.908), Model 4 was chosen as the best-fit model among the proposed models.

CONCLUSION: The developed models met multiple linear regression assumptions and could be used to estimate the rate of household solid waste generation. This study generated large amounts of organic waste present in municipal solid waste sources that can contaminate the environment and have an impact on human health while also having a massive energy recovery capability.

NUMBER OF REFERENCES	NUMBER OF FIGURES	NUMBER OF TABLES
51	5	8

*Corresponding Author:
Email: *yirdawmeride@gmail.com*
Phone: +2510581141231
ORCID: 0000-0002-4598-5179

Note: Discussion period for this manuscript open until July 1, 2023 on GJESM website at the "Show Article".

INTRODUCTION

The population of the universe has rapidly expanded, from 3.1 billion in 1960 to almost 7 billion in 2010. By 2050, 9.3 billion people are projected to exist on Earth (Malav *et al.*, 2020). Municipal solid waste (MSW) production worldwide is reportedly between 1.7 and 1.9 billion metric tons per year (Wilson *et al.*, 2016). Also, solid waste generation will increase from 1.3 billion to 2.5 billion metric tons per year by 2025, with developing countries accounting for the majority of the growth (Pandey *et al.*, 2015). The amount of solid waste produced has increased over time due to population growth and urbanization worldwide. However, there are fewer rooms accessible to keep waste (Eboh *et al.*, 2016). Owing to the differences in population growth, geography, climate, and living standards, solid waste generation trends fluctuate from area to area, country to country, and city to city (Noufal *et al.*, 2020). Developed countries can produce more solid waste than developing countries, but because of institutional competency, access to technology, and sufficient costs for sustainable solid waste treatment, most developed countries are effective in regulating waste (Shahzad *et al.*, 2013). Since solid waste managementhas an impact on both the environment and human health, as well as having the potential to considerably increase resource conservation, it is becoming a concern for both national and municipal governments (Ghinea *et al.*, 2016). An effort is being made in Africa for a range of waste streams to develop and put into effect rules, regulations, and policies that facilitate the management and collection of urban solid waste, including recycling, recovery, and environmentally sound disposal (Mukwana *et al.*, 2014). To manage waste effectively, it is important to gather a lot of data from several sources, including accurate estimates of the quantity of waste that will be produced in the future as well as data on the factors that will affect that generation of waste (Grazhdani, 2016). The development of current waste management infrastructures as well as their continued sustainable development and optimization are based on future projections of the generation of MSW (Abasi and El Hanandeh, 2016). For proper decision-making about the management of solid waste in urban areas, it is crucial to know the amountand kind of waste produced (Intharathirat *et al.*, 2015). MSW is diverse in both quantity and composition. The changes in the seasons and household income levels affect it differently (Monavari *et al.*, 2012). Investigators have conducted studies on the factors that influence the rate of waste formation. The studies' findings demonstrate that factors such as educational level, age, family size, and income have a substantial impact on the amount of household waste generated (Zulkifli *et al.*, 2019; Noufal*et al.*, 2020). The categorization and measurement of waste quantity and composition are made more challengingdue tothis fluctuation. Domestic solid waste generation and composition in various regions of the world have been evaluated by severalstudies (Noufal *et al.*, 2020). The studies revealed that analyzing the characteristics of MSW is critical for a variety of reasons, including determining the potential of waste resources for recycling, reuse, and recovery processes; estimating solid waste generation sources; and designing simple treatment facilities. However, solid waste generated in households varies greatly and is largely dependent on socioeconomic status (Amaya *et al.*, 2019). Forecasts of solid waste from mathematical prediction models are regarded as a crucial tool for decision-makers, policy-makers, and stakeholders in creating the best and most comprehensive solid waste management policies (Abbasi and El Hanandeh, 2016). To estimate the solid waste generation rate, several multiple regression models have been built for various cities around the world (Verma *et al.*, 2019). Unfortunately, the social, economic, and geographic heterogeneity of the various regions of the world makes it difficult to draw conclusions or make projections with the suggested models. It is necessary to adapt models and their variables to the circumstances in other places, often with varying degrees of success. Some of the difficulties associated with adapting these models, according to Kumar and Samandder (2017), are related withinadequate or unavailable information in databases from other countries. The majority of the work put into creating models for estimating the generation of solid waste is based on the data that is only available for one country, which makes it unrepresentative of the elements of Ethiopian MSW. There is littlecurrent, trustworthy data on the composition and quantity of solid waste in Ethiopia, including thestudy location. Because there are so few solid wastecharacteristic data points, the Yirgalem town Administration appears to struggle to create effective site-specific SWM programs and initiatives. Similar to other Ethiopian towns, Yirgalem rarely

has access to accurate waste statistics about the rates and types of solid waste that are generated, the effectiveness of solid waste collection, and the quantity of recycled and disposed solid waste. Due to the absence of accurate waste statistics, the rate of generation of solid waste must be anticipated by using predictive techniques based onthe limited amount of available data.When modeling genuine MSW, it iscritical that you employ the right preparation method. Therefore, the study aims to identify the quantity and composition of solid waste, as well as correlate waste quantity with relevant socioeconomic parameters of households, and develop a model for forecasting solid waste generation. The study was carried out in Yirgalem town, in Ethiopia, using information from the two seasons' variations in 2021.

MATERIALS AND METHODS

Study site description

This study was carried out in Yirgalemtown, Sidama Regional State, Ethiopia. It is located at 6º44´-6º46´ N latitude and 38º24´ - 38 °26´ E longitudes (Fig. 1). The study area has an elevation of 1600–1960 meter (m). In addition, it is the biggest settlement in the Daleworeda (Yusuf *et al*., 2018). It is situated 311 kilometers (km) south of Addis Ababa and 47 km from Hawassa, the capital of the Southern Nations, Nationalities, and Peoples'and Sidama regions. The total population of Yirgalem town is 64,507, of whom 31,737 are male and 32,770 are female (Yusuf *et al*., 2018). Yirgalem town has a moderate climate, with minimum and maximum annual temperatures of 14 °C and 30 °C, respectively. The study area experienced bimodal rainfall with peaks in April, June, and August, with an annual rainfall of 1138-1690 millimeters (mm) (Yusuf *et al*., 2018).

Hypotheses

The hypotheses are drawnfrom the study's goal. The rates of solid waste generation inhouseholds in Yirgalem town are constant throughout the wet and dry seasons;there is no significant difference between the solid waste generation rate and socioeconomic income levels; the quantity of solid waste produced and socioeconomic characteristics do not significantly correlate with one another.

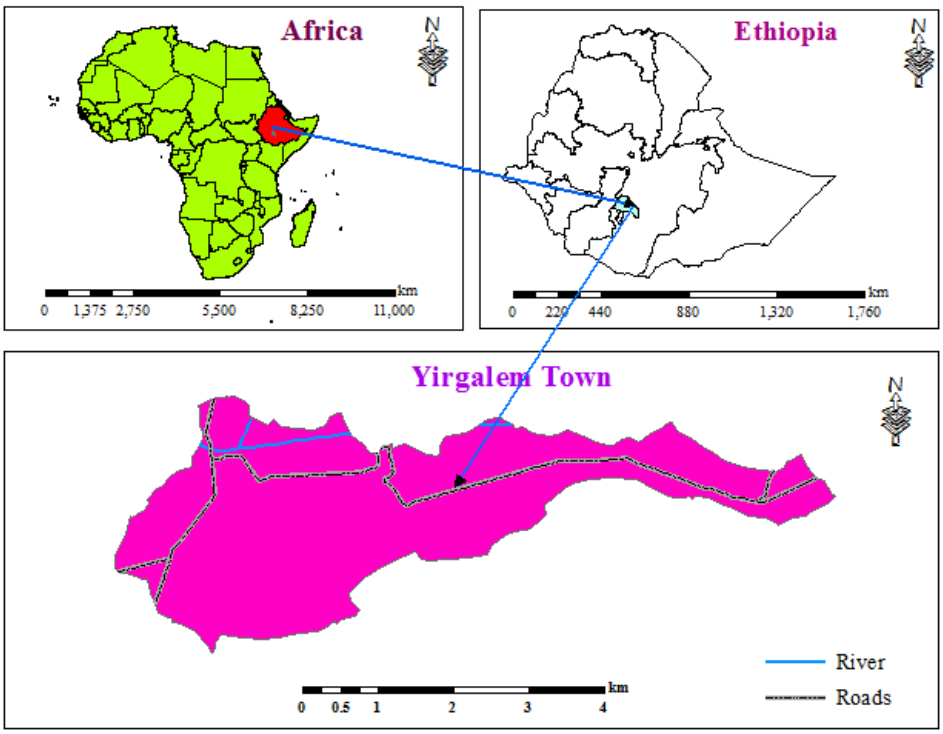

Fig. 1: Geographic location of the study area in Yirgalem town, Sidama Regional State, Ethiopia

Sampling design and techniques

Solid waste data were collected in a longitudinal study.Information on MSW was gathered from both residential and non-residential locations. A stratified sampling technique was used because of the variety of sources used to generate MSW. The municipality was classifiedinto five categories based on the sources of the production of solid waste; residential, commercial areas, institutions, healthcare facilities, and street sweepings (Okey *et al.*, 2013). For each municipal solid waste source, representative samples were gathered using a systematic sampling technique. Household samples were selected based on income, housing types, and the presence of fundamental social services, which serve to divide socioeconomic status into low-, middle-, and high-income categories (Nyankson *et al.*, 2015). The residential zones were divided into three housing types: low-cost landed (low-cost houses), middle-cost landed (living in flats and medium-cost), and high-cost landed (living in high-cost homes) (Yahya *et al.*, 2013). In the study, questionnaires were utilized to collect data on a variety of topics, including the personal and socioeconomic background of the residentials and the overall amount of waste produced.

Sample size determination

According to waste management recommendations, a total of thirty household samples were taken fromeach of the three social-economic groups (low, middle, and high) for a MSW survey (Yahya *et al.*, 2013; Mucyo, 2013). A total of 90 household samples were collected for this study, representing all socioeconomic levels.A previous study (Yahya *et al.*, 2013) that looked intothe generation of solid waste from diverse sources, such as commercial areas, institutions, healthcare facilities, and street sweeping, was the basis for the determination of total samples for non-residential locations. Each waste source was given five sample recommendations. For this investigation, 44 samples from commercial areas, 12 samples from institutions, 9 samples from healthcare facilities, and 7 km of street sweeping were collected twice during the dry and wet seasons.

Solid waste data collection methods

Depending on the amount and type of material generated in the area, MSW was measured at each source using plastic bags with one or more of their daily waste collections. Data on MSW were collected over seven consecutive days (Sachi and Mensah, 2020). To determine the weight of the waste for each solid waste collection location, the collected waste was weighed first. All samples were manually classified into eight waste categories (paper and paper products, plastics, organic (compostable) materials, glass, metals, textiles, wood, and others) at each collectionstationas indicated in Table 1 (Osei-Mensah *et al.*, 2014). To account for seasonal variation, data on solid waste were gathered in two seasons (dry and wet). Dry season data were collected from December 2020 to February 2021, and wet season data were collected from June to August 2021.

Table 1: Waste categories of MSW

Waste categories	Waste description
Organic materials	All biodegradable materials like food waste, yard trimming, grass including *Khat*, agricultural crop residues, manures, and other organic
Paper and paper products	Office paper, computer paper, magazines, glossy paper, waxed paper, and newsprint
Plastics	All plastic materials like polyethylene terephthalate (PET) bottles, high-density polyethylene (HDPE), film plastic, plastic bag,
Glass	All glass materials like windows and mirror glass as well as broken bottles and other containers
Metal	The waste originating from Ferrous (Iron, steel, tin cans, and bi-metal cans), aluminum, and non-ferrous non-aluminum metals
textiles	Waste of clothes, carpets, pillows
wood	The waste which includes sawn timber, wooden boards, furniture
others	Dust, ash, e-wastes, stone

Solidwaste generation and composition calculations

Solid waste generation rate

Household solid waste generation (HSWG) kilogram per capita per day (Kg/c/day) was determined as per the mixed or total waste collected in a day and the separated fractions using Eq. 1 (Miezah*et al*., 2015).

$$\mathrm{HSWG}\left(\frac{\frac{\mathrm{kg}}{\mathrm{c}}}{\mathrm{day}}\right)=\frac{\begin{array}{c}Total\ weight\ of\ HSW\\ generated\ within\ 7\ days\end{array}}{\begin{array}{c}a\ total\ number\ of\ \ families\ in\ the\\ household\ X\ number\ of\ the\ day\end{array}} \quad (1)$$

The total amount of household solid waste (HSW) produced by all houses in a town was calculated using Eq. 2 (Miezah *et al*., 2015).

$$\mathrm{Total\ HSW}\left(\frac{\mathrm{kg}}{\mathrm{day}}\right)=$$

$$\text{Number of population in the town}\ X\frac{\mathrm{HSWG}\frac{\mathrm{Kg}}{\mathrm{c}}}{\mathrm{day}} \quad (2)$$

Composition of solid waste

The total weight of all constituents in the sample was combined to compute the weight of the entire sample. The percentage composition of each componentis calculated using Eq. 3 (Miezah*et al*., 2015).

$$\text{Percentage composition waste fraction} = \frac{\text{weight of separated waste}}{\text{the total mixed weight sample}}\mathrm{X100} \quad (3)$$

Methods of model development

A solid waste generation forecasting model was built based on socioeconomic characteristics, such as household size, monthly income, age of the household head, gender, job status,marital status,andeducational level. All these most common traits have an impact on HSWG rates integrated with other variables (Poplie*t al*., 2021). Multiple linear regression was used to develop solid waste generation models. Multiple linear regression assumptions, such as linear relationshipsbetween dependent and independent variables, normality of the tested data, multicollinearity test, and homoscedasticity, were evaluated before the data were analyzed (Tabachnicke*t al*., 2019). Bivariate Pearson correlation coefficient (r) and a statistical significance test were used to ensure that the dependent and independent variables had a linearrelationship. To make sure the data was normal, a graphic representation of the P-P plot, histograms, and the Kolmogorov-Smirnov test were also utilized. Additionally, the multicollinearity of independent variables was examined using the variance inflation factor (VIF) to identify multivariate correlations and the Pearson correlation coefficient (r) to identify bivariate associations.An illustration of a scatter plot was used to study the homoscedasticity of the standardized residual and predictive values.Four fundamental criteria—the mean absolute error (MAE), the sum of square error (SSE), standard error of the estimate (SEE), and coefficient of multiple determination—were used to select the best-fit model (R^2) (Kulisz and Kujawska, 2020). The average absolute error is expressed using Eq. 4 (Chhay *et al*., 2018).

$$\mathrm{MAE}=\frac{1}{\mathrm{n}}\sum_{\mathrm{i=1}}^{\mathrm{n}}\left|\mathrm{SWG}-\mathrm{SWGp}\right| \quad (4)$$

Where, *SWG* and *SWGp* denote the actual solid waste generation data and the predicted values, respectively. where n represents the number of observations.

The sum of square error can be given using Eq. 5 (Wang *et al*., 2021).

$$SSE=\sum_{i=1}^{n}\left(SWG-SWGp\right)2 \quad (5)$$

The standard error of the estimate can be shown as Eq. 6 (Wang *et al*., 2021).

$$SEE=\sqrt{\frac{\sum_{i=1}^{n}\left(SWG-SWGp\right)2}{n-p}} \quad (6)$$

Where, *p*is the number of parameters in the regression model.

The coefficient of multiple determinations can be expressed using Eq. 7 (Chhay *et al*., 2018).

$$\mathrm{R}^{2}=\frac{\sum_{\mathrm{i=1}}^{\mathrm{n}}\left(\mathrm{SWGp}-\overline{\mathrm{SWG}}\right)2}{\sum_{\mathrm{i=1}}^{\mathrm{n}}\left(\mathrm{SWG}-\overline{\mathrm{SWG}}\right)2} \quad (7)$$

Where, $\overline{\mathrm{SWG}}$ is the arithmetic mean of the observed data.

Statistical analysis

The association between the amount of waste produced and socioeconomic factors such as household size, monthly income, age of the household head, gender, employment status, marital status, and educational attainment was assessed using correlation analysis. One-way analysis of variance (ANOVA) was used to examine the statistically significant variations in waste generation rates based on income class, and the Student's t-test was used to examine seasonal change.Version 25.0 of SPSS statistics for Windows was used to conduct all statistical analyses. The Tukey test was applied to compare statistical differences and means.There is a p-value < 0.05 for each analysis presented in this study.

RESULTS AND DISCUSSION

Solidwaste generation rate

Table 2 displays the average solid waste generation for the three income levels and two seasonal variations. Based on a statistical analysis of variance, it was discovered that there was a significant difference ($p < 0.05$) between the socioeconomic income level and the rate of HSWG. A multiple comparison analyses of the solid generation rate (kg/c/day) between low- and middle-income groups showed a significant difference ($p = 0.000$). The rate of solid waste generation between the low and high socioeconomic income levels also showed a statistically significant difference ($p = 0.000$). Between the middle- and high-income categories, there was no discernible difference in the rate of solid waste generation ($p = 0.222$). According to this finding, the high- and middle-income socioeconomic categories generated more solid waste than the low-income group. This is because the activities of higher-income families consume more resources than those of lower-income families. According to Amaya *et al.* (2019) households generate more solid waste as their socioeconomic status improves. This outcome is consistent with the findings reported by other researchers (Heriantoet *al.*, 2019). Yirgalemtown's mean HSWG rate is 0.39 kg /c/day, with low-income (0.28), middle-income (0.42), and high-income groups (0.47). The result of the predicted solid waste generation rate aids in the development of effective solid waste management strategies. A similar study was reported in Addis Ababa, Ethiopia (Tassie *et al.*, 2019), Shire-Endasilasie, Ethiopia (Zewdu and Mohammedbirhan, 2014), Dhanbad, India (Khan *et al.*, 2016), Ghana cities (Miezah *et al.*, 2015), Thika Municipality, Kenya (Kinyua and Njogu, 2015), and Laga Dadi town, Ethiopia (Assefa and Muktar, 2017). The current solid wastegeneration rate is higher than elsewhere reported for Bahir Dar city (Asmare, 2019), Robetown (Erasu *et al.*, 2018), Chiro town (Umer *et al*., 2019), and Debre Berhan town, Ethiopia (Abera, 2017). Thisstudy is less than the report made in Jima town (Getahun *et al.*, 2012) and Sawla town, Ethiopia (Haile *et al*., 2020). The result found fromthis study is within the range of 0.2-0.8 kg/c/day of solid waste generation for most of Sub-Saharan African countries (Miezah *et al*., 2015) and developing countries within the range of 0.3 to 0.9 kg/c/day (Nadeem and Farhan, 2016). Location, climate, lifestyle, urbanization, and economic development of cities contribute to differences in solid waste generation rates. At $p<0.05$, there was also significant variation in the solid waste generation between the wet and dry seasons. The wet season (0.43) had a higher per capita HSWG rate than did the dry season (0.35 kg/c/day). This is because the wet season produces more vegetables, fruits, *Khat*, grass, and other resources than the dry season does. Several studies (Kamran et al., 2015; Mshelia, 2015; Zia *et al*., 2017), have found that the rate of solid waste generation decreases from the wet season to the dry season. Households generated almost 80% of the solid waste, followed by commercial areas (12.13%) and institutions (4.59%). Previous studies have shown that solid waste generation comes from a variety of sources, including residential areas (50–80%), commercial areas (10–30%), street sweeping, and institutions, all of which have varying proportions (Sachiand Mensah, 2020), which is consistent with the results of this study.

Solid waste composition

The majority of organic wastewas generated by street sweeping (78.79%), followed by institutions (71.26%), commercial areas (69.98%), and residential areas (68.91%) as shown in Table 3. Institutions (22.55%) and commercial areas (5.89%) produced larger amounts of paper waste. As shown in Fig. 2, Yirgalemtown generated a high amount of organic waste (71.28%), followed by miscellaneous waste (9.77%), paper (6.71%), and plastic waste (6.41%). The overall results of the present study indicated that organic (compostable) waste had the highest

Table 2: Analysis of variance of solid waste generation under the three income levels and seasons

Income level	n	solid waste generation (kg/c/day)		f-value	p-value
		Mean*	S.E.**		
Low income	60	0.28[a]	0.017	19.77	0.000
Middle-income level	60	0.42[b]	0.024		
High-income Level	60	0.47[b]	0.023		
Total	180	0.39	0.014		
Seasons					
Wet	90	0.43[a]	0.020	10.741	0.001
Dry	90	0.35[b]	0.018		
Total	180	0.39	0.014		

*Means with different superscript letters are significantly different at (α< 0.05)
**Standard error

Table 3: Types of solid wastes under different generated sources

Types of solid waste	Sources of solid waste (%)			
	Residential	Commercial	Institutions	Street sweeping
Organic	68.91	69.98	71.26	78.79
paper	2.15	5.89	22.55	4.84
plastic	5.85	5.57	6.19	7.12
Glass	1.09	1.13	0.00	1.24
Metal	0.59	7.98	0.00	0.00
Textile	5.07	2.01	0.00	1.09
woods	0.21	0.00	0.00	0.00
others	16.14	7.45	0.00	6.92
total	100.00	100.00	100.00	100.00

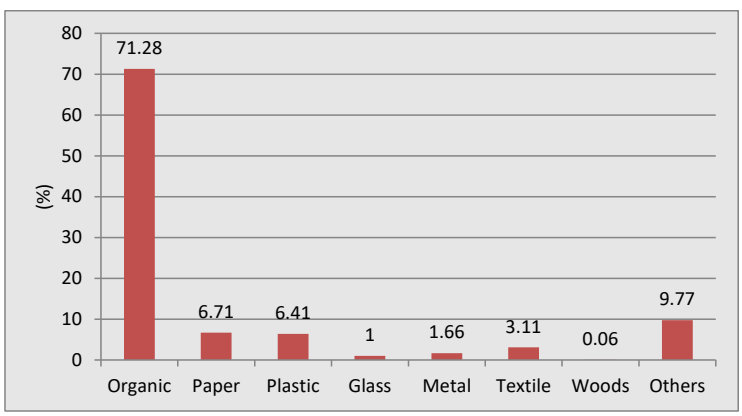

Fig. 2: Overallsolid waste composition in Yirgalem town

percentage. Comparable studies were found in Laga Dadi town, Ethiopia (Assefa and Muktar, 2017), Guayaquil, Ecuador (Amaya *et al.*, 2020), Homs City, Syria (Noufal *et al.*, 2020), Thu Dau Mot, Vietnam (Trang *et al.*, 2017), and Sulaimanyah, Iraq (Hamza, 2020). Lower organic waste was found in this study compared to work done by Umer *et al.* (2019) for Chiro town, Ethiopia.

The *relation between HSWGrate and socioeconomic factors*

Table 4 shows the relationship between the rate of HSWG and socioeconomic factors. Household monthly income (r = 0.476, p = 0.000), educational level (r = 0.327,

Table 4: Relation between HSWG rate and socioeconomic factors

	Socioeconomic factors	Pearson correlation (r)	P-value
Solid waste generation rate (kg/c/day)	Gender	0.181	0.087
	Age	-0.053	0.620
	Marital status	0.183	0.084
	Education level	0.327	0.002
	household size	-0.436	0.000
	House ownership	-0.058	0.587
	Job-status	-0.007	0.950
	Monthly income	0.606	0.000

p = 0.002), and solid waste generation rate all showed positive correlations.Solid waste production increases in direct proportion to household prosperity. This is due to the different home consumption habits, which is consistent with a study conducted by Batu *et al*. (2016). Severalstudiesobtained a negative correlation between household monthly income and the solid generation rate per capita each day (Monavari *et al*., 2012; Trang *et al*., 2017). It means that those with a greater income generated a lower rate of solid waste production per capita than lower-income households. There was a negative relationship between household family size and the solid waste generation rate (r =-0.436, p =0.000). In comparison to large families, more people in their homes live together with shared common resources and consume more items, resulting in fewer waste disposals. This study is consistent with reports from other sources (Ogwueleka, 2013). Numerous studies have discovered a positivecorrelation between the size of a household's family and the rate of solid waste produced per capita (Noufal *et al*., 2020). Households with a large number of people generate more solid waste than those with small families. The differences in the outcomes of various studies are related to differences in economic and cultural standing as well as techniques. A higher level of education in the household results in a higher rate of solid waste generation due to increased household income and work prospects. Several academics endorse this study (Getahun *et al*., 2012). Other socioeconomic factors such as job status, marital status, home ownership, and gender had no significant impact on the solid waste generation rate in this study. Similar studies were carried out by earlier researchers (Batu *et al*., 2016).

Model development

The rate of HSWG was not normally distributed when examined using the Kolmogorov–Smirnov method at a significance level of 0.05. To match the data normality, the logarithm data transformation approach for the solid waste generation rate (response variable) was used. For independent variables, Pearson correlation (r) less than 0.3 and VIF less than 5 revealed no multicollinearity issues (Ghinea *et al*., 2016), which meets the current study as shown in Table 6. Normality in terms of error was assessed using normal probability plots and histograms, as shown in Figs. 3 and 4. The homoscedasticity assumption was further tested using a graphical depiction of the scatter plot between the standardized residual and expected response variables, as illustrated in Fig. 5. Using independent variables such as household size, educational level, monthly income, and age of the household head, four types of models were proposed at a significance level of ANOVA analysis (Table 5). Because these independent variables had the greatest impact on the rate of solid waste production at the study site, which is used in the development model. Model 4 (Eq. 9) is the best-fit model, followed by Model 3 (Eq. 8), as described below, based on a high R^2 and low values of mean absolute error (MAE), the sum of square error (SSE), and standard error of the estimate (SEE), as shown in Table 7.

Model 3:

$$\log Y = 0.600 + 0.007MI + 0.034Edu - 0.152Hs \quad (8)$$

Model 4:

$$\log Y = 0.687 + 0.007MI + 0.031Edu - 0.153Hs - 0.026 \quad (9)$$

Where, logY is the log-transformed solid waste generation rate (kg/c/day), MI is household monthly income (US dollars), Edu is the educational level of the household head, and Hs is the household size. In the final model, variables (monthly income, family size, educational level, and age) of the household head explained 72% of the solid waste generation

Table 5: Analysis of variance for solid waste prediction model development

	Model	Sum of squares	df	Mean square	F	Sig.
1	Regression	1.677	1	1.677	51.167	.000[a]
	Residual	2.885	88	.033		
	Total	4.562	89			
2	Regression	2.970	2	1.485	81.183	.000[b]
	Residual	1.592	87	.018		
	Total	4.562	89			
3	Regression	3.211	3	1.070	68.159	.000[c]
	Residual	1.351	86	.016		
	Total	4.562	89			
4	Regression	3.281	4	.820	54.445	.000[d]
	Residual	1.281	85	.015		
	Total	4.562	89			

Table 6: Estimated regression coefficient of independent variables

Model		Unstandardized coefficients		t	Sig.	Collinearitystatistics	
		B	S.E.			Tolerance	VIF
1	(Constant)	.392	.035	11.227	.000		
	Monthly income	.006	.001	7.153	.000	1.000	1.000
2	(Constant)	.669	.042	15.916	.000		
	Monthly income	.007	.001	10.720	.000	.978	1.023
	Household size	-.150	.018	-8.407	.000	.978	1.023
3	(Constant)	.600	.043	14.042	.000		
	Monthly income	.007	.001	10.576	.000	.940	1.064
	Household size	-.152	.017	-9.226	.000	.976	1.024
	Educational level	.034	.009	3.917	.000	.957	1.045
4	(Constant)	.687	.058	11.822	.000		
	Monthly income	.007	.001	11.010	.000	.908	1.101
	Household size	-.153	.016	-9.432	.000	.976	1.024
	Educational level	.031	.009	3.628	.000	.935	1.069
	Age	-.026	.012	-2.155	.034	.953	1.050

Table 7: Selection of best-fitted multiple linear regression model

Model	Regression equation	R^2	MAE	SSE	SEE	Sum rank	Total rank
1	logY=0.392+0.006MI	0.37(4)	0.140(4)	2.902(4)	1.338(4)	16	4
2	logY =0.669+0.007MI - 0.150HS	0.65(3)	0.107(3)	1.597(3)	1.025(3)	12	3
3	logY=0.600+0.007MI+0.034 Edu - 0.152HS	0.70(2)	0.097(2)	1.366(2)	0.937(2)	8	2
4	logY=0.687+0.007MI+0.031 Edu - 0.153HS-0.026Age	0.72(1)	0.094(1)	1.28(1)	0.908(1)	4	1

rate. This research was similar to that of Lebersorger and Beigl (2011), who reported an R^2 of 74.3 percent. The R^2 rarely exceeded 50%, except in studies with a large number of predictors and a small sample size (Lebersorger and Beigl, 2011), which supports the current study. When compared to the findings of the earlier studies (Beitez *et al.,* 2008), the developed models produced lower solid waste per capita. These discrepancies have occurred as a result of differences in the influencing factors of independent variables in

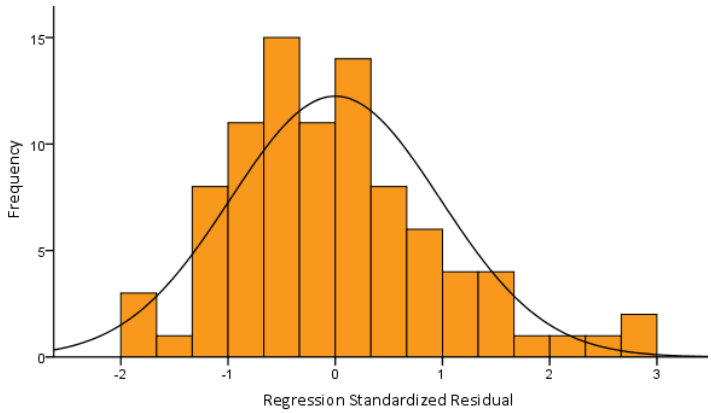

Fig. 3: Residual histogram plots for normality assumption

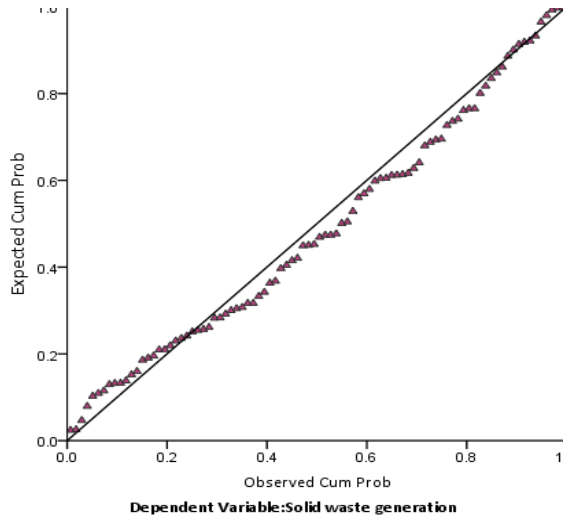

Fig. 4: Residual P-P plots for normality assumption

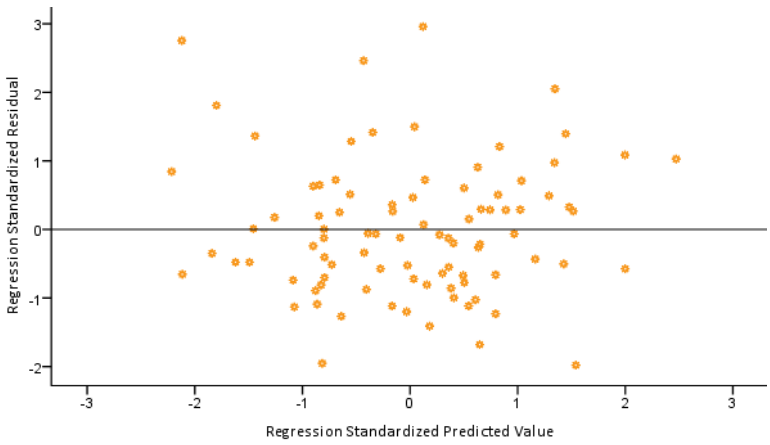

Fig. 5: residual scaterplots for homoscedasticity assumption

Table 8: Comparisons of the observed and predicted value of solid waste generation rate

Models	Paired differences				t	df	Sig.
Model No.	S.D.*	S.E.	95% confidence Interval of the difference				
			Lower	Upper			
Model 3	.12341	.01301	-.01445	.03724	.876	89	.383
Model 4	.12028	.01268	-.02324	.02715	.154	89	.878

*Standard deviation (S.D.)

various locations, nations, cities, and climates. The multiple regression coefficient determination value (R^2 = 0.51) estimated by Beitez *et al.* (2008), which is a minor relative measure of fit compared to this study model (R^2 = 0.72), was also used to explain variances in model prediction values. The different independent variables utilized during the model development caused this difference in coefficient determination (R^2). This way, the study was conductedto close the information gaps that the nation and the study area were encountering.The model established in this study can be used to estimate solid waste generation rates in Yirgalem and other similar towns.

Validation of developed models

The residual errors' behavior, notably their normal distribution, independence, and homoscedasticity—the gap between the dependent variable's observed and predicted values—determines the validity of the MLR models (Kumar and Samandder, 2017). To ensure the validity and correctness of the findings, the values of R^2 (a relative measure of fit) and performance indicators (an absolute measure of fit), such as mean absolute error (MAE), sum of square error (SSE), and standard error of the estimate (SEE), were computed (Table 7). Using a pair-wise t-test of the anticipated and actual values of a response variable (solid waste generation rate), the superior model was further validated.In Models 3 and 4, there was not a statistically significant difference ($p > 0.05$) between the dependent variable's observed and predicted values. Due to the higher value of $p = 0.878$, model 4 is more precise and accurate in this investigation, as shown in Table 8.

CONCLUSION

The characterization of solid waste is crucial for long-term sustainable planning and development. The analysis of the solid waste in Yirgalem town and its characteristics, along with the Pearson correlation results, show the significant impact of socioeconomic factors on waste generation. The most important aspect in identifying the best alternatives for solid waste treatment and investment is the composition of the waste. Low-income groups generated less solid waste per capita than high- and middle-class groups. In contrast to the dry season, the wet season showed a higher per capita generation rate of household solid waste. The majority of MSW was generated by households, followed by commercial areas and institutions in this study area. The overall results of the current study revealed that organic (compostable) waste received the highest percentage of coverage. The rate of solid waste generation was positively correlated with the monthly household income and educational level. While household size and age of the household headwere negatively associated with the rate of solid waste generation, theresult indicated that households with a large number of people generate more solid waste than those with small families. Other socioeconomic factors such as job status, marital status, home ownership, and genderhad no significant impact on the solid waste generation rate. Four models were developed using the most influential socioeconomic factors such as household monthly income, household size, age, and level of education as predictors and solid waste generation as a response variable. Based on the high regression coefficient determination, least mean absolute error, sum square error, and standard error of the estimate, the last equation (model 4) was selected as the best-fit model among these models. The model developed in this study can be used to estimate solid waste generation rates in the study area and other towns of comparable size. Although, the models generated in this study only consider socioeconomic factors, other researchers should integrate other environmental factors to improve model prediction accuracy.Large amounts of biodegradable (organic) waste present in municipal solid waste sources can contaminate the

environment and have an impact on human health, while also having a massive energy recovery capability. MSW composition should be segregated further into sub-categories of solid waste, which is crucial for in-depth analysis. The town administration of Yirgalem should utilise this organic waste as compost for urban agriculture and the manufacture of biogas fuel to decrease the amount of solid waste and energy consumption. This study can serve as a basis for more research in the field as it provides a solid foundation for comparison.

AUTHOR CONTRIBUTIONS

Y.M. Teshome performed the data collection, experimental design, sampling campaigns, solid waste analysis, and prepared the manuscript text. N.G. Habtu performed the literature review and the model configuration and simulations, analyzedand interpreted the data and results, and edited the manuscript. M.B. Mollaorganized the methodology, analyzed, and interpreted the data and results, prepared the manuscript text, and edited the manuscript. M.D. Ulsido organized the methodology, analyzed and interpreted the data and results, prepared the manuscript text, and edited the manuscript.

ACKNOWLEDGMENTS

Hawassa University, Wondo Genet College of Forestry and Natural Resources, University of Gondar, and the German Academic Exchange Service (DAAD) provided financial support [1712874] and educational opportunities. The authors appreciated the invaluable feedback from anonymous reviewers.

CONFLICT OF INTEREST

The authors declare no potential conflict of interest regarding the publication of this work. In addition, the ethical issues including plagiarism, informed consent, misconduct, data fabrication and, or falsification, double publication and, or submission, and redundancy have been completely witnessed by the authors.

ABBREVIATIONS

%	Percent
′	Minute
°	Degree
°C	Degree celsius
ANOVA	Analysis of variance
DAAD	German Academic Exchange Service
df	Degree of freedom
E	East
Edu	Educational level
Eq.	Equation
Fig.	Figure
HDPE	High-density polyethylene
Hs	Household size
HSW	Household solid waste
HSWG	Household solid waste generation
Kg/c/day	Kilogram per capita per Day
kg	Kilogram
m	Meter
Km	Kilometer
logY	Logarithm of solid waste generation
MAE	Mean absolute error
MI	Household monthly income
mm	millimeters
MSW	Municipal solid waste
n	Number of samples
N	North
p	Number of regression parameters
PET	Polyethylene terephthalate
r	Pearson correlation coefficient
R^2	Coefficient of multiple determinations
S.D.	Standard deviation
S.E.	Standard error
SEE	Standard error of the estimate
Sig.	Significance value
SPSS	Statistical package for the social sciences

SSE	Sum of square error
Student's t-test	Parametric tests based on the Student's or t-distribution
SWG	Solid waste generation
SWG_p	Solid waste generation prediction value
VIF	Variance inflation factor

REFERENCES

Abbasi, M.; El Hanandeh, A., (2016). Forecasting municipal solid waste generation using artificial intelligence modelling approaches. Waste Manage., 56: 13–22 **(10 pages).**

Abera, K.A., (2017). Household solid waste generation rate and onsite handling practices in Debre Berhan Town, Ethiopia. Sci. J. Public Health. 1(5): 1-9 **(9 pages)**.

Amaya, J.L.; Hidalgo, J.; Jervis, F.; Moreira, C., (2019). Influence of socio-economic factors on household solid waste generation of the city of Guayaquil, Ecuador. in: Proceedings of the 17th LACCEI International Multi-Conference for Engineering, Education, and Technology: "Industry, Innovation, and Infrastructure for Sustainable Cities and Communities". Latin American and Caribbean Consortium of Engineering Institutions.

Asmare, M., (2019). Bahir Dar City municipal solid waste potential assessment for clean Energy. Am. J. Energy Eng., 7(1): 1-8 **(8 pages)**.

Assefa, M.; Muktar, M., (2017). Solid waste generation rate and characterization study for LagaTafo Laga Dadi Town, Oromia, Ethiopia. Int. J. Environ. Prot. Policy. 5(6): 84-93 **(10 pages)**.

Batu, M.M.; Admasu, E.; Tolosa, F., (2016). Determinants of households' willingness to pay for improved solid waste management in Ethiopia: The case study of Jimma Town. J Environ. Earth Sci., 6(7): 1–14 **(14 pages).**

Benitez, S.O.; Lozano-Olvera, G.; Morelos, R.A.; Vega, C.A., (2008). Mathematical modeling to predict residential solid waste generation. Waste Manage., 28: 7–13 **(7 pages)**.

Chhay, L.; Reyad, M.A.; Suy, R.; Islam, M.R.; Mian, M.M., (2018). Municipal solid waste generation in China: Influncing factors analysis and multi-model forecasting. J. Mater. Cycles Waste Manage., 20(3): 1761-1770 **(10 pages).**

Eboh, F.C.; Ahlstrom, P.; Richards, T., (2016). Estimating the specific chemical exergy of municipal solid waste. Energy Sci. Eng., 4(3): 217–231 **(15 pages)**.

Erasu, D.; Feye, T.; Kiros, A.; Balew, A., (2018). Municipal solid waste generation and disposal in Robe town, Ethiopia. J. Air Waste Manage. Assoc., 68(12): 1391–1397 **(7 pages)**.

Getahun, T.; Mengistie, E.; Haddis, A.; Wasie, F.; Alemayehu, E.; Dadi, D.; Van Gerven, T.; Van der Bruggen, B., (2012). Municipal solid waste generation in growing urban areas in Africa: Current practices and relation to socioeconomic factors in Jimma, Ethiopia. Environ. Monit. Assess., 184(10): 6337–6345 **(9 pages)**.

Ghinea, C.; Dragoi, E.N.; Comanita, E.D.; Gavrilescu, M.; Campean, T.; Curteanu, S.; Gavrilescu, M., (2016). Forecasting municipal solid waste generation using prognostic tools and regression analysis. J. Environ. Manage., 182: 80–93 **(14 pages)**.

Grazhdani, D., (2016). Assessing the variables affecting on the rate of solid waste generation and recycling: An empirical analysis in Prespa Park. Waste Manage., 48: 3–13 **(11 pages)**.

Haile, M.Z.; Mohammed, E.T.; Gebretsadik, F.D., (2020). Physicochemical characterization of municipal solid waste in Sawla town, Gofa Zone, Ethiopia. J. Appl. Sci. Environ. Manage., 23(11): 2023-2029 **(7 pages)**.

Hamza, A.A., (2020). Municipal solid waste quantity, ingredients, and site disposal problems in Pshdar District in Sulaimanyah: Iraqi Kurdistan Region, Iraq. Kufa J. Eng., 11(4): 1–18 **(18 pages)**.

Herianto, H.; Maryono, M.; Budihardjo, M.A., (2019). Factors affecting waste generation: household study in Palangka Raya City, Central Kalimantan. E3S Web of Conference 125: 07007 **(5 pages)**.

Intharathirat, R.; Abdul Salam, P.; Kumar, S.; Untong, A., (2015). Forecasting of municipal solid waste quantity in a developing country using multivariate grey models. Waste Manage., 39: 3–14 **(12 pages)**.

Kamran, A.; Chaudhry, M.N.; Batool, S.A., (2015). Effects of socio-economic status and seasonal variation on municipal solid waste composition: a baseline study for future planning and development. Environ. Sci. Eur., 27(1): 1-16 **(16 pages)**.

Khan, D.; Kumar, A.; Samadder, S.R., (2016). Impact of socioeconomic status on municipal solid waste generation rate. Waste Manage., 49: 15–25 **(11 pages)**.

Kinyua, R.; Njogu, Paul., (2015). An analysis of solid waste generation and characterization in Thika Municipality of Kiambu County, Kenya. J. Environ. Sci. Eng., 4(4): 210-215 **(6 pages)**.

Kulisz, M.; Kujawska, J., (2020). Prediction of municipal waste generation in Poland using neural network modeling. Sustainability. 12(23): 10088 **(16 pages).**

Kumar, A.; Samadder, S.R., (2017). An empirical model for prediction of household solid waste generation rate – A case study of Dhanbad, India. Waste Manage., 68: 3–15 **(13 pages)**.

Lebersorger, S.; Beigl, P., (2011). Municipal solid waste generation in municipalities: Quantifying impacts of household structure, commercial waste and domestic fuel. Waste Manage., 31(9): 1907–1915 **(9 pages)**.

Malav, C.L.; Yadav, K.K.; Gupta, N.; Kumar, S.; Sharma, G.K.; Krishnan, S.; Rezania, S.; Kamyab, H.; Pham, Q.B.; Yadav, S.; Bhattacharyya, S.; Yadav, V.K.; Bach, Q.V., (2020). A review on municipal solid waste as a renewable source for waste-to-energy project in India: Current practices, challenges, and future opportunities. J. Clean. Prod., 277: 123227 **(80 pages)**.

Miezah, K.; Obiri-Danso, K.; Kadar, Z.; Fei-Baffoe, B.; Mensah, M.Y., (2015). Municipal solid waste characterization and quantification as a measure towards effective waste management in Ghana. Waste Manage., 46: 15–27 **(13 pages)**.

Monavari, S.M.; Omrani, G.A.; Karbassi, A.; Raof, F.F., (2012). The effects of socioeconomic parameters on household solid-waste generation and composition in developing countries: A case study Ahvaz, Iran. Environ. Monit. Assess., 184(4): 1841–1846 **(6 pages)**.

Mshelia, A.D., (2015). Seasonal variations of household solid waste generation in Mubi, Nigeria. Int. J. Innovations Educ. Res., 3(5): 115–124 **(10 pages)**.

Mucyo, S., (2013). Analysis of key requirements for effective implementation of biogas technology for municipal solid waste management in Sub-Saharan Africa. A Case Study of Kigali City, Rwanda. Abertay University, Rwanda.

Mukwana, K.C.; Samo, S.R.; Tunio, M.M.; Jakhrani, A.Q.; Luhur, M.R., (2014). Study of energy potential from municipal solid waste of Mirpurkhas city. J. Eng. Sci. Technol., 13(2): 3 **(3 pages).**

Nadeem, K.; Farhan, K., (2016). Waste amount survey and physio-chemical analysis of municipal solid waste generated in Gujranwala-Pakistan. Int. J. Waste Resour., 6(1): 1-8 **(8 pages)**.

Noufal, M.; Yuanyuan, L.; Maalla, Z.; Adipah, S., (2020). Determinants of household solid waste generation and composition in Homs City, Syria. J. Environ. Public Health. 2020: 1–15 **(15 pages)**.

Nyankson, E.A.; Fei-Baffoe, B.; Gorkeh-Miah, J., (2015). Household solid waste generation rate and physical composition analysis: Case of Sekondi-Takoradi Metropolis in the Western Region, Ghana. Int. J. Environ., 4 (2): 1-15 **(15 pages)**.

Ogwueleka, T.C., (2013). Survey of household waste composition and quantities in Abuja, Nigeria. Resour. Conserv. Recycl., 77: 52–60 **(9 pages)**.

Okey, E.N.; Umana, E.J.; Markson, A.A.; Okey, P.A., (2013). Municipal solid waste characterization and management in Uyo, Akwalbom State, Nigeria. WIT Trans. Ecol. Environ., 173: 639–648 **(10 pages)**.

Osei-Mensah, P.; Adjaottor, A.A.; Owusu-Boateng, G., (2014). Characterization of solid waste in the Atwima-Nwabiagya District of

the Ashanti Region, Kumasi-Ghana. Int. J. Waste Manage. Technol., 2: 1–14 **(14 pages)**.
Pandey, B.K.; Vyas, S.; Pandey, M.; Gaur, A., (2016). Municipal solid waste to energy conversion methodology as physical, thermal, and biological methods. Curr. Sci. Perspect. 2: 1–6 **(6 pages)**.
Popli, K.; Park, C.; Han, S.M.; Kim, S., (2021). Prediction of solid waste generation rates in urban region of laos using socio-demographic and economic parameters with a multi linear regression approach. Sustainability. 13(6): 3038 **(15 pages)**.
Sachi, P.J.; Mensah, E.A., (2020). Household characteristics and waste generation paradox: What influences solid waste generation in Bolgatanga.Int. J. Environ. Waste Manage., 26(2): 212–233 **(22 pages)**.
Shahzad, S.; Butt, A.; Anwar, S.; Ahmad, S.; Sarwar, T.; Asghar, N., (2017). Municipal solid waste as a renewable source of energy: an overview from the Lahore District in Punjab, Pakistan. Pol. J. Environ. Stud., 26(6): 2721–2729 **(9 pages)**.
Tabachnick, B.G.; Fidell, L.S.; Ullman, J.B., (2019). Using multivariate statistics, Seventh edition. ed. Pearson, N.Y.
Tassie, K.; Endalew, B.; Mulugeta, A., (2019). Composition, generation and management method of municipal solid waste in Addis Ababa City, Central Ethiopia: A Review. Asian J. Environ. Ecol., 9(2): 1–19 **(19 pages)**.
Trang, P.T.; Dong, H.Q.; Toan, D.Q.; Hanh, N.T.; Thu, N.T., (2017). The effects of socio-economic factors on household solid waste generation and composition: A case study in Thu Dau Mot, Vietnam. Energy Procedia., 107: 253–258 **(7 pages)**.
Umer, N.; Shimelis, G.; Ahmed, M.; Sema, T., (2019). Solid waste generation rate and management practices in the case of Chiro Town, West Hararghe Zone, Ethiopia. Am. J. Environ. Prot., 8(4): 87-93 **(7 pages)**.
Verma, A.; Kumar, A.; Singh, N.B., (2019). Application of multi linear model for forecasting municipal solid waste generation in Lucknow City: A case study. Curr. World Environ., 14(3): 421–432 **(12 pages)**.
Wang, D.; Tang, Y.T.; He, J.; Yang, F.; Robinson, D., (2021). Generalized models to predict the lower heating value of municipal solid waste. Energy. 21: 1-29 **(29 pages)**.
Wilson, D.C.; Rodic, L.; Modak, P.; Soos, R.; Rogero, A.C.; Velis, C.; Simonett, O., (2015). Global waste management outlook. United Nations Environment Programme.
Yahya, N.; Mohd, A.B.; Abdullah, P.F.; Hj, N.B., (2013). Survey on solid waste composition, characteristics and existing practice of solid waste recycling in Malaysia.Perumahan Dan Kerajaan Tempatan, Malaysia.
Yusuf, E.; Fiseha, F.; Dulla, D.; Kassahun, G., (2018). Utilization of kangaroo mother care and influencing factors among mothers and care takers of low birth weight babies in Yirgalem Town, Southern, Ethiopia. Divers. Equal. Health Care. 15(2): 87-92 **(6 pages)**.
Zewdu, A.; Mohammedbirhan, M., (2014). Municipal solid waste management and characterization in Aksum and Shire-Endaslassie Towns, North Ethiopia. J. Environ. Earth Sci., 4(13): 1-8 **(8 pages)**.
Zia, A.; Batool, S.; Chauhdry, M.; Munir, S., (2017). Influence of income level and seasons on quantity and composition of municipal solid waste: A case study of the capital City of Pakistan. Sustainability. 9(9): 1568 **(13 pages)**.
Zulkifli, A.A.; MohdYusoff, M.Z.; AbdManaf, L.; Zakaria, M.R.; Roslan, A.M.; Ariffin, H.; Shirai, Y.; Hassan, M.A., (2019). Assessment of municipal solid waste generation in Universiti Putra Malaysia and its potential for green energy production. Sustainability. 11(14): 3909 **(15 pages)**.

AUTHOR (S) BIOSKETCHES

Teshome, Y.M., Ph.D. Candidate, Climate Change and Bioenergy Development, Wondo Genet College of Forestry and Natural Resources, Hawassa University, Ethiopia.
- Email:*yirdawmeride@gmail.com*
- ORCID: 0000-0002-4598-5179
- Web of Science ResearcherID: NA
- Scopus Author ID: NA
- Homepage: https://hu.edu.et/index.php/academics/all-programs/316-all-programs-wcofnr

Habtu, N.G., Ph.D., Associate Professor, Chemical, Environmental and Process Engineering, Institute of Technology, Bahir Dar University, Ethiopia.
- Email: *nigus.gabiye@bdu.edu.et*
- ORCID: 0000-0002-0725-8771
- Web of Science ResearcherID: GPF-8910-2022
- Scopus Author ID: NA
- Homepage: https://bit.bdu.edu.et/fcfe/?q=staffprofile/http://bdu.edu.et/

Molla, M.B., Ph.D., Assisstant Professor, GIS-Remote Sensing and Environmental Management, Wondo Genet College of Forestry and Natural Resources, Hawassa University, Ethiopia.
- Email: *mikiasb@hu.edu.et*
- ORCIDD: 0000-0002-6694-4579
- Web of Science ResearcherID: AAY-1347-2020
- Scopus Author ID: NA
- Homepage: https://hu.edu.et/index.php/academics/all-programs/316-all-programs-wcofnr

Ulsido, M.D., Ph.D., Associate Professor, Water Supply and Environmental Engineering, Institute of Technology, Hawassa University, Ethiopia.
- Email:*mihret@gmail.com*
- ORCID:0000-0002-6961-3193
- Web of Science ResearcherID: NA
- Scopus Author ID: 57190020367
- Homepage: https://www.researchgate.net/profile/Mihret-Ulsido-2

HOW TO CITE THIS ARTICLE

Teshome, M.Y.; Habtu, G.N.; Molla, B.M.; Ulsido, D.M., (2023).Municipal solid waste quantification and model forecasting. Global J. Environ. Sci Manage., 9(2): 227-240.

DOI: 10.22034/gjesm.2023.02.04

url: https://www.gjesm.net/article_254253.html

Global J. Environ. Sci. Manage. 9(2): 241-260, Spring 2023, Serial #34

Global Journal of Environmental Science and Management
(GJESM)

Homepage: https://www.gjesm.net/

ORIGINAL RESEARCH PAPER

Components and predictability of pollutants emission intensity

Z. Farajzadeh[1], M.A. Nematollahi[2,*]

[1] *Department of Agricultural Economics, College of Agriculture, Shiraz University, Shiraz, Iran*

[2] *Department of Biosystems Engineering, College of Agriculture, Shiraz University, Shiraz, Iran*

ARTICLE INFO

Article History:
Received 27 June 2022
Revised 05 September 2022
Accepted 16 October 2022

Keywords:
Emission intensity
Energy
Neural network
Pollutants.

DOI: 10.22034/gjesm.2023.02.05

ABSTRACT

BACKGROUND AND OBJECTIVES: The rank of Iran in terms of pollutant emissions, which mainly originate from the consumption of energy products, is much higher than the rank of gross domestic product, placing Iran the fourth in the production and consumption of gas and oil, among the cases with the highest emission intensity in the world. Different driving forces account for the high emission intensity. This study decomposes the changes in the aggregate emission intensity of the selected pollutants into a broader scope of driving forces including energy, urbanization, output, labor, and trade-related variables. The examined pollutants were far beyond carbon dioxide, including nitrogen oxides, sulphur dioxide, and carbon monoxide, emitted from energy product consumption. The aim of this study was to investigate the emission intensity of the selected pollutants and their components.

METHODS: Decomposition analysis was done to decompose the emission intensity into a broader scope of the driving forces far beyond what examined in the literature. For this purpose, two well-known artificial neural networks, multilayer perceptron, and wavelet-based neural network were applied to forecast the emission intensity of the selected pollutants and their components.

FINDINGS: The emission intensity of nitrogen oxides and sulphur dioxide illustrated a decreasing trend. In contrast, a general increasing trend with significant fluctuation was observed for carbon monoxide and carbon dioxide emission intensity. Among the components, energy structure, population-labor ratio, and trade openness showed an intensity decreasing effect, while urban per capita output, urbanization, energy intensity, and industrial output-trade ratio contributed to higher emission intensity of the pollutants. Moreover, the multilayer perceptron and wavelet-based neural networks were recommended to examine the predictability of the emission intensity and its components.

CONCLUSION: It was found that intensive and extensive growth and energy structure were the most significant driving forces of the emission intensity. The forecast results indicated that the emission intensity of nitrogen oxides, sulphur dioxide, and carbon monoxide might be predicted by the applied networks with a prediction error of less than 0.2 percent. However, the prediction error for carbon dioxide emission intensity was much higher.

NUMBER OF REFERENCES	NUMBER OF FIGURES	NUMBER OF TABLES
54	10	2

*Corresponding Author:
Email: *manema@shirazu.ac.ir*
Phone: +9871 3613 8382
ORCID: 0000-0001-5780-2723

Note: Discussion period for this manuscript open until July 1, 2023 on GJESM website at the "Show Article".

INTRODUCTION

Global carbon dioxide (CO_2) emissions increased by 1.9 percent (%) annually over 1990-2016, while the corresponding figure for production was 3.2% (World Bank, 2016), indicating a decreasing trend in CO_2 emissions intensity. However, regarding the role of greenhouse gases (GHGs) in climate change (Naderipour *et al.*, 2020), more efforts are needed to lower the emission intensity. Emission mitigation has received more attention after the Paris Agreement in 2015, leading to a reinforcement of developing countries' involvement (Rodríguez and Pena-Boquete, 2017). Accordingly, Iran intends to abate its GHGs emissions to 4% below baseline by 2030, having the potential of an additional 8% (UNFCCC, 2015). Globally, about 65% of the GHGs are emitted from the production and use of energy (Marrero, 2010). The corresponding figure for Iran is over 80% (Farajzadeh, 2018). Despite the global attempts to diminish the energy intensity, it has been increasing in Iran over decades (Farajzadeh and Nematollahi, 2018). Iran, as the 8th biggest CO_2 emitter in the world (World Bank, 2018a), is ranked the 18th in terms of gross national income (GNI) based on purchasing power parity (PPP) (World Bank, 2019), indicating its higher emission intensity compared to the world. The CO_2 emission intensity of Iran is around 0.56 kg, which is more than twice the world's emission intensity (World Bank, 2018b). To the best of authors' knowledge, the increasing intensity of emissions and their driving forces have not received adequate attention in Iran. Although the CO_2 emission is more important since it plays a central role in global warming (Böhringer and Löschel, 2006), other GHGs such as methane (CH_4), and nitrous oxide (N_2O), acidifying substances such as sulphur dioxide (SO_2), and nitrogen oxides (NO_x), and health-damaging pollutants such as carbon monoxide (CO) are also important (Farajzadeh *et al.*, 2017). These pollutants are highly important in the Iranian economy, which is ranked the fourth in the production and consumption of gas and oil in the world (Farajzadeh, 2018). The estimated energy-related emissions of CO_2, NO_x, SO_2, and CO in 2018 have been equal to 635.2, 2.05, 0.82, and 11.75 million tons, respectively (Iran's Energy Balance, 2018). Considering the medium damage costs (World Bank, 2004), around 43.7% of total damage caused by the selected pollutants are related to NO_x, SO_2, and CO, and the remaining share pertains to CO_2. In other words, in terms of damage cost, other pollutants are also extremely important. Although energy intensity is an important factor in emission intensity, there is a great room for further progress in examining other driving forces, including output structure, urbanization, industrialization, and energy composition (Rodríguez and Pena-Boquete, 2017; Zhang *et al.*, 2019). The decomposition technique is a tool that can help in examining the possible variables affecting the emission intensity. Attempts to examine the emissions intensity have been increasing over the last decade. Xu and Ang (2013) believed that a few studies examined the emission intensity. Accordingly, Steckel *et al.* (2011) suggested to decrease the energy intensity in order to reduce the emissions and especially carbon intensity in China. A similar result was also found by Cheng *et al.* (2014). Rodríguez and Pena-Boquete (2017) suggested that higher output stemming from increased labor productivity led to lower carbon intensity in Asian Dragons countries, while an increase in industrial energy use per worker contributed to the reverse direction. Dong *et al.* (2018) reported the negative effect of per capita gross domestic product (GDP) on Chinese carbon emission intensity. In the same vein, Zhang and Hao (2020) found a negative relationship between SO_2 and chemical oxygen demand (COD) intensities and per capita GDP in Chinese provinces. Han *et al.* (2019) found that 1% increase in GDP resulted in 2.61% increase in carbon emission intensity in China. GDP was also found as the main driving force for carbon intensity among the countries membered in the Organization for Economic Cooperation and Development (OECD) (Pan *et al.*, 2019). Although the economy's structure is mainly examined using output composition or industrial output share, as discussed by Farajzadeh and Nematollahi (2018), urbanization may also reveal the level of economic development. Similar to the income effect, both positive and negative effects have been highlighted for urbanization. For example, some empirical works showed that urbanization could lead to negative environmental consequences (Lean and Smyth, 2010; Mishra *et al.*, 2009), which is mainly assigned to more energy-intensive activities (Holtedahl and Joutz, 2004). On the other hand, urbanization may make it possible to enjoy economies of scale and more efficient use of energy (Jones, 1991). Dong *et al.* (2018) and Han *et al.* (2019) reported the dampening

effect of urbanization on carbon intensity in China. In a different view, it was suggested that the impact of urbanization depended on the level of economic development (Sadorrsky, 2013). However, as implicitly declared by Naderipour *et al.* (2021), urban services include emissions. As for energy intensity, goods-producing and industrial activities are expected to raise energy intensity (Poumanyvong and Kaneko, 2010; Adom, 2015), leading to higher emissions as well. Dong *et al.* (2018) showed that more industrialization of China's economy might be accompanied by higher carbon intensity. However, there is an evidence for energy intensity reduction (Adom and Kwakwa, 2014) and even emissions-reducing effects of industrialization (Zhang *et al.*, 2019). Other components of emission intensity are emission coefficient factor, employment, and energy structure (mix). Zhang *et al.* (2019) reported an emissions-reducing effect for the emission coefficient in China. However, Rodríguez and Pena-Boquete (2017) and Han *et al.* (2019) found a positive relation between this variable and carbon intensity in China. The emission intensity reducing effect of urban employment was found to be enormously significant in China (Han *et al.*, 2019). Similarly, Zhang and Hao (2020) and Long *et al.* (2015) reported a positive impact of unemployment on SO_2 emissions intensity and carbon emissions in China, respectively. There is also an evidence for positive impact of energy mix on carbon intensity (Dogan and Seker, 2016; Dong *et al.*, 2018). There is a great body of literature indicating the significant role of trade openness in energy intensity. The energy intensity reducing effect of trade openness has been suggested for Nigeria (Adom, 2015), Chinese provinces (Herrerias *et al.*, 2013), and emerging economies (Rafiq *et al.*, 2016). However, Shahbaz *et al.* (2019) found that for the United States, trade openness decreased the CO_2 emissions, while foreign direct investment (FDI) adversely affected it. The CO_2 emission increasing role of FDI or trade has been reported for the emerging economies such as Malaysia (Lau *et al.*, 2014), Tunisia (Shahbaz *et al.*, 2014), Brazil, China, Egypt, Mexico, Nigeria, and South Africa (Onafwora *et al.*, 2014). The contribution of the present study to the current literature is fourfold. First, it extends the index decomposition analysis using a broader scope of the driving forces far beyond what examined in the literature. Second, the decomposition of pollutants is extended beyond CO_2 to SO_2, NO_x, and CO. Third, the relevance of the applied components as driving forces in the emissions intensity determination is evaluated. Fourth, the multilayer perceptron (MLP) and the wavelet-based neural networks (WNNs) are designed for all components individually, in which a set of economic determinants are applied. The distinguishing feature of WNNs is that they use a class of functions named "wavelets". The objective of the current study was to examine the components of the selected pollutants' emission intensity. Moreover, a time series covering the period of 1988-2018 was applied as the required data. This study was carried out in Iran in 2020.

MATERIALS AND METHODS

Decomposition method

Decomposition analysis is widely used to identify the driving forces affecting energy consumption and environmental deterioration (Ang and Zhang, 2000; Su and Ang, 2012). There are two major decomposition techniques, i.e., index decomposition analysis (IDA), and structural decomposition analysis (SDA). Generally, IDA is easier to be empirically used compared to SDA (Zhang *et al.*, 2019). IDA approach enjoys various formulations and applications. These methods can be divided into Laspeyres and Divisia families (Ang, 2015; Zhang *et al.*, 2019). The log mean Divisia index (LMDI) method in the Divisia family, which is preferred to other methods (Greening *et al.*, 1997; Ang, 2004), has been broadly used to decompose CO_2 emissions for its advantages in working with the remaining items and zero values (Ang, 2015). It should be noted that the LMDI technique has been adopted in this study. Following the index decomposition method, the emission intensity of the selected pollutants was expressed using Eq. 1 (Rodríguez and Pena-Boquete, 2017; Zhang *et al.*, 2019).

$$P^k = \sum_i \sum_j P_{ij}^k = \sum_i \sum_j \frac{P_{ij}^k}{E_{ij}} \times \frac{E_{ij}}{E_i} \times \frac{E_i}{Y_i} \times \frac{Y_i}{Y} \times \frac{Y}{P} \times P \quad (1)$$

Where, P^k is total amount of *k*th pollutant emissions; P_{ij}^k is amount of *k*th pollutant emitted in production sector *i* by fuel j; E_{ij} is a mount of *j*th energy product consumed in production sector *i*; E_i is total energy products used in production sector *i*; Y_i is output of sector *i*; Y is total output; P is total

population; $\frac{P_{ij}^k}{E_{ij}}$ is *k*th pollutant emission coefficient of energy product *j* in sector *i*; $\frac{E_{ij}}{E_i}$ is the share of *j*th energy product in total energy use of sector *i* (energy structure or energy mix including gasoline, kerosene, fuel oil, gas oil, liquid gas, natural gas, and electricity); $\frac{E_i}{Y_i}$ is energy intensity in sector *i* (sectoral energy intensity); $\frac{Y_i}{Y}$ is the output share of sector *i* in total output (economic structure), and $\frac{Y}{P}$ is per capita output (income).

The emission intensity of pollutant *k* was calculated using Eq. 2 (Zhang *et al.,* 2019).

$$PI^k = \frac{P^k}{Y} = \sum_i \sum_j \frac{P_{ij}^k}{E_{ij}} \times \frac{E_{ij}}{E_i} \times \frac{E_i}{Y_i} \times \frac{Y_i}{Y} \times \frac{Y}{P} \times P \times \frac{1}{Y} \quad (2)$$

GDP growth can be attributed to the extensive use of resources and higher productivity. By multiplying Eq. 2 by L/L, the above-mentioned sources of GDP growth could be obtained using Eq. 3 (Rodríguez and Pena-Boquete, 2017).

$$PI^k = \frac{P^k}{Y} = \sum_i \sum_j \frac{P_{ij}^k}{E_{ij}} \times \frac{E_{ij}}{E_i} \times \frac{E_i}{Y_i} \times \frac{Y_i}{Y} \times \frac{Y}{P} \times \frac{P}{L} \times \frac{L}{Y} \quad (3)$$

Where, $\frac{P}{L}$ is the *inverse of employment* rate and $\frac{L}{Y}$ is the *inverse of labor productivity*. The former element shows the extensive use of labor (extensive growth), and the latter examines the intensive nature of economic growth. The index decomposition was extended using urbanization, industrialization, and trade openness as expressed using Eq. 4 (Li *et al.,* 2017; Zhang *et al.,* 2019).

$$PI^k = \frac{P^k}{Y} = \sum_i \sum_j \frac{P_{ij}^k}{E_{ij}} \times \frac{E_{ij}}{E_i} \times \frac{E_i}{Y_i} \times \frac{Y_i}{U} \times \frac{U}{P} \times \frac{P}{L} \times \frac{L}{Y} \times \frac{Y}{M} \times \frac{M}{T} \times \frac{T}{Y} \quad (4)$$

Where, $\frac{Y_i}{U}$ is the output of sector *i* – urban population ratio; $\frac{U}{P}$ is urbanization; $\frac{Y}{M}$ is the GDP-industrial output ratio or the *inverse of industrialization*; $\frac{M}{T}$ is the industrial output-trade ratio; and $\frac{T}{Y}$ is trade openness (*economic integration*). Applying the logarithmic mean weighting scheme, the emissions intensity components could be presented by Eq. 5 (Ang, 2015; Zhang *et al.,* 2019).

$$\Delta PI^k = \Delta PE^k + \Delta EE + \Delta EY + \Delta YU + \Delta UP + \Delta PL + \Delta LY + \Delta YM + \Delta MT + \Delta TY \quad (5)$$

Emissions intensity changes from the base year 0 to target year *t* could be decomposed using Eq. 6 (Ang, 2015).

$$\begin{aligned}\Delta PI^k &= PI_t^k - PI_0^k \\ &= \sum_{ij} L_{ij} \cdot ln\frac{PE_{ij.t}^k}{PE_{ij.0}^k} + \sum_{ij} L_{ij} \cdot ln\frac{EE_{ij.t}}{EE_{i.0}} + \sum_{ij} L_{ij} \cdot ln\frac{EY_{i.t}}{EY_{i.0}} + \\ &\sum_{ij} L_{ij} \cdot ln\frac{YU_{i.t}}{YU_{i.0}} + \sum_{ij} L_{ij} \cdot ln\frac{UP_t}{UP_0} \\ &+ \sum_{ij} L_{ij} \cdot ln\frac{PL_t}{PL_0} + \sum_{ij} L_{ij} \cdot ln\frac{LY_t}{LY_0} + \sum_{ij} L_{ij} \cdot ln\frac{YM_t}{YM_0} + \\ &\sum_{ij} L_{ij} \cdot ln\frac{MT_t}{MT_0} + \sum_{ij} L_{ij} \cdot ln\frac{TY_t}{TY_0}\end{aligned} \quad (6)$$

Where, $L_{ij} = \left(PI_{ij.t} - PI_{ij.0}\right) / \left(lnPI_{ij.t} - lnPI_{ij.0}\right)$ for $PI_t \neq PI_0$ and $L_{ij} = PI_{ij.t}$ when $PI_t = PI_0$.

Artificial neural network model

In this study, two well-known artificial neural networks (NNs), multilayer perceptron (MLP), and wavelet-based neural network (WNN) were employed to forecast the emission intensity and its components for the selected pollutants. The NNs include some interconnected computing elements (neurons) inspired by the biological brain. The feed-forward type is a topology widely used in the NNs structure for many applications in engineering and science, such as forecasting (Fig. 1). The aim of the learning process is to adjust the weights and biases in the NNs structure, while an error function in the output layer is minimized using Eq. 7 (Nematollahi *et al.,* 2012).

$$E = \sum_{k=1}^{K} \left[(EI_M)_k - (EI_P)_k \right]^2 \quad (7)$$

Where, EI_M is the observed (target) data presented to the NNs as input; EI_P is predicted by the NNs, including the weights and biases; and *K* denotes the number of outputs. To adjust the weights, the back-propagation (BP) as an iterative algorithm was employed using Eq. 8 (Nematollahi *et al.,* 2012).

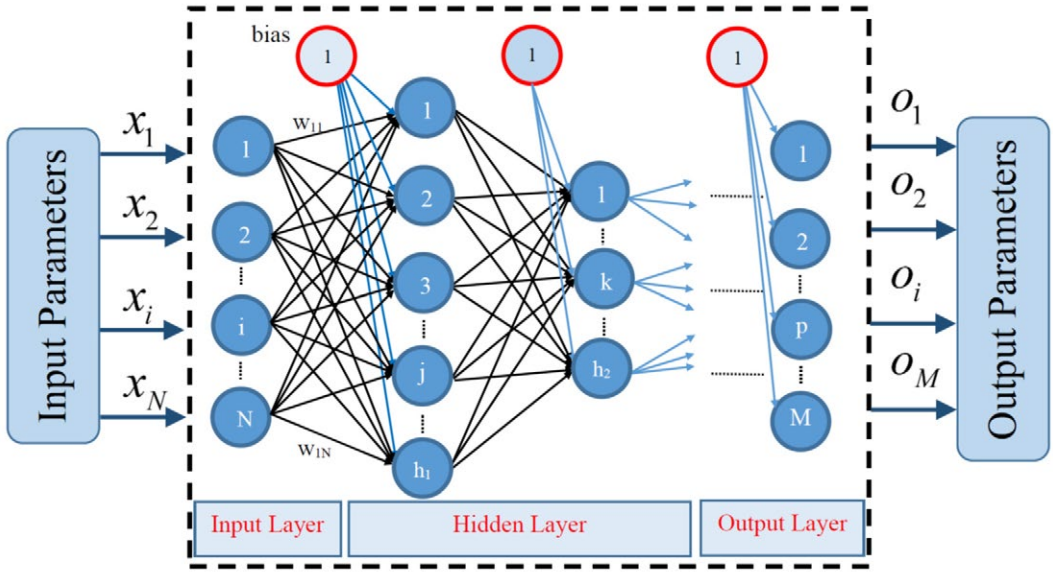

Fig. 1: Structure of the MLP-feedforward network

$$w_{ji}(k+1) = w_{ji}(k) + \Delta w_{ji}(k) \quad (8)$$

The generalized delta learning rule is usually used to compute $\Delta w_{ji}(k)$. Details of the structures and training algorithms of the NNs are presented in Fig. 1 (Rojas, 1996; Nematollahi *et al.,* 2020; Nematollahi and Mousavi Khaneghah, 2019).

The wavelet-based neural network (WNN)

WNN consists of a class of localized basis functions, namely wavelets. The useful features of wavelets are orthonormality, fast implementation, and locality in time and frequency (Daubechies, 1992; Mallat, 1989). A multi-resolution framework was developed by Mallat (1989), in which any function $F(\mathbf{X}) \in \mathrm{L}^2(\mathrm{R})$ could be approximated by wavelets as the basis functions using Eq. 9 (Nematollahi *et al.,* 2012).

$$\mathbf{F}(\mathbf{X}) = \sum_{k=-\infty}^{+\infty} a_{0,k}\varphi_{0,k}(\mathbf{X}) + \sum_{m=-\infty}^{0}\sum_{k=-\infty}^{k=+\infty} d_{m,k}\psi_{m,k}(\mathbf{X}) \quad (9)$$

Where, $\varphi_{0,k}$ and $\psi_{m,k}$ denote the scaling and wavelet functions, respectively; and $a_{0,k}$ $d_{m\,k}$ denote an approximation and detail coefficients, respectively. These coefficients are determined using discrete wavelet transform (DWT). Fig. 2 presents two types of wavelet and their corresponding scaling functions.

The WNN training

The original time series for training the NNs initially pass through two filters and are decomposed into low (approximations) and high-frequency (details) portions (Fig. 3a and 3b).

One signal could be decomposed into lower resolution using multiple-level decomposition (Fig. 3b). Next, the NN was trained with the above-mentioned coefficients. The NN output, after training, was used to reconstruct the approximated signal as compared to the original signal (Fig. 4). To improve the performance of the NN, the training data were normalized.

To examine the accuracy of the predicted values, root mean squared error (RMSE), mean absolute error (MAE), mean absolute percentage error (MAPE), and Theil Inequality coefficient were applied.

Data

The time series related to the aggregate emissions intensity index of the selected pollutants and their components were applied as the data. The data related to the intended period (1988-2018) were obtained from the Central Bank of Iran (2018),

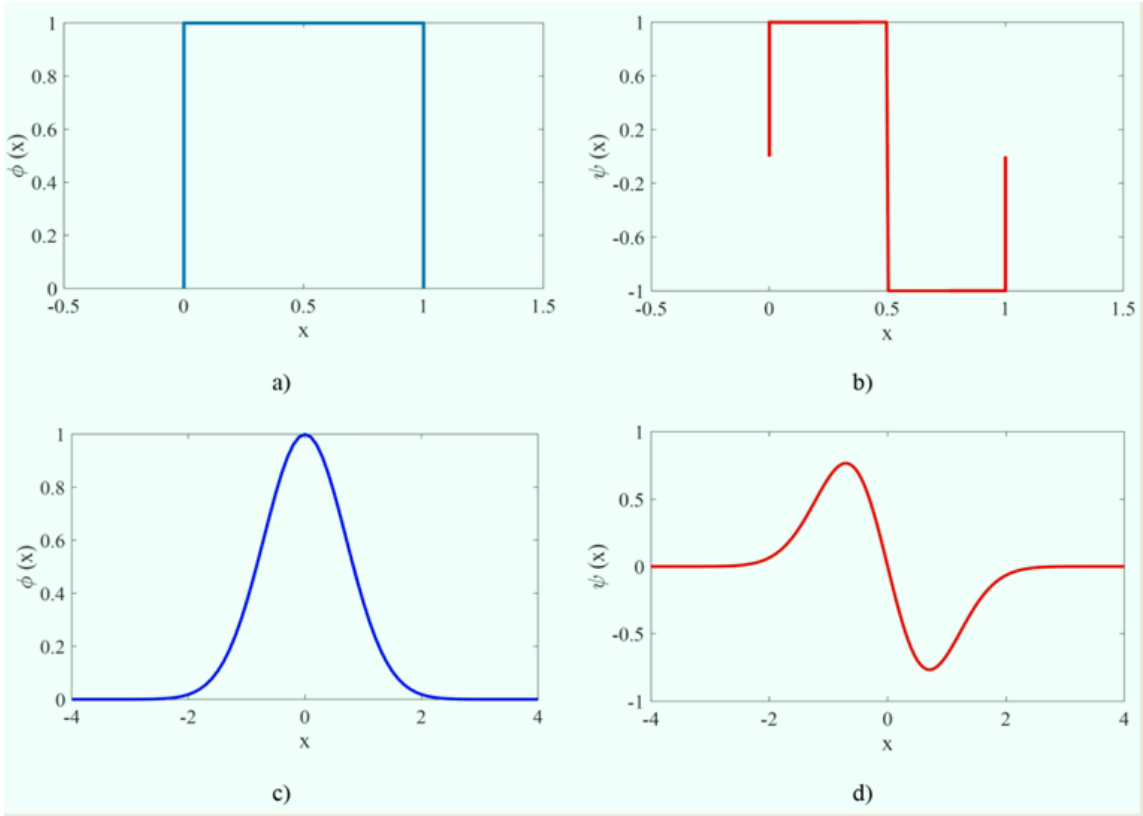

Fig. 2: Two types of wavelet and their corresponding scaling functions: a) Haar scaling function; b) Haar wavelet function; c) Gaussian scaling function; d) Gaussian wavelet function

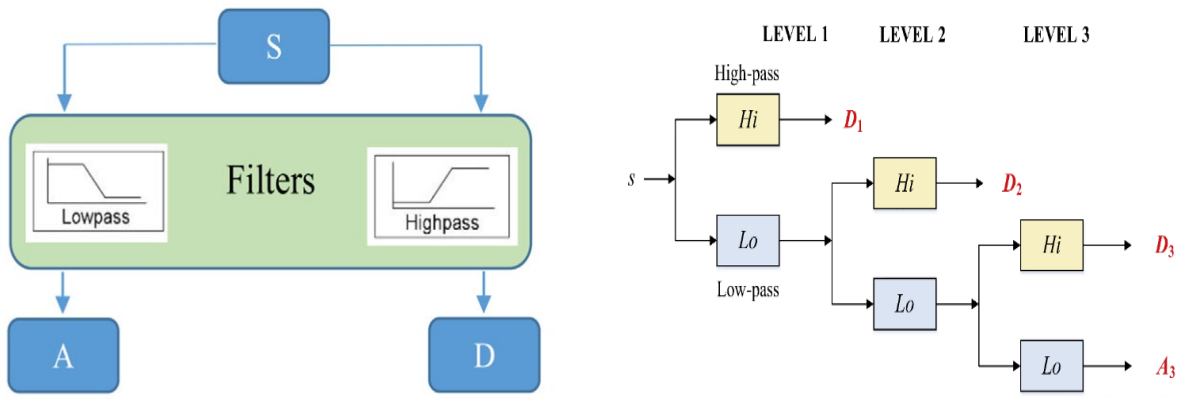

(a) (b)

Fig. 3: a) Transformation of a discrete wavelet into approximation (A) and detail (D) segments; and b) multi-level decomposition of a signal at level 3

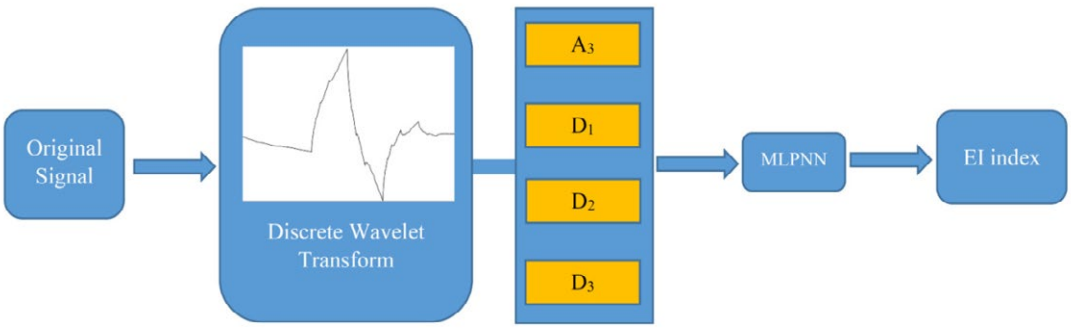

Fig. 4: The schematic structure of the wavelet neural network models

Table 1: Descriptive statistics of the selected pollutants

Pollutants	Average emission intensity	Growth of intensity (%)	Coefficient of variation	Correlation coefficients			
				NO_x	SO_2	CO	CO_2
NO_x	3.05	-0.59	0.06	1.00	0.88	-0.15	0.61
SO_2	3.24	-4.34	0.31	-	1.00	-0.39	0.23
CO	16.66	0.86	0.11	-	-	1.00	0.03
CO_2	765.10	-0.03	0.05	-	-	-	1.00

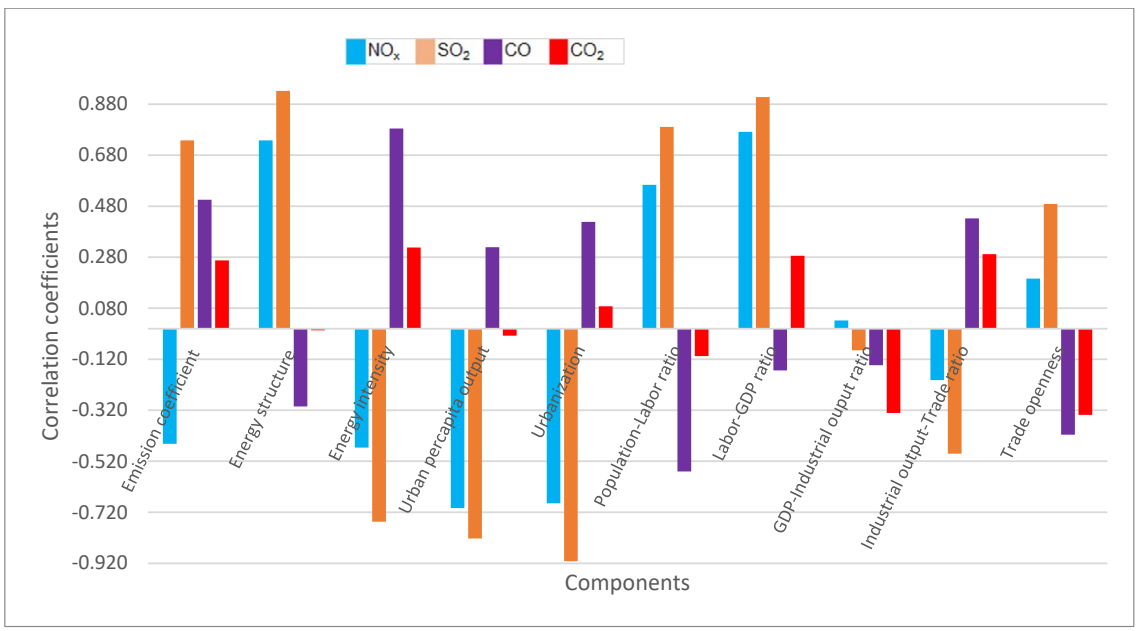

Fig. 5: Correlation coefficients of the components and emission intensity

the Statistical Center of Iran (2018), and Iran's Energy Balance (2018). Subsequently, the data were examined for the selected pollutants including NO_x, SO_2, CO, and CO_2. In NN models, data of 1988-2016 were applied for training and the data of the last two years were used for the forecast evaluation.

RESULTS AND DISCUSSION

Results of emissions intensity

Table 1 presents the descriptive information about the selected pollutants. The emission intensity of SO_2 and NO_x decreased over the study horizon by 4.34% and 0.59%, respectively. This was mainly due to the reduction in fuel oil consumption as the main origin of SO_2 and NO_x emissions. CO_2 emission intensity did not show significant changes, while CO emission intensity increased by 0.86% annually. Gasoline plays a central role in CO emissions, accounting for around 97% of emissions (Iran's Energy Balance, 2018), and the continuing growth of gasoline consumption resulted in CO emission growth. In terms of average emission intensity, CO_2 is tremendously different from other pollutants. However, considering the health damage associated with emissions, the total damage of NO_x, SO_2 and CO was comparable with that of CO_2. Higher fluctuations in SO_2 and CO emissions intensity were mainly due to fuel oil consumption. The dominant role of gasoline in CO emission was the main reason for negativity or insignificance of the correlation between CO coefficient and other pollutants (less than 0.4 in absolute value). Gas oil and gasoline were also responsible for NO_x, CO_2, and SO_2 emissions, resulting in positive and higher correlation coefficients ranging from 0.23 to 0.88. It should be mentioned that natural gas is the main source of CO_2 emission (Iran's Energy Balance, 2018).

The decomposition results of the selected pollutants are presented in Figs. 6-9. Considering the large number of components and pollutants examined, the correlation coefficients of the components and the emission intensity are presented in Fig. 5. As explained by Eq. 6, the changes in emission intensity were decomposed into ten components as influencing factors. It should be noted that the

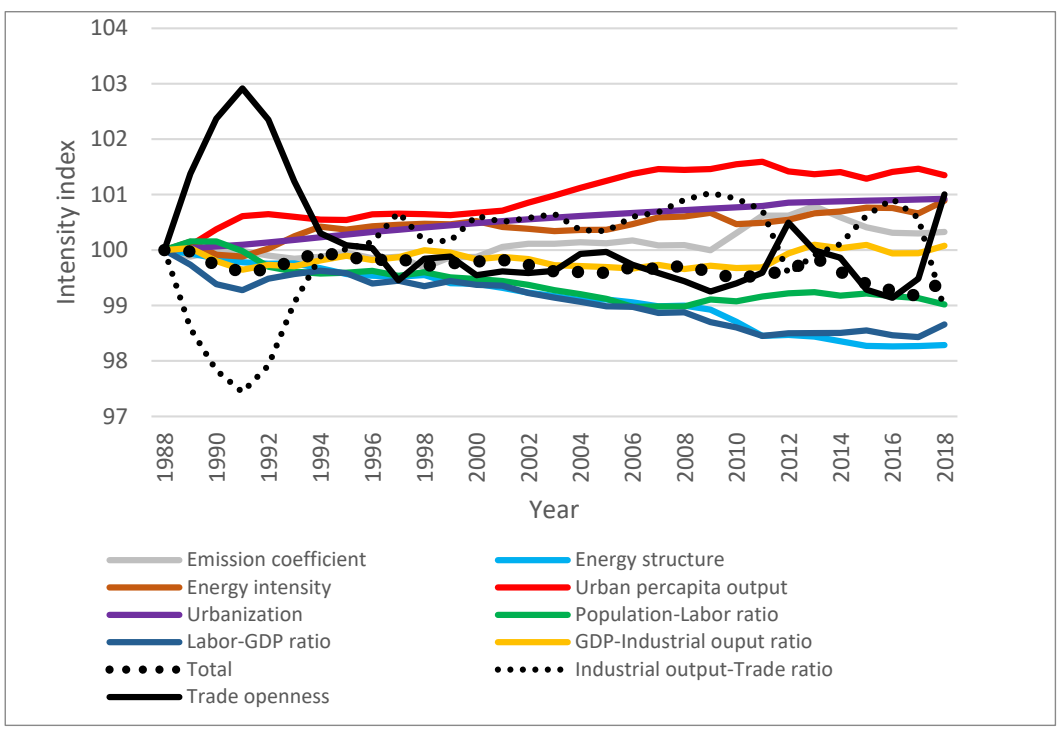

Fig. 6: NO_x emission intensity and its components

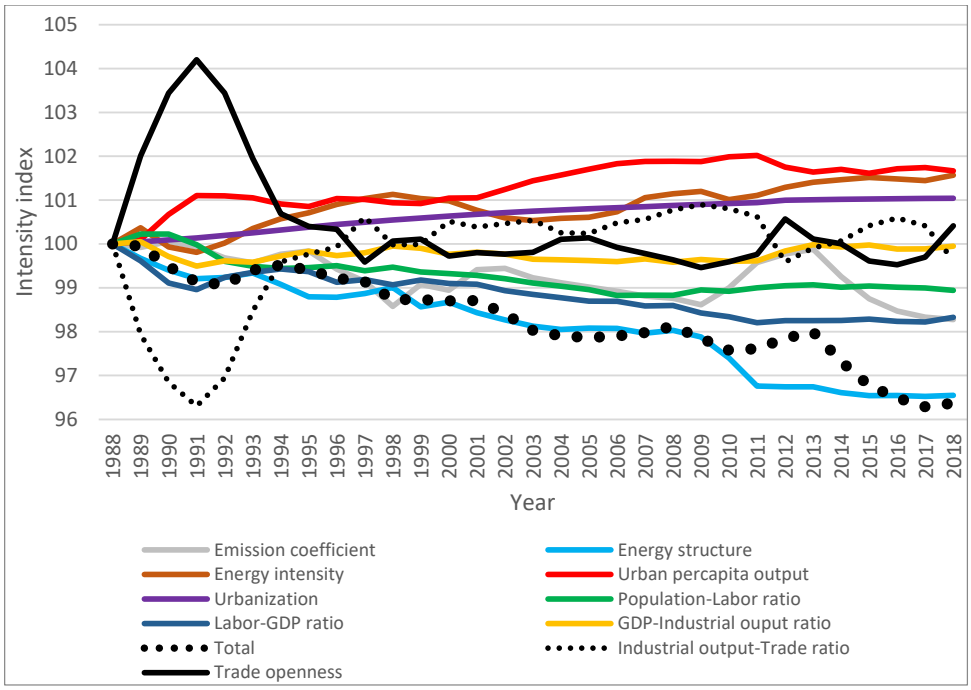

Fig. 7: SO_2 emission intensity and its components

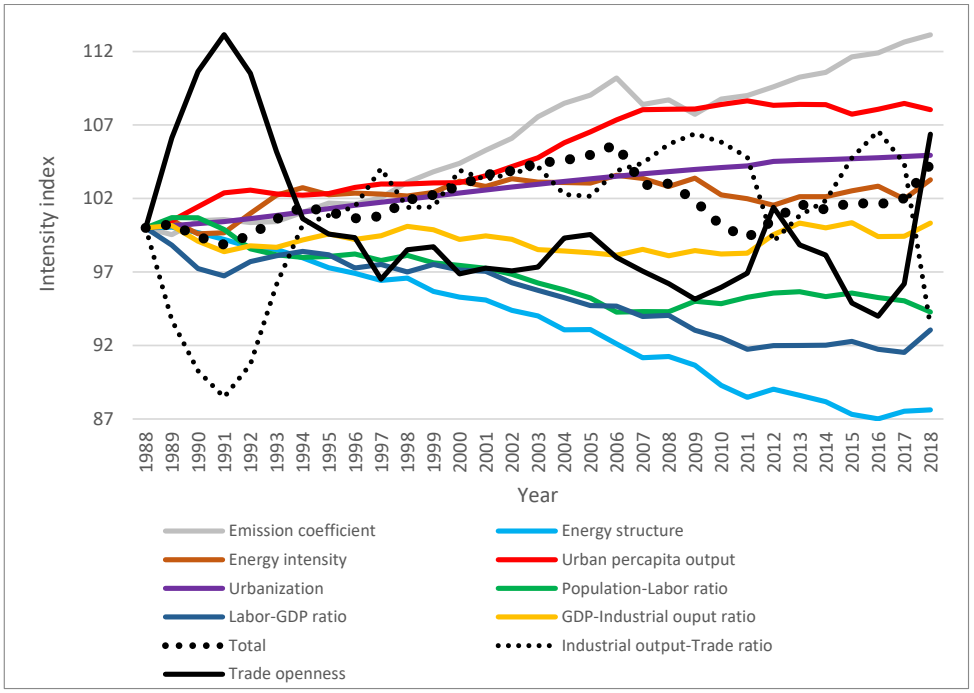

Fig. 8: CO emission intensity and its components

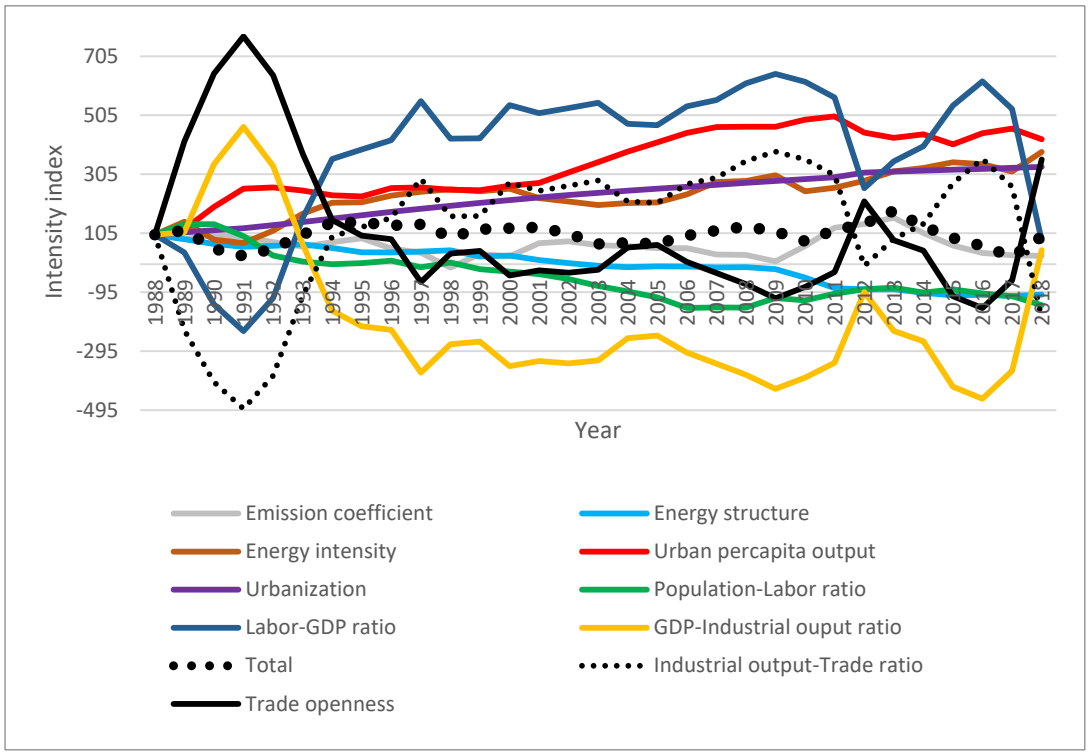

Fig. 9: CO_2 emission intensity and its components

changes in each component and emission intensity are presented in an index format starting from 100 for the base year of 1988. This allowed for observing the changing trend of the influential factors over the study horizon.

Although most of the components had a similar direction of correlation, a higher similarity was observed between NO_x and SO_2 emissions. This also applied to CO and CO_2. Thus, the results of NO_x and SO_2 were discussed together. It should be noted that the common sources of NO_x and SO_2 emissions are gasoline and gas oil, so that over 56% of NO_x and more than two-thirds of SO_2 are emitted from these products. As for CO and CO_2, gasoline and natural gas play a central role in CO and CO_2 emissions, respectively. However, in this study, gasoline and natural gas consumptions were significantly correlated, resulting in similar behavior of CO and CO_2 emissions intensity components (Iran's Energy Balance, 2018).

NO_x and SO_2 emissions intensity components

As shown in Figs. 5 and 6 and 7, there are marked similarities between the results found for NO_x and SO_2. Comparison of the results of NO_x and SO_2 components revealed some points: 1) the total emission intensity of NO_x and SO_2 showed a decreasing trend. However, a steeper trend was observed for SO_2 emissions intensity. 2) only two components (i.e., emissions coefficient, and GDP-industrial output ratio) illustrated a different direction of correlation. Since the emission coefficient reduced the emission intensity of NO_x, it was expected to contribute to higher emission intensity of SO_2 with a significant correlation coefficient as high as 0.74. The reverse order was observed for the GDP-industrial output ratio. However, the magnitude of the coefficients for this component was not significant as it was less than 0.10 in absolute value. 3) the magnitude of the correlation coefficients related to the remaining components of SO_2 was higher than that of the

correlation coefficients related to the components of NO_x. Most of the correlation coefficients for SO_2 were over 70% and for NO_x were less than 70%. During the study period, the contribution of energy products to NO_x emissions changed in favor of natural gas, while the contribution of energy products to SO_2 emissions did not experience a significant change. Considering the decreasing trend of NO_x and SO_2 emissions intensity, a positive correlation implied the reducing effect of emission intensity and vice versa. The components could be classified into three groups in terms of correlation coefficients. The first group included the components that were positively correlated with emission intensity, revealing a decreasing trend similar to the total emission intensity. The inverse labor productivity (Labor-GDP ratio), energy structure, population-labor ratio, and trade openness could be categorized in this group. The reduction in emission intensity due to energy structure changes probably occurred via a change in energy consumption toward the products that contained less NO_x and SO_2 such as liquid gas, kerosene, and even gasoline. The importance of energy composition was also pointed out by Rodríguez and Pena-Boquete, (2017) and Zhang *et al.* (2019). The second group included the components that contributed to higher emission intensity, including urban per capita output, urbanization, energy intensity, and industrial output-trade ratio, which revealed negative correlations. The third group included the emissions coefficient, and GDP-industrial output ratio that were discussed above.

Among the emission intensity-increasing components, urban-related components had the highest contribution as their correlation coefficients tended to be around 0.70 for NO_x and 0.82-0.91 for SO_2. This implicitly meant that while urbanization was expected to be accompanied by more energy use, it entailed a higher output, resulting in lower energy intensity and indicating the economies of scale as suggested by Sadorrsky, (2013). Another urban-related variable was urban per capita output or GDP-urban population ratio, which had the highest contribution to NO_x emission intensity. For SO_2, this variable, with a high correlation coefficient of 0.82, was ranked after urbanization. Urbanization was expected to be accompanied by a higher output as well. Urbanization was correlated with the output expansion in the services sector, in which the activities were more energy and pollution intensive. The correlation between the services sector output and urbanization was found to be 0.94 over 1967-2018 (Central Bank of Iran, 2018). Energy intensity was the next component inducing higher emission intensity with correlation coefficients of 0.47 and 0.76 for NO_x and SO_2, respectively. There is evidence of emission decreasing effect (Zhang *et al.,* 2019) expected to dampen the emission intensity. However, the emission intensity-raising effect of this component, to a great extent, could be attributed to the production technology. Farajzadeh *et al.* (2017) have also suggested that production processes in Iran are not highly technology-embodied ones. Additionally, sanctions might be responsible for a part of such recession in technology, since Iran has faced sanctions for many years (Hufbauer *et al.,* 2012). Energy plays a central role in the Iranian economy. In the study period, while GDP has been growing by 4.1% annually, the corresponding value for energy was obtained as 5.2%. Particularly, the consumption of natural gas (as a great source of emissions for NO_x) in the industrial and services sectors has increased by 10.8% and 11.4% annually, respectively (Iran's Energy Balance, 2018). Contrary to the role of energy intensity in raising the emission intensity, energy structure indicated that changes in energy mix would have an emission-reducing effect as already mentioned. The data showed that the energy composition changed in favor of natural gas and electricity, while the oil products share (accounting for most of the NO_x emissions in the energy basket) decreased. Zhang *et al.* (2019) also pointed out that emissions fading role of energy mix changed in favor of natural gas and electricity. Both labor-related components were positively correlated with NO_x emission intensity with correlation coefficients of higher than 0.56. In other words, these variables contributed to lower emissions intensity. Over the study horizon, population-labor and labor-GDP ratios would be decreased. In other words, an increase in employment and labor productivity would be associated with lower emission intensity. In terms of correlation coefficients (0.77 and 0.91 for NO_x and SO_2, respectively), labor productivity showed a high contribution to the emission intensity reduction, which agreed with the findings of Rodríguez and Pena-Boquete, (2017) for Asian Dragons. In other words, the intensive use of labor or intensive growth

of output might reduce the emission intensity. The extensive use of labor could also induce a reduction in emissions intensity, since it reduced the population-labor ratio. The extensive use of labor meant the replacement of labor for energy, leading to lower energy use and lower pollutant emissions. The contribution of trade-related components to emission intensity was not significant for NO_x. As for SO_2, the coefficients for trade components were much lower than other components' coefficients being less than 50%. However, trade openness was expected to lower the emission intensity slightly. In other words, a higher volume of trade might decrease the emission intensity. Emission reducing effect of trade could be assigned to technology transfer, positive spillover effects, productivity gains, and improved managerial skills (Shahbaz *et al.,* 2019). The slight effect of trade openness on emission intensity could be due to the significant fluctuations in trade mainly caused by sanctions. It should be noted that due to the Iran-Iraq war occurred during 1979-1988, the following years (1989-1991) were characterized by reintroducing the production capacities, leading to higher fluctuations in trade-related components. During the study horizon, the industrial output-trade ratio was increased, revealing a lower increase in trade compared to industrial output. The higher values for this ratio were accompanied by a slight increase in emission intensity since the correlation coefficient was only 20%. Accordingly, this could probably show the emissions intensity role of higher industrial output, which agreed with the effect of the inverse industrialization component (industrial output-GDP ratio) with a positive correlation coefficient. In the study horizon, industrialization and its inverse did not show a significant trend and had a slight effect on emission intensity. The related emission coefficient was expected to be closely related to the energy mix or energy structure. For SO_2, the emission coefficient, such as energy structure component, reduced the emission intensity, while for NO_x, the effect of emission coefficient on emission intensity was increasing. The corresponding coefficients were -0.45 and 0.74, respectively. During the study period, electricity use grew much higher than oil products; this could probably provide an opportunity of having lower emissions-energy use ratio i.e., lower emission coefficient. However, for NO_x, the change in energy product composition in favor of natural gas, which was more emission-embodied, played an emission intensity-increasing role. Both emissions-reducing (Zhange *et al.,* 2019) and emission-increasing effects (Rodríguez and Pena-Boquete, 2017; Han *et al.,* 2019) have been reported for this factor.

CO and CO_2 emissions intensity components

As shown in Figs. 8 and 9, a general increasing trend was observed for CO and CO_2 emission intensity, with the emission intensity of CO being slightly stronger. CO emission intensity experienced significant fluctuations, while it exceeded the base year value in most of the study period. Therefore, contrary to NO_x and SO_2 cases, the positive values for correlation coefficients (Fig. 5) meant an increase in emission intensity of the components and vice versa. Similar to the results of NO_x and SO_2, energy structure, population-labor ratio, labor-GDP ratio, inverse industrialization, and trade openness had an emission intensity-dampening effect, while energy intensity, urban per capita output, urbanization and industrial output-trade ratio were expected to raise emission intensity for both CO and CO_2. However, the contribution of these driving factors, except for inverse industrialization, was much higher for CO compared to CO_2, since the correlation coefficients for most of the components of CO were higher than 0.3 in absolute values compared to those of CO_2 which were less than 0.3. This could be due to the fact that CO was mainly emitted from gasoline, while natural gas played a central role in CO_2 emission and gasoline had a slight effect on CO_2 emission (Iran's Energy Balance, 2018). This difference in emission contribution could be attributed to the fact that the increase in these factors more significantly raised the consumption of gasoline rather than natural gas. Most of these variables were closely connected with urbanization and their expansion resulted in higher urban services which had been heavily dependent on gasoline consumption. However, Dong *et al.* (2018) and Han *et al.* (2019) found that urbanization might result in lower carbon intensity. The emission coefficient also contributed to emission intensity, as seen for NO_x. Considering the discussion presented for NO_x and SO_2, the distinguishing aspects for CO were highlighted. The range of fluctuation for the components of CO emissions was broader than that of fluctuations for NO_x and SO_2 (ranging from 100.2 to 113.2 respectively), while the corresponding

ranges for NO_x and SO_2 were 100-102.9 and 99.8-104.2, respectively. In terms of absolute values of correlation coefficients, the values obtained for CO for most components were much lower than those of SO_2. Comparison of these values with the values of NO_x was not straightforward. Although the urban-related components had a more significant role in emission intensity of NO_x and SO_2, their role in CO emission intensity, with correlation coefficients of around 0.3-0.4, was moderate compared to the other components. Despite the significant role of energy intensity in NO_x and SO_2 emissions, its contribution to the emission intensity of CO was slight (0.32). This might be due to the difference in the energy products emitting pollutants. Gas oil plays an essential role in NO_x and SO_2 emissions, while around 97% of CO is emitted from gasoline (Iran's Energy Balance, 2018). CO_2 emission intensity illustrated a strong fluctuation and an insignificant increasing trend. The components with an increasing (decreasing) trend revealed a positive (negative) correlation with the CO_2 emissions intensity. Due to the considerable fluctuations in emission intensity, the correlation coefficients between the CO_2 components and the total emission intensity were lower as compared to the other pollutants. The coefficients were less than 0.11 for four components including energy structure, urban per capita output, urbanization, and population-labor ratio. The corresponding values for other components were lower than 0.34.

Inverse industrialization or GDP-industrial output ratio showed an emission intensity-dampening contribution. As expected, higher GDP-industrial output ratio was associated with lower emission intensity, since the higher ratio was equivalent to higher GDP and resulted in lower emission intensity. The higher ratio could be interpreted as lower industrialization as well. In other words, industrialization might result in more emission intensity. In 2018, around two-thirds of CO_2 was emitted from natural gas. During the study horizon, the natural gas consumption in industrial production increased by 10.8% annually, while the corresponding value for the output was 4.1% (Iran's Energy Balance, 2018), resulting in higher emission intensity. The higher employment and output as well as the

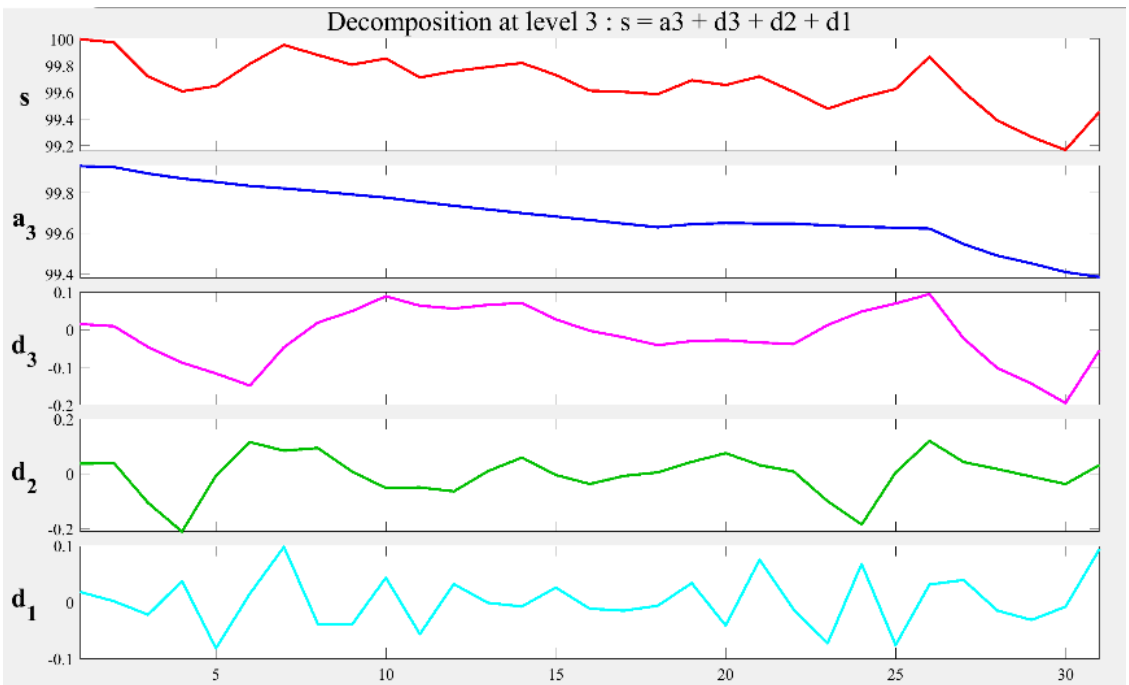

Fig. 10: Decomposition of NO_x time series with 'sym2' wavelet at level 3

Table 2: Training and test forecasting results of the components and total emission intensity

NNs			Components (MLP network)										Total (emissions intensity)		
	criterion	Period	Emission coefficient	Energy structure	Energy intensity	Urban per capita output	Urbanization	Population-labor ratio	Labor-GDP ratio	GDP-industrial output ratio	Industrial output-trade ratio	Trade openness	Based on components	Based on MLP	Based on WNN
NO_x	RMSE	Train	0.0138	0.0045	0.0211	0.0156	0.0021	0.0003	0.0117	0.0007	0.0697	0.0637	-	0.0052	0.0035
		Test	0.0166	0.0085	0.1169	0.0571	0.0056	0.0379	0.1467	0.0533	0.2178	0.1104	0.0803	0.0803	0.0157
	MAPE	Train	0.0114	0.0023	0.0107	0.0065	0.0012	0.0002	0.0088	0.0013	0.0536	0.0263	-	0.0031	0.0026
		Test	0.0137	0.0084	0.1106	0.0440	0.0048	0.0331	0.1425	0.0521	0.1601	0.0897	0.0580	0.0580	0.0154
	MAE	Train	0.0115	0.0016	0.0108	0.0066	0.0013	0.0003	0.0087	0.0003	0.0539	0.0262	-	0.0031	0.0026
		Test	0.0138	0.0081	0.1115	0.0447	0.0049	0.0328	0.1405	0.0522	0.1585	0.0904	0.0575	0.0575	0.0153
	Theil	Train	0.0002	0.0001	0.0001	0.0001	0.0002	0.0004	0.0001	0.0003	0.0004	0.0003	-	0.0002	0.0001
		Test	0.5371	0.3828	0.5799	0.2814	0.2751	0.1914	0.7446	0.2666	0.0011	0.5507	0.0004	0.0004	0.0002
SO_2	RMSE	Train	0.0241	0.0171	0.0376	0.0189	0.0043	0.0286	0.0137	0.0153	0.0895	0.0793	-	0.0732	0.0156
		Test	0.1697	0.0255	0.0270	0.0465	0.0058	0.0421	0.1544	0.1200	0.4122	0.3863	0.0624	0.0844	0.0565
	MAPE	Train	0.0243	0.0051	0.0030	0.0085	0.0015	0.0182	0.0087	0.0077	0.0658	0.0325	-	0.0233	0.0162
		Test	0.1636	0.0234	0.1264	0.0486	0.0049	0.0423	0.1572	0.0853	0.3134	0.3154	0.0645	0.0649	0.0467
	MAE	Train	0.0473	0.0050	0.0130	0.0086	0.0016	0.0181	0.0091	0.0077	0.0559	0.0324	-	0.0213	0.0155
		Test	0.1608	0.0226	0.1268	0.0444	0.0049	0.0421	0.1464	0.0852	0.3125	0.3148	0.0621	0.0625	0.0459
	Theil	Train	0.0031	0.0001	0.0003	0.0002	0.0005	0.0001	0.0003	0.0001	0.0004	0.0003	-	0.0004	0.0002
		Test	0.0010	0.1318	0.1328	0.2288	0.2503	0.0614	0.2771	0.6006	0.0021	0.0019	0.0003	0.0005	0.0003
CO	RMSE	Train	0.0751	0.0235	0.0942	0.0708	0.0068	0.0547	0.0345	0.0434	0.2419	0.3562	-	0.0713	0.0619
		Test	0.1727	0.0308	0.1540	0.0559	0.0059	0.1328	0.7411	0.1834	1.5036	1.4605	0.2046	0.2045	0.1293
	MAPE	Train	0.0360	0.0083	0.0485	0.0435	0.0028	0.0263	0.0122	0.0141	0.1250	0.1408	-	0.0823	0.0469
		Test	0.1860	0.0321	0.1271	0.0498	0.0052	0.1210	0.6820	0.0896	1.4375	1.3174	0.1819	0.1819	0.1006
	MAE	Train	0.0564	0.0064	0.0497	0.0458	0.0029	0.0253	0.0113	0.0146	0.1287	0.1385	-	0.0803	0.0459
		Test	0.1733	0.0306	0.1237	0.0475	0.0053	0.1143	0.6326	0.0861	1.3835	1.2563	0.1867	0.1867	0.1047
	Theil	Train	0.0004	0.0006	0.0005	0.0003	0.0002	0.0003	0.0002	0.0002	0.0012	0.0018	-	0.0005	0.0003
		Test	0.3221	0.6145	0.7500	0.2581	0.2513	0.7018	0.0040	0.0005	0.0076	0.0073	0.0010	0.0010	0.0006
CO_2	RMSE	Train	0.0163	1.6624	5.4318	10.1708	0.0890	0.1362	22.3816	15.8235	10.2472	0.8531	-	0.8058	0.6291
		Test	11.1617	4.3181	42.134	15.5624	1.1408	11.6715	25.0502	65.1245	34.9995	190.728	19.4909	19.4911	4.3061
	MAPE	Train	0.0725	3.6481	1.2534	1.9102	0.0207	0.0412	2.4828	2.1944	1.7376	0.9531	-	0.0912	0.0843
		Test	29.1380	3.7370	9.6207	3.5313	0.3089	9.6047	14.4315	36.0481	16.4338	54.9237	17.9776	17.9769	12.182
	MAE	Train	0.0632	0.9483	3.0834	6.8380	0.0557	0.0851	12.6933	6.0580	4.4450	0.0162	-	0.0831	0.0952
		Test	8.1121	3.9114	35.320	15.5146	1.0162	11.4666	24.3387	55.9126	34.6331	143.911	14.5946	14.5945	3.5334
	Theil	Train	0.0005	0.0149	0.0111	0.0140	0.0002	0.0007	0.0239	0.0250	0.0189	0.0008	-	0.0018	0.0015
		Test	0.1682	0.0201	0.0626	0.0176	0.0017	0.0468	0.0343	0.1439	0.0766	0.5712	0.1638	0.1638	0.0313

stabilized prices addressed by the subsidized energy product consumption have led to energy-dependent industrialization (Farajzadeh, 2018).

An increase in the trade may also lead to lower emission intensity. Greater trade would raise the openness component and decrease the industrial GDP-trade component. Given the correlations (Fig. 5), the increase in trade seemed to induce a reduction in emissions intensity. The corresponding value was around -0.34. Rafig *et al.* (2016) found that trade openness could reduce CO_2 emissions and energy intensity in emerging economies. More exposure to the global interactions may provide opportunities to enjoy modern and clean technology. This channel of trade effect on emission has been specified by Shahbaz *et al.* (2019) as well. Labor productivity component resulted in higher emission intensity of CO_2. Inverse labor productivity showed an intensity-increasing role. In other words, the intensive growth, as suggested by Berndt (1990), can increase the emission intensity since they may substitute away from labor toward energy. However, like other pollutants, the extensive growth via greater use of labor was expected to decrease the emission intensity slightly. Apparently, the extensive use of labor was accompanied by lower use of energy products, revealing a substitution relationship for labor-energy. Emissions coefficient (+0.27) and energy intensity (+0.32) were also positively correlated with the emission intensity of CO_2. The dominant role of natural gas in CO_2 emission was the reason for failure of the energy structure (mix) in affecting the emission intensity. Considering the energy structure, a reduction in emission intensity of CO meant that gasoline was replaced with other energy products, since CO was dominantly emitted by gasoline. It should be noted that over the study period, the composition of energy products changed in favor of natural gas, which was more CO_2-embodied, leading to higher emission factors.

Forecast results

The related data for the emission intensity and its components were divided into training (1980 to 2106) and forecast evaluation (test) subset (2017 and 2018). An architecture with two layers was employed to train the NNs. The Levenberg-Marquardt algorithm and sigmoid function were used as learning algorithm and transfer function, respectively. The 'sym2' wavelet was employed in the WNN training for NO_x, SO_2, and CO prediction, while the 'db2' wavelet was applied for CO_2 prediction, from which the results were obtained in the third resolution. Furthermore, to prepare the data (total case) to feed the NNs, the DWT method was applied in order to decompose the values into approximations and detail components. Fig. 10 illustrates the approximation and detail coefficients. The coefficients extracted using the DWT method were applied as the data for training the WNN.

The results of training and test forecasting of the components and total emission intensity are presented in Table 2. The forecast results were discussed for each pollutant separately. The total (aggregate) emission intensity of each pollutant was forecasted using three methods: the MLP NN model, WNN model, and aggregation of the components. These results are presented in the last three columns of Table 2.

NO_x

The results of NO_x forecast are presented in Table 2. Regarding the accuracy of the forecasts, in the training period, there were slight differences between the components since the RMSE values remained lower than 0.03, except for the trade-related variables (Table 2). MAPE also showed a highly accurate forecast with forecast errors as low as less than 0.1% over the training period. Notably, the prediction error of the training period was slight even for some components including the GDP-industrial output ratio. The significant fluctuations indicated the strong ability of the designed networks to perform predictions over the training horizon. The predictions for the test period also showed a high accuracy; however, the trade-related variables and labor-GDP ratio showed a higher prediction error compared to the other components. In the test period, for most of the components, the prediction error of the last year accounted for most of the test period error, since dramatic changes occurred in the actual values of the last year. Considering the MLP network, during the training period, the total (emission intensity) index showed the highest forecast accuracy. The prediction error presented by the total emission intensity over the test period was much higher than the prediction error in most of the components. This indicated that the decomposition of the total emission intensity to

its components could provide a better opportunity for forecasting the emission intensity more accurately. The WNN was also used for the total emissions intensity index. As presented in the last column of Table 2, the WNN prediction error was lower than the prediction error of the MLP NN. It was also found that predicting the total emission intensity based on the predicted values of the components led to a higher prediction error compared to the predicted values of the WNN. However, considering the low prediction error of less than 0.1%, predicting NO_x emission intensity using the component values was also acceptable.

SO_2

Most of the results obtained from NO_x could be applied to the SO_2 components as well. However, the prediction errors for trade-related variables were higher than those observed for NO_x over the test period (Table 2). Considering the test period, there was a significant difference among the components in terms of prediction error. Trade-related, emission coefficient, and labor-GDP ratio components illustrated a higher prediction error. In the test period, the trade-related variables showed higher prediction errors like those observed for NO_x, whereas the total index showed a lower prediction error, indicating more accurate predictions for other components of SO_2. For most of the components and the total index, the prediction error was observed in the form of an overestimation of the actual values. Similar to NO_x, the low prediction error might allow for predicting the total emission intensity using the values forecasted for the components, since the highest error did not exceed 0.4%.

CO

Table 2 presents the forecast results for CO emission intensity and its components. For CO, also trade variables played an important role in forecast error. The corresponding errors were higher than those obtained for NO_x and SO_2, reaching over 1.3% for the test period. However, the prediction error for other components were similar to those of NO_x and SO_2. Interestingly, even for highly fluctuating components like the GDP-industrial output ratio, the forecasts were presented with high accuracy, indicating the well-designed structure of the networks. While most of the components showed a fluctuating trend (Fig. 8), the forecast accuracy was high for both training and testing periods. It was also found that the second year of the testing period accounted for most of the prediction error. Similar to NO_x and SO_2, the forecasts for the prediction period for the components with lower fluctuations were significantly accurate, indicating that precise forecasts for these components were achievable. The forecast for total emissions intensity based on the predicted components had a high prediction error like NO_x and SO_2.

CO_2

As shown in Fig. 9, the CO_2 emission intensity components showed a fluctuating trend, which made it difficult to design a network with lower prediction error. In terms of forecasting accuracy, CO_2 was different. The prediction errors for other selected pollutants were less than 1.5%, whereas the prediction errors of the test period for 7 components out of 10 were around 10% or higher and around 18% for total emission intensity in MLP network. However, the prediction error over the training period for most of the components was less than 2%. As shown in Fig. 9, there were fluctuations, even for the most years of the training period and for most components, leading to higher prediction errors for the test period. Contrary to the other pollutants, the prediction error for some components of CO_2 was significantly high for the test period. These components were emission coefficient, energy intensity, population-labor ratio, labor-GDP ratio (inverse labor productivity), and GDP-industrial output ratio (inverse industrialization). Among them, emission coefficient and population-labor ratio were forecasted with an extremely high accuracy over the training period, but they showed a high prediction error over the test period. For other components with a higher prediction error, the actual value of the last period seemed to be the strongest fluctuating value over the whole study period. In particular, the comparison of the prediction errors for training and test periods showed that the test period (especially the last year) experienced significant changes. However, even with the current strongly fluctuating test period, prediction errors were acceptable, indicating that the applied networks were well-designed networks. Compared to the MLP NN, the considerable contribution of the WNN was evident as it dampened the prediction error from 18% to 12.2%.

CONCLUSION

Contrary to the current literature that focuses on CO_2 emission, this study examined the emission intensity trend and the driving forces for more pollutants, including NO_x, SO_2, and CO. In terms of the driving forces, to some extent, the emission intensity of CO_2 was found to be different from others. Based on the results, the components such as energy and urban-related variables were mostly involved in forming the trend of emission intensity, while labor, GDP, and trade-related variables, which were mainly and directly affected by the economic variables, accounted for most of the fluctuations in the emission intensity of pollutants. Energy intensity was a driving factor for higher emission intensity, which in turn was affected by a highly subsidizing energy system. It could be claimed that the low price of energy has been resulted in substitution of energy for other production inputs or energy-based industrialization, and higher emission intensity. Thus, removing energy subsidies was recommended from the viewpoint of approaching a less polluted environment. Contrary to the energy intensity, the emission intensity-dampening effect of energy structure occurred through changes in energy product composition indicated a strong chance of achieving a less polluted environment. The results showed that many other factors, such as population, urbanization, and energy-intensive industrialization, could influence the emission intensity. Moreover, both intensive (except for CO_2) and extensive sources of economic growth could reduce the emission intensity of pollutants. This implied that substitution relation might be restricted at some levels, needing to focus on energy use efficiency measures. It was also found that well-organized networks could predict the emission intensity and its components with a high accuracy. The higher prediction error of CO_2 compared to the other pollutants could be attributed to structural changes and significant shocks over the test period. As far as the relevance of the designed NNs was considered, the study horizon included some of the strong fluctuations in the Iranian economy including the Iran-Iraq war and sanctions. Thus, the high accuracy of the forecasts should be considered meantime the strong fluctuations induced by these shocks. It should be noted that the decomposition technique can be used as a tool for a broader extension of the influencing factors far beyond what considered in the present study.

AUTHOR CONTRIBUTIONS

Z. Farajzadeh, the corresponding author, has contributed to designing the paper structure, collecting the data, processing the data, performing the analysis, and writing the manuscript. Also, M. Nematollahi as another corresponding author, has been involved in designing the analysis, performing the simulations, performing the analysis and writing the paper.

ACKNOWLEDGEMENT

This study was supported by the College of Agriculture at Shiraz University [Grant No 99GRC1M84069].

CONFLICT OF INTEREST

The authors declare that they have no known conflict of interests regarding the publication of this manuscript. In addition, the ethical issues, including plagiarism, informed consent, misconduct, data fabrication and/or falsification, double publication and/or submission, and redundancy have been completely observed by the authors.

ABBREVIATIONS

%	Percent
ANN	Artificial neural network
BP	Back-propagation
CH_4	Methane
CO	Carbon monoxide
CO_2	Carbon dioxide
COD	Chemical oxygen demand
DWT	Discrete wavelet transform
FDI	Foreign direct investment
GDP	Gross domestic product
GHGs	Greenhouse gases
GNI	Gross national income
IDA	Index decomposition analysis
LMDI	Log mean Divisia index
MAE	Mean absolute error
MAPE	Mean absolute percentage error
MLP	Multilayer perceptron
N_2O	Nitrous oxide
NNs	Neural networks
NO_x	Nitrogen oxides
OECD	Organization for economic co-operation and development
PPP	Purchasing power parity
RMSE	Root mean squared error
SDA	Structural decomposition analysis
SO_2	Sulphur dioxide
WNNs	Wavelet-based neural networks

REFERENCES

Adom, P.K., (2015). Asymmetric impacts of the determinants of energy intensity in Nigeria. Energy Econ., 49: 570–580 **(11 Pages)**.

Adom, P.K.; Kwakwa, P.A., (2014). Effects of changing trade structure and technical characteristics of the manufacturing sector on energy intensity in Ghana. Renewable Sustainable Energy Rev., 35: 475–483 **(9 Pages)**.

Ang, B.W., (2004). Decomposition analysis for policymaking in energy: Which is the preferred method? Energy Policy, 32: 1131–1139 **(9 Pages).**

Ang, B.W., (2015). LMDI decomposition approach: A guide for implementation. Energy Policy, 86: 233–238 **(6 Pages).**

Ang, B.W.; Zhang, F., (2000). A survey of index decomposition analysis in energy and environmental studies. Energy. 25: 1149–1176 **(8 Pages).**

Berndt, E.R., (1990). Energy use, technical progress and productivity growth: A survey of economic issues. J. Productivity Anal., 2(1): 67–83 **(17 Pages).**

Böhringer, C.; Löschel, A., (2006). Promoting renewable energy in Europe: A hybrid computable general equilibrium approach. The Energy Journal, 27: 135–150 **(16 Pages).**

Central Bank of Iran, (2013). A Yearly Publication.

Cheng, Y.; Wang, Z.; Ye, X.; Wei, Y., (2014). Spatiotemporal dynamics of carbon intensity from energy consumption in China. J. Geogr. Sci., 24: 631–650 **(20 Pages).**

Daubechies, I., (1992). Ten lectures on wavelets, Second ed., SIAM, Philadelphia, PA, USA.

Dogan, E.; Seker, F., (2016). Determinants of CO_2 emissions in the European Union: The role of renewable and non-renewable energy. Renewable Energy, 94: 429-439 **(11 Pages).**

Dong, F.; Yu, B.; Hadachin, T.; Dai, Y.; Wang, Y.; Zhang, S.; Long, R., (2018). Drivers of carbon emission intensity change in China. Resour. Conserv. Recycl., 129: 187-201 **(15 Pages)**.

Farajzadeh, Z., (2018). Emissions tax in Iran: Incorporating pollution disutility in a welfare analysis. J. Cleaner Prod., 186: 618-631 **(14 Pages).**

Farajzadeh, Z.; Nematollahi, M.A., (2018). Energy intensity and its components in Iran: Determinants and trends. Energy Econ., 73: 161-177 **(17 Pages).**

Farajzadeh, Z.; Zhu, X.; Bakhshoodeh, M., (2017). Trade reform in Iran for accession to the World Trade Organization: Analysis of welfare and environmental impacts. Econ. Modelling, 63: 75-85 **(11 Pages).**

Greening, L.A.; Davis, W.B.; Schipper, L.; Khrushch, M., (1997). Comparison of six decomposition methods: application to aggregate energy intensity for manufacturing in 10 OECD countries. Energy Econ., 19: 375 –390 **(16 Pages).**

Han, X.; Cao, T.; Sun, T., (2019). Analysis on the variation rule and influencing factors of energy consumption carbon emission intensity in China's urbanization construction. J. Cleaner Prod., 238: 117958 **(11 Pages).**

Herrerias, M.; Caudros, A.; Orts, V., (2013). Energy intensity and investment ownership across Chinese province. Energy Econ., 36: 286-298 **(13 Pages).**

Holtedahl, P.; Joutz, F.L., (2004). Residential electricity demand in Taiwan. Energy Econ., 26: 201–224 **(24 Pages).**

Hufbauer, G.C.; Schott, J.J.; Annelliott, K.; Muir, J., (2012). Case studies in economic sanction and terrorism.

Iran's Energy Balance, (2018). Deputy of Electricity and Energy Affairs, Ministry of Energy.

Jones, D., (1991). How urbanization affects energy-use in

developing countries. Energy Policy, 19(7): 621-630 **(10 Pages).**

Lau, L.S.; Choong, C.K.; Eng, Y.K., (2014). Investigation of the environmental Kuznets curve for carbon emissions in Malaysia: Do foreign direct investment and trade matter? Energy Policy, 68: 490–497 **(8 Pages).**

Lean, H.H.; Smyth, R., (2010). CO_2 emissions, electricity consumption and output in ASEAN. Appl. Energy, 87: 1858–1864 **(7 Pages).**

Long, X.; Naminse, E.Y.; Du, J.; Zhuang, J., (2015). Nonrenewable energy, renewable energy, carbon dioxide emissions and economic growth in China from 1952 to 2012. Renewable Sustainable Energy Rev., 52: 680-688 **(9 Pages).**

Mallat, S.G., (1989). A theory for multiresolution signal decomposition: The wavelet representation. IEEE Trans. Pattern Anal. Mach. Intel., 11: 674 – 693 **(20 Pages).**

Marrero, G., (2010). Greenhouse gases emissions, growth and energy mix in Europe. Energy Econ., 32: 1356-1363 **(8 Pages).**

Mishra, V.; Smyth, R.; Sharma, S., (2009). The Energy-GDP nexus: Evidence from a panel of Pacific Island countries. Resour. Energy Econ., 31: 210–220 **(11 Pages).**

Naderipour, A.; Abdul-Malek, Z.; Ahmad, N.A,; Kamyab, H.; Ashokkumar, V.; Ngamcharussrivichai, C.; Chelliapan, S., (2020) Efect of COVID-19 virus on reducing GHG emission and increasing energy generated by renewable energy sources: a brief study in Malaysian context. Environ. Technol. Innov., 20: 101151 **(18 Pages)**.

Naderipour, A.; Abdul-Malek, Z.; Arshad, R.; Kamyab, H.; Chelliapan, S.; Ashokkumar, V.; Tavalaei, J., (2021). Assessment of carbon footprint from transportation, electricity, water, and waste generation: towards utilization of renewable energy sources. Clean Technol. Environ. Policy. 23: 183–201 **(18 Pages)**.

Nematollahi, M.A.; Farid, M.; Hematiyan, M.R.; Safavi, A.A., (2012). Crack detection in beam-like structures using a wavelet-based neural network. Proceedings of the Institution of Mechanical Engineers, Part G. Journal of Aerospace Engineering, 226(10): 1243-1254 **(11 Pages)**.

Nematollahi, M.A.; Jamali, B.; Hosseini, M., (2020). Fluid velocity and mass ratio identification of piezoelectric nanotube conveying fluid using inverse analysis. Acta Mech., 231(2): 683-700 **(18 Pages).**

Nematollahi, M.A.; Mousavi Khaneghah, A., (2019). Neural network prediction of friction coefficients of rosemary leaves. J. Food Process Eng., 42(6): 13211 **(12 Pages).**

Pan, X.; Uddin, M.K.; Saima, U.; Jiao, Z.; Han, C., (2019). How do industrialization and trade openness influence energy intensity? Evidence from a path model in case of Bangladesh. Energy Policy, 133: 110916 **(9 Pages).**

Poumanyvong, P.; Kaneko, S., (2010). Does urbanization lead to less energy use and lower CO_2 emissions? A cross-country analysis. Ecol. Econ., 70: 434-444 **(11 Pages).**

Rafiq, S.; Salim, R.; Nielsen, I., (2016). Urbanization, openness, emissions, and energy intensity: A study of increasingly urbanized emerging economies. Energy Econ., 56: 20–28 **(9 Pages).**

Rodríguez, M.; Pena-Boquete, Y., (2017). Carbon intensity changes in the Asian dragons: Lessons for climate policy design. Energy Econ., 66: 17-26 **(10 Pages).**

Rojas R., (1996). Neural Networks-A Systematic Introduction Springer-Verlag. New York.

Sadorrsky, P., (2013). Do urbanization and industrialization affect energy intensity in developing countries. Energy Econ., (37): 52-59 **(8 Pages).**

Statistical Center of Iran (SCI), (2018). National Statistics. https://www.amar.org.ir/english#10291052-national-statistics.

Shahbaz, M.; Gozgor, G.; Adom, P.K.; Hammoudeh, S., (2019). The technical decomposition of carbon emissions and the concerns about FDI and trade openness effects in the United States. Int. Econ., 159: 56-73 **(18 Pages).**

Shahbaz, M.; Khraief, N.; Uddin, G.S.; Ozturk, I., (2014). Environmental Kuznets curve in an open economy: A bounds testing and causality analysis for Tunisia. Renewable Sustain. Energy Rev., 34: 325–336 **(12 Pages).**

Steckel, J.C.; Jakob, M.; Marschinski, R.; Luderer, G., (2011). From carbonization to decarbonization? Past trends and future scenarios for China's CO_2 emissions. Energy Policy, 39: 3443–3455 **(13 Pages).**

Su, B.; Ang, B.W., (2012). Structural decomposition analysis applied to energy and emissions: Some methodological developments. Energy Econ., 34: 177–188 **(12 Pages).**

UNFCCC (United Nations Framework Convention on Climate Change), (2015). UNFCCC Country Brief 2014: Iran.

World Bank, (2004). Islamic Republic of Iran energy-environment Review Policy Note. Report No. 29062-IR. Washington D.C. **(63 Pages).**

World Bank, (2014). Data. IEA Statistics. Energy Use. Washington D.C.

World Bank, (2016). Data. Climate Watch. GHG Emissions. Washington D.C.

World Bank, (2018a). Data. Climate Watch. GHG Emissions. Washington D.C.

World Bank, (2018b). Data. Climate Watch. GHG Emissions. Washington D.C.

World Bank, (2019). Data. World Development Indicators database. Washington D.C.

Xu, X.; Ang, B., (2013). Index decomposition analysis applied to CO_2 emission studies. Ecol. Econ., 93: 313–329 **(17 Pages).**

Zhang, C.; Su, B.; Zhou, K.; Yang, S., (2019). Decomposition analysis of China's CO_2 emissions (2000–2016) and scenario analysis of its carbon intensity targets in 2020 and 2030. Sci. Total Environ., 668: 432-442 **(11 Pages).**

Zhang, P.; Hao, Y., (2020). Rethinking China's environmental target responsibility system: Province-level convergence analysis of pollutant emission intensities in China. J. Cleaner Prod., 242: 118472 **(10 Pages).**

AUTHOR (S) BIOSKETCHES

Farajzadeh, Z., Ph.D., Associate Professor, Department of Agricultural Economics, College of Agriculture, Shiraz University, Shiraz, Iran.
- Email: *zakariafarajzadeh@gmail.com*
- ORCID: 0000-0002-5971-947X
- Web of Science ResearcherID: AGD-1851-2022
- Scopus Author ID: 56708802100
- Homepage: https://agri.shirazu.ac.ir/en/~zakariafarajzadeh

Nematollahi, M.A., Ph.D., Assistant Professor, Department of Biosystems Engineering, College of Agriculture, Shiraz University, Shiraz, Iran.
- Email: *manema@shirazu.ac.ir*
- ORCID: 0000-0001-5780-2723
- Web of Science ResearcherID: W-5769-2018
- Scopus Author ID: 57197262608
- Homepage: https://agri.shirazu.ac.ir/en/~m.nematollahi

HOW TO CITE THIS ARTICLE

Farajzadeh, Z.; Nematollahi , M.A., (2023). Components and predictability of pollutants emission intensity. Global J. Environ., Sci. Manage., 9(2): 241-260.

DOI: 10.22034/gjesm.2023.02.05

url: https://www.gjesm.net/article_255152.html

Global J. Environ. Sci. Manage. 9(2): 261-274, Spring 2023, Serial #34

Global Journal of Environmental Science and Management
(GJESM)

Homepage: https://www.gjesm.net/

ORIGINAL RESEARCH PAPER

Ecological and human health implications of mercury contamination in the coastal water

A. Mallongi[1,*], A.U. Rauf[1], R.D.P. Astuti[1], S. Palutturi[2], H. Ishak[1]

[1] *Department of Environmental Health, Faculty of Public Health, Hasanuddin University, Indonesia*

[2] *Department of Health Policy and Administration, Faculty of Public Health, Hasanuddin University, Indonesia*

ARTICLE INFO

Article History:
Received 28 June 2022
Revised 06 September 2022
Accepted 15 October 2022

Keywords:
Exposure time
Mercury
Risk assessment
Water pollution

DOI: 10.22034/gjesm.2023.02.06

ABSTRACT

BACKGROUND AND OBJECTIVES: The increasing population and anthropogenic activities in coastal areas affects the presence of mercury in coastal waters. Therefore, this study aims to 1) assess the ecological and human health risk of mercury contamination in coastal water; 2) analyze the effectiveness of polymer sulfur as an absorbent for mercury.

METHODS: A total of fifteen water samples were obtained from the coastal areas of Makassar and were analyzed using cold vapor atomic absorption spectrophotometry. Ecological and human health risks were assessed using established assessment methods by the United States Environmental Protection Agency. The uncertainty and sensitivity tests for independent variables in human health risk were assessed by the Monte Carlo Simulation method. Furthermore, polymer sulfur was used as a promising technique for capturing and reducing the level of mercury in the water column.

FINDINGS: The results showed that the mean concentration of mercury was very high and exceeded the values established by the World Health Organization, United States of Environmental Protection Agency, and Indonesian National Standards, indicating elevated risks to the ecosystem and human health in the future. Additionally, the Monte Carlo simulation model revealed that the non-carcinogenic risk caused by mercury exposure in adults and children was greater than 1 (Total Hazard Index>1), indicating the health adverse effects for both receptors. From the simulation results, the concentration of mercury at 23.3 percent and exposure time of 21.3 % were the most influential and dominant factors in non-cancer risk for adults and children, respectively. Therefore, mercury concentration needs to be reduced in coastal areas. The application of polymer sulfur is effective for reducing mercury concentration in water with a percentage reduction range of 39 – 100 percent and p-value of 0.001.

CONCLUSION: Mercury contamination of coastal water in Makassar city poses ecological and health risks. The application of polymer sulfur is an effective way for reducing mercury in the water column.

NUMBER OF REFERENCES	NUMBER OF FIGURES	NUMBER OF TABLES
79	3	3

*Corresponding Author:
Email: *rawnaenvi@gmail.com*
Phone: +62 821-8772-4636
ORCID: 0000-0001-6438-1154

Note: Discussion period for this manuscript open until July 1, 2023 on GJESM website at the “Show Article”.

INTRODUCTION

Mercury (Hg) pollution has become a serious threat to the marine environment, especially those adjacent to industrial zones and high urbanization due to its toxicity, accumulation, persistence, and non-biodegradable nature (Basri *et al*., 2020; Fioramonti *et al*., 2022; Rauf *et al*., 2020; Aravind *et al.,* 2016; Tariq *et al.,* 2015). Naturally, weathering and heavy metal pollution affect the composition of coastal sediments which are related to seawater quality (Armstrong-Altrin *et al*., 2021; Astuti *et al*., 2021a). In Jiangsu coastal region, China, the industrial activities from photovoltaic electronics, mechanical metallurgy, printing, and dyeing industries lead to increased levels and accumulation of Hg (Zhao *et al*., 2018). Hg enters the marine environment mainly from atmospheric deposition, reduces to Elemental mercury (Hg^0), and is then released back into the atmosphere, or taken up from the water column by particulate matter and eventually buried in sea sediments (Lamborg *et al*., 2014; Zaferani and Biester, 2021). In the coastal areas, pollutants are released from various sources including the spill of oil from shipping activities, land reclamation, industrial runoff, and solid waste accumulation by human. Among the various chemical forms of Hg, Methylmercury (Me-Hg) is known to be highly neurotoxic and has been identified as the cause of Minamata disease (Sakamoto *et al*., 2018). The disease stemmed from methylmercury poisoning due to the consumption of aquatic edible biota such as fish and shellfish contaminated by methylmercury in Minamata bay, Japan (Harada, 1995). It was first discovered in 1956, where the people injured by methylmercury exposure had several symptoms including auditory, motoric, and sensoric disturbances, as well as dysarthria, ataxia, tremor, and visual constriction (Harada, 1995). Furthermore, Hg exposure can attack neurological systems. Its pollution recorded at the Kao Bay has exceeded the maximum exposure limit thereby causing a high potential health risk for humans (Amqam *et al*., 2020). Skin contact with Hg from acute and repeated exposure in humans also causes pruritic skin rashes, allergies, reddening, and peeling skin on the palms of the hands, and erythematous soles of the feet (Rauf *et al*., 2020). The initial effect of Hg exposure is characterized by fever fatigue, chills, fever, and elevated leukocyte count. For acute and chronic exposure, several studies reported increased tremors, muscle fasciculations, myoclonus, or muscle pain (ATSDR, 1999). Meanwhile, South Sulawesi as the largest national marine products producer has been contaminated by pollutants released from land-based sources through rivers and land runoff over several years due to urbanization and industrialization activities (Lestari *et al*., 2021; Yap and Al-Mutairi, 2022). This condition influences the potential damage to marine ecosystems, a decline in tourism, and affects the quality of the food chain, especially seafood consumed by the community (Li *et al*., 2013). Moreover, exposure to Hg, even in small amounts, can cause serious health problems. Previous assessments have found elevated mercury in samples of hair, blood, and urine in residents. Fetuses and infants are highly susceptible to mercury exposure, and this is associated with neurological effects (Gonzalez *et al*., 2019; Ashe, 2012). Several studies on the impact of heavy metals have been carried out in the coastal areas of Sulawesi. However, the contamination of Hg in the coastal environment has not been examined. Industrial runoff and land change have a potentially great contribution to the release of Hg metal into the aquatic environment in the Makassar coastal area. This implies that Hg removal from seawater is urgently needed to prevent adverse effects and protect the ecosystem. Efforts to apply simple remediation and economical materials are a major consideration, especially for the low-middle income region. Polymer sulphur is one of the candidate mercury adsorbents for water ecosystems. This absorption method is very easy to use, convenient, cost-effective, has high competence, low-cost, and is environmentally friendly (Azman *et al.,* 2020). Elemental sulphur can adsorb and stabilize mercury (Azman *et al.,* 2020). Additionally, it can easily be fused into the backbone of polymers and this mixture has a large surface area with a porous structure (Xu *et al.,* 2017). Based on several experimental studies, polymer sulphur can adsorb mercury effectively (Azman *et al.,* 2020; Chowdhury *et al.,* 2021; Mann *et al.,* 2021; Xu *et al.,* 2017). These previous studies focused on the experimental aspects in laboratory settings. Consequently, this study was conducted in the actual coastal water of Makassar city. To obtain a high level of accuracy, the Monte-Carlo simulation (MCS) model was also applied to determine the predictive value of non-cancer risk and the most influential health factor through sensitivity analysis.

Previous results in health risk assessment relied on the input variables without assessing the level of correlation and contribution of each assumption. Therefore, this study used the probabilistic risk assessment which is more developed and highly accurate than the regular assessment. The Monte Carlo model was used to investigate the distribution of a selected variable by simulating random numbers. The specific contribution of health risk due to mercury exposure can be analyzed for further policy making. Furthermore, enhanced simulation reliability can improve the information contributing to the cost-effective approach in the prevention of further damage caused by water pollution (Puno *et al.,* 2022). The results are expected to form the basis of large-scale reductions in Hg levels in this area. The aims of the present study is to investigate the ecological damage and health risk assessment of Hg pollution from estuarine water of Makassar coastal area, South Sulawesi Province, Indonesia in 2022.

MATERIALS AND METHODS

Study area descriptions

Makassar city is one of the coastal areas in the South Sulawesi Province, Indonesia located at 119°18”27,97” – 119°32”31,03” east longitude and 5°30”18” – 5°14”49” south latitude. Its climate is tropical with a distinct wet and dry season, where the wet season start from November to May, while the dry season commences from June to October. Furthermore, high humidity and an average temperature of 27.8 °C occur in the dry season. There is only a slight temperature variation throughout the year, ranging from 24°C and 32°C for minimum and maximum respectively. The areas of the city lie along the three rivers namely the Jeneberang, Tallo, and Maros. The city has experienced significant environmental degradation caused by uncontrolled land use and the geomorphological condition of the coastal area (Suleman *et al.,* 2018). The several areas that have experienced degradation include Akarena, Tanjung Bayang, Tanjung Bunga, and Losari beach. Consequently, these areas tend to have high porosity and are affected by abrasion (Suleman *et al.,* 2018). The coastal area of Makassar is the final site of pollutants carried by the water from the Jeneberang watershed and Tallo river. This area is also surrounded by various anthropogenic activities including industry, domestic, hotel, hospital, harbor, and shopping centers. These conditions might influence the accumulation of heavy metals such as Hg in the coastal area. The existence of traders who process and sell gold also contributes to the accumulation of Hg pollution in this area (Ishak, 2017).

Sampling method

The grab water samples were obtained from 15 sampling sites in the Makassar coastal area. This sample site included in this study was selected using the purposive sampling method based on the potential sources or effluent flow of water to the coastal water ecosystems as presented in Fig. 1. The sampling was performed by a water sampler in 30 – 50 Centimeter (cm) depth of water. All samples were placed in a 1 liter (L) pre-sterilized High-density polyethylene (HDPE) bottle, then acidified using nitric acid (HNO_3) to examine the potential of hydrogen (pH) to minimize precipitation and adsorption on the wall of containers. Next, a bottle of the sample was placed in the box with ice cubes to avoid Hg evaporation. A global positioning system (GPS) was used to determine the geographic coordinates of each sampling site. All samples were transported to the chemical laboratory in Makassar to determine Hg concentration after the water collection.

Total Hg concentration analysis

Total mercury concentration (THg) was determined by Cold vapor atomic absorption spectrophotometry (CV-AAS) with wavelength 253.7 nanometer (nm) following Indonesia’s standard for Hg analysis in water samples namely Indonesian National Standard (INS) 6989.78.2011. About 100 milliliters (mL) of the diluted sample was placed in a 250 mL erlenmeyer glass. Next, 5 mL of sulphuric acid (H_2SO_4) and 2.5mL of nitric acid (HNO_3) were added to the water sample and homogenized. About 15 mL of Potassium permanganate ($KMnO_4$) solution was also added and left for 15 minutes until the solution changed to purple. The solution was further added with 8 mL of Potassium persulfate ($K_2S_2O_8$), homogenized, and heated for two hours at 95°C in a water bath. Afterward, the solution was cooled to room temperature and added with 5 mL of Tin(II) chloride ($SnCl_2$). The samples were then analyzed in Cold vapor atomic absorption spectrophotometry (CVAAS): Shimadzu AA-7000 with mercury analyzer. To ensure procedure validity, Certified Reference

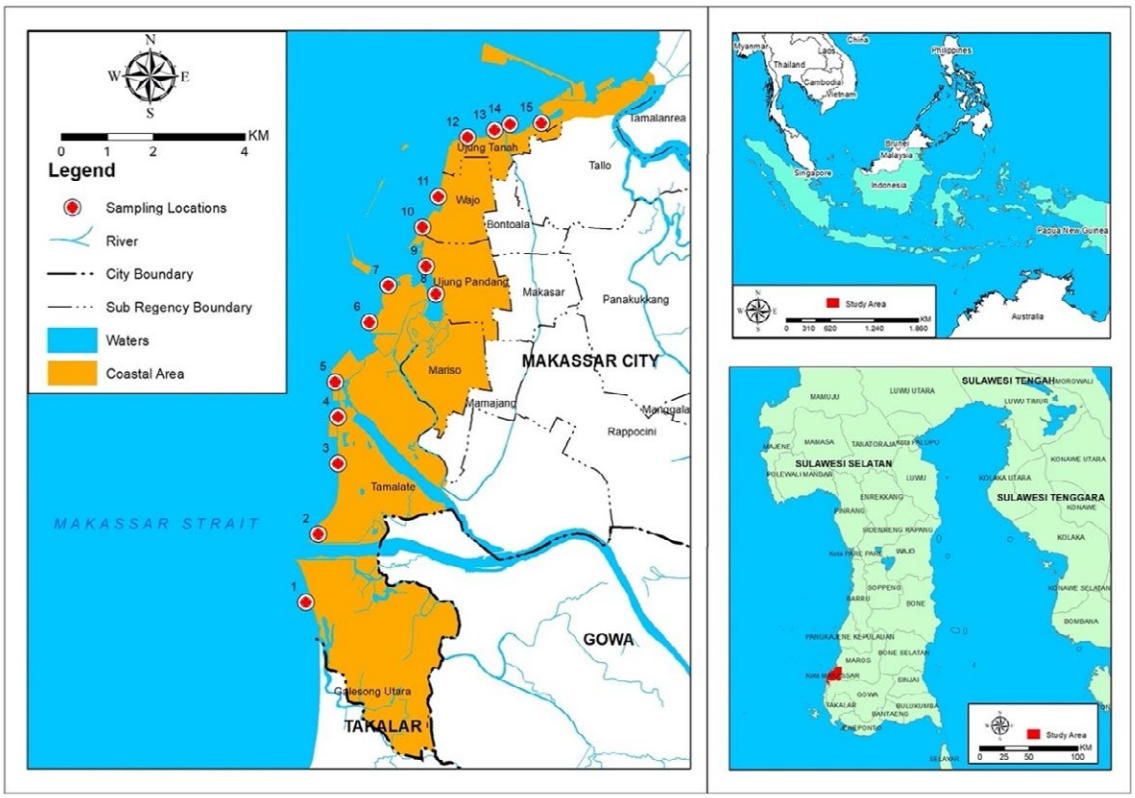

Fig. 1: Geographic location of the study area in estuarine water of Makassar coastal area, South Sulawesi Province, Indonesia

Material (CRM) from National Institute Standards and Technology (NIST) 1646a sediment estuarine was included in the analysis procedure. Moreover, sample blanks and three replications were analyzed attentively. The percent (%) recovery achieved was > 90% with linear curves R^2 of 0.95.

Ecological risk estimation

The ecological risk was estimated using Eq. 1 (Mallongi *et al*., 2020a).

$$HQ = \frac{C_{Hg}}{\text{Eco screening benchmark}} \quad (1)$$

Where, Hazard quotient (HQ) is the hazard quotient (no unit); Hg concentration (C_{Hg}) is in water (mg/L); Eco screening benchmark for Hg is 0.0011 milligram per liter (mg/L) (USEPA, 1996; Mallongi *et.al*., 2020b). HQ >1 indicates that there are adverse ecological consequences that might occur with Hg contamination in the coastal water.

Human health risks estimation

The United States Environmental Protection Agency (USEPA) method was used to estimate the human health risk caused by Hg exposure during recreational activities such as swimming, bathing, and fishing in the coastal area of Makassar city. The equations for human health risk are depicted in Eqs. 2, 3 and 4 (USEPA, 2015; USEPA, 2016; USEPA, 2021a; USEPA, 2021b; Astuti *et al*., 2022).

$$THQ_{ingestion} = \frac{C_{Hg} \times IR_{rec} - w \times EF_{rec} \times ED_{rec} \times EV_{rec} \times ET_{rec}}{BW \times AT \times RfD_o} \quad (2)$$

$$THQ_{dermal} = \frac{C_{Hg} \times SA \times K_p \times ET_{rec} \times EV \times EF_{rec} \times ED_{rec} \times CF_w}{BW \times AT \times RfD_d} \quad (3)$$

$$THI = THQ_{ingestion} + THQ_{dermal} \quad (4)$$

Where, THQ is the target hazard quotient for ingestion ($THQ_{ingestion}$) and dermal contact (THQ_{dermal}) of Hg in water, total hazard index (THI); Hg concentration in water (C_{Hg}) is the level of Hg; Ingestion rate of water during recreation activity (IR_{rec-w}) is 0.12 L/hour for

children and 0.11 for adults L/hour (USEPA, 2015; USEPA, 2021c); Exposure frequency during recreation (EF_{rec}) is 135 days/year; Duration for recreational exposure (ED_{rec}) is 26 years for adults and 6 years for children (USEPA, 2021c); Event of recreation (EV_{rec}) is the amount event of recreation (1 event/day) (USEPA, 2021c); Exposure time during recreation (ET_{rec}) is recreator time 0.54 hours/event for children and 0.71 hours/event for adults (USEPA, 2021c); human body weight (BW) is 70 kg for adults and 15 Kg for children (USEPA, 2021c); Exposure averaging time (AT) is ED x 365 = days; Skin exposed area (SA) is 19652 cm^2 for adults and 6365 cm^2 for children (USEPA, 2015); dermal permeability constant (Kp) is 0.001 cm/hour (USEPA, 2016; USEPA, 2021a); volumetric conversion for water (CF_w) is 0.001 L/cm^3 (USEPA, 1991; USEPA, 2004); Oral reference dose (RfD_o) for Hg is 0.0003 mg/kg/day (RAIS, 2020); Dermal reference dose (RfD_d) for Hg is 0.000021 (RAIS, 2020).

Monte Carlo simulation

The Monte Carlo simulation (MCS) is a mathematical approach that is applied to calculate risks (Mallongi *et al*., 2022b; Rauf *et al*., 2021a). In the past, health risks due to chemical exposure are determined only by conventional data which usually culminate in a single point of risk. Through the use of MCS, the calculation of uncertainty associated with the estimated risk is identified as a probability distribution to predict risk or exposure. It involves large random numbers from some specified theoretical probability distribution and can find the most sensitive variables contributing to the health risk (Millard, 1998). This simulation is operated by ORACLE inc software, United States of America (USA) (Crystal ball version 11.1.2) in Microsoft Excel 2019. MCS simulation is used to estimate uncertainty and health risk parameter's sensitivity with 10,000 replication. After THI calculation, independent health risk variables such as exposure time (ET), exposure frequency (EF), body weight (BW), ingestion rate from recreational activities (IR Rec-w), concentration (C), and exposed skin surface area (SA) were included in the simulation. The cumulative distribution is expressed in the 5^{th} percentile and 95^{th} percentile, THI or THQ < 1 is the safe limit for Hg exposure. Additionally, the sensitivity test was performed to determine the most influential factor in THI value to develop efficient risk management for the population.

Hg removal from water

The porous polymer version of the Hg absorber was fabricated and prepared by mixing and synthesizing this polymer model with sodium chloride. This process produced a rubber sorbent capable of capturing Hg species such as liquid, vapor, inorganic, and highly toxic alkyl compounds to capture the Total mercury concentration (THg) in the water along the coast area of Makassar. Application of polymer bag was carried out for 10 weeks, then, the samples were found to have no more than 1 milligram per kilogram (mg/kg) mercury. A characteristic methoxy ethyl mercuric chloride (MEMC) red color was observed from the top of the bag up to 10 cm where MEMC was applied and also for the polymer bag installed in the drain hole. After 7 and 10 weeks, all samples up to a depth of 36 centimeters (cm) contained between 0.03-0.04 mg/kg of mercury, while after 10 and 15 weeks, no more than 1 mg/kg was detected in the polymer.

Statistical analysis

A non-parametric test namely Wilcoxon was conducted using Statistical Package for the Social Sciences (SPSS) software version 22 (IBM inc) to determine the efficiency of Hg removal using co-polymerization of sulfur and cooking oil in the sampling site, and the probability value (p-value) of <0.05 was considered significant. Moreover, descriptive statistics such as mean, standard deviation (SD), and range were calculated in SPSS software.

RESULTS AND DISCUSSION

Hg concentration in water

The Hg concentration as shown in Table 1 is higher compared to the value obtained by (Mallongi, 2014). This shows that the accumulation in Makassar coastal area will become more worrisome over time without any controlling action. Previous studies in Europe, South America, and Asia region are shown in Table 1. The mean of Hg concentration in this study exceeded the acceptable limit of the World Health Organization (WHO), United States Environmental Protection Agency (USEPA), and Canadian and Indonesian standards. This implies the possibility of high ecological risk, contaminated seafood, and bioaccumulation of Hg in the aquatic ecosystem (Fioramonti *et al.,* 2022; Yap and Al-Mutairi, 2022).

Table 1: Comparison of Hg concentration in the study area with water quality standards and previous results from other countries

Organization/ Countries	Hg concentration (mg/L)	Reference
Makassar coastal water	0.205 ± 0.41	This study
Indonesia standard	0.002	Peraturan Pemerintah, 2021
WHO standard	0.006	WHO, 2017
USEPA standard	0.002	USEPA, 2009
Canada standard	0.001	Government of Canada, 1979
Background concentration	0.000015	Kowalski *et al.,* 2007
Slovenia	0.0002 ± 0.0015	Bratkič *et al.,* 2018
Argentina	0.2700	La Colla *et al.,* 2019
Saudi Arabia	0.3000	Youssef *et al.,* 2016
China	0.023	Liu *et al.,* 2022
China	0.025	Zhao *et al.,* 2018

Ecological risk assessment

Based on the calculation of ecological risk assessment in Table 2, the contamination of Hg in the coastal area of Makassar city can induce adverse impacts on the marine aquatic ecosystem (HQ > 1). This result is in line with Zhang *et al.* (2017) which mentioned that Hg contamination in water (HQ >1) has potentially harmful effects on the health and ecosystem of marine organisms such as invertebrates and phytoplankton. The highest value of HQ was located in sampling sites 9, 14, and 15 which are near the ship harbor. This result is in accordance with previous reports (Zhang *et al.,* 2012; Ndungu *et al.,* 2017). Areas near the ship harbor are polluted by various pollutants such as Hg from coal combustions or residual fuel oil, ballast water, petroleum hydrocarbon oil, organic pollutant, oil spill, and dredging (Zhang *et al.,* 2012; Ndungu *et al.,* 2017; Tang *et al.,* 2018; Wang *et al.,* 2019; Kakar *et al.,* 2021). Furthermore, Kakar *et al* (2021) found that naval and non-naval vessels contained 44 and 75 Kilogram (Kg) of Hg, respectively, per million Gross tonnage (GT). Heavy metals and other organic pollutants from various anthropogenic activities such as urban artisanal gold mining (UAGM), gas station, domestic waste, shipbuilding yard, as well as industrial and hospital waste accumulate in the coastal area (Mallongi 2014; Abbas *et a*l., 2017; Abbas *et al*., 2020; Mallongi *et al*., 2023; Mallongi *et al*., 2020b; Astuti and Mallongi 2020; Astuti *et al.,* 2021b; Mallongi *et al*. 2022a; Rauf *et al*., 2021b; Rauf *et al*., 2022). The canals or rivers are the main input of pollutants in this area. Lack of proper wastewater treatment and low environmental law enforcement influence the high accumulation of heavy metals including Hg in the coastal area of Makassar city. A higher concentration of Hg is associated with elevated ecological risks (Mao *et al.,* 2020; Masni *et al,* 2016). Based on previous studies, Hg not only contaminates the water but also the sediment and marine aquatic biotas while a high ecological risk was detected in Losari beach (Ishak *et al*. 2014; Ishak 2017). The result obtained in this study is higher than the level of total Hg concentration in Poland and Taiwan. In Poznan, the total Hg concentration in the surface water was 0.00002 mg/L (Kowalski *et al.,* 2007), while the value obtained in Northern Taiwan was approximately 0.00005 mg/L (Fang and Lien, 2021). According to previous reports, the total concentration of Hg in the estuary and coastal sediments varies, depending on the contamination and pollution status.

Human health risk assessment

Table 2 shows the point estimate of human health risk from the coastal community of Makassar city. The majority of the Total hazard quotient (THQ) and index (THI) values was lower than 1, except for the community in the sampling site 9, 14, and 15. This indicates that adverse health impacts are unlikely to occur in these areas or people should avoid carrying out recreational activities around places near the ship harbor. The mean value of THI in adults was higher than 1, implying that this population is at risk of health problems in the future due to Hg exposure from recreational activities such as swimming, fishing, or playing around the coastal area. Based on the results, adults had a lower value of THQ and THI compared to the children which imply that children are more at risk of Hg exposure than adults. This is in accordance with another study conducted in Ankobrah and Pra, Ghana, where the THQ value of children due to Hg exposure was greater than that of adults (Kortei *et al.,* 2020). The toxic response factors of Cd and Hg

Table 2: Water Hg concentration, ecological risk (HQ), and human health risk (THQ and THI) of the Makassar coastal community

Sampling site	Ecotoxicity screening value	Reference	Measured Hg concentration (mg/L)	HQ	THQ Ingestion		THQ dermal		THI	
					Adult	Children	Adult	Children	Adult	Children
S1	0,0011	(USEPA 1996)	0.0071	6	0.010	0.0003	0.025	0.029	0.035	0.029
S2			0.0081	7	0.011	0.0003	0.028	0.033	0.040	0.033
S3			0.0055	5	0.008	0.0002	0.019	0.022	0.027	0.022
S4			0.0081	7	0.011	0.0003	0.028	0.033	0.040	0.033
S5			0.0052	5	0.007	0.0002	0.018	0.021	0.025	0.021
S6			0.0025	2	0.003	0.0001	0.009	0.010	0.012	0.010
S7			0.0032	3	0.004	0.0001	0.011	0.013	0.016	0.013
S8			0.0035	3	0.005	0.0001	0.012	0.014	0.017	0.014
S9			0.0095	9	0.013	0.0004	0.033	0.038	0.046	0.039
S10			1.0013	910	1.377	0.0395	3.515	4.041	4.893	4.080
S11			0.0091	8	0.013	0.0004	0.032	0.037	0.044	0.037
S12			0.0056	5	0.008	0.0002	0.020	0.023	0.027	0.023
S13			0.0089	8	0.012	0.0004	0.031	0.036	0.043	0.036
S14			1.0019	911	1.378	0.0395	3.517	4.043	4.895	4.083
S15			1.007	915	1.385	0.0397	3.535	4.064	4.920	4.104
Mean			0.205	187	0.283	0.0081	0.722	0.830	1.005	0.839
Standard deviation			0.410	375	0.5	0.01	1.4	1.6	2	1.6
Minimum value			0.0025	2	0.003	0.0001	0.009	0.010	0.012	0.01
Maximum value			1.007	915	1.385	0.0397	3.535	4.064	4.920	4.104

are significantly higher than other heavy metals, this indicates that exposure to Hg is more dangerous to human health, especially among young children (Renieri *et al.,* 2014).

Based on Fig. 2, the Total hazard index (THI) values in percentile 95th of adults at 1.008 and children 1.554 exceeds the acceptable limit from the United States Environmental Protection Agency (USEPA) namely THI >1 (USEPA, 1989). Both age categories are at risk of experiencing adverse effects of Hg exposure through multiple sources. However, children have a greater non-cancer risk than adults. This is due to the different body ratios where the amount of intake is greater in children. Early stage of neurodevelopment, the physiological structure, and the vulnerable immune system put children at greater risk (Al-Saleh *et al*., 2020; Du *et al*., 2021). These results are consistent with previous studies conducted in Italy and Japan where repeated exposure to total Hg and methylmercury (Me-Hg) made young children more vulnerable to neurologic changes than adults due to greater sensitivity during the early stages of brain development (Barone *et al*., 2021; Iwai-Shimada *et al*., 2021).

Fig. 3 shows that Hg concentration (C) 23.3% and exposure time (ET) 21.3% are the most dominant or influential variables in non-cancer risk for adults and children, respectively. These results indicate that an increase in chemical concentration will affect the intake value and elevate the risk of developing adverse health effects (Saha *et al*., 2016; Rauf *et al*., 2021c). Meanwhile, body weight (BW) has no effect on the non-cancer risk for adults and children. This is consistent with a previous study which stated that BW has a negative and insignificant contribution to health risk assessment (Orosun *et al.,* 2020). The limitation of this study is that human exposure pattern was not collected directly from the people around coastal areas. The human data used was adapted from the USEPA standard value.

Hg removal application

Based on the Monte Carlo Simulation (MCS), Hg concentration is the most influential factor in human health risk. Therefore, there is a need to control Hg concentration in the coastal area of Makassar city. Polymerized sulfur and unsaturated cooking oil were used to absorb mercury in the water column along the sampling sites. From the non-parametric test result, this method is effective for absorbing mercury from water with a p-value <0.005. The range of percentage (%) reduction of Total mercury concentration (THg) in the water column was 39 – 100%. This implies that polymer sulfur can be alternatively used by local authorities to reduce mercury from the water and prevent ecological as well as human health

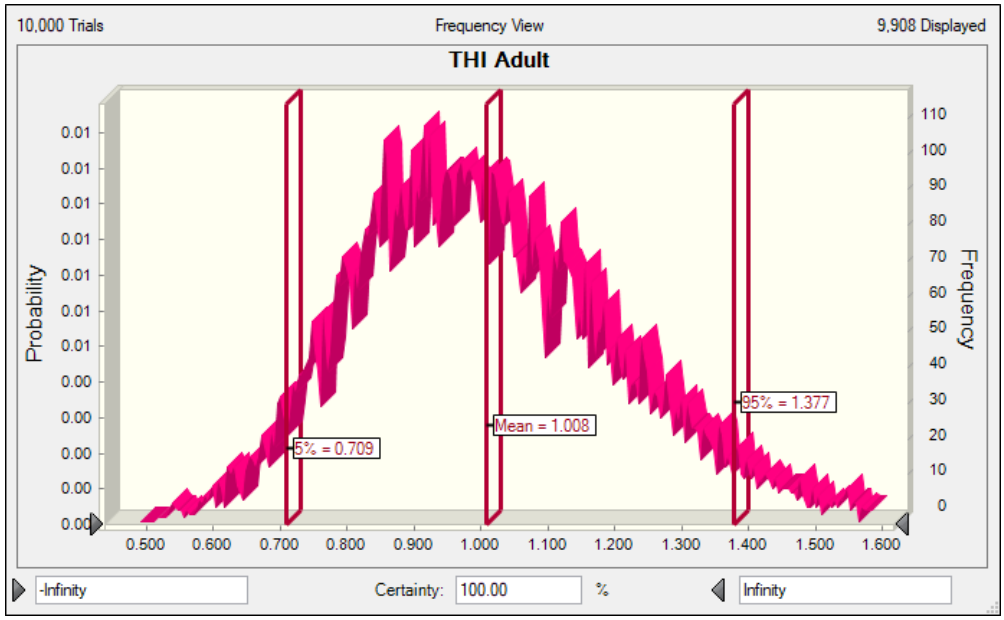

(a)

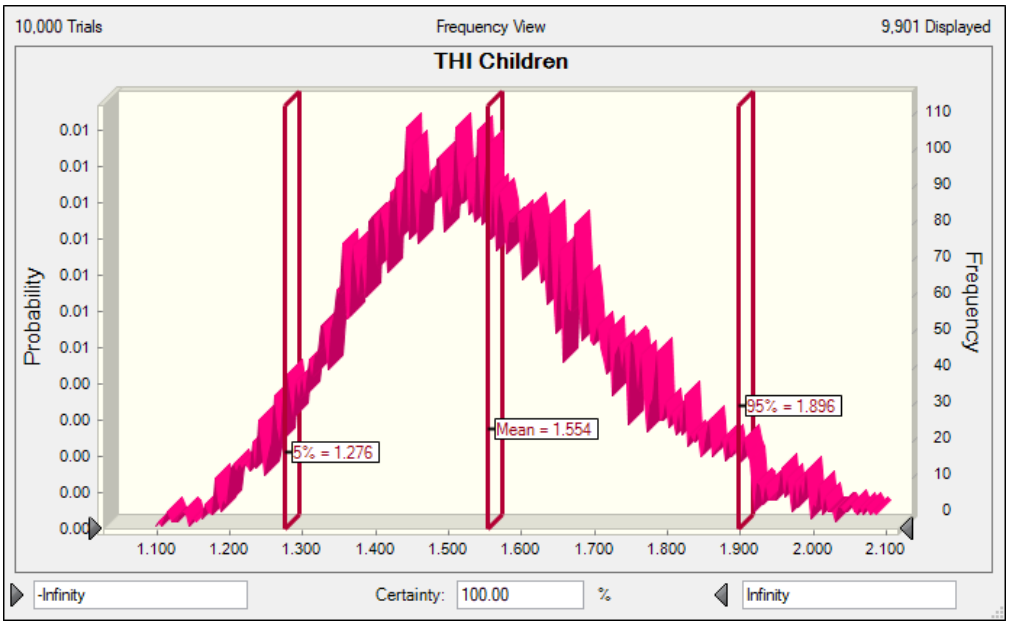

(b)

Fig. 2: Total Hazard Index (THI) of adults (a) and children (b) using the MCS model

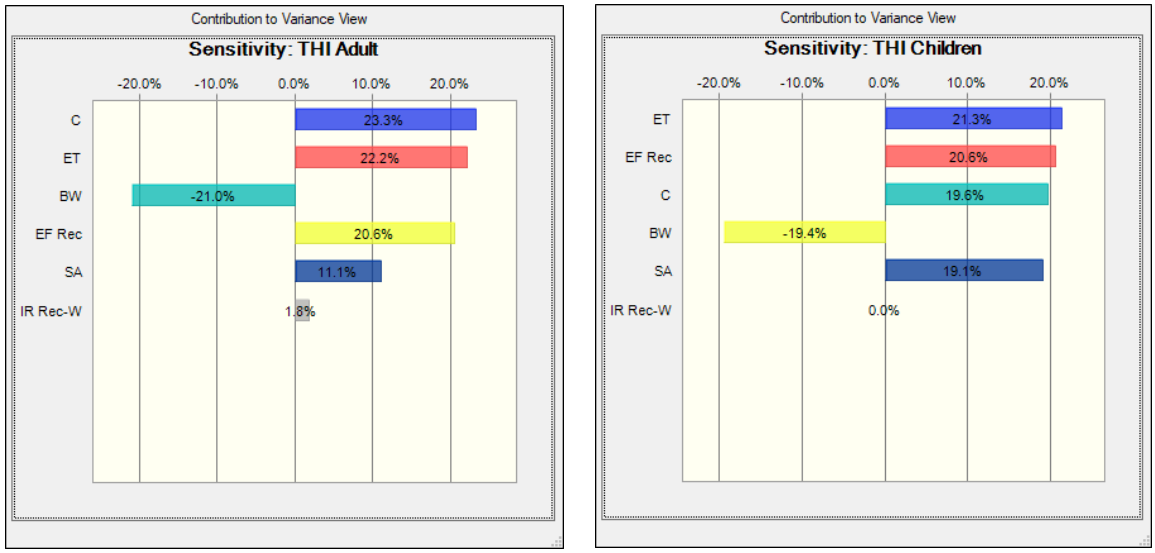

Fig. 3: Sensitivity analysis for all selected variables in health risk

Table 3: The percent reduction of polymer sulfur (PS) to total Hg concentration in coastal water of Makassar City

Sampling sites	THg before application PS	THg after application PS	reduction (%)	p-value
S1	0.0071	0.0043	39	
S2	0.0081	0.0032	60	
S3	0.0055	0.0012	78	
S4	0.0081	0.0023	72	
S5	0.0052	0.0022	58	
S6	0.0025	0.0003	88	
S7	0.0032	0.0011	66	
S8	0.0035	0.0012	66	0.001
S9	0.0095	0.0032	66	
S10	1.0013	0.0011	100	
S11	0.0091	0.0043	53	
S12	0.0056	0.0024	57	
S13	0.0089	0.0041	54	
S14	1.0019	0.0993	90	
S15	1.007	0.0487	95	

adverse impacts in the future. Additionally, strict environmental monitoring and pollution control in coastal areas such as reducing vehicle activities and throwing garbage into the sea are needed.

CONCLUSION

The mean Hg concentration in the coastal water of Makassar city is high and above the water quality standard value in several countries. The Hazard quotient (HQ) was >1 in all sampling sites, which indicates that Hg contamination is likely to cause adverse impacts on the ecosystem, especially in invertebrates and phytoplankton. Based on the Human health risk estimation, communities near the ship harbor namely sites 9, 14 and 15 are at risk of adverse health impacts from Hg exposure. Furthermore, the Monte Carlo simulation (MCS) showed that children are at higher risk of Hg exposure than adults. This condition allows for the possibility of developing non-cancer risk. Children are the most vulnerable subject in terms of rudimentary development. They absorb more Hg during neurodevelopment compared to adults. The most impactful factor for health risk is Hg concentration with a contribution of 23.3 %. The

presence and high level of Hg in the environment will cause ecological damage and health problems. Efforts are needed from the government and all institutions for protection policy and remediation of Hg, especially in coastal areas. This metal is one of the most dangerous and has been shown to cause cardiovascular disease and cancer from long-term exposure. Therefore, the applicable risk reduction effort is reducing Hg concentration in the water column. Based on the results, the application of polymer sulfur (PS) is effective in reducing Hg concentration in the coastal water of Makassar city in the range of 39 – 100%. Due to its high efficiency, polymer sulfur (PS) has broad prospects for the remediation of Hg or other heavy metals in various contaminated media.

AUTHOR CONTRIBUTIONS

A. Mallongi prepared the original draft, methodology and conceptualization. A.U. Rauf performed the data analysis, software and editing. R.D.P. Astuti organized the data curation and validation. S. Palutturi performed the draft review, interpreted the data and results. H. Ishak performed the draft review and data curation.

ACKNOWLEDGMENTS

All authors are very grateful to Higher Education Directorate, Republic of Indonesia for the study grant [No. 8044/UN4.1.2.3/PL.02.00/2021], through Lembaga Penelitian dan Pengabdian Kepada Masyarakat (LPPM) of Hasanuddin University, 2021.

CONFLICT OF INTEREST

The authors declare no potential conflict of interest regarding the publication of this work. In addition, the ethical issues including plagiarism, informed consent, misconduct, data fabrication and, or falsification, double publication and, or submission, and redundancy have been completely witnessed by the authors.

ABBREVIATIONS

%	Percent
°C	Degree of Celcius
AT	Exposure averaging time
ATSDR	Agency for toxic substances and disease registry
BW	Body weight
C	Concentration
CF_w	Volumetric conversion for water
CHg	Hg concentration in water
cm	Centimeter
CRM	Certified Reference Material
CVAAS	Cold vapor atomic absorption spectrophotometry
EF	Exposure frequency
EF_{rec}	Exposure frequency during recreation
ED_{rec}	Exposure duration during recreation
EV_{rec}	Event of recreation
ET	Exposure time
ET_{rec}	Exposure time during recreation
GPS	Global positioning system
GT	Gross tonnage
HDPE	High-density polyethylene
Hg	Mercury
Hg^0	Elemental mercury
H_2SO_4	Sulphuric acid

HNO_3	Nitric acid
INS	Indonesian National Standard
IR	Ingestion rate
IR Rec-w	Ingestion rate of water from recreational activities
HQ	Hazard quotient
Kg	Kilogram
K_p	Dermal permeability constant
$KMNO_4$	Potassium permanganate
$K_2S_2O_8$	Potassium persulfate
L	Liter
Me-Hg	Methylmercury
MCS	Monte carlo simulation
MEMC	Methoxy ethyl mercuric chloride
mL	Milliliter
mg/kg	Miligram per kilogram
mg/L	Milligram per liter
NIST	National Institute of Standards and Technology
nm	Nanometer
pH	Potential of hydrogen
p-value	Probability value
R^2	R-squared
RfD_o	Reference dose for oral exposure
RfD_d	Reference dose for dermal
PS	Polymer sulfur
SA	Exposed skin surface area
SD	Standard deviation
$SnCl_2$	Tin(II) chloride
SNI	National standard of Indonesia
SPSS	Statistical package for the social sciences
THg	Total mercury concentration
THI	Total hazard index
THQ	Target hazard quotient
$THQ_{ingestion}$	Target hazard quotient for ingestion
THQ_{dermal}	Target hazard quotient for dermal
THI	Total hazard index
UAGM	Urban artisanal gold mining
USA	United States of America
USEPA	United States Environmental Protection Agency
WHO	World Health Agency

REFERENCES

Abbas, H.H.; Sakakibara, M.; Sera, K.; Arma, L.H., (2017). Mercury exposure and health problems in urban artisanal gold mining (UAGM) in Makassar, South Sulawesi, Indonesia. Geosci., 7(3): 1-15 (**15 Pages**).

Abbas, H.H.; Sakakibara, M.; Sera, K.; Arma, L.H.; Sididi M., (2020). Socioeconomic and mercury exposure to the Goldsmiths in Manggal Subdistrict of urban artisanal gold mining (UAGM) Area in Makassar, South Sulawesi, Indonesia. IOP Conference Series: Earth and Environmental Science. 589: 1–7 (**7 Pages**).

Al-Saleh, I.; Moncari, L.; Jomaa, A.; Elkhatib, R.; Al-Rouqi, R.; Eltabache, C.; Al-Rajudi, T.; Alnuwaysir, H.; Nester, M.; Aldhalaan, H., (2020). Effects of early and recent mercury and lead exposure on the neurodevelopment of children with elevated mercury and/or developmental delays during lactation: A follow-up study. Int. J. Higiene Environ. Health., 230: 113629 (**15 Pages**).

Amqam, H.; Thalib, D.; Anwar, D.; Mallongi, A.; Sirajuddin, S., (2020). Human health risk assessment of heavy metals via consumption of fish from kao bay., Rev. Environ. Health., 35(3): 257–263 (**7 Pages**).

Aravind, J.; Kanmani, P.; Sudha, G.; Balan, R., (2016). Optimization of chromium(VI) biosorption using gooseberry seeds by response surface methodology. Global J. Environ. Sci. Manage., 2(1): 61-68 **(8 pages).**

Armstrong-Altrin, J.S.; Madhavaraju, J.; Vega-Bautista, F.; Ramos-Vázquez, M.A.; Pérez-Alvarado, B.Y.; Kasper-Zubillaga, J.J.; Ekoa Bessa, A.Z., (2021). Mineralogy and geochemistry of Tecolutla and Coatzacoalcos beach sediments, SW Gulf of Mexico. Appl. Geochem., 134: 105103 (**15 pages**).

Ashe, Katy, (2012). Elevated mercury concentrations in humans of Madre de Dios, Peru. PLos One., 7(3): 1-6 (**6 pages**).

Astuti, R.D.P.; Mallongi, A., (2020). Using system dynamic modeling for improving water security in the coastal area: a literature review. Open Access Maced. J. Med. Sci., 8(F): 143–154 (**12 pages**).

Astuti, R.D.P.; Mallongi, A.; Amiruddin, R.; Hatta, M.; Rauf, A.U., (2021a). Risk identification of heavy metals in well water surrounds watershed area of Pangkajene, Indonesia. Gac. Sanit., 35: S33–S37 (**5 pages**).

Astuti, R.D.P.; Mallongi, A.; Rauf, A.U., (2021b). Risk identification of Hg and Pb in soil: a case study from Pangkep Regency, Indonesia. Soil Sci. Annu., 72(1): 1–15 (**15 pages**).

Astuti, R.D.P.; Mallongi, A.; Choi, K.; Amiruddin, R.; Hatta, M.; Tantrakarnapa, K.; Rauf, A.U., (2022). Health risks from multiroute exposure of potentially toxic elements in a coastal community: A probabilistic risk approach in Pangkep Regency, Indonesia. Geomatics Nat. Hazards Risk., 13(1): 1-32 (**32 pages**).

ATSDR, (1999). Toxicological profile for mercury. Department of Health and Human Services, Public Health Service. Agency for toxic substances and disease registry (**847 pages**).

Azman, N.A.A.; Azoddein, A.A.M.; Ali, M.F., (2020). Polymer sorbent for mercury removal from aqueous solution. IOP Conference Series: Materials Science and Engineering. 736: 052020 (**9 pages**).

Barone, G.; Storelli, A.; Meleleo, D.; Dambrosio, A.; Garofalo, R.; Busco, A.; Storelli, M.M., (2021). Levels of mercury, methylmercury and selenium in fish: insights into children food safety. Toxics., 9(2): 1-14 (**14 pages**).

Basri; Sakakibara, M.; Sera, K., (2020). Mercury in soil and forage plants from artisanal and small-scale gold mining in the Bombana Area, Indonesia. Toxics., 8(1): 1-10 (**10 pages**).

Bratkič, A.; Tinta, T.; Koron, N.; Guevara, S.R.; Begu, E.; Barkay, T.; Horvat, M.; Falnoga, I.; Faganeli, J., (2018). Mercury transformations in a coastal water column (Gulf of Trieste, northern Adriatic Sea). Mar Chem., 200: 57–67 (**11 pages**).

Chowdhury, A.; Das, S.K.; Mondal, S.; Ruidas, S.; Chakraborty, D.; Chatterjee, S.; Bhunia, M.K.; Chandra, D.; Hara, M.; Bhaumik, A., (2021). Sulfur-containing nitrogen rich robust hierarchcally porous organic polymer for adsorptive removal of mercury: experimental and theoritical insights. Environ. Sci. Nano., 8: 2641 – 2649 (**9 pages**).

Du, B.; Li, P.; Feng, X.; Yin, R.; Zhou, J.; Maurice, L., (2021). Monthly variations in mercury exposure of school children and adults in an industrial area of southwestern China., Environ. Res., 196: 110362 (**36 pages**).

Fang,T.H.; Lien, C.Y., (2021). Different mercury species partitioning and distribution in the water and sediment of a eutrophic estuary in Northern Taiwan. Water., 13: 2471 (**19 pages**).

Fioramonti, N.E.; Ribeiro, G.S.; Becker, Y.A.; Riccialdelli, L., (2022). Mercury transfer in coastal and oceanic food webs from the Southwest Atlantic Ocean. Mar. Pollut. Bull., 175: 113365 (**10 pages**).

Gonzalez, D.J.X.; Arain, A.; Fernandez, L.E., (2019). Mercury exposure, risk factors, and perceptions among women of childbearing age in an artisanal gold mining region of the Peruvian Amazon. Environ. Res., 179: 108786 (**9 pages**).

Government of Canada, (1979). Guidelines for Canadian drinking water quality.

Harada, M., (1995). Minamata disease: methylmercury poisoning in Japan caused by environmental pollution. Crit. Rev. Toxicol., 25(1): 1-24 (**24 pages**).

Ishak N.I., (2017). Analisis risiko lingkungan logam berat merkuri pada sedimen laut di wilayah pesisir kota Makassar. Promot. J. Kesehat. Masy., 7(2): 88–92 (**5 pages**).

Ishak, N.I.; Daud, A.; Naiem F. (2014). Risiko logam berat (Hg, Cd, As) pada sedimen laut, ikan, dan kerang terhadap kesehatan masyarakat pesisir Makassar. JST Kesehat., 4(4): 370–376 (7 **pages**).

Iwai-Shimada, M.; Kobayashi, Y.; Isobe, T.; Nakayama, S.F.; Sekiyama, M.; Taniguchi, Y.; Yamazaki, S.; Michikawa, T.; Oda, M.; Mitsubuchi, H.; Sanefuji, M.; Ohga, S.; Mise, N.; Ikegami, A.; Suga, R.; Shimono, M., (2021). Comparison of simultaneous quantitative analysis of methylmercury and inorganic mercury in cord blood using LC-ICP-MS and LC-CVAFS: the pilot study of the Japan environment and children's study. Toxics., 9(4): 1-14 (**14 pages**).

Kakar, A.; Liem-Nguyen, V.; Mahmood, Q.; Jonsson, S., (2021). Elevated concentrations of mercury and methylmercury in the Gadani shipbreaking area, Pakistan. Mar. Pollut. Bull., 165: 112048 (**8 pages**).

Kortei, N.K.; Heymann, M.E.; Essuman, E.K.; Kpodo, F.M.; Akonor, P.T.; Lokpo, S.Y.; Boadi, N.O.; Ayim-Akonor, M.; Tettey, C., (2020). Health risk assessment and levels of toxic metals in fishes (Oreochromis noliticus and Clarias anguillaris) from Ankobrah and Pra basins: Impact of illegal mining activities on food safety. Toxicol Rep., 7: 360–369 (**10 pages**).

Kowalski, A.; Siepak, M.; Boszke, L., (2007). Mercury contamination of surface and groundwaters of Poznań, Poland. Polish J. of Environ. Stud., 16(1): 67-74 (**8 pages**).

La Colla, N.S.; Botté, S.E.; Marcovecchio, J.E., (2019). Mercury cycling and bioaccumulation in a changing coastal system: From water to aquatic organisms. Mar. Pollut. Bull., 140: 40–50 (**11 pages**).

Lamborg, C.H.; Hammerschmidt, C.R.; Bowman, K.L.; Swarr, G.J.; Munson, K.M.; Ohnemus, D.C.; Lam, P.J.; Heimbürger, L.E.; Rijkenberg, M.J.A.; Saito, M.A., (2014). A global ocean inventory of anthropogenic mercury based on water column measurements. Nature., 512 (7512): 65–68 (**4 pages**).

Lestari, H.A.; Samawi, M.F.; Faizal, A.; Moore, A.M.; Jompa, J., (2021). Diversity and abundance of phytoplankton in the coastal waters of South Sulawesi. Hayati J. Biosci., 28(3): 199-211 (**13 pages**).

Li, P.; Feng, X.; Liang, P.; Chan, H.M,; Yan, H.; Chen, L., (2013). Mercury in the seafood and human exposure in coastal area of Guangdong province, South China. Environ. Toxicol. Chem., 32(3): 541–547 (**7 pages)**.

Liu, Y.; Kuang, W.; Xu, J.; Chen, J.; Sun, X.; Lin, C.; Lin, H., (2022). Distribution, source and risk assessment of heavy metals in the seawater, sediments, and organisms of the Daya Bay, China. Mar. Pollut. Bull., 174: 113297 (**12 pages)**.

Mallongi, A., (2014). Environmental risks of mercury contamination in Losari Coastal Area of Makassar City, Indonesia. Int. J. Sci. Res. Publ., 4(2): 1-6 (**6 pages)**.

Mallongi, A.; Birawida, A.B.; Astuti, R.D.P.; Saleh, M., (2020a). Effect of lead and cadmium to blood pressure on communities along coastal areas of Makassar, Indonesia. Enferm. Clin., 30: 313–317 (**5 pages**).

Mallongi, A.; Stang, S.; Manyullei, S.; Natsir, M.F.; Astuti, R.D.P.; Rauf, A.U.; Rachmat, M.; Muhith, A., (2020b). Potential ecological risks of mercury contamination along communities area in tonasa cement industry Pangkep, Indonesia. Enferm. Clin., 30: 119–122 **(4 pages)**.

Mallongi, A.; Rauf, A.U.; Daud, A.; Hatta, M.; Al-Madhoun, W.; Amiruddin, R.; Stang, S.; Wahyu, A.; Astuti, R.D.P., (2022a). Health risk assessment of potentially toxic elements in Maros karst groundwater: a monte carlo simulation approach. Geomatics Nat. Hazards Risk., 13(1): 338–363 (**26 pages**).

Mallongi, A.; Astuti, R.D.P.; Amiruddin, R.; Hatta, M.; Rauf A.U., (2022b). Identification source and human health risk assessment of potentially toxic metal in soil samples around karst watershed of Pangkajene, Indonesia. Environ. Nanotechnol. Monit. Manage., 17: 100634 (**10 pages**).

Mallongi, A.; Stang, S.; Astuti, R.D.P.; Rauf, A.U.; Natsir M.F., (2023). Risk assessment of fine particulate matter exposure attributed to the presence of the cement industry. Global J. Environ. Sci., Manage., 9(1): 1-16 (**16 pages**).

Mann, M.; Luo, X.; Tikoalu, A.D.; Gibson, C.T.; Yin, Y.; Al-attabi, R.; Andersson, G.G.; Raston, C.L.; Henderson, L.C.; Pring, A.; Hasell, T.; Chalker, J.M., (2021). Carbonisation of polymer made from sulfur and canola oil. Chem. Commun., 57: 6296 -6299 (**3 pages**).

Mao, G.; Zhang, Y.; Tong, Y.; Huang, X.; Mehr, F., (2020). Ecological risk assessment of heavy metals to aquatic organisms in the

Lhasa River, Tibet, China. Environ. Sci. Pollut. Res., 27(21): 26091–26102 (**13 pages**).

Ndungu, K.; Beylich, B.A.; Staalstrøm, A.; Øxnevad, S.; Berge, J.A.; Braaten, H.F.V.; Schaanning, M.; Bergstrøm, R., (2017). Petroleum oil and mercury pollution from shipwrecks in Norwegian coastal waters. Sci. Total Environ., 593–594: 624–633 (**10 pages**).

Masni.; Sirajuddin, S.; Syaharuddin.; Syam, A., (2016). Influence of a red palm oil emulsion on the level of retinol in the plasma of primary school children in the coastal area of Makassar City. Pak. J. Nut., 15(5): 465-473 (**9 pages**).

Millard, S.P., (1998). Monte carlo simulation and risk assessment. In: EnvironmentalStats for S-Plus. Springer.

Orosun, M.M.; Adewuyi, A.D.; Salawu, N.B.; Isinkaye, M.O.; Orosun, O.R.; Oniku, A.S., (2020). Monte carlo approach to risks assessment of heavy metals at automobile spare part and recycling market in Ilorin, Nigeria. Sci. Rep., 10(1): 22084 (**16 pages**).

Peraturan Pemerintah, (2021). PP No. 22 tentang penyelenggaraan perlindungan dan pengelolaan lingkungan hidup.

Puno, G.R.; Puno, R.C.C.; Mahhuyop, I.V., (2022). Flood hazard simulation and mapping using digital elevation models with different resolutions. Global J. Environ. Sci. Manage. 8(3):339 – 352 (**14 pages**).

RAIS, (2020). Toxicity profiles for mercury - CAS Number 7439976.

Rauf, A.U.; Mallongi, A.; Astuti, R.D.P., (2020). Mercury and chromium distribution in soil near maros karst ecosystem. Carpathian J. Earth Environ. Sci., 15(2): 453–460 (**8 pages**).

Rauf, A.U.; Mallongi, A.; Daud, A.; Amiruddin, R.; Stang, S.; Wahyu, A.; Astuti, R.D.P., (2022). Spatial distribution and ecological Risk of potentially toxic elements in Maros Regency, Indonesia. Carpathian J. Earth Environ. Sci., 17(1): 93–100 (**8 pages**).

Rauf, A.U.; Mallongi, A.; Lee, K.; Daud, A.; Hatta, M.; Al Madhoun, W.; Astuti, R.D.P., (2021a). Potentially toxic element levels in atmospheric particulates and health risk estimation around industrial areas of Maros, Indonesia. Toxics., 9(12): 328 (**14 Pages**).

Rauf, A.U.; Mallongi, A.; Daud, A.; Hatta, M.; Al-Madhoun, W.; Amiruddin, R.; Rahman, SA.; Wahyu, A.; Astuti, R.D.P., (2021b). Community health risk assessment of total suspended particulates near a cement plant in Maros Regency, Indonesia. J. Health Pollut., 11(30): 1–13 (**13 pages**).

Rauf, A.U.; Mallongi, A.; Daud, A.; Hatta, M.; Astuti, R.D.P., (2021c). Ecological risk assessment of hexavalent chromium and silicon dioxide in well water in Maros Regency, Indonesia. Gac Sanit., 35: S4–S8. (**5 pages**).

Renieri, E.A.; Alegakis, A.K.; Kiriakakis, M.; Vinceti, M.; Ozcagli, E.; Wilks, M.F.; Tsatsakis, A.M., (2014)."Cd, Pb and Hg biomonitoring in fish of the mediterranean region and risk estimations on fish consumption," Toxics., 2(3): 417–442 (**26 pages**).

Saha, N.; Ahmed, M.B.; Ngo, H.H.; Guo, W.; Zhou, J.L.; Rahman, M.S., (2016). Industrial metal pollution in water and probabilistic assessment of human health risk. J. Environ. Manage., 185: 70–78 (**9 pages**).

Sakamoto, M.; Tatsuta, N.; Izumo, K.; Phan, P.T.; Vu, L. D.; Yamamoto, M.; Nakamura, M.; Nakai, K.; Murata, K., (2018). Health Impacts and biomarkers of prenatal exposure to methylmercury: lessons from Minamata, Japan. Toxics., 6(45): 1-9 (**9 pages**).

Suleman, Y.; Rachman, T.; Paotonan, C., (2018). Tinjauan degradasi lingkungan pesisir dan laut kota Makassar terhadap kebijakan penge-lolaan kawasan pesisir. Seminar sains teknologi kelautan. (**8 Pages**).

Tang, H.; Ke, Z.; Yan, M.; Wang, W.; Nie, H.; Li, B.; Zhang, J.; Xu, X.; Wang J., (2018). Concentrations, distribution, and ecological risk assessment of heavy metals in Daya Bay, China. Water., 10(6): 1-15 (**15 pages**).

Tariq, A.; Athar, M.; Ara, J.; Sultana, V.; Ehteshamul-Haque, S.; Ahmad, M, (2015). Biochemical evaluation of antioxidant activity and polysaccharides fractions in seaweeds. Global J. Environ. Sci. Manage., 1(1): 47-62 **(6 pages).**

USEPA, (1989). Risk assessment guidance for superfund human health evaluation manual (Part A). Vol. I.

USEPA, (1991). Risk assessment guidance for superfund. Volume I human health evaluation manual Part (B, Development of Risk-basedPreliminary Remediation Goals.

USEPA, (1996). ECO update: ecotox thresholds. ECO Updat. 3(2): EPA 540/F-95/038.

USEPA, (2004). Risk assessment guidance for superfund volume i: Human health evaluation manual. Part E, supplemental guidance for dermal risk assessment. 1–156 **(156 pages).**

USEPA, (2009). National primary drinking water regulations.

USEPA, (2015). Mid-Atlantic risk assessment: equations (June 2015). Mid-Atlantic Risk Assessment.

USEPA, (2016). Risk based concentration table. Mid-Atlantic Risk.

USEPA, (2021a). Exposure assessment tools by routes – dermal.

USEPA, (2021b). Regional screening levels (RSLs) - equations.

USEPA, (2021c). Regional screening levels (RSLs) - user's guide.

Wang, X.; Shen, Y.; Lin, Y.; Pan, J.; Zhang, Y.; Louie, P.K.K.; Li, M.; Fu, Q., (2019). Atmospheric pollution from ships and its impact on local air quality at a port site in Shanghai. Atmos Chem. Phys., 19(9): 6315–6330 (**16 pages**).

WHO, (2017). Guideline for drinking water quality: fourth edition incorporating the first addendum. 1–631 **(631 pages).**

Xu, D.; Wu, W.D.; Qi, H.J.; Yang, R.X.; Deng, W.Q., (2017). Sulfur rich microporous polymer enables rapid and efficient removal (II) from water. Chemosphere. 196: 174 – 181 (**8 pages**).

Yap, C.K.; Al-Mutairi, K.A., (2022). Ecological-health risk assessments of heavy metals (Cu, Pb, and Zn) in aquatic sediments from the ASEAN-5 emerging developing countries: A review and synthesis. Biology., 11(1): 1-40 (**40 pages**).

Youssef, M.; El-Sorogy, A.; Al-Kahtany, K., (2016). Distribution of mercury in molluscs, seawaters and coastal sediments of Tarut Island, Arabian Gulf, Saudi Arabia. J. African Earth Sci., 124: 365–370. (**6 pages**).

Zaferani, S.; Biester, H., (2021). Mercury accumulation in marine sediments – a comparison of an upwelling area and two large river mouths. Front. Mar. Sci., 8: 732720 (**13 pages**).

Zhang, Q.; Wang, L.; Zhao, L.; Sun, H.; Lu, Y., (2012). Analysis and assessment of heavy metal pollution in sediments of tianjin harbor and Dagu Drainage Canal in Bohai Bay, China. Fresenius Environ. Bull., 21(7): 1777–1785 (**9 pages**).

Zhang, Y.; Liu, Y.; Niu, Z.; Jin, S., (2017). Ecological risk assessment of toxic organic pollutant and heavy metals in water and sediment from a landscape lake in Tianjin City, China. Environ. Sci. Pollut. Res., 24(13): 12301–12311 (**11 pages**).

Zhao, Y.; Xu, M.; Liu, Q.; Wang, Z.; Zhao, L.; Chen, Y., (2018). Study of heavy metal pollution, ecological risk and source apportionment in the surface water and sediments of the Jiangsu coastal region, China: A case study of the Sheyang Estuary. Mar. Pollut. Bull., 137: 601–609 (**10 pages**).

AUTHOR (S) BIOSKETCHES

Mallongi, A., Ph.D., Professor, Department of Environmental Health, Faculty of Public Health, Hasanuddin University, Indonesia Jl. Perintis Kemerdekaan KM 10, Tamalanrea, Kota Makassar, 90245 Indonesia.
- Email: *rawnaenvi@gmail.com*
- ORCID: 0000-0001-6438-1154
- Web of Science ResearcherID: GSO-1993-2022
- Scopus Author ID: 57196100558
- Homepage: https://fkm.unhas.ac.id/teacher/anwar-mallongi-skm-phd/?lang=en

Rauf, A.U., Ph.D. Candidate, Department of Environmental Health, Faculty of Public Health, Hasanuddin University, Indonesia. Jl. Perintis Kemerdekaan KM 10, Tamalanrea, Kota Makassar, 90245 Indonesia.
- Email: *annisautamirauf@gmail.com*
- ORCID: 0000-0002-7808-3374
- Web of Science ResearcherID: AAY-2834-2020
- Scopis Author ID: 57215346048
- Homepage: https://fkm.unhas.ac.id/ilmu-kesehatan-masyarakat-dr-km/

Astuti, R.D.P., Ph.D. Candidate, Department of Environmental Health, Faculty of Public Health, Hasanuddin University, Indonesia. Jl. Perintis Kemerdekaan KM 10, Tamalanrea, Kota Makassar, 90245 Indonesia.
- Email: *ratnadwipujiastuti@gmail.com*
- ORCID: 0000-0001-9693-557X
- Web of Science ResearcherID: ABB-2962-2020
- Scopus Author ID: 57215353200
- Homepage: https://fkm.unhas.ac.id/ilmu-kesehatan-masyarakat-dr-km/

Palutturi, S. Ph.D., Professor, Department of Health Policy and Administration, Faculty of Public Health, Hasanuddin University, Indonesia. Jl. Perintis Kemerdekaan KM 10, Tamalanrea, Kota Makassar, 90245, Indonesia.
- Email: *sukritanatoa72@gmail.com*
- ORCID: 0000-0002-1074-7445
- Web of Science ResearcherID: NA
- Scopus Author ID: 57189250331
- Homepage: https://fkm.unhas.ac.id/teacher/57-2/

Ishak, H, Ph.D. Professor, Department of Environmental Health, Faculty of Public Health, Hasanuddin University, Indonesia. Jl. Perintis Kemerdekaan KM 10, Tamalanrea, Kota Makassar, 90245 Indonesia.
- Email: *hasanuddin.ishak@unhas.ac.id*
- ORCID: 0000-0001-9802-1501
- Web of Science ResearcherID: NA
- Scopus Author ID: 6507848974
- Homepage: https://fkm.unhas.ac.id/ilmu-kesehatan-masyarakat-dr-km/

HOW TO CITE THIS ARTICLE

Mallongi, A.; Rauf, A.U.; Astuti, R.D.P.; Palutturi, S.; Ishak, H., (2023). Ecological and human health implications of mercury contamination in the coastal water. Global J. Environ., Sci. Manage., 9(2): 261-274.

DOI: 10.22034/gjesm.2023.02.06

url: https://www.gjesm.net/article_255151.html

Global J. Environ. Sci. Manage. 9(2): 275-286, Spring 2023, Serial #34

Global Journal of Environmental Science and Management
(GJESM)

Homepage: https://www.gjesm.net/

ORIGINAL RESEARCH PAPER

Environmental assessment of river water quality near oil and gas fields

A.S. Patimah[1], A. Prasetya[2], S.H.M.B. Santosa[3,*]

[1] *Department of Environmental Science, Postgraduate School of Gadjah Mada University, Yogyakarta, Indonesia*

[2] *Department of Chemical Engineering, Faculty of Engineering, Gadjah Mada University, Yogyakarta, Indonesia*

[3] *Department of Geographic Information Science, Faculty of Geography, Gadjah Mada University, Yogyakarta, Indonesia*

ARTICLE INFO

Article History:
Received 24 June 2022
Revised 03 September 2022
Accepted 20 October 2022

Keywords:
Agriculture
Oil and gas industry
Pollution index
River water quality

DOI: 10.22034/gjesm.2023.02.07

ABSTRACT

BACKGROUND AND OBJECTIVES: The research aimed to evaluate the water quality of the Cangkring River in Tuban Regency, East Java Province, Indonesia, at the segment near the oil and gas fields (Mudi Pad A, B, and C).

METHODS: Water samples were collected from January to September 2021 at seven locations along the river segment and tested ex-situ using six parameters, including physical, chemical, and microbiological. The pollution index formula was used to calculate, determine, and analyze the river water quality status. Samples at three locations were further tested with 13 additional chemical parameters due to potential contamination by other substances as they were located the closest to the production site and office area.

FINDINGS: Sample analysis with six parameters showed a pollution index value of 0.558 or within the predefined standard at one location (SW6) and 1.080–2.721 at the other six locations, indicating slight pollution. Another test at three selected locations (i.e., SW1, SW2, and SW7) with 13 additional parameters increased the pollution index to 5.556–6.170 (moderate pollution). This status change was due to the high presence of nitrite and ammonia in the water samples.

CONCLUSION: The oil and gas industry near the Cangkring River has strictly complied with the regulations in treating their produced water. However, it still contains a high amount of nitrite and ammonia, moderately polluting the river water. Therefore, it is necessary to regularly test the river water near oil and gas fields to ensure its quality and safety.

NUMBER OF REFERENCES	NUMBER OF FIGURES	NUMBER OF TABLES
38	1	7

*Corresponding Author:
Email: *sigit.heru.m@ugm.ac.id*
Phone: 0000-0002-6821-6364
ORCID: +62811 470 6027

Note: Discussion period for this manuscript open until July 1, 2023 on GJESM website at the "Show Article".

INTRODUCTION

Environmental pollution is often linked to the growth of economic activities and industrialization (Carvalho *et al.*, 2018; Tran *et al.*, 2019; Nasrollahi *et al.*, 2020). Manufacturing and mining industries are the primary economic sectors in the Asian region that generate different types of pollutants. Industrial activities have been known to contaminate rivers around the business district (Vu *et al.*, 2017; Li *et al.*, 2019; Hoang *et al.*, 2020), including those of the oil and gas sector that potentially diminish the water quality near and downstream of its operational areas. For instance, crude oil extraction brings water to the surface, termed produced water (PW), which constitutes more than 80% of the total wastewater (Bagheri *et al.*, 2018) and contains hydrocarbons and their derivatives. PW is often discharged into the ocean from offshore operations (Jepsen *et al.*, 2018), which can pollute the marine environment, a problem frequently caused by the oil and gas industry that should be handled seriously (Carpenter, 2019). Similarly, on-shore operations often release PW into rivers (McLaughlin *et al.*, 2020). Introducing pollutants into a river can have vast adverse impacts on the ecology and the surrounding communities that depend on its water and many other benefits (Khan and Zhao, 2019). Therefore, PW and other domestic wastes generated by the oil and gas industry should meet a certain standard of quality prior to disposal or reuse (Patimah *et al.*, 2022). According to many previous studies, PW can be utilized to irrigate food crops and other agricultural plants on dry terrains (Echchelh *et al.*, 2018; Sedlacko *et al.*, 2019; McLaughlin *et al.*, 2020). For this purpose, PW is commonly treated using produced water reinjection (PWRI) by adsorption (Costa *et al.*, 2022). However, this method can damage the reservoir formations if it is not conducted carefully and in compliance with the procedures (Liang *et al.*, 2018). It is necessary to be vigilant even when existing processing technologies and processes have been shown to meet the quality criteria, mainly because PW is generated daily in a large volume and can thus endanger the ecosystem around the production area (Ganiyu *et al.*, 2022). PW management requires a structured framework and a risk-based strategy and incorporates various issues, including environmental, technical, and financial (Ghafoori *et al.*, 2022). In some cases, it solely relies on the most cost-efficient alternative (Sabie *et al.*, 2022). Subpar management practices can reduce soil fertility, microbial diversity, agricultural yields (Miller *et al.*, 2020), and lead to river pollution. Therefore, river segments near and downstream of oil and gas fields should be regularly inspected to ensure the water quality standard is met. The water quality index (WQI) is often proposed to estimate and monitor water quality (Aliyu *et al.*, 2019; Lkr *et al.*, 2020). However, because the quality standards vary across countries and purposes, the estimation method should refer to or be adjusted to local government regulations (Costa *et al.*, 2022). For instance, in Indonesia, one of the techniques used to assess river water quality is the pollution index (PI), as outlined in the Decree of the Minister of the Environment No. 115 of 2003 (Hamuna and Tanjung, 2021; Wikurendra *et al.*, 2022). This study primarily aimed to evaluate the river water quality using PI. Samples were collected along the Cangkring River segment near the Mudi Field in 2021. It is one of the locations in Tuban, East Java, Indonesia, where the oil and gas industry operates.

MATERIALS AND METHODS

Bengawan Solo River and one of its tributaries, Cangkring River, run close to the Mudi Field, an oil and gas exploration site in Tuban Regency, East Java Province, Indonesia. The field lies between 7° 04’41” and 7° 08’45”S and between 111° 57’02” and 111° 59’46”E (Fig. 1). It is about 32 km from Tuban Regency and 101 km from Surabaya City, the capital of East Java Province. Tuban has two seasons during which various disasters have been reported: drought and forest fires in dry seasons and floods and landslides in multiple places in rainy seasons (Rustinsyah *et al.*, 2021). It is one of the regencies in the province that relies on agricultural commodities, and the livelihood of its people is mostly in the farming sector (Widiatmaka *et al.*, 2016).

Water sampling

Samples were collected from January to September 2021 at several points along the Cangkring River segment near the oil and gas production site (Mudi Pad B) and the office areas (Mudi Pad A and Mudi Pad C) (Fig.1). The sampling points were selected based on their turbidity level and their position relative to potential sources of pollutants. Different hypotheses were formulated for each point so that the data obtained could describe the entire study area. Table 1 describes the condition and the hypothesis of each sampling location.

Test parameters and quality standards

The water samples collected at seven points were tested ex-situ at the Hydrology Laboratory, Gadjah

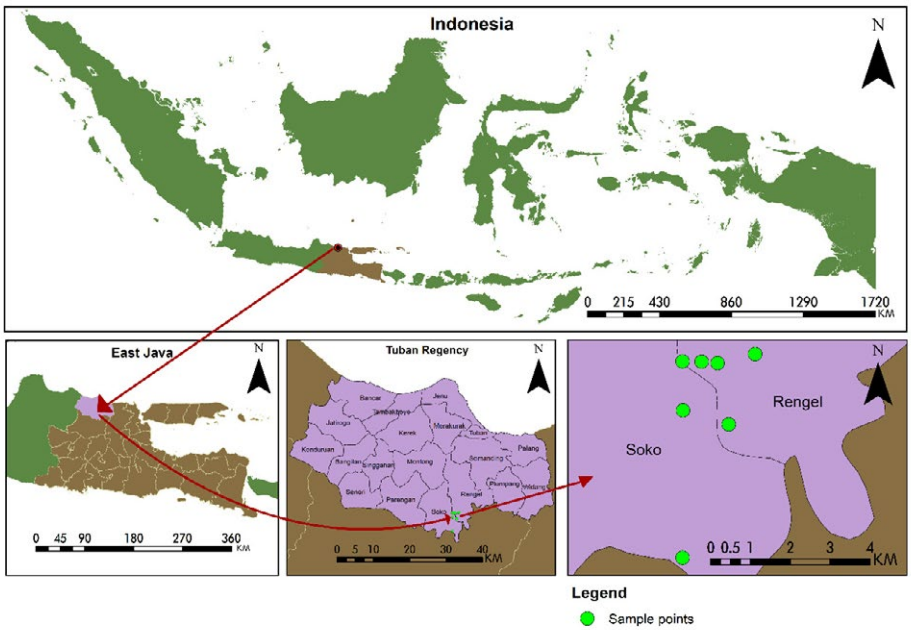

Fig. 1: Geographical location of the Cangkring River, Indonesia, along with the seven sampling points

Mada University, Yogyakarta, Indonesia. The primary characteristics used to gauge the water pollution level were total dissolved solids (TDS), total suspended solids (TSS), biological oxygen demand (BOD_5), chemical oxygen demand (COD), oil and grease, and total coliform, on which the test parameters were based. Three of the seven sampling points, namely SW1, SW2, and SW7, were in direct contact with Mudi Pad B (oil and gas production site) and were assumed to have a higher pollution potential than other points. Thirteen additional organic chemical parameters, including pH, nitrate, nitrite, chloride, sulfate, ammonia, phosphate, detergent, hexavalent chrome, cadmium (Cd), lead (Pb), zinc (Zn), and copper (Cu), were tested at these points. Table 2 summarizes the test parameters, units of measurement, and standards or requirements for the river water quality. These parameters were assessed using specific methods according to applicable laws and regulations (MLHK, 2016). All parameter values were compared against their respective quality standards for class III purposes according to Government Regulation Number 82 of 2001 because the Cangkring River was designated for agricultural activities. Water quality standards measure the highest amount or level of substances, energy, living organisms, or other components a body of water can tolerate without changing its desired condition for specific utilization.

Calculation of the pollution index value

According to the ministerial decree, PI is a method used to assess the river water quality in Indonesia (Hamuna and Tanjung, 2021; Wikurendra *et al.*, 2022). It calculates the pollution level of a water body in relation to water quality parameters measured directly in the field or assessed in the laboratory using collected water samples (Martinus *et al.*, 2018; Suriadikusumah *et al.*, 2021). However, unlike the water quality index, PI is produced to inform about the designated uses of one segment or the entire body of water (Effendi *et al.*, 2015). In other words, it decides the water quality status for a specific purpose (Ikhsan *et al.*, 2021) and lays the groundwork for improving water quality due to high pollutant content (Rahmatillah *et al.*, 2021).

Following the ministerial decree, the pollution index (PI) was used to generate and analyze the water quality parameter values at each sampling point in the Microsoft Excel program. In this study, the PI value was calculated using Eq. 1 (MNLH, 2003).

$$PI_j = \sqrt{\frac{\left(\frac{C_i}{L_{ij}}\right)_M^2 + \left(\frac{C_i}{L_{ij}}\right)_R^2}{2}} \quad (1)$$

Table 1: Water sampling locations and tested hypotheses

Sampling location	Information
Point 1 (SW1)	- Near Mudi Pad B, upstream of the oil and gas production site - The water flows to point 2 (SW2) - Selected to determine the river's water quality before traversing Mudi Pad B, assumed to be the source of pollutants
Point 2 (SW2)	- Near Mudi Pad B, downstream of the oil and gas production site - Water flows from point 1 (SW1) to point 6 (SW6) - Selected to determine the river's water quality after traversing Mudi Pad B. Hypothesis: pollution has occurred at this point
Point 3 (SW3)	- Just upstream of Mudi Pad A (the industry's office area) - Water flows to point 5 (SW5) - Selected to determine the river's water quality before traversing Mudi Pad A, assumed to be the source of pollutants
Point 4 (SW4)	- The outlet of the Cangkring River, before it meets the main river (Bengawan Solo) - Selected to determine the river's water quality before entering Bengawan Solo River, with the assumption that the water is slightly polluted because it is connected to several other water sources
Point 5 (SW5)	- Near Mudi Pad A, just downstream of the oil and gas production site - The water flows from point 3 (SW3) and traverses Mudi Pad A before reaching this point - Selected to determine the river's water quality after flowing through Mudi Pad A. Hypothesis: pollution has occurred at this point
Point 6 (SW6)	- Downstream of Mudi Pad B and upstream of Mudi Pad C, but this point also receives water from other sources. - Water flows from point 2 (SW2) to point 7 (SW7). - Selected to study the conditions around Mudi Pad B (production site) and Mudi Pad C (office area), fed by other water sources assumed to be slightly polluted
Point 7 (SW7)	- Downstream of Mudi Pad C (office area) - Water flows from point 6 (SW6) - Selected to determine the river's water quality after traversing Mudi Pad C. Hypothesis: slight pollution has occurred at this point

Where, L_{ij} is the maximum allowable concentration of water parameter (i) for designated use (j), C_i is the value of the water parameter (i) based on the test results, PI_j is the pollution index for designated use (j), *M* on C_i / L_{ij} is the highest value, and R on C_i / L_{ij} is the average value.

The level of damage or water pollution is difficult to determine if two C_i / L_{ij} values are close to the reference value (1.0), e.g., C_1 / L_{1j} = 0.9 and C_2 / L_{2j} = 1.1, or if they are substantially different, e.g., C_3 / L_{3j} = 5.0 and C_4 / L_{4j} = 10.0. The points below should be considered in solving these problems:

1) If C_i / L_{ij} < 1.0, then the PI is the same as the measurement result

2) Suppose C_i / L_{ij} > 1.0. In that case, $(C_i / L_{ij})_{New}$ is calculated using Eq. 2 (MNLH, 2003). *P* is a constant, and its value can be flexibly chosen depending on the results of environmental observations and the intended criteria for a designated use. The commonly used *P* value is 5.

$$\left(\frac{C_i}{L_{ij}}\right)_{New} = 1.0 + P.log\left(\frac{C_i}{L_{ij}}\right) \quad (2)$$

The derived PI values were then converted into water quality status, which indicates if a body of water is suitable for a particular purpose or polluted at a predefined time (MNLH, 2003). Table 3 classifies the status into four: good condition for PI smaller than 1, slight, moderate, and heavy pollution for PI larger than 1. Each water quality parameter directly correlates to and strongly influences the PI value.

RESULTS AND DISCUSSION

River water quality

Table 4 shows the water quality test results of the Cangkring River between January and September 2021. Seven water samples were collected from different sites along the river segment near the oil and gas production site and office areas and analyzed using six physical, chemical, and microbiological parameters (see Table 2). The two physical parameters, TDS and TSS, were 146–682 mg/L and 12–36 mg/L, or below the upper threshold of 1,000 and 400 mg/L for class III purposes. TDS is influenced by several anthropogenic and natural activities on the surface, while TSS is

Table 2: Test parameters and their maximum allowable presence (MLHK, 2016)

No	Parameter	Abbreviation	Unit	Quality standard for class III**	Sample water (SW)
	Physical				
1	Total dissolved solids	TDS	mg/L	1,000	1–7
2	Total suspended solids	TSS	mg/L	400	1–7
	Chemical				
3	Five-day biological oxygen demand	BOD_5	mg/L	6	1–7
4	Chemical oxygen demand	COD	mg/L	50	1–7
5	Power of hydrogen*	pH	-	6–9	1, 2, 7
6	Nitrate*	NO_3^-	mg/L	20	1, 2, 7
7	Nitrite*	NO_2^-	mg/L	0.06	1, 2, 7
8	Chloride*	Cl	mg/L	600	1, 2, 7
9	Sulfate*	SO_4	mg/L	400	1, 2, 7
10	Ammonia*	NH_3-N	mg/L	0.5	1, 2, 7
11	Phosphate*	PO_4^{3-}	mg/L	1	1, 2, 7
12	Detergent*		mg/L	0.2	1, 2, 7
13	Chromium hexavalent*	Cr^{6+}	mg/L	0.05	1, 2, 7
14	Cadmium*	Cd	mg/L	0.01	1, 2, 7
15	Leads*	Pb	mg/L	0.03	1, 2, 7
16	Zinc*	Zn	mg/L	0.05	1, 2, 7
17	Copper*	Cu	mg/L	0.02	1, 2, 7
18	Oil and grease		mg/L	1	1–7
	Microbiological				
19	Total coliform		Σ/100 mL	10,000	1–7

*additional organic chemical parameters
**per the Decree of the Indonesia Minister of Environment Number 115 of 223

determined by plant roots and their role in nutrient adsorption, dust distribution from the air, and root decomposition (Suriadikusumah *et al.*, 2021). The chemical parameters tested were BOD_5, COD, and oil and grease contents. BOD_5 values varied widely from 1.70 to 20.60 mg/L. SW1, SW4, SW5, and SW7 had BOD_5 above its maximum allowable presence for class III purposes. Moreover, SW7 had the highest BOD_5 of 20.6 mg/L or three times greater than the upper limit. The cause is impurities from agricultural and domestic waste disposed of into the river. On the contrary, the COD values of all the points were below the upper limit. Nevertheless, there is a linear relationship between COD and BOD_5 (Qi *et al.*, 2021). The next chemical parameter was oil and grease content, which exceeded its maximum allowable presence at SW1, SW2, and SW3. The only microbiological parameter tested in this study was total coliform, and the results showed that it was below the upper threshold of 10,000 per 100 mL at all the sampling points. Based on the physical and microbiological parameter values, the Cangkring River segment near the oil and gas production site and office

Table 3: Water quality status based on pollution index values (MNLH, 2003)

$\mathbf{PI_j}$ Score	Water quality status
$0 \leq \mathbf{PI_j} \leq 1.0$	Good condition (the quality standards are met)
$1.0 < \mathbf{PI_j} \leq 5.0$	Slight pollution
$5.0 < \mathbf{PI_j} \leq 10.0$	Moderate pollution
$\mathbf{PI_j} > 10.0$	Heavy pollution

Table 4: Water quality test results of the seven samples along the Cangkring River segment near the oil and gas production site and office areas in Tuban

No.	Parameters	Unit	Quality standards for class III	Parameter values						
				SW1	SW2	SW3	SW4	SW5	SW6	SW7
1	TDS	mg/L	1,000	146.00	170.00	268.00	506.00	430.00	457.00	682.00
2	TSS	mg/L	400	13.00	13.00	13.00	24.00	20.00	25.50	36.00
3	BOD_5	mg/L	6	6.53	4.60	1.70	9.70	7.40	4.30	20.60
4	COD	mg/L	50	17.38	13.95	12.31	14.20	11.00	7.80	36.70
5	Oil and grease	mg/L	1	1.60	1.60	1.60	0.80	0.40	0.50	0.80
6	Total coliform	/100 mL	10,000	2,400	2,400	1,100	3,600	2,200	850	8,000

areas still meets the water quality standards and is thus suitable for supplying agricultural irrigation water. However, the chemical conditions put a limit to this purpose because the upper thresholds were exceeded at SW1, SW2, and SW7, which were close to Mudi Pad B (production site). Of the seven points, SW6 is the only location whose parameter values were below their respective maximum allowable presence. It is located between Mudi Pad B (production site) and Mudi Pad C (office area) and receives water from other sources.

Additional testing of chemical parameters

Because the BOD_5 and oil and grease content at SW1, SW2, and SW7 exceeded their maximum allowable presence for class III purposes, the three points were further tested using 13 additional organic chemical parameters. Their selection for the additional test was also based on their proximity to the potential sources of pollutants. SW1 and SW2 were in direct contact with the oil and gas production site Mudi Pad B, while SW7 was located between Mudi Pad B and the office area Mudi Pad A. In addition, they had a higher pollution potential than the other four sampling points, and SW7 had a slightly higher value than the rest for some parameters. Of the 13 additional parameters, the nitrite, ammonia, and phosphate concentrations exceeded their respective upper limits for class III purposes, as shown in Table 5.

Pollution index and water quality status

PI values determine the river's water quality at each sampling location based on their physical, chemical, and microbiological parameter values (see Table 4). The PI of each parameter was calculated using Eqs. 1 and 2 to obtain the value of C_i / L_{ij} and $\left(C_i / L_{ij}\right)_{New}$ for class III purposes, i.e., agricultural irrigation, before being classified into one of the four water quality statuses (see Table 3). Table 6 shows the entire calculation results for the six parameters and the water quality status of each point. Tables 4 and 6 also indicate a linear relationship between the parameter values, PI values, and water quality status. The water quality test results showed that SW6 was the only point that met all the criteria for class III water. Similarly, its PI value, 0.558, categorized the water quality as good condition. On the contrary, the PI values of other points ranged from 1.080 to 1.522, indicating slight pollution. This pollution level is also characterized by the PI value of each tested parameter.

Table 5: Test results of three selected sampling points with additional 13 chemical parameters

No	Parameters	Unit	Quality standards class III	Sample test results		
				SW1	SW2	SW7
1	TDS	mg/L	1,000	146.00	170.00	682.00
2	TSS	mg/L	400	13.00	13.00	36.00
3	Power of hydrogen*	-	9	7.80	7.76	7.61
4	BOD_5	mg/L	6	6.53	4.60	20.60
5	COD	mg/L	50	17.38	13.95	36.70
6	Nitrate*	mg/L	20	2.35	2.29	20.00
7	Nitrite*	mg/L	0.06	2.00	1.55	1.33
8	Chloride*	mg/L	600	28.00	28.40	28.40
9	Sulfate*	mg/L	400	18.00	12.30	11.90
10	Ammonia*	mg/L	0.5	4.25	4.07	6.13
11	Phosphate*	mg/L	1	1.15	1.06	0.99
12	Detergent*	mg/L	0.2	0.0480	0.1200	0.0640
13	Chromium hexavalent*	mg/L	0.05	0.0100	0.0036	0.0036
14	Cadmium*	mg/L	0.01	0.0033	0.0033	0.0033
15	Leads*	mg/L	0.03	0.0130	0.0130	0.0130
16	Zinc*	mg/L	0.05	0.0180	0.0096	0.0140
17	Copper*	mg/L	0.02	0.0860	0.0086	0.0086
18	Oil and grease	mg/L	1	1.60	1.60	0.80
19	Total coliform	/100 mL	10,000	2,400	2,400	8,000

*Additional organic chemical parameters

For instance, BOD_5 and oil and grease content at other locations had a PI value of between 1 to 5, contributing to slight pollution. The sampling points other than SW6 were classified as slightly polluted, with the primary contributing factors being BOD_5 and oil and grease content because only both parameters had the C_i / L_{ij} and $(C_i / L_{ij})_{New}$ of higher than 1.

Table 7 shows the PI calculation for the six parameters measured at the initial stage and the additional 13 chemical parameters at SW1, SW2, and SW7. Compared with the PI values of the six parameters (Table 6), there was a considerable increase in value and water quality status from slight to moderate pollution. The three selected points were previously identified as potentially polluted by the production activities of the oil and gas sector because BOD_5 and oil and grease content had the C_i / L_{ij} and $(C_i / L_{ij})_{New}$ of higher than 1 (see Table 6). Aside from these two chemical parameters, the additional test also revealed that nitrite, ammonia, and phosphate contributed to the high PI values. However, nitrite and ammonia contents (dissolved nitrogen) were found to be substantially above their upper limits for class III water. The total nitrogen calculated using Total Kjeldahl Nitrogen (TKN) includes ammonia and all organic nitrogen molecules that can cause the formation of a hypoxic zone, resulting in oxygen deprivation (Al-Ghouti *et al.*, 2019). The high nitrite contents indicated that the organic matter breakdown along the Cangkring River segment consumed oxygen, thereby decreasing the oxygen content in the water. Meanwhile, an increase in nitrogen levels, specifically nitrite, is caused by the influx of waste from agricultural activities (John *et al.*, 2020).

The average and maximum C_i / L_{ij} and/or $(C_i / L_{ij})_{New}$ values of all the parameters are components of PI calculation formula. PI values determine the water quality status; thus, if one parameter value increases to very high, it will also increase the PI value and worsens the status. The maximum C_i / L_{ij} and/or $(C_i / L_{ij})_{New}$ values of nitrite and ammonia were higher than 5, indicating moderate pollution. Both parameters caused the water quality status at SW1, SW2, and SW7 to change from slightly to moderately polluted. Nitrite and ammonia, which include nitrogen, are not always produced by the oil and gas industry but can also result from agricultural

Table 6: Pollution Index values and water quality status at seven points along the Cangkring River segment near the oil and gas production site and office areas in Tuban

No.	Parameters	SW1		SW2		SW3	
		C_1/L_{1j}	$(C_1/L_{1j})_{New}$	C_2/L_{2j}	$(C_2/L_{2j})_{New}$	C_3/L_{3j}	$(C_3/L_{3j})_{New}$
1	TDS	0.146	0.146	0.170	0.170	0.268	0.268
2	TSS	0.033	0.033	0.033	0.033	0.033	0.033
3	BOD_5	1.088*	1.184	0.767	0.767	0.283	0.283
4	COD	0.348	0.348	0.279	0.279	0.246	0.246
5	Oil and Grease	1.600*	2.021	1.600*	2.021	1.600*	2.021
6	Total Coliform	0.240	0.240	0.240	0.240	0.110	0.110
Average		$(C_1/L_{1j})_R$	0.662	$(C_2/L_{2j})_R$	0.585	$(C_3/L_{3j})_R$	0.493
Maximum		$(C_1/L_{1j})_M$	2.021	$(C_2/L_{2j})_M$	2.021	$(C_3/L_{3j})_M$	2.021
Pollutant Index		PI_{1j}	1.503	PI_{2j}	1.487	PI_{3j}	1.471
	Quality status	Slightly polluted		Slightly polluted		Slightly polluted	

No.	Parameters	SW4		SW5		SW6	
		C_4/L_{4j}	$(C_4/L_{4j})_{New}$	C_5/L_{5j}	$(C_5/L_{5j})_{New}$	C_6/L_{6j}	$(C_6/L_{6j})_{New}$
1	TDS	0.506	0.506	0.430	0.430	0.457	0.457
2	TSS	0.060	0.060	0.050	0.050	0.064	0.064
3	BOD_5	1.617*	2.043	1.233*	1.455	0.717	0.717
4	COD	0.284	0.284	0.220	0.220	0.156	0.156
5	Oil and Grease	0.800	0.800	0.400	0.400	0.500	0.500
6	Total Coliform	0.360	0.360	0.220	0.220	0.085	0.085
Average		$(C_4/L_{4j})_R$	0.676	$(C_5/L_{5j})_R$	0.463	$(C_6/L_{6j})_R$	0.330
Maximum		$(C_4/L_{4j})_M$	2.043	$(C_5/L_{5j})_M$	1.455	$(C_6/L_{6j})_M$	0.717
Pollutant Index		PI_{4j}	1.522	PI_{5j}	1.080	PI_{6j}	0.558
	Quality status	Slightly polluted		Slightly polluted		Good condition (Quality standards are met)	

No.	Parameters	SW7	
		C_{i7}/L_{ij}	$(C_{i7}/L_{ij})_{New}$
1	TDS	0.682	0.682
2	TSS	0.090	0.090
3	BOD_5	3.433*	3.679
4	COD	0.734	0.734
5	Oil and Grease	0.800	0.800
6	Total Coliform	0.800	0.800
Average		$(C_7/L_{7j})_R$	1.131
Maximum		$(C_7/L_{7j})_M$	3.679
Pollutant Index		PI_{7j}	2.721
	Quality status		Slightly polluted

*C_i/L_j >1, indicating the need for a new C_i/L_j calculation, $(C_i/L_j)_{New}$.

practices that apply nitrogen-based fertilizers. Even though nitrite and ammonia are non-carcinogenic, their high presence in moderately contaminated water is still harmful to human health (Adimalla and Qian, 2019). Nevertheless, Cangkring River water can still be used for agricultural irrigation, provided that a further investigation into the effect of high nitrate and ammonia content on plant growth be conducted.

Table 7: Pollution Index values and water quality status at three selected points near the oil and gas production site and office areas in Tuban with 13 additional chemical parameters

No	Parameters	SW1		SW2		SW7	
		C_1/L_{1j}	$(C_1/L_{1j})_{New}$	C_2/L_{2j}	$(C_2/L_{2j})_{New}$	C_7/L_{7j}	$(C_7/L_{7j})_{New}$
1	TDS	0.146	0.146	0.170	0.170	0.682	0.682
2	TSS	0.033	0.033	0.033	0.033	0.090	0.090
3	pH	0.867	0.867	0.862	0.862	0.846	0.846
4	BOD_5	1.088*	1.184	0.767	0.767	3.433*	3.679
5	COD	0.348	0.348	0.279	0.279	0.734	0.734
6	Nitrate	0.118	0.118	0.115	0.115	1.000	1,000
7	Nitrite	33.333*	8.614	25.833*	8.061	22.167*	7,729
8	Chloride	0.047	0.047	0.047	0.047	0.047	0.047
9	Sulfate	0.045	0.045	0.031	0.031	0.030	0.030
10	Ammonia	8.500*	5.647	8.140*	5.553	12.260*	6.442
11	Phosphate	1.150*	1.303	1.060*	1.127	0.990	0.990
12	Detergent	0.240	0.240	0.600	0.600	0.320	0.320
13	Chromium hexavalent	0.200	0.200	0.072	0.072	0.072	0.072
14	Cadmium	0.330	0.330	0.330	0.330	0.330	0.330
15	Leads	0.433	0.433	0.433	0.433	0.433	0.433
16	Zinc	0.360	0.360	0.192	0.192	0.280	0.280
17	Copper	4.300*	4.167	0.430	0.430	0.430	0.430
18	Oil and grease	1.600*	2.021	1.600*	2.021	0.800	0.800
19	Total coliform	0.240	0.240	0.240	0.240	0.800	0.800
Average		$(C_1/L_{1j})_R$	1.386	$(C_2/L_{2j})_R$	1.124	$(C_7/L_{7j})_R$	1.420
Maximum		$(C_1/L_{1j})_M$	8.614	$(C_2/L_{2j})_M$	8.061	$(C_7/L_{7j})_M$	7.729
Pollutant index		PI_{1j}	6.170	PI_{2j}	5.755	PI_{7j}	5.556
Quality status		Moderately polluted		Moderately polluted		Moderately polluted	

*C_i/L_j >1, indicating the need for a new C_i/L_j calculation, $(C_i/L_j)_{New}$.

CONCLUSION

The water quality of the Cangkring River segment near the oil and gas fields has been determined at seven sampling points using six main physical, chemical, and microbiological parameters, i.e., TDS, TSS, BOD_5, COD, oil and grease, and total coliform. Furthermore, points SW1, SW2, and SW7 have been selected for further analysis using 13 more chemical parameters because of their high BOD_5 and oil and grease levels and proximity to the production site and office areas. Based on the additional analysis, the river's nitrite, ammonia, and phosphate concentrations are above their maximum allowable presence in water for class III purposes. For these reasons, their water quality status is moderately polluted. The nitrite and ammonia contents are substantially above their upper limits, presumably caused by an increase in nitrogen. Nitrite and ammonia are not always associated with the oil and gas industry but also agricultural activities. Nevertheless, the Cangkring River water can still be used to irrigate farmlands despite its low to moderate contamination levels. The research has found that even with the strict regulations currently enforced in treating the produced water (PW) from the oil and gas fields, the discharged PW still contains a significant amount of nitrite and ammonia, resulting in moderately polluted river water. Also, conducting an additional test with 13 chemical parameters at three locations closest to the fields has provided a good comparison for the six-parameter water quality test results and confirmed this finding. Therefore, to address the high nitrite and ammonia contents, it is also necessary to regularly assess the river water quality near the fields to ensure that it is safe for the agricultural sector and the environment and to investigate the effect of moderately contaminated water on crop health.

AUTHOR CONTRIBUTIONS

A.S. Patimah conducted the literature review, designed the research, performed data collection, data

analysis and interpretation, and prepared the article. A. Prasetya performed the literature review for chemical parameters and analyzed and interpreted the data, especially on the water test results. S.H.M.B. Santosa conducted the literature review for site selection for the research, sampling, and data collection and analyzed and interpreted the data, especially those related to location and mapping.

ACKNOWLEDGMENT

The authors would like to express their gratitude to the Doctoral Program in Environmental Sciences at Gadjah Mada University in Yogyakarta, Indonesia, for funding this research through the dissertation research grant program (PDD) in 2022 [Grant Number 1873/UN1/DITLIT/Dit-Lit/PT.01.03/2022]. Gratitude is also extended to the Hydrology Laboratory of Gadjah Mada University and Pertamina LLC in Tuban for their support in acquiring field data and test results.

CONFLICT OF INTEREST

The authors declare no potential conflict of interest regarding the publication of this work. In addition, the ethical issues, including plagiarism, informed consent, misconduct, data fabrication and/or falsification, double publication and/or submission, and redundancy, have been completely witnessed by the authors.

OPEN ACCESS

PUBLISHER'S NOTE

ABBREVIATIONS

BOD_5	Five-day biological oxygen demand
Cd	Cadmium
C_i	Parameter value at point (i) based on the test results
Cl	Chloride
COD	Chemical oxygen demand
Cr^{6+}	Chromium hexavalent
Cu	Copper
Eq.	Equation
et al.	*et alia* (others)
Fig.	Figure
L_{ij}	Water quality standards for purpose (j) at point (i)
mg/L	Milligrams per liter
MLHK	*Menteri Lingkungan Hidup dan Kehutanan* (Minister of Environment and Forestry of the Republic of Indonesia)
MNLH	*Menteri Negara Lingkungan Hidup* (Secretary of State for Environment of the Republic of Indonesia)
NH_3-N	Ammonia
NO_2^-	Nitrite
NO_3^-	Nitrate
P	Constants (usually filled with the number 5)
Pb	Lead
pH	Power of hydrogen
PI	Pollution Index
PI_j	Pollution index value for purpose (j)
PO_4^{3-}	Phosphate
PP	*Peraturan Pemerintah* (Government Regulation of the Republic of Indonesia)
PT	*Perseroan Terbatas* (limited liability company)
PW	Produced Water
PWRI	Produced water reinjection
SO_4	Sulfate
SW	Water sample
TDS	Total dissolved solid
TKN	Total Kjeldahl Nitrogen

TSS	Total suspended solid
WQI	Water Quality Index
Zn	Zinc
Σ/100 mL	A certain amount in every 100 milliliters
$\left(\frac{C_i}{L_{ij}}\right)$	Pollution index of each parameter
$\left(\frac{C_i}{L_{ij}}\right)_M$	The maximum value of the pollution index of all parameters
$\left(\frac{C_i}{L_{ij}}\right)_{New}$	Pollution index of each new parameter (if the value of the previously calculated pollution index is higher than 1)
$\left(\frac{C_i}{L_{ij}}\right)_R$	The average value of the pollution index of all parameters

REFERENCES

Adimalla, N.; Qian, H., (2019). Groundwater quality evaluation using water quality index (WQI) for drinking purposes and human health risk (HHR) assessment in an agricultural region of Nanganur, South India. Ecotoxicol. Environ. Saf., 176: 153-161 **(9 pages)**.

Al-Ghouti, M.A.; Al-Kaabi, M.A.; Ashfaq, M.Y.; Da'na, D.A., (2019). Produced water characteristics, treatment and reuse: A review. J. Water Process Eng., 28: 222-239 **(18 pages)**.

Aliyu, G.A.; Jamil, N.R.B.; Adam, M.B.; Zulkeflee, Z., (2019). Assessment of Guinea Savanna River system to evaluate water quality and water monitoring networks. Global J. Environ. Sci. Manage., 5(3): 345-356 **(12 pages)**.

Bagheri, M.; Roshandel, R.; Shayegan, J., (2018). Optimal selection of an integrated produced water treatment system in the upstream of oil industry. Process Saf. Environ. Protect., 117: 67-81 **(15 pages)**.

Carpenter, A., (2019). Oil pollution in the North Sea: the impact of governance measures on oil pollution over several decades. Hydrobiol., 845: 109-127 **(19 pages)**.

Carvalho, N.; Chaim, O.; Cazarini, E.; Gerolamo, M., (2018). Manufacturing in the fourth industrial revolution: A positive prospect in sustainable manufacturing. Procedia Manuf., 21: 671-678 **(8 pages)**.

Costa, T.C.; Hendges, L.T.; Temochko, B.; Mazur, L.P.; Marinho, B.A.; Weschenfelder, S.E.; Florido, P.L.; da Silva, A.; de Souza, A.A.U.; de Souza, S.M.A.G.U., (2022). Evaluation of the technical and environmental feasibility of adsorption process to remove water soluble organics from produced water: A review. J. Pet. Sci. Eng., 208: 109360 **(15 pages)**.

Echchelh, A.; Hess, T.; Sakrabani, R., (2018). Reusing oil and gas produced water for irrigation of food crops in drylands. Agric. Water Manage., 206: 124-134 **(11 pages)**.

Effendi, H.; Romanto, R.; Wardiatno, Y., (2015). Water Quality Status of Ciambulawung River, Banten Province, Based on Pollution Index and NSF-WQI. Procedia Environ. Sci., 24: 228-237 **(10 pages)**.

Ganiyu, S.O.; Sable, S.; El-Din, M.G., (2022). Advanced oxidation processes for the degradation of dissolved organics in produced water: A review of process performance, degradation kinetics and pathway. Chem. Eng. J., 429: 132492 **(24 pages)**.

Ghafoori, S.; Omar, M.; Koutahzadeh, N.; Zendehboudi, S.; Malhas, R.N.; Mohamed, M.; Al-Zubaidi, S.; Redha, K.; Baraki, F.; Mehrvar, M., (2022). New advancements, challenges, and future needs on treatment of oilfield produced water: A state-of-the-art review. Sep. Purif. Technol., 289: 120652 **(24 pages)**.

Hamuna, B.; Tanjung, R.H.R., (2021). Heavy metal content and spatial distribution to determine the water pollution index in Depapre Waters, Papua, Indonesia. Current Appl. Sci. Technol., 21(1): 1-11 **(11 pages)**.

Hoang, H.G.; Lin, C.; Tran, H.T.; Chiang, C.F.; Bui, X.T.; Cheruiyot, N.K.; Shern, C.C.; Lee, C.W., (2020). Heavy metal contamination trends in surface water and sediments of a river in a highly-industrialized region. Environ. Technol. Innovation, 20: 101043 **(14 pages)**.

Ikhsan, J.; Kurniati, R.; Rozainy, M.R., (2021). Analysis of river water quality in the upstream of the Code River, Indonesia. IOP Conference Series: Earth and Environmental Science, 794: 012044 **(8 pages)**.

Jepsen, K.L.; Bram, M.V.; Pedersen, S.; Yang, Z., (2018). Membrane fouling for produced water treatment: A review study from a process control perspective. Water, 10(7): 847 **(28 pages)**.

John, E.M.; Krishnapriya, K.; Sankar, T.V., (2020). Treatment of ammonia and nitrite in aquaculture wastewater by an assembled bacterial consortium. Aquaculture, 526: 735390 **(6 pages)**.

Khan, I.; Zhao, M., (2019). Water resource management and public preferences for water ecosystem services: A choice experiment approach for inland river basin management. Sci. Total Environ., 646: 821-832 **(11 pages)**.

Liang, Y.; Ning, Y.; Liao, L.; Yuan, B., (2018). Special focus on produced water in oil and gas fields: Origin, management, and reinjection practice. In: Formation Damage During Improved Oil Recovery. Gulf Professional Publishing, 515-586 **(71 pages)**.

Li, Y.; Zhou, Q.; Ren, B.; Luo, J.; Yuan, J.; Ding, X.; Bian, H.; Yao, X., (2019). Trends and health risks of dissolved heavy metal pollution in global river and lake water from 1970 to 2017. Rev. Environ. Contam. Toxicol., 251: 1-24 **(24 pages)**.

Lkr, A.; Singh, M.R.; Puro, N., (2020). Assessment of water quality status of Doyang River, Nagaland, India, using water quality index. Appl. Water Sci., 10: 46 **(13 pages)**.

Martinus, Y.; Astono, W.; Hendrawan, D., (2018). Water quality study of Sunter River in Jakarta, Indonesia. IOP Conference Series: Earth and Environmental Science, 106: 012022 **(6 pages)**.

McLaughlin, M.C.; Borch, T.; McDevitt, B.; Warner, N.R.; Blotevogel, J., (2020). Water quality assessment downstream of oil and gas produced water discharges intended for beneficial reuse in arid regions. Sci. Total Environ., 713: 136607 **(12 pages)**.

Miller, H.; Dias, K.; Hare, H.; Borton, M.A.; Blotevogel, J.; Danforth, C.; Wrighton, K.C.; Ippolito, J.A.; Borch, T., (2020). Reusing oil and gas produced water for agricultural irrigation: Effects on soil health and the soil microbiome. Sci. The Total Environ., 722: 137888 **(9 pages)**.

MLHK, (2016). Peraturan Menteri Lingkungan Hidup dan Kehutanan Republik Indonesia Nomor: P.68/Menlhk/Setjen/Kum.1/8/2016

tentang Baku Mutu Air Limbah Domestik. Jakarta: Kementerian Lingkungan Hidup dan Kehutanan.

MNLH, (2003). Keputusan Menteri Negara Lingkungan Hidup Nomor: 115 Tahun 2003 tentang Pedoman Penentuan Status Mutu Air. Jakarta: Menteri Negara Lingkungan Hidup.

Nasrollahi, Z.; Hashemi, M.S.; Bameri, S.; Taghvaee, V.M., (2020). Environmental pollution, economic growth, population, industrialization, and technology in weak and strong sustainability: using STIRPAT model. Environ. Dev. Sustainability, 22(2): 1105-1122 **(18 pages)**.

Patimah, A.S.; Prasetya, A.; Murti, S.H., (2022). Study of domestic wastewater in oil and gas field: A case study in the Cangkring River, Tuban, East Java. IOP Conference Series: Earth Environmental Science, 963: 012051 **(12 pages)**.

Peraturan Pemerintah, (2001). Peraturan Pemerintah Republik Indonesia Nomor 82 Tahun 2001 tentang Pengelolaan Kualitas Air dan Pengendalian Pencemaran Air. Jakarta: Pemerintah Republik Indonesia.

Qi, M.; Han, Y.; Zhao, Z.; Li, Y., (2021). Integrated determination of chemical oxygen demand and biochemical oxygen demand. Pol. J. Environ. Stud., 30(2): 1785-1794 **(10 pages)**.

Rahmatillah, R.; Meilina, H.; Ramli, I., (2021). Water quality index and the sediment criteria due to anthropogenic activity in West Aceh District, Indonesia. IOP Conference Series: Earth and Environmental Science, 922: 012042 **(9 pages)**.

Rustinsyah, R.; Prasetyo, R.A.; Adib, M., (2021). Social capital for flood disaster management: Case study of flooding in a village of Bengawan Solo Riverbank, Tuban, East Java Province. Int. J. Disaster Risk Reduct., 52: 101963 **(10 pages)**.

Sabie, R.; Langarudi, S.P.; Perez, K.; Thomson, B.; Fernald, A., (2022). Conceptual framework for modeling dynamic complexities in produced water management. Water, 14(15): 2341 **(13 pages)**.

Sedlacko, E.M.; Jahn, C.E.; Heuberger, A.L.; Sindt, N.M.; Miller, H.M.; Borch, T.; Blaine, A.C.; Cath, T.Y.; Higgins, C.P., (2019). Potential for beneficial reuse of oil and gas–derived produced water in agriculture: Physiological and morphological responses in Spring Wheat (Triticum aestivum). Environ. Toxicol. Chem., 38(8): 1756-1769 **(14 pages)**.

Suriadikusumah, A.; Mulyani, O.; Sudirja, R.; Sofyan, E.T.; Maulana, M.H.R.; Mulyono, A., (2021). Analysis of the water quality at Cipeusing river, Indonesia using the pollution index method. Acta Ecol. Sin., 41(3): 177-182 **(6 pages)**.

Tran, H.; Vi, H.; Dang, H.; Narbaitz, R., (2019). Pollutant removal by Canna Generalis in tropical constructed wetlands for domestic wastewater treatment. Global J. Environ. Sci. Manage., 5(3): 331-344 **(14 pages)**.

Vu, C.T.; Lin, C.; Shern, C.C.; Yeh, G.; Le, V.G.; Tran, H.T., (2017). Contamination, ecological risk and source apportionment of heavy metals in sediments and water of a contaminated river in Taiwan. Ecol. Indic., 82: 32-42 **(11 pages)**.

Widiatmaka, W.; Ambarwulan, W.; Setiawan, Y.; Walter, C., (2016). Assessing the Suitability and Availability of Land for Agriculture in Tuban Regency, East Java, Indonesia. Appl. Environ. Soil Sci., 2016: 7302148 **(13 pages)**.

Wikurendra, E.A.; Syafiuddin, A.; Nurika, G.; Elisanti, A.D., (2022). Water quality analysis of pucang river, sidoarjo regency to control water pollution. Environ. Qual. Manage., 1-12 **(12 pages)**.

AUTHOR (S) BIOSKETCHES

Patimah, A.S., Ph.D. Candidate, Department of Environmental Science, School of Postgraduate, Universitas Gadjah Mada, Yogyakarta, Indonesia.
- Email: *fatimah13lee@gmail.com*
- ORCID: 0000-0002-3381-3193
- Web of Science ResearcherID: GSE-6331-2022
- Scopus Author ID: 57440910300
- Homepage: http://www.pasca.ugm.ac.id/v3.0/id/programs.sub-40

Prasetya, A., Ph.D., Associate Professor, Department of Chemical Engineering, Faculty of Engineering, Universitas Gadjah Mada, Yogyakarta, Indonesia.
- Email: *aguspras@ugm.ac.id*
- ORCID: 0000-0001-5126-6253
- Web of Science ResearcherID: GWC-3938-2022
- Scopus Author ID: 36154870700
- Homepage: https://chemeng.ugm.ac.id/web/?page_id=2263

Santosa, S.H.M.B., Ph.D., Associate Professor, Department of Geographic Information Science, Faculty of Geography, Universitas Gadjah Mada, Yogyakarta, Indonesia.
- Email: *sigit.heru.m@ugm.ac.id*
- ORCID: 0000-0002-6821-6364
- Web of Science ResearcherID: G-2594-2017
- Scopus Author ID: 57193140660
- Homepage: https://acadstaff.ugm.ac.id/MTk3MjA5MjQxOTk4MDMxMDAy

HOW TO CITE THIS ARTICLE

Patimah, A.S.; Prasetya, A.; Santosa, S.H.M.B, (2022). Environmental assessment of river water quality around the oil and gas field. Global J. Environ. Sci. Manage., 9(2): 275-286.

DOI: 10.22034/gjesm.2023.02.07

url: https://www.gjesm.net/article_696591.html

Global J. Environ. Sci. Manage. 9(2): 287-298, Spring 2023, Serial #34

Global Journal of Environmental Science and Management
(GJESM)

Homepage: https://www.gjesm.net/

ORIGINAL RESEARCH ARTICLE

Drought stress tolerance based on selection indices of resistant crops variety

R. Daneshvar Rad[1], H. Heidari Sharifabad[1,*], M. Torabi[2], R. Azizinejad[1], H. Salemi[3], M. Heidari Soltanabadi[3]

[1]Department of Agronomy and Horticultural Science, Faculty of Agriculture science and Food Industries, Science and Research Branch, Islamic University, Tehran, Iran

[2]Horticulture Crops Research Department, Isfahan Agriculture and Natural Resource Research and Education Center, AREEO, Isfahan, Iran

[3]Agriculture Engineering Research Department, Isfahan Agriculture and Natural Resource Research and Education Center, AREEO, Isfahan, Iran

ARTICLE INFO

Article History:
Received 30 April 2022
Revised 06 July 2022
Accepted 19 August 2022

Keywords:
Ash content
Crude Protein
Fodder
Nitrogen
Sorghum

DOI: 10.22034/gjesm.2023.02.08

ABSTRACT

BACKGROUND AND OBJECTIVES: The stress caused by dryness can affect plant growth and physiology. Several coping mechanisms (recovery, avoidance, tolerance and drought escape) have been developed to mitigate the impact of drought stress, and most strategies involve survival during stress condition. The aim of this study was to compare the morphological and physiological characteristics of two varieties of sorghum forage (Pegah and Speedfeed) under drought stress conditions in order to provide beneficial and functional recommendations to farmers in the study area.

METHODS: This study was performed as a spit-plot plot in a complete randomised design with 3 replications for two years in Esfahan, Iran. Experimental treatments included drought stress at three levels for two varieties of sorghum. Mechanisms of sorghum response to drought stress, including physiological and morphological alterations, were also proposed. Treatment means were compared by the Duncan test at 5% and 1% levels of probability. The statistical analysis was applied to the data using the R software.

FINDINGS: Lower irrigation showed a gradual decrease in plants height, number of leaves per plant, stem diameter, nitrogen and crude protein, with an increase in the length and weight of their panicle. Compared to Pegah variety, Speedfeed cultivar with 12% increase enhanced the contents of chlorophyll (1.7 times) in the two years of experiment. It could be concluded that Speedfeed variety exhibited better yield and quality characteristics against drought stress compared to Pegah variety. Considering the tolerance index and the harmonic mean index, Pegah showed the highest sensitivity to drought stress.

CONCLUSION: This study indicated that sorghum had several adaptive mechanisms for dealing with drought stress, so that it could be applied as a suitable alternative for other crops with higher water needs such as Zea.

NUMBER OF REFERENCES	NUMBER OF FIGURES	NUMBER OF TABLES
41	4	2

*Corresponding Author:
Email: *heidari_sharif_abad@yahoo.com*
Phone: +98 261 3660 5612
ORCID: 0000-0003-0504-9316

Note: Discussion period for this manuscript open until July 1, 2023 on GJESM website at the "Show Article".

INTRODUCTION

Over 80% of Iran is located in arid and semiarid regions and has extremely dry periods with no precipitation and strong evapotranspiration (Nouri *et al.,* 2020). Moreover, in this country, precipitation does not have appropriate spatial and temporal distributions (Amiri and Eslamian, 2010). Agriculture accounts for 72 billion cubic meters (94%) of the country's total water output. Models Crops under drought stress have predicted severe droughts by the end of the 21st century, causing severe water crises and double yields (Kang *et al.,* 2019; Yu *et al.,* 2018). As a result, finding a solution to reduce water consumption and increase its productivity seems to be necessary more than ever. Drought stress is one of the most significant factors in reducing the growth, development and production of cultivated plants. This stress represents a loss of 55% of crop varieties worldwide (Bray *et al.,* 2000). Water stress is more or less affected by all aspects of the plant, including morphology, physiology and metabolism (Zhao *et al.,* 2020; Deepak *et al.,* 2019; Jabereldar *et al.,* 2017; Tariq *et al.,* 1325). Therefore, drought has become the world's most destructive strain (Zhao *et al.,* 2020; Mohammadi and Shams, 2012). Decline in irrigation, as a beneficial economic strategy mostly targeting the use of water volume unit, is known as a step towards the stability of agricultural commodities. This means that the trained plants receive less water than they need. Today, global deficiency is considered as a method for increasing the water consumption efficiency by eliminating the irrigation systems that have the least contribution to productivity or use more water (Karam *et al.,* 2007). Although, with less aggregation, the plant is slightly exposed to water stress, by adjusting the irrigation and implementing optimization steps, the unit of water volume can be used (Kirnak *et al.,* 2002). The problem is that farmers are looking for an alternative product rather than the crops that require more water. In search of the best measure of genotype selection under water stress, various selection criteria have been recommended to choose the genotypes with optimal performance under stress and non-stress conditions among other groups (Fernandez, 1992; Naghavi *et al.,* 2013; Afolabi *et al.,* 2020). Estimating the drought tolerance indices is fundamental in assessing the drought-tolerant hybrids (Hussain *et al.,* 2019). In recent years, sorghum drought resistance has been considered as an appropriate alternative for maize with higher water requirements (Smith and Friedriksen, 2008). Sorghum is one of the top five cereal types after wheat, rice, maize and Hordeum which is ranked as the fourth largest grain in the world. Sorghum provides food for millions of animals. For example, over 55% and approximately 33% of sorghum seeds are used for human consumption and livestock feed in the world, respectively (Aghaalikhani *et al.,* 2012). The quality and value of sorghum feed are similar to that of maize, but its use is significantly different. Sorghum can be used for dry matter or direct grazing, whereas maize silage is the most expendable feed type (Sarshad *et al.,* 2021). In addition, a good growth capacity of sorghum after harvest has made it economically more valuable and suitable than corn (De Oliveria Santos *et al.,* 2020). In Iran, the lack of fodder is one of the main livestock issues (Karimi *et al.,* 2018). Considering the lack of rich pastures and the pressure posed by cattle on them, evaluation of the cultivation of these plants is especially important. Regarding the compromise of sorghum, drought conditions on the one hand and dryness of large areas in Iran on the other hand, investigation of plant yield in drought stress in the country seems essential. Considering the growth of population, their need to provide the required food and poultry and the need for research on plants and drought-resistant forage, such as sorghum, have received more attention (Iqbal *et al.,* 2015). Optimizing plant water use efficiency in arid and semiarid areas is one of the most important factors in sustainable agriculture. An appropriate method for dealing with drought in the agricultural sector should be based on cultivation of drought-resistant plants instead of highly consumed plants, leading to an increase in the yield and quality of the product. Consequently, the aim of the current study is to evaluate the impacts of drought stress on different varieties of sorghum in terms of morpho-physiological traits and compare morphological and physiological characteristics of two varieties of sorghum forage (Pegah and Speedfeed) under drought stress conditions in order to provide beneficial and functional recommendations to farmers. This study has been carried out in Isfahan, Iran, within 2017 and 2018 crop seasons.

MATERIALS AND METHODS

Site description and planting

A spit-plot experiment was performed in a randomized block design with 3 replications within 2017 and 2018 crop seasons. The treatments comprised irrigation managements with 3 levels: High irrigation (HI) (100% irrigation), Medium irrigation (MI) (80% full irrigation), and Low irrigation (LI) (60% full irrigation), with sorghum varieties: Pegah (late mature) and Speedfeed (early mature). Varieties belonging to Iranian fodder sorghum cultivars, were gained from the Seed Improvement Research Centre of Isfahan, Iran. The harrowing and ploughing were performed prior to sowing in order to prepare the soil. Seeds were sown on the mound at a density of 250,000 plants/ha in early June (calculated according to prevailing plantan dates in the area) for two years. The length of each edge was set to 12 m and the separate between the edges was 60 cm in each plot. Therefore, spacing among the seedlings in the row was 60 cm. Prior to planting, the physical and chemical properties of the soil were Clay: 18%, Silt: 12%, Sand: 70%, EC: 1.23 dS/m, pH: 7.2, Organic Carbon: 0.97%, Absorbable potassium: 700 ppm, Absorbable phosphorus: 40.50 and Total nitrogen: 0.1%. Potassium sulfate and ammonium phosphate fertilizers were connected with the doses of 150 and 250 kg/ha individually. When the plants reached 40-cm tall with a water framework system, urea fertilizer was utilized as dressing. The water system was established by drip-strip and water system cycle was based on a steady cycle and water net prerequisite of plant (evaporation pan class A). Water requirement was estimated according to daily evapotranspiration values of reference tree (ETO) and crop specific coefficient (KC) of the combined Penman-Montes-FAO model (Allen *et al.,* 1998). The irrigation water quality included EC: 1.9 dS/m, pH: 7.2, HCO^{3}: 4.6 meq/L, Cl: 9.2 meq/L, SO_4^{-2}: 6.5 meq/L, Ca^{2+}: 6.6 meq/L, Mg^{2+}: 3 meq/L, and Na^{+}:10.3 meq/L. Water consumption was also measured by a calibrated meter. Water consumptions during the growing season, during 18 to 20 irrigations in 100%, 80% and 60% full irrigation treatments, were 5,038, 42,250 and 3,350 m^3/ha in 2017 and 4,400, 5,445 and 3,225, in 2018 respectively. The total rainfalls in the whole area were 14 mm and 25.2 mm for 2017 and 2018, respectively.

Laboratory analyses

Important crop traits, including plant height, stem diameter, length, leaf number, and weight of the panicle, were measured. In order to determine the dry weight, one kilogram sample was placed in a temperature of 70-75 °C for 24 hours to dry. Ash content was determined using the dry ash method when weighing an empty crucible and placing 2 g of the sample in a crucible at 550 °C in a furnace until the sample turned gray after complete heating. The crucible was placed in desiccator and allowed to cool, and then the sample was reweighed and calculated. The kjeldahl method was applied for determination of total nitrogen and crude protein (Bremner, 1982). Total chlorophyll content was estimated as sum of chlorophyll a and b and expressed as mg/g fresh weight. Drought tolerance indices were calculated using Eqs. 1 to 4 (Bonea and Urechean, 2011).

$$\text{Tolerance index (TOL)}=(Yp–Ys) \quad (1)$$

$$\text{Mean productivity (MP)}=(Ys + Yp)/2 \quad (2)$$

$$\text{Geometric mean productivity (GMP)}=(Yp*Ys)^{½} \quad (3)$$

$$\text{Harmonic mean index (HAR)}=2(Ys.Yp)/Ys+Yp \quad (4)$$

Where, $\hat{Y}s$ and $\hat{Y}p$ are the means of all genotypes under stress and well water conditions, respectively.

Statistical analysis

The analysis of variance (ANOVA) was conducted for each year to verify the statistical differences among the two sorghum varieties, various irrigation levels (3 levels) and their interaction. Moreover, correlation analyses of the studied parameters were performed by a linear regression model. Several data sets were altered for logarithm to provide the prerequisites of ANOVA for homogeneity of variance and normality. Treatment means were compared using the Duncan test at 5% and 1% levels of probability. The statistical analysis was applied to the data using the R software (version 4.3.19).

RESULTS AND DISCUSSION

According to analysis of variance, the effect of experimental years on all morphological characteristics, except for the weight of the plate at

the level of 1%, was significant (Table 1). The irrigation effect on all morphological traits, except for number of leaves and plant height, was also significant. The effect of varieties on all traits, except for the length of the plate and plant height, was significant. The interaction of factors was also different in other traits.

The results of variance analysis of physiological traits indicated that the effect of experimental years on all studied characteristics was not significant at the level of 5% (Table 2). The effect of irrigation on all traits, except for chlorophyll and ash content, was important, and the effect of varieties on all traits, except for ash content, was important. The interaction of factors in most traits, except for chlorophyll content and dry weight plant, was not significant.

Results of mean comparison showed that the difference in mean plant height in the first year between the two varieties was insignificant and, in the second year, it was higher in HI than in MI and LI and only in LI it was significantly higher (Fig. 1). In general, stem diameter had the highest value in Speedfeed variety in MI compared to other treatments, while both varieties in LI showed the lowest value in both years (Fig. 1). Due to sorghum's resistance to environmental stresses, most of its vegetative and functional characteristics remained unaffected by the increase of temperature in the second year. Jabereldar *et al.* (2017) reported similar results. The dry matter, protein and minerals (ash) of Speedfeed are higher than Pegah variety. While, its soluble fibers and lignin or, in other words, digestibility is less than that of Pegah (Mokhtarpour *et al.,* 2000). Due to the lack of significance of dry matter in water stress levels with control treatment, it has been reported that sorghum can drain more moisture from the soil in low water conditions (Pardales Jr and Kono 1990). As a result, the average number of leaves of the two varieties was meaningfully higher in the first year than in the second year. No marked difference was observed in the mean length of panicle in the two varieties in different irrigation years. The weight of the panicle showed different values, with values for Pegah cultivar being less than the values observed in HI levels in both years. Finally, the mean DM in Speedfeed variety at HI level was significantly higher than Pegah variety and it was vice versa at MI (Fig. 1). Naseri *et al.* (2011) showed that shortening of the length of the panicle due to the impact of drought

Table 1: Two-way ANOVA results of morphological variables of the two varieties of sorghum at different years under different irrigation levels

Variables	df	Plant height (cm)	Leaf number	Panicle length (cm)	Panicle weight (g)	Stem diameter (mm)
Time (A)	1	4436.89 **	86.64**	29.5**	11.82ns	15**
Irrigation (B)	2	1111.84 ns	0.18ns	19.62**	192.99**	21.5**
A×B	2	145/74 ns	1.69ns	7.7*	3ns	0.1ns
Variety (C)	1	76 ns	32.2**	7.62ns	132.44*	455.5**
B×C	2	568/92*	1.4ns	0.91ns	142.87*	2.4**
A×C	1	756.43*	1.22ns	2ns	0.45ns	0.1ns
A×B×C	2	645/13*	0.09*	11 ns	117.21*	0.08ns

ns: not significant; * and **: significant at $p < 0.05$ and $p < 0.01$, respectively

Table 2: Two-way ANOVA results of variables of the two varieties of sorghum at different years under different irrigation levels

Variables	df	Chlorophyll content (mg/g)	Nitrogen (%)	Dry matter weight (g)	Crude protein (%)	Ash (%)
Time (A)	1	0.07ns	0.0003ns	0.008ns	0.01ns	1.88ns
Irrigation (B)	2	0.2ns	0.1**	25.14**	4.69**	3.73ns
A×B	2	3.7**	0.005ns	2.27 ns	0.2 ns	1.97ns
Variet y(C)	1	13.9**	0.1**	404.27**	4.89**	3.75ns
B×C	2	33.6**	0.007ns	60*	0.3ns	3ns
A×C	1	31.7**	0.003ns	1.36ns	0.13ns	1.69ns
A×B×C	2	3.6**	0.007ns	2.6ns	0.28ns	2.59ns

ns: not significant; * and **: significant at $p < 0.05$ and $p < 0.01$, respectively

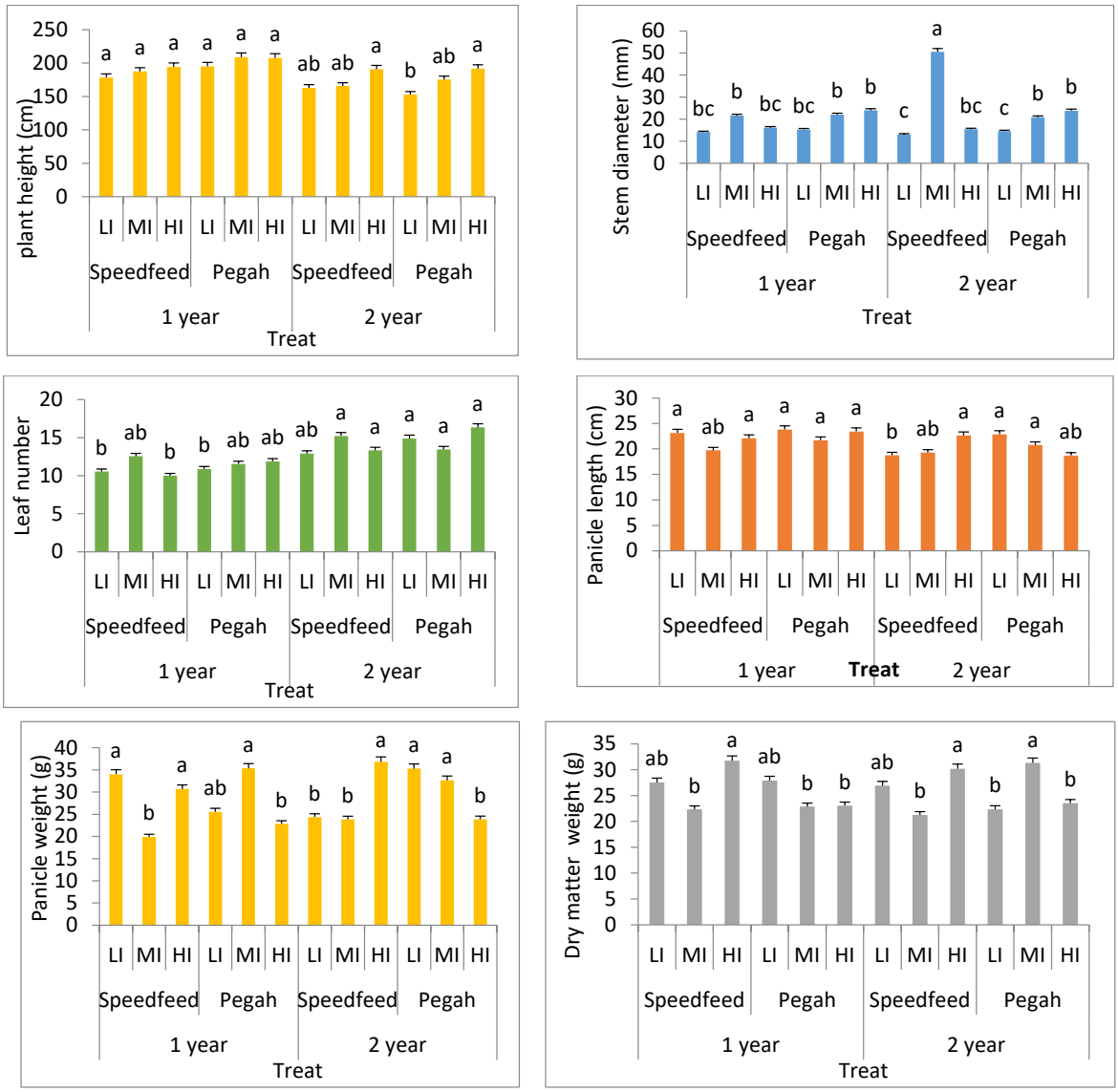

Fig. 1: Variations in morphological properties of the two varieties of sorghum at different years under different irrigation levels. Different lower-cases for interaction on the bars show significant differences (Duncan, $P < 0.05$). (HI): High irrigation, (MI): Medium irrigation and (LI): Low irrigation

stress on the development of the panicle was reported as contradictory.

Results showed that the amount of nitrogen was not significantly different in any treatment, but it decreased with the decrease of irrigation (Fig. 2). The amount of forage nitrogen in HI treatment had the highest amount (averagely 1.4%) and decreased with the decrease of access to water. Therefore, the lowest amount upto an average of 1.2% was related to the treatment of 60% of complete irrigation. The study of drought stress evaluation on forage quality of millet forage implied that the highest amount was related to complete irrigation of plants (Keshavarz *et al.*, 2013). Considering the reduction of nitrogen due to water stress, it can be said that one of the most detrimental effects of water stress is the disruption of nutrient uptake and accumulation, leading to reduced crop yields and animal feed, in addition to loss of

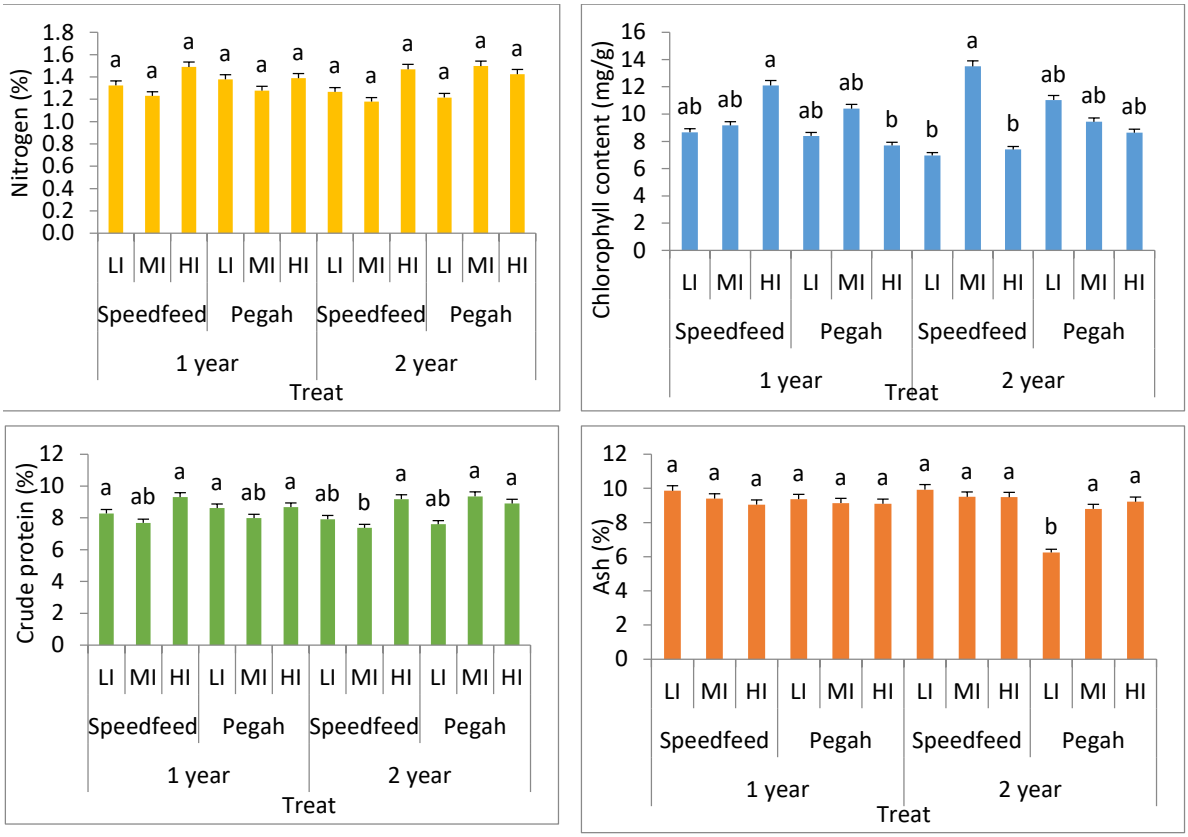

Fig. 2: Variations in chemical properties of the two varieties of sorghum under different irrigation levels in different years. Different lower-cases for interaction on the bars show significant differences (Duncan, $P < 0.05$). (HI): High irrigation, (MI): Medium irrigation and (LI): Low irrigation

fertilizer (Irannejad, 1991). Bock (1984) stated that in order to absorb nitrogen, it must move in aqueous solution to reach the roots. Therefore, providing the right amount of water is one of the most efficient ways to move nitrate to the roots through the mass flow. The amount of crude protein differences was small, so that the values were higher in HI than in LI, but the values were not significant. Compared to Pegah variety, Speedfeed cultivar with a 12% increase had a higher chlorophyll content in both years of experiment (Fig. 2). According to results, during the two years of experiment and due to the temperature difference, the amount of crude protein of sorghum in both years was nearly 8% higher in natural irrigation than in the two levels of low irrigation stress applied in the study. Barati *et al.* (2015) explored the effect of low irrigation regimes on barley and showed that stress reduced the protein concentration. The ash percentage of Pegah variety had the lowest amount in the second year compared to other treatments. Accordingly, Speedfeed variety in full irrigation produced about 19% more crude protein than Pegah variety at 60% full irrigation. The interaction between irrigation and variety demonstrated a slight difference among the irrigation regimes in terms of forage ash percentage of the two sorghum varieties. Therefore, it could be stated that the ash contents of the two varieties in the present study were not affected by irrigation treatments. In a study comparing the physiological traits of the two sorghum cultivars in response to water restriction, it was observed that there was a difference in the leaf chlorophyll content of the cultivars (Goche *et al.*, 2020). Drought stress can lead to changes in chlorophyll content and thus changes in photosynthetic efficiency (Xu *et al.*, 2020). These findings showed that the effect of water

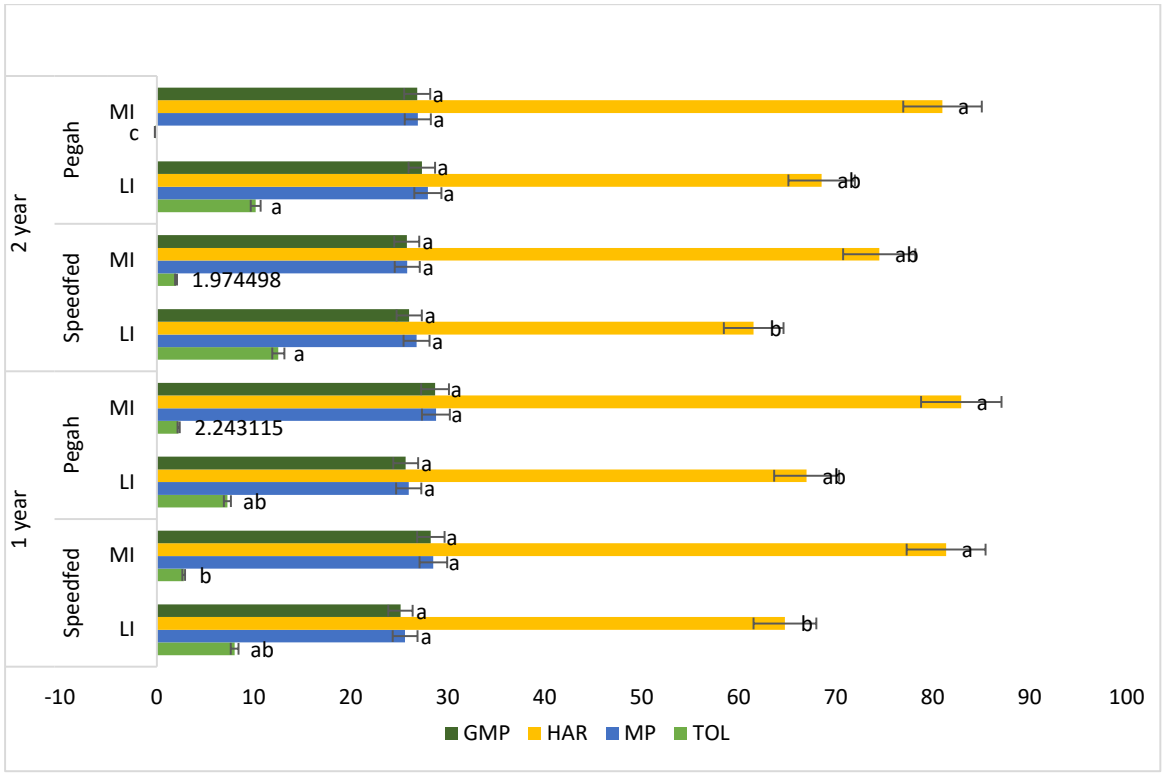

Fig. 3: Values of drought tolerance indices for maize hybrids under different irrigation levels. Different lower-cases for interaction on the bars show significant differences (Duncan, P < 0.05). Medium irrigation (MI) and Low irrigation (LI)

stress on plant chlorophyll could be very different depending on the environmental conditions and genotype of the plants (Jnandabhiram and Sailen Prasad, 2012). The superiority of the chlorophyll content of sorghum over other plants can be related to its genetic characteristics. There are many differences between plant species and even different cultivars of a species in terms of changes in a trait. Some plants or cultivars of a plant, under drought stress conditions, can prevent the reduction of leaf chlorophyll by maintaining the relative content of leaf water and photosynthetic power (Najafinejad et al., 2019). Drought stress is a key environmental factor that inhibits photosynthesis. Drought stress typically affects the stomatal conductance and photosynthetic activity in leaves, and since photosynthesis is necessary for plant materialization, drought stress reduces photosynthetic efficiency, growth retardation, and relative growth rate (Maddah and Farhangian Kashani, 2011). Sorghum can grow and produce crops in a hot, dry environment that is unappropriate for most crops. As a result, among the two varieties, Speedfeed seemed to have a higher content of cholorophyll under water deficit. The increase in chlorophyll content at 60% stress in the second year observed in the present study was in agreement with the results presented by Goche *et al.* (2020).

TOL and HAR indices showed an intensive tolerance and better performance than MP and GMP (Fig. 3). Based on TOL and HAR indices, Pegah had the highest sensitivity to drought stress. The large amount of TOL index can be a good criterion for selecting the variety which is tolerant to drought stress. Speedfeed cultivar appeared to be more responsive to water shortage in chlorophyll content and photosynthetic efficiency than Pegah cultivar. Pegah is a relatively late Iranian cultivar suitable for forage silage production because of its high soluble sugar content and is considered genetically pure. Speedfeed is one of

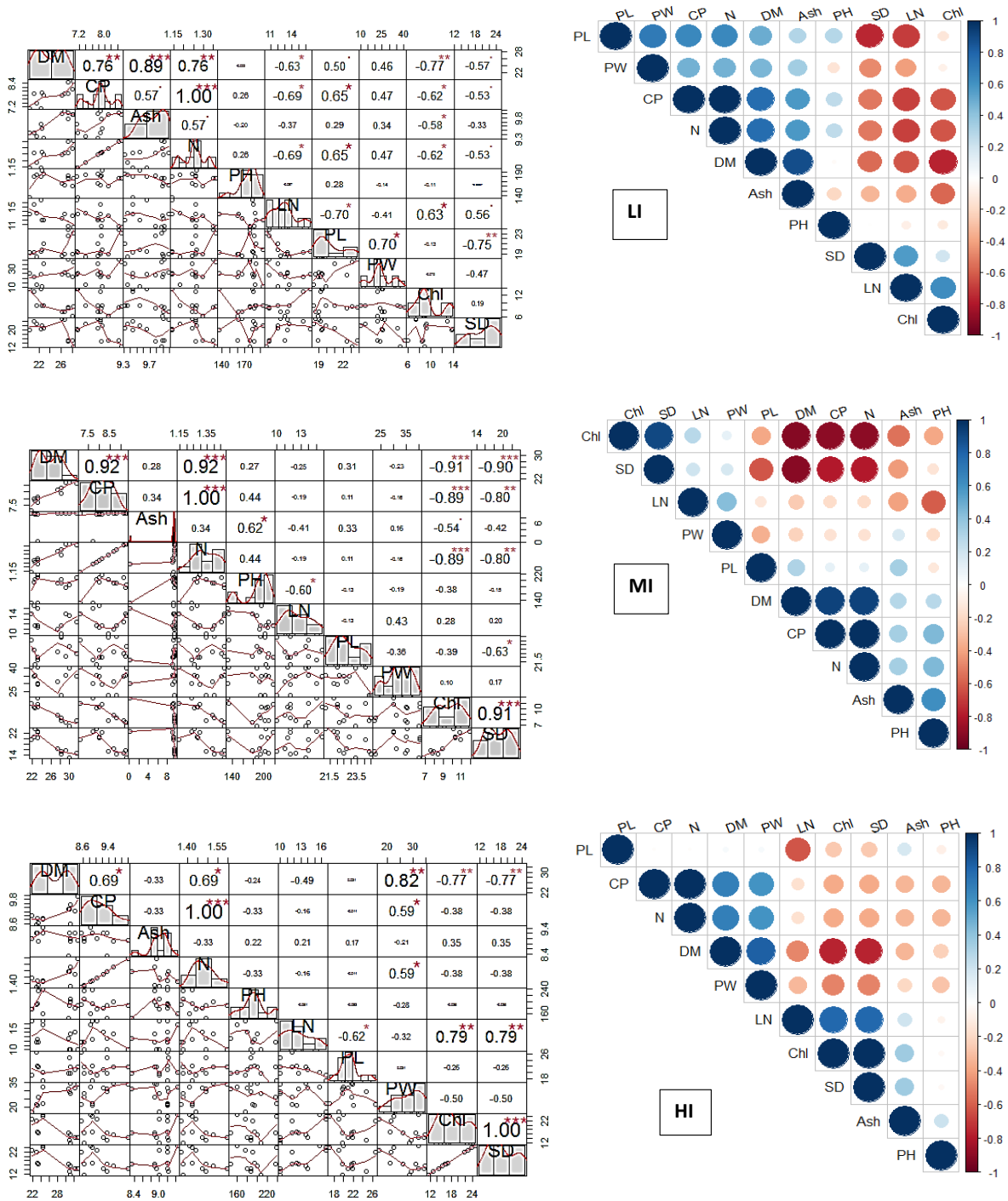

Fig. 4: Correlation plot of sorghum traits under irrigation levels; (HI): High irrigation, (MI): Medium irrigation and (LI): Low irrigation. DM: dry matter, CP: crude protein, PH: plant height, LN: leaf number, PW: panicle weight, PL: Panicle lengh, Ash: Ash content, and Chl: Total Chlorophyll.

the varieties of Australian hybrid cultivar modified by Pacific Seyed Australia. This variety is multi-grained and is suitable for direct grazing and, in terms of low sugar content, it is not suitable for producing forage silage. Compared to Pegah variety, Speedfeed hybrid variety has a shorter growth period due to its multiplicity and, except for amount of soluble sugar. It has also preference over Pegah variety in terms of some qualitative parameters.

The correlation between the studied traits at LI level showed a strong negative correlation among the amount of panicle length, stem diameter and number of leaves, between the dry weight and chlorophyll content, and between nitrogen and the number of leaves (Fig. 4). However, the amount of raw protein had a strong positive relationship with nitrogen and the amount of ash in dry weight. According to Abdi and Habibi (2017), fiber up to a low amount is needed for forage crops to have a high quality of, but its higher content can negatively affect the quality of forage. At MI level, chlorophyll content and stem diameter were strongly correlated with dry weight, crude protein, and nitrogen traits, while the dry matter content was strongly correlated with crude protein and nitrogen, and nitrogen content was strongly correlated with ash. However, at HI level, the dry weight had a strong negative correlation with chlorophyll and stem diameter, while a strong positive correlation was observed between crude protein and nitrogen and between chlorophyll and ash (Fig. 4). Evaluating the impact of drought stress through the association among the traits under different stress treatments displayed that the drought stress induction had no significant effect on yield-related and morphological traits in sorghum compared to control. However, it was capable of changing the relationship among the traits, and this was verified by the correlation plot results. The results obtaioned by Cho *et al.* (2006) revealed a significant reduction in yield and biomass yield-related characteristics of sorghum under severe water shortage conditions. If the moisture content decreases, the intensity and amount of nutrient uptake would change. Since some element transfer systems, such as diffusion, require less moisture to absorb nutrients, reducing the moisture content to the critical threshold can trigger the process of absorption and transfer of some nutrients by the roots. However, other traits, including mass flow, are highly dependent on the amount of moisture, and by reducing the moisture, the elements would be transferred by the flow and the process would have a negative absorption (Taize and Zeiger, 1998; Aravind *et al.,* 2016).

CONCLUSION

The development of drought tolerant cultivars suitable for a wide range of agro-climatic conditions, particularly in arid and semiarid regions, is important to avoid the adverse effects of water stress. Forages have a key role in producing protein and energy required by livestock. In forage selection, the improvement of forage yield and quality is of particular importance and one of the main factors is the introduction of improved cultivars. The results demonstrated that the quality-related traits were implicated in stress tolerance mechanisms. These factors could enhance the nutritional quality of cereals. The difference between nutrient contents was non-significant for different irrigation levels. Besides, the relationships among the studied traits were affected by the drought stress. The lower irrigation significantly affected all the tested parameters. The decrease in fodder yield with drought application could be attributed to lower plant height, the number of leaves per plant, stem diameter, and panicle weight. The yield-related and morphological traits along with tolerance and susceptibility indices revealed that the Speedfeed variety exhibited better yield and quality characteristics against drought stress than Pegah variety. It could be concluded that Sorghum variety was compatible against drought stress. Hence, a mild water stress along with saving water resources could increase the sorghum quality. This study, among others, focused merely on the effects of drought stress occurring at particular plant growth stages. For a more comprehensive understanding of the characteristics, it is essential to perform an in-depth study covering the growth and developmental stages of the whole plant. Despite the closeness of the ecological characteristics and nutritional composition of sorghum to those of corn, the relative advantages of sorghum against drought stress have led to its significant superiority over corn. Encouraging farmers and ranchers to grow sorghum and use this fodder in production units is one of the important results of this study.

AUTHOR CONTRIBUTIONS

H. Heidari Sharifabad, the corresponding author, contributed in supervising the first author in the data

analysis and interpreting the results. R. Daneshvar rad prepared the manuscript, performed the data analysis, and plotted the figures. M. Torabi and R. Azizinejad designed the field experiments. H. Salemi and M. Heidarisoltanabadi prepared the text and figures.

ACKNOWLEDGMENTS

The authors would like to acknowledge the Agricultural Engineering Research Department of Isfahan Agricultural and Natural Resources Research and Education Center and the Department of Horticultural Science of Faculty of Agricultural Sciences and Food Industries of Science and Research Branch of Tehran for their valuabe assistance provided when required.

CONFLICT OF INTEREST

The authors declare no potential conflict of interest regarding the publication of this work. In addition, the ethical issues including plagiarism, informed consent, misconduct, data fabrication and, or falsification, double publication and, or submission, and redundancy have been completely witnessed by the authors.

ABBREVIATIONS

%	Percent
^{O}C	degrees centigrade
ANOVA	Analysis of variance
Ca^{2+}	Calcium
Chl	Total Chlorophyll
cm	Centimeter
CP	Crude protein
df	Degrees of freedom
dS/m	DeciSiemens/meter
DM	Dry matter
EC	Electrical conductivity
Eq.	Equatioon
ETO	Evapotranspiration
FAO	Food and Agriculture Organization
Fig.	Figure
g	Gram
GMP	Geometric mean productivity
ha	hectares
HAR	Harmonic mean
HCO^{3}	Bicarbonate
HI	High irrigation
KC	Crop specific coefficient
kg	Kilogram
LI	Low irrigation
LN	Leave number
meq/L	*Milliequivalents per liter*
Mg^{2+}	*Magnesium*
mg/g	*Milligrams* per gram
MI	Medium irrigation
mm	Millimeter
m^{3}	Cubic meter
MP	Mean productivity
Na^{+}	Sodium
ns	not significant
SO_{4}^{-2}	Sulphate
pH	potential of hydrogen
PL	Panicle lengh
ppm	Part per million
PW	Panicle weight
TOL	Tolerance

REFERENCES

Abdi, M.; Habibi, M., (2017). Effect of drought stress on quantitative and qualitative traits of two forage sorghum cultivars in Jiroft region. Agroecology Journal, 13(3): 35-39 **(5 pages)**.

Afolabi, M.S.; Murtadha, M.A.; Lamidi, W.A.; Waheed, J.A.; Salami, A.E.; Bello, O.B., (2020). Evaluation of yield and yield components of low n maize (Zea mays l.) varieties under low and high nitrogen conditions. Afr. J. Agric. Res., 15: 66–72 **(7 pages)**.

Aghaalikhani, M.; Etemadi, F.; Ajirlo, A.F., (2012). Physiological basis of yield difference for grain sorghum (Sorghum bicolor (L.) Moench) in a semi-arid environment. J. Agric. Biol. Sci., 7: 488-496 **(9 pages)**.

Allen, R.G.; L.S.Pereira, D. Raes.; M. Smith., (1998). Crop evapotranspiration-Guidelines for computing crop water requirements-FAO Irrigation and drainage paper 56. Fao., Rome, 300(9): D05109.

Amiri, M.J.; Eslamian, S.S., (2010). Investigation of climate change in Iran. J. Environ. Sci. Technol., 3(4): 208-216 **(9 pages)**.

Aravind, J.; Kanmani, P.; Sudha, G.; Balan, R., (2016). Optimization of chromium(VI) biosorption using gooseberry seeds by response surface methodology. Global J. Environ. Sci. Manage., 2(1); 61-68 (**8 pages**).

Barati, V.; Ghadiri, H.; Zand-Parsa, S.; Karimian, N., (2015). Nitrogen and water use efficiencies and yield response of barley cultivars under different irrigation and nitrogen regimes in a semi-arid Mediterranean climate. Archives Agron. Soil Sci., 61(1): 15-32 **(18 pages)**.

Bock, B.R., (1984). Efficient use of nitrogen in cropping systems. Nitrogen in crop production. 273-294 **(22 pages).**

Bonea, D.; Urechean, V., (2011). The evaluation of water stress in maize (Zea mays L.) Using selection indices. Rom. Agric. Res., 28: 79-86 **(8 pages).**

Bray, EA.; Bailey-Serres, J.; Weretilnyk, E., (2000). Responses to abiotic stresses. In: Gruissem, W.; Jones, R., Eds., Am. Soc. Plant Physiol., Rockville, 1158-1203 **(46 pages).**

Bremner, J.M., (1982). Total nitrogen. Methods of soil analysis' Am. Soc. Agron. Mongrn., 10(2): 594-624 **(31 pages).**

Cho, K.; Toler, H.; Lee, J.; Ownley, B.; Stutz, J.C.; Moore, J.L.; Augé, R.M., (2006). Mycorrhizal symbiosis and response of sorghum plants to combined drought and salinity stresses. J. Plant Physiol., 163(5): 517-528 **(12 pages).**

De Oliveria Santos, A.; Garcia Von Pinho, O.; Fillipe de Souza, V.O.; José Moreira Guimarães, L.; Balestre, M.; Paulo Miranda Pires, L.; Pereira da Silva, C., (2020).Grain yield, anthesis-silking interval and drought tolerance indices of tropical maize hybrids. Crop Breed. Appl. Biotechnol., 20(1): 1-9 **(9 pages).**

Deepak, S. B.; Thakur, A.; Singh, S.; Bakshi, M.; Bansal, S., (2019). Changes in crop physiology under drought stress: A review. J Pharmacogn. Phytochem., 8: 1251-1253 **(3 pages).**

Fernandez, G.C.J., (1992). Effective selection criteria for assessing plant stress tolerance. In Proceedings of the International Symposium on Adaptation of Vegetables and other Food Crops in Temperature andWater Stress, Taipei., 257–270 **(14 pages).**

Goche, T.; Shargie, N. G.; Cummins, I.; Brown, A. P.; Chivasa, S.; Ngara, R., (2020). Comparative physiological and root proteome analyses of two sorghum varieties responding to water limitation. Sci. Rep., 10(1): 1-18 **(18 pages).**

Hussain, H.A.; Men, S.; Hussain, S.; Chen, Y.; Ali, S.; Zhang, S.; Wang, L., (2019). Interactive effects of drought and heat stresses on morpho-physiological attributes, yield, nutrient uptake and oxidative status in maize hybrids. Sci., Rep., 9: 1–12 **(12 pages).**

Iqbal, M. A.; Bilal, A.; Shah, M. H. U.; Kashif, A., (2015). A study on forage sorghum (Sorghum bicolor L.) production in perspectives of white revolution in Punjab, Pakistan: Issues and future options' Agric. Environ. Sci., 15(4): 640-647 **(8 pages).**

Irannejad, H., (1991). The effect of food in increasing the quantity and quality of grain corn. Olive J., 16-19 **(4 pages).**

Jabereldar, A. A.; El Naim, A. M.; Abdalla, A. A.; Dagash, Y. M., (2017). Effect of water stress on yield and water use efficiency of sorghum (Sorghum bicolor L. Moench) in semi-arid environment. Int. J. Agric. For., 7(1): 1-6 **(6 pages).**

Jnandabhiram, C.; Sailen Prasad, B., (2012). Water stress effects on leaf growth and chlorophyll content but not the grain yield in traditional rice (Oryza sativa Linn.) genotypes of Assam, India II. Protein and proline status in seedlings under PEG induced water stress. Am. J. Plant Sci., 3(7): 1-4 **(4 pages).**

Kang, Z.; Babar, M.A.; Khan, N.; Guo, J.; Khan, J.; Islam, S.; Shahi, D., (2019). Comparative metabolomic profiling in the roots and leaves in contrasting genotypes reveals complex mechanisms involved in post-anthesis drought tolerance in wheat. PLoS One., 14(3): 213502.

Karam, F.; Lahoud, R.; Masood, R.; Kabalan, R.; Breid, J.; Chalita, C.; Rouphael, Y., (2007). Evaporanspiration, seed yield and water use efficiency of drip irrigation sunflower under full and deficit irrigation conditions. Agric. Water Manage., 90: 213-223 **(11 pages).**

Karimi, V.; Karami, E.; Keshavarz, M., (2018). Vulnerability and adaptation of livestock producers to climate variability and change. Rangeland Ecol. Manage., 71(2): 175-184 **(10 pages).**

Keshavarz, L.; Farahbakhsh, H.; Golkar, P., (2013). Effect of hydrogel and irrigation regimes on chlorophyll content, nitrogen and some growth indices and yield of forage millet (Pennisetum glaucum L.). J. Crop Product. Process., 3(9): 147-161 **(16 pages).**

Kirnak, H.; Tas, I.; Kaya, C.; Higgs, D., (2002). Effects of deficit irrigation on growth, yield and fruit quality of eggplant under semi-arid conditions. Aus. Agric. Res., 53(12): 1367-1373 **(7 pages).**

Maddah, S.M.; Farhangian Kashani, S., (2011). Investigation of growth and chlorophyll concentration. Crop Physiol. J., 3(11): 89-102 **(14 pages).**

Mohammadi, H.; Shams, A.S., (2012). Evaluation of drought stress effects on yield components and seed yield of three maize cultivars (Zea mays L.) in Isfahan region. Int. J. Agric. Crop Sci., 4(19): 1436-1439 **(4 pages).**

Mokhtarpour, H.; Kashiri, M.; Anaghli, A., (2000). Evaluation of domestic varieties of forage sorghum in comparison with Speedfeed hybrid variety. J. Agric. Sci. Nat. Resour., 7(4): 73-84 **(12 pages).**

Naghavi, M.R.; Aboughadareh, A.P.; Khalili, M., (2013). Evaluation of drought tolerance indices for screening some of corn (Zea mays L.) cultivars under environmental conditions. Not. Sci. Biol., 5: 388-393 **(6 pages).**

Najafinejad, H.; Javaheri, MA.; Koohi, N.; Shakeri, P., (2019). Yield and quality of forage and water use efficiency of Kochia, sorghum and corn under water stress. Seed Plant Breed. Neighborhood. 2-35(2): 261-283 **(23 pages).**

Naseri, P.; Faramarzi, A.; Khorshidi, Bm.; Shahrokhi, S., (2011). Effect of irrigation intervals on yield and yield components of sorghum bicolor varieties in Miyaneh region, Iran. J. Crop Ecophysiol., (19): 93-103 **(11 pages).**

Nouri, E.; Matinizadeh, M.; Moshki, A.; Zolfaghari, A.; Rajaei, S.; Janoušková, M., (2020). Arbuscular mycorrhizal fungi benefit drought-stressed Salsola laricina., Plant Ecol., 221(8): 683-694 **(12 pages).**

Pardales Jr, J. R.; Kono, Y., (1990). Development of sorghum root system under increasing drought stress [Sorghum bicolor]., Japan. J. Crop Sci., 59(4): 752-761 **(10 pages).**

Sarshad, A.; Talei, D.; Torabi, M.; Rafiei, F.; Nejatkhah, P., (2021). Morphological and biochemical responses of Sorghum bicolor (L.) Moench under drought stress., SN. Appl. Sci., 3(1): 1-12 **(12 pages).**

Smith, C.W.; Frederiksen, R.A., (2008). Sorghum: Origin, History, Technology, and Production. John Wiley and Sons, New York. **731-749 (19 pages).**

Taize, L.; Zeiger, E., (1998). Plant Physiology' (2nd). Sinager Associates. Inc. Publisher. Sunderland Massa Chussets., 757.

Tariq, A.; Athar, M.; Ara, J.; Sultana, V.; Ehteshamul-Haque, S.; Ahmad, M., (2015). Biochemical evaluation of antioxidant activity in extracts and polysaccharide fractions of seaweeds. Global J. Environ. Sci. Manage., 1(1): 47-62 **(6 pages).**

Xu, J.; Zhou, Y.; Xu, Z.; Chen, Z.; Duan, L., (2020). Combining physiological and metabolomic analysis to unravel the regulations of coronatine alleviating water stress in tobacco (Nicotiana tabacum L.). Biomol., 10(1): 1-16 **(16 pages).**

Yu, C.; Huang, X.; Chen, H.; Huang, G.; Ni, S.; Wright, J. S.; Yu, L., (2018). Assessing the impacts of extreme agricultural droughts in China under climate and socioeconomic changes. Earth's Future. 6(5): 689-703 **(15 pages).**

Zhao, W.; Liu, L.; Shen, Q.; Yang, J.; Han, X.; Tian, F.; Wu, J., (2020). Effects of water stress on photosynthesis, yield and water use efficiency in winter wheat. Water. 12: 1-19 **(19 pages).**

AUTHOR (S) BIOSKETCHES

Daneshvar Rad, R., Ph.D. Candidate, Department of Agronomy and Horticultural Science, Faculty of Agriculture science and Food Industries, Science and Research Branch, Islamic University, Tehran, Iran.
- Email: *Rd1981@yahoo.com*
- ORCID: 0000-0001-8160-0814
- Web of Science ResearcherID: NA
- Scopus Author ID: NA
- Homepage: https://srb.iau.ir/en

Heidari Sharifabad, H., Ph.D., Professor, Department of Agronomy and Horticultural Science, Faculty of Agricultural Sciences and Food Industries, Science and Research Branch, Islamic Azad University, Tehran, Iran.
- Email: *heidari_sharif_abad@yahoo.com*
- ORCID: 0000-0003-0504-9316
- Web of Science ResearcherID: NA
- Scopus Author ID: NA
- Homepage: https://www.adelaide.edu.au

Torabi, M., Ph.D., Assistant professor, Horticulture Crops Research Department, Isfahan Agricultural and Natural Resources Research and Education Center (AREEO), Isfahan, Iran.
- Email: *masoud.agro.ir@gmail.com*
- ORCID: 0000-0002-2645-2270
- Web of Science ResearcherID: M-3161-2017
- Scopus Author ID: NA
- Homepage: https://www.researchgate.net/profile/Masoud-Torabi

Azizinejad, R., Ph.D., Assistant Professor, Department of Agronomy and Horticultural Science, Faculty of Agriculture science and Food Industries, Science and Research Branch, Islamic University, Tehran, Iran.
- Email: *r.azizi@srbiau.ac.ir*
- ORCID: 0000-0003-1752-2975
- Web of Science ResearcherID: NA
- Scopus Author ID: 54797550100
- Homepage: http://www.scopus.com/inward/record.url?eid=2-s2.0-85099086505&partnerID=MN8TOARS

Salemi, H., Ph.D., Assistant professor, Agriculture Engineering Research Department, Isfahan Agriculture and Natural Resource Research and Education Center, AREEO, Isfahan, Iran.
- Email: *hrsalemiwk@gmail.com*
- ORCID: 0000-0002-0413-2874
- Web of Science ResearcherID: NA
- Scopus Author ID: S-4323-2016
- Homepage: http://www.aeri.ir/WebGenerator/PageView.aspx?src=1011&Dynamic

Heidari Soltanabadi, M., Ph.D., Assistant professor, Agriculture Engineering Research Department, Isfahan Agriculture and Natural Resource Research and Education Center, AREEO, Isfahan, Iran.
- Email: *mheisol@gmail.com*
- ORCID: 0000-0001-7892-3487
- Web of Science ResearcherID: NA
- Scopus Author ID: 37099933400
- Homepage: https://scientometric.areeo.ac.ir/Mohsen_Heidarisoltanabadi

HOW TO CITE THIS ARTICLE

Daneshvar rad, R.; Heidari Sharifabad, H.; Torabi, M.; Azizinejad, R.; Salemi, H.; Heidarisoltanabadi, M., (2023). Drought stress tolerance based on selection indices of resistant crops variety. Global J. Environ. Sci Manage., 9(2): 287-298.

DOI: 10.22034/gjesm.2023.02.08

url: https://www.gjesm.net/article_254145.html

Global J. Environ. Sci. Manage. 9(2): 299-308, Spring 2023, Serial #34

Global Journal of Environmental Science and Management
(GJESM)

Homepage: https://www.gjesm.net/

ORIGINAL RESEARCH PAPER

Microplastics contamination in two peripheral fish species harvested from a downstream river

M.R. Maulana[1], S. Saiful[2], Z.A. Muchlisin[3,*]

[1] Department of Integrated Coastal Zone Resources Management , Postgraduate Program, Universitas Syiah Kuala, Banda Aceh 23111, Indonesia

[2] Department of Chemistry, Faculty of Mathematics and Natural Sciences, Universitas Syiah Kuala, Banda Aceh 23111, Indonesia

[3] Department of Aquaculture, Faculty of Marine and Fisheries, Universitas Syiah Kuala, Banda Aceh 23111, Indonesia Marine and Fisheries Research Center, Syiah Kuala University, Banda Aceh 23111, Indonesia

ARTICLE INFO

Article History:
Received 14 June 2022
Revised 22 August 2022
Accepted 01 October 2022

Keywords:
Fiber
Film
Fourier transform infrared (FT-IR)
Plastic waste
Water pollution

DOI: 10.22034/gjesm.2023.02.09

ABSTRACT

BACKGROUND AND OBJECTIVES: The occurrence of plastic waste pollution in waters has become a major issue globally. One of the waters which tend to be polluted with plastic waste such as bags, food wrappers, and unused fishing nets, is the Krueng Aceh River, which is located in the center of Banda Aceh city, Indonesia. Microplastics in the rivers potentially contaminate the fish through the food chains, and are then transferred to humans once consumed. The two species of fish that are frequently caught by fishermen in the Krueng Aceh River and consumed by the local people are mullet *Mugil cephalus* and bagok catfish *Hexanematichthys sagor*. Both have the potential of being contaminated with microplastics that enter the river. Therefore, this study aims to analyze the status of microplastic pollution in mullet *M. cephalus* and bagok catfish *H. sagor* harvested downstream of the Krueng Aceh River, Banda Aceh, Indonesia.
METHODS: The fish samples were caught in three locations, namely in the river estuary, residential, and agricultural areas. A total of 50 mullets and 46 bagok catfish were employed for analysis. Microplastics were analyzed in the digestive tract using a microscope, while waste in the carcass was detected using the fourier transform infrared analysis.
FINDINGS: In mullet, the highest number of microplastic particles were found in fish samples caught in river estuary (16 particles/fish on average), followed by the sample from residential areas (10 particles/fish on average). Meanwhile, the lowest abundance of microplastic was recorded in sample near agriculture areas (5 particles/gram body weight). In bagok catfish, microplastic abundance in samples from the river estuary and residential areas was almost the same, and it ranged from 7-8 particles/fish. The lowest particle number was in bagok catfish caught in the region near agricultural areas. This study indicated fiber as the most dominant microplastic in the two fish species at all sampling locations. It also had three colors in the alimentary tract of mullet and bagok catfish, namely red, blue, and black, which was predominant. The fourier transform infrared spectrum showed several wavenumber peaks signifying alkane compounds' presence, which are microplastic characteristics. Based on the peak values, the presence of two polymer types was suspected, namely polyethylene, and polypropylene.
CONCLUSION: Fiber and film microplastics were found in the digestive tract of mullet and bagok catfish, where the number of particles was most abundant in the mullet. The fourier transform infrared test was also detected the presence of microplastic pollutants in both species. This indicates that mullet and bagok catfish in Krueng Aceh River have been contaminated by microplastics and are not safe for consumption.

NUMBER OF REFERENCES	NUMBER OF FIGURES	NUMBER OF TABLES
52	2	3

*Corresponding Author:
Email: *muchlisinza@unsyiah.ac.id*
Phone: +62 651 7553205
ORCID: 0000-0002-0858-1853

Note: Discussion period for this manuscript open until July 1, 2023 on GJESM website at the "Show Article".

INTRODUCTION

Water pollution is one of the major issues in the world, and it is often caused by waste from various sources including industries, oil spills, as well as anthropogenic waste, such as plastic, which is difficult to degrade in a short period (Rodrigues *et al*., 2020). Plastic waste is often obtained from lands in coastal areas, where the waste drifts off to open seas, and some sink to the sea bottom (Depledge *et al*., 2013; Hardesty *et al*., 2017; Law, 2017). Furthermore, Kubota *et al*. (2005) and Hardesty *et al*. (2017) stated that the distribution of plastic debris in the oceans is caused by currents, tides, and winds. Eriksen *et al*. (2014) reported that more than 250,000 tons of plastic waste have been floating in the ocean, while Haward (2018) estimated 4.8 – 12.7 million tons of waste, including plastic. According to Derraik (2002), approximately 6.5 million tons of plastic waste have been polluting the ocean since the 1990s. In the last 4 years, there has been a significant increase in the volume, which is 16-48 times higher than the previously recorded value. A similar phenomenon also occurred in Indonesia, and Purba *et al*. (2017) revealed that 68-80% of the waste found in the Indonesian sea contains plastics, it was higher than in China approximately 44.9% (Zhou *et al*. 2011). According to Hastuti *et al*. (2014), approximately 165,000 tons of plastic waste have been polluted the Indonesian water annually. Assuyuti *et al*. (2018) reported that its contamination in Pramuka, Panggang, and Air Islands in Jakarta causes low coral cover in these areas. Djaguna *et al*. (2019) stated that various sizes of plastic waste have been recorded in the coastal waters of Tongkaina and Talawaan Bajo, North Sulawesi. Furthermore, Joesidawati (2018) revealed that sediments in coastal areas near rivers in Tuban Regency have been contaminated with microplastics. Takarina *et al*. (2022) reported that the surface water and sediment in Jakarta Bay were contaminated by microplastic. Microplastics in the sea mostly come from the inland (Browne, 2015; Duhec *et al*., 2015; Nur and Obbard, 2014), and this microplastic contaminate marine biota, including plankton, benthos, and fish (Smith and Markic 2013; Wright *et al*., 2013), and also salt produced from contaminated seawater (Tahir *et al*., 2019). Wastes in the plankton are then transferred into other aquatic biotas through the food chains once the biotas feed on contaminated plankton (Mearns *et al*., 2014). For instance, approximately 80% of *Sardinella lemuru* the planktivorous fish harvested from Northern Mindanao Philippines were contaminated by microplastics (Palermo *et al*., 2020). This indicates that it has the potential to cause damage to digestive organs, reduce growth rates, inhibit enzyme production, reduce steroid hormone levels, and inhibit the reproductive process (Wright *et al*., 2013). Therefore, microplastic pollution now threatens the health of aquatic wildlife and humans (Priya *et al*., 2022). Banda Aceh is an urban city located in a coastal area with rapid development. Furthermore, this development is followed by an increase in population density and activities, which also increase the production of waste, including plastics with the potential to pollute waters. One of the potentially polluted waters is the Krueng Aceh River, originating from Aceh Besar District and flowing into the city of Banda Aceh. This river crosses agricultural, residential, and urban areas that are densely populated and fond of discharging wastes into the Lampulo village where there is a fish landing and fish market. Sources of plastic waste that have the potential to pollute the Krueng Aceh River include plastic bags, food wrappers, and unused fishing nets. According to Evode *et al*. (2021), stated that approximately 40% of plastics were used for packaging materials in various industries. A previous report by Hadi *et al*. (2008) showed that the Krueng Aceh river has been contaminated with heavy metals, such as Lead (Pb), Cadmium (Cd), and Zinc (Zn) at a moderate level. A similar report was also published by Sarong *et al*. (2015) that oysters (*Crassoscrea* sp.) in the estuary of the Lamnyong River, one of the tributaries of the Krueng Aceh River were contaminated by these elements, which indicates the presence of plastics. However, no study has examined the status of plastic waste pollution in Krueng Aceh. In this study, microplastic contamination is determined in two fish species that are often caught downstream of Krueng Aceh, namely mullet (*Mugil cephalus*) and bagok catfish (*Hexanmatichthys sagor*). This study is crucial because the local community uses the bagok catfish and mullets commercially as a protein source. Yulianto *et al*. (2020) stated that mullets feed on algae and detritus at the bottom of the waters, while bagok is an omnivore. The two species have the potential to be polluted by microplastics due to their feeding habit. The current results obtained can be applied as scientific information to strategize

a better waste management policy, specifically for plastics waste disposal in urban city of Banda Aceh, and Indonesia in general. These tend to also become a theoretical basis for further studies. Therefore, this study aims to analyze the presence of microplastics in the digestive tract and carcass of mullet and bagok catfish harvested in the estuary of the Krueng Aceh River, Banda Aceh City, Indonesia in 2021. .

MATERIALS AND METHODS

Date and sampling

This study was carried out from January to February 2021 at the Laboratory of the Faculty of Marine and Fisheries, Universitas Syiah Kuala, Banda Aceh. The fish sample was collected at three stations in the estuary of Krueng Aceh River. Station 1 was located at the river mouth close to the fish market, jetty, and garbage processing station; Station 2 was situated approximately 7.46 Kilometers (km) from the river mouth, and was close to the residential area; Station 3 was located approximately 16.10 Kilometers (km) from river mouth close to agricultural plantations, as shown in Fig. 1. The fish sample was caught using two sets of gillnets with the mesh size of 15 millimeters (mm) and 20 mm with 25 meters (m) length and 1.2 m depth. The sampling was carried out at one-week intervals for one month. The samples were kept in an ice box at 4 degrees Celsius (°C), and then transported to the laboratory in Universitas Syiah Kuala Banda Aceh for further analysis.

Sample preparation

The fish samples were measured for their total length using digital calipers and weighed with a digital balance. The abdomen of the fish was dissected using scissors, after which the alimentary tract, namely the stomach and intestine was removed from the body cavity, and then preserved with 4% formaldehyde (Jantz *et al.*, 2013). Subsequently, the fish were weighed, dissected, and their contents were removed and placed on separate plates. The contents were then diluted using saturated NaCl three times the weight of the stomach and intestines.

Microplastics and data analysis

Approximately, 1 milliliter (mL) of the stomach and intestines content that was diluted with NaCl was taken and then placed on a sample plate. The sample was observed with the eye naked, where microplastic particles that are visible were separated from the rest. Meanwhile, those that are invisible were identified using stereo and binocular microscopes at 40x and 100x magnification. The microplastics obtained were then measured in size, followed by identification of their type and color. The abundance of microplastics was also calculated based on Boerger *et al.* (2010).

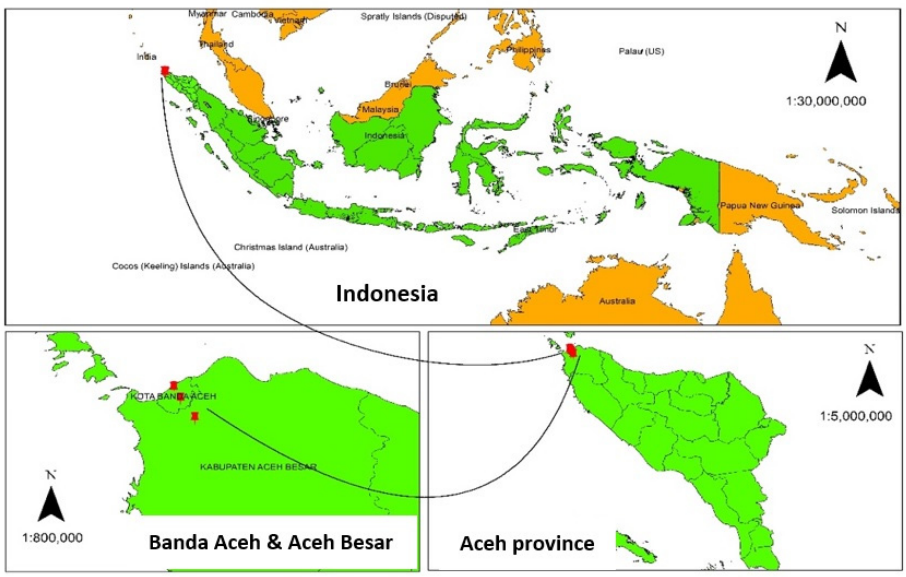

Fig. 1: Geographic location of the Indonesian archipelago showing the sampling location (red dots) from the river mouth to agricultural plantations

Table 1: The average abundance of microplastic at the alimentary tract of mullet *Mugil cephalus* and bagok catfish *Hexanematichthys sagor* according to location and type of microplastics

Species	Sampling site	N*	The average weight of fish (g)	Type of microplastic		Particles/ fish	Particles/ gram of fish
				Fiber	Film		
M. cephalus	River mouth	20	78	8	8	16	0.21
	Residential	15	106	5	5	10	0.10
	Agricultural	15	85	3	2	5	0.06
H. sagor	River mouth	16	118	4	4	8	0.07
	Residential	15	136	4	3	7	0.05
	Agricultural	15	129	2	1	3	0.02

*N= number of fish sample

Table 2: The average abundance of microplastic at the alimentary tract of mullet *Mugil cephalus* and bagok catfish *Hexanematichthys sagor* according to the location and colour of microplastics.

Species	Sampling site	Fish sample (N*)	Colour of microplastic (Particles/ fish)			
			Red	Blue	Black	Total
M. cephalus	River mouth	20	4	4	8	16
	Residential	15	2	3	5	10
	Agricultural	15	1	1	3	5
H. sagor	River mouth	16	1	3	4	8
	Residential	15	1	2	4	7
	Agricultural	15	1	1	1	3

*N= number of fish sample

FT-IR analysis

The type of microplastic polymer in fish carcasses was detected using Fourier Transform Infrared (FT-IR) spectroscopy with the KBr (Potassium Bromide) pellet method (Nor and Obbard, 2014). The wavelength spectrum of the polymeric produced by FT-IR was analyzed using a software to read the spectrum and then compared to the standard spectrum from the plastic polymer database using Euclidean Distance to determine the type of polymer in the sample (Lusher *et al.,* 2013).

Data analysis

The data were presented in the tables and figures, followed by descriptive analysis using comparison with the previous reports and other related references.

RESULTS AND DISCUSSION

A total of 50 mullets and 46 bagok catfish were caught from three sampling sites. The results showed that in mullet, the highest number of microplastic particles was found in samples caught in the river mouth close to the fish market and garbage processing station, namely 16 particles/fish on average, followed by the residential areas with 10 particles/fish on average. The lowest value was recorded at the sampling site close to agriculture areas, namely 5 particles/fish. In bagok catfish, the abundance of microplastics in samples from the river mouth and residential areas was almost the same, and it ranged from 7-8 particles/fish. The lowest abundance of microplastic (3 particles/fish) was in catfish caught in the region near agricultural areas, as shown in Table 1.

The fiber was the most dominant microplastic in the two species of fish at all sampling locations. It also had three colors in the alimentary tract of mullet and bagok catfish, namely red, blue, as well as black, which were predominant, as shown in Table 2.

The results showed that the size of microplastics in the mullet ranged from 20 micrometers (µm) to 120 µm, and from 20 µm to 80 µm in bagok catfish, where the dominant size was 20-40 µm in both species, as summarized in Table 3.

FT-IR analysis on the carcass of both fish species showed that the wavenumber of 3,570/cm – 3,200/ cm, indicated that there was a peak of OH stretch. The range of 2,935/cm – 2,915/cm indicated the presence

Table 3: The size ranges of the microplastic found in the alimentary tract of the mullet *Mugil cephalus* and bagok catfish *Hexanematichthys sagor* according to location.

Fish species	Microplastic size	Sampling site (Particles/ fish)			Total
		River mouth	Residential	Agricultural	
M. cephalus	<20 µm	5	3	2	10
	20-40 µm	7	5	3	15
	40-60 µm	2	1	-	3
	60-80 µm	1	1	-	2
	80-120 µm	1	-	-	1
H. sagor	<20 µm	2	2	1	5
	20-40 µm	4	4	2	10
	40-60 µm	1	1	-	2
	60-80 µm	1	-	-	1
	80-120 µm	-	-	-	-

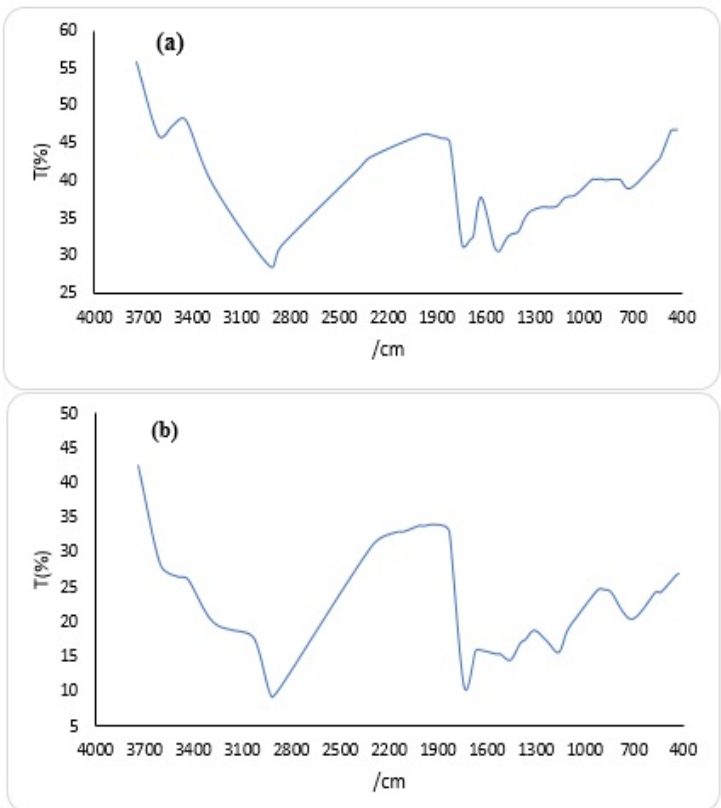

Fig. 2: The graph of the FT-IR analysis of carcass of (a) the mullet *Mugil cephalus*, and (b) bagok catfish *Hexanematichthys sagor*

of a peak of C-H stretch with strong intensity, while 1,375-1,450 showed CH_3 bending. A sharp and strong peak also occurred at 1,740/cm due to C=O from acid, as shown in Fig. 2. Therefore, the study showed that mullet and bagok catfish harvested from Krueng Aceh River estuary were contaminated by microplastics, and mullets contained more pollutants than the bagok catfish in all sampling sites.

The highest number of microplastic particles were found in fish samples caught in the river mouth area, followed by a site close to residential areas. The plastic waste in the river mouth mostly comes from

the garbage processing station and market near this site. The pollutant is blown by the wind into the river, and eaten by fish accidentally or through the food chain, for instance, plankton and other small fish that have been contaminated by microplastic. In sampling locations close to the residential area, the waste produced is often organic waste mixed with plastics. People who live on the banks of the river have a bad habit of throwing garbage directly into the water. Some of the waste are carried by the current to the river mouth, and this increases the plastic content of fish in this region, as recorded in this study. The study showed that the abundance of microplastics in the fish from Krueng Aceh river ranged from 10 -16 particles/fish. The stated values were higher than in fish from the Bengal Bay up to 2.2 particles per fish (Gosh *et al*., 2021). Conversely, they were lower compared to fish harvested from Great Lake, North America namely 35-59 particles/fish (Munno *et al*., 2021), and in cultured fish at the Pearl River estuary, South China, namely 35 particles/fish (Lam *et el*., 2022). In general, microplastic pollution in freshwaters such as rivers and lakes is greater than in the sea because freshwater is very intense and close to community activities, inlcuding industrial and residential areas (Rezania *et al*., 2018). The results showed that two types of microplastics were found, namely fiber, and film. These particles were most likely produced from used plastic bags, food wrappers, and gillnet that were dumped by fishermen into the river. This is because the first location (river mouth) was also close to the fish landing jetty. Napper *et al.* (2022) stated that fiber can be sourced from boat ropes and fishing gear discarded by fishermen. A'yun (2019) reported that it was dominantly found at the mouth of the Begawan Solo river, Gresik, Indonesia, which is a site for fishing boat mooring. Nor and Obbard (2014) also stated that fiber was produced from the degradation of various types of gillnet and boat ropes that broke down into the waters, and settled in the sediment. Pivokonsky *et al*. (2018) revealed that it is the most common morphotype of microplastics found in water samples. The abundance of microplastics in water depends on their density, where low-density particles, such as Polyethylene (PE) and Poly Propylene (PP) float in water, while others with high density, including High-Density Polyethylene (HDPE), tend to sink and be deposited in sediments (Sul and Costa, 2014). The PP and PE have densities of 900 kg/m^3 and 857 kilograms per cube meter (kg/m^3), respectively, while the density of surface water ranges from 1001.50 - 1021.33 kg/m^3. It was suspected that the microplastics found at the sampling sites mostly belonged to the PE and PP group, which came from used plastic bags, nylon gillnet, and fishing lines discarded by fishermen as mentioned above. Saleem *et al*. (2018) stated that these two categories are the most common plastic waste (Saleem *et al*., 2018), and these microplastics are frequently found in the waters in the forms of film and fiber (Liu *et al*., 2022; Zhang *et al*., 2019). Microplastic contamination in fish occurs through plastic waste that is eaten by fish accidentally. These particles cannot be digested and are difficult to discharge, hence, these wastes are left in the alimentary tract and absorbed into the tissue (Yona *et al*., 2020). This finding is in line with the FT-IR analysis, where microplastics were detected in the carcass (muscles) of the two species. The results showed that the abundance of these particles in the digestive tract of mullet was higher than that bagok catfish. This is caused by the feeding habit of mullets as detritophages (Jamabo and Maduako, 2015), and the mullet fed on detritus mixed with plastic waste at the bottom of the waters. Therefore, it was suspected that the sediment of the Krueng Aceh has also been polluted by microplastics. A series of studies are currently being carried out to examine this speculation. Black microplastics were the dominant particles in all fish samples due to their long duration in the waters or in the digestive tract of fish, and the color changed because of the discoloration process. Microplastics with dark colors probably come from polyethylene polymers, which have low density and are the main material for plastic bags and container production (GESAMP, 2015). Hidalgo-Ruz *et al*. (2012) stated that the dark coloration indicates the presence of many contaminants and other organic particles. The dark microplastics have a high ability to absorb pollutants (Basri *et al*., 2021; Shuo *et al*., 2021), including polycyclic aromatic hydrocarbons (PAHs), which are commonly found in aquatic ecosystems. Phenanthrene compounds (Phe) are one of the PAHs reported being toxic in fish and humans (Karami *et al*., 2016). Therefore, when these microplastics absorb the pollutants, their texture becomes coarse and dense (Hiwari, 2019). All types and colors of microplastics are harmful to health, but it was suspected that dark particles are more toxic because its contain higher pollutants. Sugandi *et al*. (2021), and Ghaffar *et al*.

(2022) reported that microplastics harm human health, including causing brain inflammation. This compound can also cause oxidative stress, which is a condition where the number of free radicals in the body exceeds the limits. Microplastics can also enter the intestines through food, and interfere with the digestive system (Hollman *et al*., 2013). The microplastic in the digestive tract is then further absorbed, then enters the blood circulation to cause cancer, diabetes, skin irritation, cardiovascular disease, as well as respiratory and reproductive problems (Murray and Cowie, 2011; A'yun, 2019). The results showed that the size of microplastics varied in fish samples, where the dominant size was 20-40 µm. According to Ng and Obbard (2006) and Barnes *et al*. (2009) microplastic of sizes 1 µm to 500 µm are commonly found in seawater. It was influenced by several factors, one of which is the duration of time in the waters. The longer the time taken, the more it decomposes, which makes the size becomes smaller. Small microplastics are easier to enter the body because they are difficult to detect (Lim, 2021). The FT-IR analysis showed that the carcass of mullet and bagok catfish harvested from Krueng Aceh River have been contaminated by microplastics. The spectrum of the FT-IR shows several wavenumber peaks indicating the presence of alkane compounds, which are characteristic of microplastic. Based on peak values, it was suspected that there are two types of polymers present, namely polyethylene (PE) and polypropylene (PP). This was indicated by the peak wavenumber in the range of 2,935-2,915 cm^{-1}, which shows the presence of CH stretch bonds and 1,375-1,450 cm^{-1} for $–CH_3$ bending. The CH bond can be used as an indication of the presence of PE and PP (Syakti, 2017). The PE was produced from plastic bags, detergent packages, and shampoo bottles, while PP can be obtained from bottle caps, straws, buckets, and plastic toys (Barron and Spark, 2020; Hoseini and Bond, 2022).

CONCLUSIONS

Presently, the Krueng Aceh river in Banda Aceh city, Indonesia is potentially polluted by domestic wastes including microplastics. Similar to other urban cities in Indonesia, unresponsible people use rivers as a place for direct waste disposal without any processing it. Previous study has also reported the contamination of biotas such as the oyster *Crassostrea gigas* from this river with heavy metals. The current study examined microplastic contents in the two dominant fish species found in the downstream of Krueang Aceh river, namely the mullet *M. cephalus*, and the bagok catfish *H. sagor*. The fish samples were collected from several locations in the downstream river of Krueng Aceh. The digestive tract of both fish was discovered to be contaminated with microplastics. The highest particle content was found in mullet and bagok catfish caught at the river estuary. There were two types of microplastics in this study, namely film and fiber. The dominant particle was black with a size range of 20 - 80 µm. The FT-IR analysis spectrum of the carcass mullet and bagok catfish samples showed several wavenumber peaks. This indicates Alkane compound's presence as a characteristic of microplastics with two polymer types, namely Polyethylene, and Polypropylene which mean the fish are not safe for consumption. Therefore, a better management strategy needs to be planned for the Krueng Aceh river by developing the laws and socializing with the people followed by consistent law enforcement. In Banda Aceh, even in Aceh province, a plastic waste recycling facility should be built immediately as an effort to reduce plastic waste disposed into the environment. The policy of selecting wastes based on their type and form also needs to be implemented to ensure plastic waste are separated and then recycled. In the short term, the obtained results have to be socialized to people in Banda Aceh that the two studied fish species and possibly other species living in this river are not safe for consumption because their microplastic content is harmful to health.

AUTHORS CONTRIBUTIONS

M.R. Maulana performed survey, collecting data, processing data, and prepared the first draft of the manuscript**.** S. Saiful conducted survey, analyzed and processed the FTIR data, and prepared the first draft. Z.A. Muchlisin developed the research concepts, data analysis, financial acquisition, and approval of the final draft of the manuscript

ACKNOWLEDGEMENTS

This study was financed by Universitas Syiah Kuala through Professorship Research Scheme 2021. Therefore, the authors thank the Rector of Universitas Syiah Kuala for supporting this study [Grant No.: 1/UN11.2.1/PT.01.03/PNBP/2021].

CONFLICT OF INTEREST

The authors declare no potential conflict of interest regarding the publication of this work. In addition, the ethical issues including plagiarism, informed consent, misconduct, data fabrication and, or falsification, double publication and, or submission, and redundancy have been completely witnessed by the authors.

OPEN ACCESS

PUBLISHER'S NOTE

ABBREVIATIONS

µm	Micrometer
%	Percent
°C	Degrees Celsius
Cd	Cadmium
CH	Alkane
CH_3	Methyl
C=O	Carbonyl
cm	Centimeter
FT-IR	Fourier Transform Infrared
g	Gram
HDPE	High density polyethylene
KBr	Potassium bromide
kg	Kilogram
km	Kilometer
m	Meter
mL	Milliliter
mm	Milimeter
m^3	Cube meter
N	Number of fish samples
OH	Hydroxyl
sp.	Species
PAHs	Polycyclic Aromatic Hydrocarbons
Pb	Lead
PE	Polyethylene
Phe	Phenanthrene
PP	Poly Propylene
Zn	Zinc

REFERENCES

Assuyuti, Y.M.; Zikrillah, R.B.; Tanzil, M.A.; Banata, A.; Utami, P., (2018). Distribusi dan jenis sampah laut serta hubungannya terhadap ekosistem terumbu karang Pulau Pramuka, Panggang, Air, dan Kotok Besar di Kepulauan Seribu Jakarta. Biosfera: A Sci. J., 35(2): 91-102 **(12 pages).**

A'yun, N.Q., (2019). Analisis mikroplastik menggunakan FT-IR pada air, sedimen, dan ikan belanak (*Mugil cephalus*) di segmen Sungai Bengawan Solo yang melintasi Kabupaten Gresik. Doctoral Dissertation, UIN Sunan Ampel, Surabaya.

Barron, A.; Spark, T.D., (2020). Commercial Marine-Degradable Polymers for Flexible Packaging. Science. 23: 101353 **(13 pages).**

Barnes, D.K.A.; Galgani, F.; Thompson, R.C.; Barlaz, M., (2009). Accumulation and fragmentation of plastic debris in global environments. Phil. Trans. R. Soc., B. 364: 1985–1998 **(14 pages)**.

Basri, S.; Basri.; Eko, M.S.; Handayani, S., (2021). Microplastic pollution in waters and its impact on health and environment in Indonesia: a review. J. Public Health Trop. Coastal Reg., 4(2): 63-77 **(15 pages).**

Boerger, C.M.; Lattin, G.L.; Moore, S.L.; Moore, C.J., (2010). Plastic ingestion by planktivorous fishes in the North Pacific Central Gyre. Mar. Poll. Bull. 60: 2275-2278 **(4 pages).**

Browne, M.A., (2015). Sources and pathways of microplastics to habitats. Marine Anthropogenic Litter. Springer Int. Publ., 229-244 **(16 pages).**

Depledge, M.H.; Galgani, F.; Panti, C.; Caliani, I.; Casini, S.; Fossi, M.C., (2013). Plastic litter in the sea. Mar. Environ. Res., 92: 279-281 **(3 pages).**

Derraik, J.G.B., (2002). The pollution of the marine environment by plastic debris: a review. Mar. Pollut. Bull., 44: 842–852 **(11 pages).**

Djaguna, A.; Pelle, W.E.; Schaduw, J.N.; Manengkey, H.W.; Rumampuk N.D.; Ngangi, E.L., (2019). Identifikasi sampah laut di Pantai Tongkaina dan Talawaan Bajo. J. Pes. Laut Trop., 7(3): 174-182 **(9 pages).**

Duhec, A.V.; Jeanne, R.F.; Maximenko, N.; Hafner, J., (2015). Composition and potential origin of marine debris stranded in the Western Indian Ocean on remote Alphonse Island, Seychelles. Mar. Pollut. Bull., 96: 76-86 **(11 pages).**

Eriksen, M.; Mason, S.; Wilson, S.; Box, C.; Zellers, A.; Edwards, W.; Farley, H.; Amato, S., (2013). Microplastic pollution in the surface waters of the Laurentian Great Lakes. Mar. Poll. Bull., 77(1): 177-182 **(6 pages).**

Evode, N.; Qamar, S.A.; Bilal, M.; Barcelo, D.; Iqbal, H.M.N., (2021). Plastic waste and its management strategies for environmental sustainability. Case Stud. Chem. Environ. Eng., 4 : 100142 **(8 pages).**

GESAMP, (2015). Sources, fate and effect of micropalstics in the marine oceans: a global assessment. International Maritme Organization, London **(98 pages).**

Ghaffar, M.; Rashid, M.; Akmal, M.; Hussain, A., (2022). Plastics in the environment as potential threat to life: an overview. Environ. Sci. Pollution Res., 29: 56928–56947 **(20 pages).**

Gosh, G.C.; Akter, S.M.; Islam, R.M.; Habib, A.; Chakraborty, T.K.; Zaman, S.; Kabir, A.H.M.E.; Shipin, O.S.; Wahid, M.A., (2021). Microplastics contamination in commercial marine fish from the Bay of Bengal. Reg. Stud. Mar. Sci., 44: 101728 **(8 pages).**

Hadi, I.; Suhendrayatna, S.; Muchlisin, Z.A., (2018). Water quality status and heavy metal content in water and sediment at the estuary of Krueng Aceh. Depik. 7(2): 91-99 **(9 pages).**

Hardesty, B.D.; Harari, J.; Isobe, A.; Lebreton, L.; Maximenko, N.; Potemra, J.; Wilcox, C., (2017). Using numerical model simulations to improve the understanding of micro-plastic distribution and pathways in the marine environment. Front. Mar. Sci., 4(3): 1-9 **(9 pages).**

Hastuti, A.R.; Yulianda, F.; Wardianto, Y., (2014). Distribusi spasial sampah laut di ekosistem mangrove Pantai Indah Kapuk, Jakarta. Bonoworo Wetlands. 4(2): 94-107 **(14 pages).**

Haward, M., (2018). Plastic pollution of the world's seas and oceans as a contemporary challenge in ocean governance. Nat. Commun., 9: 667 **(3 pages).**

Hidalgo-Ruz, V.; Gutow, L.; Thompson, R.C.; Thiel, M., (2012). Microplastics in the marine environment: a review of the methods used or identification and quantification. Environ. Sci. Technol., 46(6): 3060-3075 **(15 pages).**

Hiwari, H.; Purba, N.P.; Ihsan, Y.N.; Yuliadi, I.P.; Mulyani, P.G., (2019). Condition of microplastic garbage in sea surface water at around Kupang and Rote, East Nusa Tenggara Province. Prosiding Seminar Nasional Masyarakat Biodiversitas Indonesia. 5(2): 165-171 **(7 pages).**

Hollman, P.C.; Bouwmeester, H.; Peters, R.J., (2013). Microplastics in the aquatic food chain; Sources, measurement, occurence and potential health risks. RIKILT Report. **(32 pages).**

Hoseini, M.; Bond, T., (2022). Predicting the global environmental distribution of plastic polymers. Environ. Pollut., 300: 118966 **(10 pages).**

Jamabo, N.A.; Maduako, N.C., (2015). Food and feeding habits of *Mugil cephalus* (Linnaeus, 1758) in Elechi Creek, Niger Delta, Nigeria. Int. J. Fish. Aquac., 7(3): 25-29 **(5 pages).**

Jantz, L.A.; Morishige, C.L.; Bruland, G.L.; Lepczkyk, C.A., (2013). Ingestion of microplastic marine debris by Longnose lancet fish (*Alepisaurus ferox*) in the North Pacific Ocean. Mar. Poll., Bull., 69(2): 97-104 **(8 pages).**

Joesidawati, M.I., (2018). Pencemaran mikroplastik di sepanjang pantai Kabupaten Tuban. Prosiding Seminar Nasional Hasil Penelitian dan Pengabdian Kepada Masyarakat III Universitas PGRI Ronggolawe. 8-15 **(8 pages).**

Karami, A.; Romano, N.; Galloway, T.; Hamzah, H., (2016). Virgin microplastics cause toxicity and modulate the impacts of phenanthrene on biomarker responses in African catfish (*Clarias gariepinus*). Environ. Res., 151: 58–70 **(13 pages).**

Kubota, M., Takayama, K.; Namimoto, D., (2005). Pleading for the use of biodegradable polymers in favor of marine environments and to avoid an asbestos-like problem for the future. Appl. Microbiol. Biotechnol., 67(4): 469-476 **(8 pages).**

Lam, T.W.L.; Fok, L.; Ma, A.T.H.; Li, H.; Xu, X.R.; Cheung, L.T.O.; Womg, M.H., (2022). Microplastic contamination in marine-cultured fish from the Pearl River Estuary, South China. Sci. Total Environ., 827: 154281 **(9 pages).**

Law, K.L., (2017). Plastics in the marine environment. Ann. Rev. Mar. Sci., 9(1): 205-232 **(28 pages).**

Lim, X., (2021). Microplastics are everywhere— but are they harmful? Nature. 593: 23-25 **(3 pages).**

Liu, D.; Guo, Z.; Xu, Y.; Chan, F.K.S.; Xu, Y.; Johnson, M.; Zhu, Y., (2022). Widespread occurrence of microplastics in marine bays with diverse drivers and environmental risk. Environ. Int., 168: 107483 **(10 pages).**

Lusher, A.L.; McHugh, M.; Thompson, R.C., (2013). Occurrence of microplastics in the gastrointestinal tract of pelagic and demersal fish from the English channel. Mar. Poll. Bull., 67(1-2): 94–99 **(6 pages).**

Mearns, A.J.; Reish, D.J.; Oshida, P.S; Ginn, T., Rempel-Hester, M.A.; Arthur, C.; Rutherford, N., (2014). Effects of pollution on marine organisms. Water Environ. Res., 86(10): 1832-1868 **(37 pages).**

Mohamed, G.A.; Reuy, K.C.; Joses, H.; Seetha, K.; Farhan, M.; Adam, C.C.; Suresh, J., (2017). Optical inhibition of larval zebrafish behaviour with anion channel rhodopsins. BMC Biol., 15(103): 1-12 **(12 pages).**

Munno, K.,; Helm, P.A.; Rochman, C.; George, T.; Jackson, D.A., (2021). Microplastic contamination in Great Lakes fish. Conserv. Biol., 36(1): e13794.

Murray, F.; Cowie, P.R., (2011). Plastic contamination in the decapod crustacean *Nephrops norvegicus* (Linnaeus, 1758). Mar. Pollut. Bull., 62: 1207-1217 **(11 pages).**

Napper, I.E.; Wright, L.S.; Barrett, A.C.; Parker-Jurd, F.N.F.; Thompson, R.C., (2022). Potential microplastic release from the maritime industry: Abrasion of rope. Sci. Total Environ., 804: 150155 **(6 pages).**

Ng, K.L., Obbard, J.P., (2006). Prevalence of microplastics in Singapore's coastal marine environment. Mar. Pollut. Bull., 52: 761–767 **(7 pages).**

Nor, N.H.M.; Obbard, J.P., (2014). Microplastics in Singapore's coastal mangrove ecosystems. Mar. Poll. Bull., 79(1-2): 278-283 **(6 pages).**

Palermo, J.D.H.; Labrador, K.L.; Follante, J.D.; Agmata, A.B.; Pante, M.J.R.; Rollon, .N.; David, L.T., (2020). Susceptibility of *Sardinella lemuru* to emerging marine microplastic pollution. Global J. Environ. Sci. Manage., 6(3): 373-384 **(12 pages).**

Pivokonsky, M.; Cermakova, L.; Novotna, K.; Peer, P.; Cajthami, T.; Janda, V., (2018). Occurrence of microplastics in raw and treated drinking water. Sci. Total Environ., 643: 1644-1651 **(8 pages).**

Priya, A.; Anusha, G.; Thanigaivel, S.; Karthick, A.; Mohanavel, V.; Velmurugan, P.; Balasubramanian, B.; Ravichandran, M.; Kamyab, H., Kirpichnikova, I.M.; Chelliapan, S., (2022).Removing microplastics from wastewater using leading-edge treatment technology: a solution to microplastic pollution—a review. Bioprocess Biosyst Eng., 2022.

Purba, N.P., (2017). Sampah dan solusi untuk kesehatan laut. Indonesia Youth Marine Debris Summit, Jakarta **(25 pages).**

Rezania, S.; Park, J.; Din, M.F.M.; Taib, S.M.; Talaiekhozani, A.; Yadav, K.K.; Kamyab, H., (2018). Microplastics pollution in different aquatic environments and biota: A review of recent studies. Mar. Poll. Bull., 133: 191-208 **(18 pages).**

Rodrigues, S.M.; Almeida, C.M.R.; Ramos, S., (2020). Microplastics contamination along the coastal waters of NW Portugal. Case Stud. Chem. Environ. Eng., 2: 100056 **(6 pages).**

Saleem, J.; Riaz, M.A.; McKay, G., (2018). Oil sorbents from plastic wastes and polymers: a review. J. Hazard. Mat., 5(341): 424 – 437 **(14 pages).**

Sarong, M.A.; Jihan, C.; Muchlisin, Z.A.; Fadli, N.; Sugianto, S., (2015). Cadmium, lead and zinc on the oyster *Crassostrea gigas* muscle harvested from the estuary of Lamnyong River, Banda Aceh City, Indonesia. AACL Bioflux., 8(1): 1-6 **(6 pages).**

Smith, S.D.A.; Markic, A., (2013). Estimates of marine debris accumulation on beaches are strongly affected by the temporal scale of sampling. Plos One. 8(12): 8-13 **(6 pages).**

Shuo, W.; Duan, W.; Huanming, L.; Sun, R.; Zhu, X., (2021). The pollution of atmospheric microplastics and their potential risks to humans. IOP Conference Series: Earth and Environmental Science. 793(1): 012016 **(8 pages).**

Sul, J.A.I.; Costa, M.F., (2014). The present and future of microplastics pollution in the marine enviroment. Environ. Pollut., 185(1): 352-364 **(13 pages).**

Sugandi, D.; Deri, A.; Shafira, V.F.; Yulius, Y.; Nelly, W., (2021). Identifikasi jenis mikroplastik dan logam berat di air Sungai Kapuas Kota Pontianak. Positron. 11(2): 112-120 **(9 pages).**

Syakti, A.D., (2017). Microplastics monitoring in marine environment. Omni Akua. J. Fish. Mar. Res., 13(2): 1-6 **(6 pages).**

Tahir, A., Taba, P.; Samawi, M.F.; Werorilangi, S, (2019). Microplastics in water, sediment and salts from traditional salt producing ponds. Global J. Environ. Sci. Manage., 5(4): 431 440 **(10 pages).**

Takarina, N.D.; Purwiyanto, A.I.S.; Rasudi, A.A.; Arifin, A.A.; Suteja, Y., (2022). Microplastic abundance and distribution in surface water and sediment collected from the coastal area. Global J. Environ. Sci. Manage., 8(2): 183-196 **(14 pages).**

Wright, S.L.; Thompson, R.C.; Galloway, T.S., (2013). The physical impacts of microplastics on marine organisms: a Review. Environ. Poll., 178(1): 483-492 **(10 pages).**

Yulianto, D.; Indra, I.; Batubara, A.S.; Efizon, D.; Nur, F.M.; Rizal, S.; Muchlisin, Z.A., (2020). Length–weight relationships and condition factors of mullets Liza macrolepis and Moolgarda engeli (Pisces: Mugilidae) harvested from Lambada Lhok Waters in Aceh Besar, Indonesia. FI000 Res., 9(259): 1-10 **(10 pages).**

Yona, D.; Mela, D.M.; Mohammad, R.C.; Yuyun, E.I.; Wayan, E.D., (2020). Analisis mikroplastik di insang dan saluran pencernaan ikan karang di tiga pulau kecil dan terluar Papua, Indonesia: Kajian awal. J. Ilm. Teknol. Kel. Trop., 12(2): 495-505 **(11 pages).**

Zhang, X.; Leng, Y.; Liu, X.; Huang, K.; Wang, J., (2019). Microplastics pollution and risk assessment in an urban river: a case study in the Yongjiang River, Nanning City, South China. Expos. Health. 34(2): 1-11 **(11 pages).**

Zhou, P.; Huang, C.; Fang, H.; Cai, W.; Li, D.; Li, X., Yu, H., . (2011). The abundance, composition and sources of marine debris in coastal seawaters or beaches around the northern South China Sea (China). Mar. Poll Bull., 62: 1998–2007 **(10 pages).**

AUTHOR (S) BIOSKETCHES

Muchlisin, Z.A., Ph.D., Professor, Dean, Faculty of Marine and Fisheries, Syiah Kuala University, Banda Aceh 23111, Indonesia.
- Indonesia.Email: *muchlisinza@unsyiah.ac.id*
- ORCID: 0000-0002-0858-1853
- Web of Science ResearcherID: E-2317-2015
- Scopus Author ID: 55937322900
- Homepage: https://fsd.unsyiah.ac.id/muchlisinza/

Saiful, S., Ph.D., Associate Professor, Department of Chemistry, Faculty of Mathematics and Natural Sciences, Universitas Syiah Kuala, Banda Aceh 23111, Indonesia.
- Email: *saiful@unsyiah.ac.id*
- ORCID: 0000-0002-4133-7086.
- Web of Science ResearcherID: NA
- Scopus Author ID: 23095220900
- Homepage: https://fsd.unsyiah.ac.id/saiful/

Maulana, M.R., M.Sc., Postgraduate student, Department of Integrated Coastal Zone Resources Management, Postgraduate Program, Universitas Syiah Kuala, Banda Aceh 23111, Indonesia.
- Email: *rizki.rm47@gmail.com*
- ORCID: 0000-0002-3663-2056
- Web of Science ResearcherID: GRJ-3660-2022
- Scopus Author ID: NA
- Homepage: http://fkp.unsyiah.ac.id

HOW TO CITE THIS ARTICLE

Maulana, M.R.; Saiful, S.; Muchlisin, Z.A., (2023). Microplastics contamination in two peripheral fish species harvested from downstream river. Global J. Environ. Sci Manage., 9(2): 299-308.

DOI: 10.22034/gjesm.2023.02.09

url: https://www.gjesm.net/article_255004.html

Global J. Environ. Sci. Manage. 9(2): 309-322, Spring 2023, Serial #34

Global Journal of Environmental Science and Management
(GJESM)

Homepage: https://www.gjesm.net/

ORIGINAL RESEARCH ARTICLE

Geospatial visualization and seasonal variation of heavy metals in river sediments

D. Justus Reymond, K. Sudalaimuthu*

Department of Civil Engineering, SRM Institute of Science and Technology, Kattankulathur, Chengalpattu, Tamil Nadu, India

ARTICLE INFO

Article History:
Received 14 June 2022
Revised 19 August 2022
Accepted 22 October 2022

Keywords:
Contamination factor
Contamination degree
Geographical information system
Heavy metals
Pollution load index

DOI: 10.22034/gjesm.2023.02.10

ABSTRACT

BACKGROUND AND OBJECTIVES: Heavy metals can enter the food chain in the aquatic environment and become available for accumulation in biota. Industrialization and agricultural developments are progressively causing ecological concerns, which must be addressed. This study aimed to ascertain the heavy metals in Tamiraparani River sediments using contamination factor and contamination degree, which would help administrative bodies implement control measures. For heavy metal analysis, this study is unique in that it focuses on the far downstream, where the sediment deposition is higher.

METHODS: Using an atomic absorption spectrophotometer, the abundance of iron, manganese, copper, and chromium was determined in this study. In this study, the heavy metals in the sediments are selected on the basis of previous studies. Additionally, to assess sediment pollution status, contamination factor, contamination degree, and pollution load index were used. Furthermore, a geographical information system was used to analyse the temporal variations of heavy metals in the sediments for different spatial locations downstream of the river.

FINDINGS: The study revealed that iron > manganese > chromium > copper concentration ranges from 3838 to 853, 68 to 7.8, 8.3 to 0.5, and 5.6 to 0.26 milligram per kilogram, respectively. The contamination factor ranges from 0.006 to 0.093 among all the sampling locations, heavy metals, and seasons, indicating that the pollution is in a low-level category. The contamination degree ranges from 0.039 to 0.378 among sampling stations and seasons, also indicating low-category pollution. The pollution load index value ranges from 0.004 to 0.092, which is less than 1 (guideline value), indicating less pollution impact. The seasonal variation shows that the post-monsoon is highly polluted because of the excessive sediment deposit from upstream after monsoon rainfall.

CONCLUSION: The contamination factor and contamination degree are within the acceptable limit. However, they are in an increasing phase during monsoon seasons, which indicates that heavy metals are from industries and are built up along the river banks upstream. Additionally, chromium and copper are in high concentrations during post-monsoon (chromium = 6.643, copper = 5.636) than during pre-monsoon because of anthropogenic activities and industrial waste discharge into the river stream.

NUMBER OF REFERENCES	NUMBER OF FIGURES	NUMBER OF TABLES
40	7	5

*Corresponding Author:
Email: *karuppas@srmist.edu.in*
Phone: 9791 695481
ORCID: 0000-0001-6612-6763

Note: Discussion period for this manuscript open until July 1, 2023 on GJESM website at the “Show Article”.

INTRODUCTION

The accumulation of heavy metals in sediments in rivers is drastically increasing because of various industrial and anthropogenic activities on the river banks. Pollution due to heavy metal sediments in water is a serious issue, and it is drawing international attention. Hence, sediments have been widely considered a heavy metal source because of their biogeochemical association (Annammala *et al*., 2021). These complex biogeochemical association mechanisms indicate pollutant availability, mobility, and toxicity in sediments. Therefore, heavy metals are bioaccumulated in sediments because of their slow removal rates and in turn biomagnified, which is posing serious health risks to humans and aquatic organisms (Ramesh and Nagalakshmi, 2022). It is known that there are various sources for the generation of heavy metals, in which weathering of rocks (Hu *et al.,* 2013), untreated sewage, untreated industrial effluents, agricultural runoff, metal leaching from garbage (Michael *et al.,* 2022), and solid waste heaps are the major sources for the same (Reymond and Sudalaimuthu, 2021). The discharge of sewage, untreated or partially treated industrial effluent, and agricultural waste accumulated in the river, which disturbs the natural balance of the riverine system and eventually creates problems across the globe (Kumar *et al*., 2013). Various researchers have been using advanced instruments such as inductively coupled plasma–optical emission spectrometry and graphite furnace atomic absorption spectroscopy (AAS) and AAS for analyzing heavy metal pollution in sediments for more than decades. Magesh and Chandrasekar (2014) have used AAS in their study for the detection and quantification of chemical elements relying on the absorption of optical radiation (light) by gaseous atoms. The aforementioned high-end sophisticated instruments are used extensively to determine the presence of toxic metal in sediment from the river sample. In the current scenario, the advent of remote sensing and geographical information system (GIS) is inevitable for analysing the spatiotemporal variation of heavy metals in the water body. Skordas *et al*. (2015) have used GIS in their study to analyse the spatial distribution of heavy metal concentration in sediments. Recently, GIS software has been used in the spatial modelling field, and several studies in interpolation analyses for zoning contamination sites have been conducted (Brady *et al*., 2015). GIS is evolving as the most essential tool for researching environmental geochemistry issues (Kuchelar *et al*., 2022). Using GIS, numerous studies have directly addressed whether reported contamination is a result of natural sources or anthropogenic (Sojka *et al*., 2018). The indices contamination factor (CF) and contamination degree (CD) are used to evaluate the impact of anthropogenic activities. The CF is clear and concise, and a single-index indicator was used to assess metal contamination. It gives a ratio of an element at the sampling site to the same element at a background site, as well as a reference value (Said *et al*., 2019). Generally, sediments have been used as environmental indicators, in which, their ability to monitor contaminants and identify heavy metal contamination sources is well documented. Additionally, the pollution load index (PLI) is used to determine the overall toxicity and quality of the sediments; moreover, it is utilized effectively to determine the consequence of the contribution of the metals like chromium (Cr), copper (Cu), iron (Fe), manganese (Mn), and zinc (Zn) (Khorasani *et al*., 2013). According to the literature, metal accumulation in sediments is strongly influenced by the nature of the substrate as well as the physiochemical characteristics controlling dissolution and precipitation (Vaezi *et al*., 2015). The Tamiraparani River receives a significant quantity of effluents from numerous industries like fertilizer production, petrochemicals, rice mills, copper smelting plants, mineral-based industries, coal-fired power stations, and other sources as it flows through the industrial area. The literature shows that although few studies were conducted to determine the heavy metal sediments in the Tamiraparani River, no studies have been done downstream of the river (Bai and Reji, 2015). Generally, the heavy metals in the sediments especially in the flood plains interact with the surrounding ecosystem and accumulate in it. Most times directly or indirectly it affects human health by creating skin diseases, cancers, and other harsh diseases. Hence, this study primary focused on the heavy metal analysis at the downstream delta region of Tamiraparani River where the sediment deposits are at their maximum. The catchment region has many industries and cities discharging untreated effluent into the Tamiraparani River, creating the dissolving of heavy metals and gradually it is adsorbed by the sediments and get deposited in the downstream deltaic regions. Therefore, this

study focused on the spatiotemporal analysis of the heavy metals in the sediments of the deltaic region of the Tamiraparani River using various pollution assessment indices such as CF, CD, and PLI. The visual representation and spatial analysis are carried out using GIS techniques (Vaezi *et al*., 2014). To fulfill the expected outcome of the study, the following objectives are framed: i) sampling and laboratory analysis to derive the toxic metals of the study area; ii) assessment of the contamination levels through indices such as CF, CD, and PLI; and iii) spatiotemporal variation analysis using geospatial techniques to monitor the heavy metal pollution levels in sediments for Tamiraparani River. This study has been carried out in the Tamiraparani River of India in 2020 and 2021.

Study area

The study area is the Tamiraparani River (Fig. 1), which is the only perennial river providing drinking water for Tirunelveli and Tuticorin districts. It lies between 78°4′8.4″ and 78°5′20.4″E longitudes and 8°37′33.6″ and 8°38′13.2″N latitudes of Thoothukudi, Tamil Nadu. Thoothukudi is well known for pearl fishing, coral reefs, industries, minerals, and salt pans (Okedeyi *et al*., 2014). It has one of the oldest ports in the world. The river extends approximately 126 km in the mountains and plains, covering a catchment area of 5369 km^2. For the present study, 6 km from the downstream was considered. This area has a semiarid tropical wet climate and is characterized by South West and North East monsoons, with the annual rainfall ranging from 1000 to 1100 mm. The temperature and wind velocity vary from 20°C to 38°C and 2.8 to 35.5 km/h, respectively (Mukesh *et al*., 2018). The major rock types found in the area are garnet–biotite–sillimanite gneiss, calc–granulite, quartzite, and charnockite groups; limestone of the khondalite group; and migmatite complex of the Eastern Ghats super group. The area has four dominant soil textures, namely, loamy, fine loamy, coarse loamy, sandy, and fine sandy. The main sources of pollution in the study area includes wastewater from residence, industries, agricultural activities, and sand mining (Nayagam

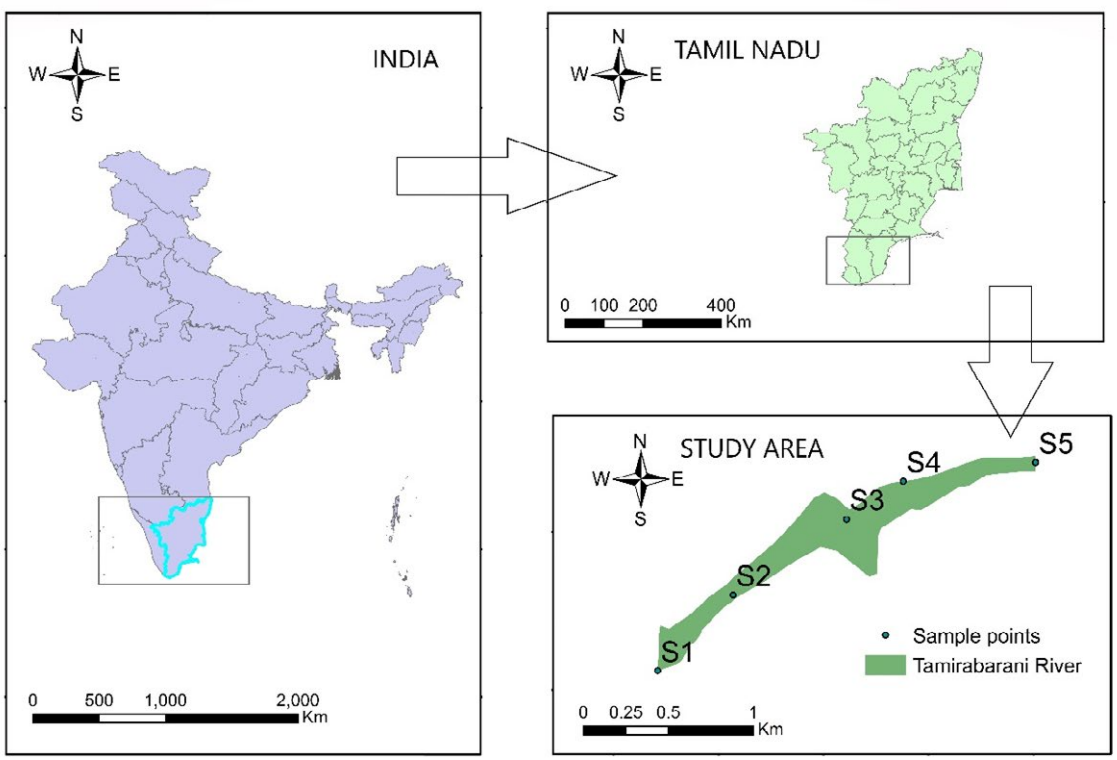

Fig. 1: Geographic location of the study area in the Tamiraparani River in India

et al., 2019). Fig. 1 shows the downstream of the Tamiraparani River as a study area.

MATERIALS AND METHODS

Sample collection

Study area delineation was carried out from the Top sheet, a scale of 1:50,000 with the help of the Aeronautical Reconnaissance Coverage Geographic Information System. Delineation of the study area includes geo-referencing of top sheet followed by onscreen digitization. Successively, sediment sampling from the field was carried out as per the standard procedures, and their locations were marked using global positioning system. The sampling primarily focused on downstream, and the location was chosen based on reconnaissance surveys such as potential pollutant sources, sites with inhabitants, and significant human activities (Pandey *et al.,* 2015). Eventually, the sediment samples are collected from Authoor, Mukkani, and Sernthamangalam from the study area. The Sernthamangalam area contains the mineral separation industry at a distance of 1.2 km from the riverbank (Singh *et al.,* 2017). To study the seasonal variation of heavy metals in river sediments, the sampling was carried out in three stages, namely, pre-monsoon, post-monsoon, and monsoon seasons. Hence, samples were collected during pre-monsoon (July 2020), monsoon (November 2020), and post-monsoon (March 2021). The Van Veen grab sampler was used for sampling the sediments from the river bed, and the samples were packed and tagged properly before laboratory analysis. The collected samples were refrigerated at 4°C for further analysis (Perumal *et al.,* 2021). Table 1 presents the details of the sampling stations along with the observed activities.

In the three seasons, a total of 75 surface sediment samples were collected. Additionally, five composite samples were collected at each station in the respective season to reduce sampling error.

Sediment digestion and heavy metals analysis

The sediments were air dried in a hot air oven at 60°C for 24 h and powdered using mortar and pestle and sieved through a 63 µm sieve. The fraction that settled was referred to as sand, whereas the fraction that passed through the sieve was referred to as clay and silt. The samples were placed on a clean and waterproof board and divided into four parts, with the diagonal portions mixed and quartered again until a homogeneous sample was obtained (Chen *et al*., 2012). Homogenized subsamples of 1 g were subjected to the digestion process. In a Teflon bomb, 1 g homogenized subsample and 1 mL aqua regia (mixed concentrated acid of HNO_3 and HCl in a ratio of 1:3) were mixed with 6 mL hydrogen fluoride; the Teflon bomb was kept in a 95°C hot water bath for approximately 2.5 h. During the digestion process, fluorides from unreacted hydrogen fluoride precipitate were added to the solution, to re-dissolve the precipitated boric acid crystals (Guo *et al*., 2016). Then, distilled water was added to the digested samples in a 100 mL volumetric flask and filled to the mark. After centrifuging, the heavy metals were determined via AAS, Thermo Fisher Scientific, designed in the United Kingdom and manufactured in China (Model-ICE 3300). All the chemicals used were of analytical grade. The reagent blanks were included in each analysis. All absorbance readings were taken thrice. The results were presented in milligrams per kilogram of the dry mass of sediments (Jaishankar *et al*., 2014). The experimental analysis of the sediment samples was conducted using the AAS instrument. Samples were analysed for heavy metal concentrations such as Cr, Cu, Mn, and Fe for the pre-monsoon, post-monsoon, and monsoon months.

Pearson's correlation matrix

Pearson's correlation was performed for the different metals under consideration to see if there was any correlation between them. Table 2 shows the outcomes.

Table 1: Details of the sampling places in the Tamiraparani River

Sampling station	Place	Latitude	Longitude	Observations/activities
S1	Authoor	8.626°	78.069°	Agricultural, bathing and washing, sewage outfall, and solid waste dumping
S2	Mukkani	8.630°	78.073°	Agricultural, sewage outfall, and Brick kiln
S3	Shasta Thirukkovil	8.634°	78.079°	Agricultural, sewage outfall, and Brick kiln
S4	Sernthamangalam	8.636°	78.082°	Mineral separation industry
S5	Sri Pathirakali ammankovil	8.637°	78.089°	Mineral separation industry

Table 2: Correlation matrix of heavy metals

Heavy metal	Cr	Fe	Mn	Cu
Cr	1			
Fe	0.979849	1		
Mn	0.993816	0.969517	1	
Cu	0.982353	0.942409	0.986026	1

Table 3: Sediment quality according to contamination factor and contamination degree

C_f	C_d	Class	Quality of sediment
$C_f < 1$	$C_d < 6$	1	Low pollution
$1 \geq C_f \geq 3$	$6 \geq C_d \geq 12$	2	Moderate pollution
$3 \geq C_f \geq 6$	$12 \geq C_d \geq 24$	3	Considerable pollution
$C_f > 6$	$C_d > 24$	4	Very high pollution

In this study, Cr, Fe, Mn, and Cu all had significant correlation coefficients, indicating that they have closely associated origins and may be influenced by an exclusive factor. Cu had a strong positive relationship with Cr and Mn and, to a lesser extent, Fe. Heavy metals are present due to anthropogenic sources such as municipal and industrial wastewater, but agricultural wastewaters are the original sources of copper.

Contamination factor and contamination degree

Followed by the experimental analysis, contamination factor (C_f) and contamination degree (C_d) were estimated to analyse the intensity of the pollution in the study area. CF and CD were calculated by using Eqs. 1 and 2, respectively (Islam *et al*., 2015).

C_f = Sediment metal content/Background metal content (1)

The evaluation of contamination of sediments by heavy metals is generally carried out by determining CF and CD. The sum of all contamination factors is used to calculate the contamination degree (Islam *et al*., 2015). Sediment quality is categorized according to CF and CD values represented in Table 3.

$$C_d = C_{f1} + C_{f2} + C_{f3} \quad (2)$$

Eventually, spatial analyst tools named the Inverse Distance Weighted Interpolation Techniques from GIS techniques were used to prepare the geospatial pollution vulnerability map of the study area.

Pollution load index

The PLI is a popular approach for determining the toxicity level of sediment. The succeeding formula was employed to calculate PLI using Eq. 3 (Islam *et al*., 2015).

$$PLI = (CF_1 \text{ X } CF_2 \text{ X } CF_3 \text{ X } \ldots \text{ X } CF_n)^{1/n}, \quad (3)$$

Where, CF denotes the contamination factor and n denotes the number of metals considered for the derivation of the resultant. PLI values greater than 1 indicate heavy metal pollution, whereas PLI values less than 1 indicate no pollution (Rakib *et al*., 2021).

RESULTS AND DISCUSSION

Heavy metal concentration

AAS instrument was used to analyse trace metal concentrations in sediments for the various season such as pre-monsoon, post-monsoon, and monsoon seasons, and Fig. 2 presents the results. It was revealed that the highest concentration as 3837 milligram per kilogram (mg/kg) and the lowest concentration (2275 mg/kg) of Fe were found in Station 5 at post-monsoon and Station 1 at pre-monsoon, respectively. The reason behind the higher concentration of Fe was due to lithogenic and detrital components in the sand. The experimental analysis shows that Mn levels were higher (68.1 mg/kg) at Station 5 during post-monsoon and lower (48.1 mg/kg) at Station 1 during the pre-monsoon. It is caused by the influence of industrial effluent and farming activities near the study area. The aforementioned sampling location recorded the highest (5.6 mg/kg) and lowest (4.4 mg/

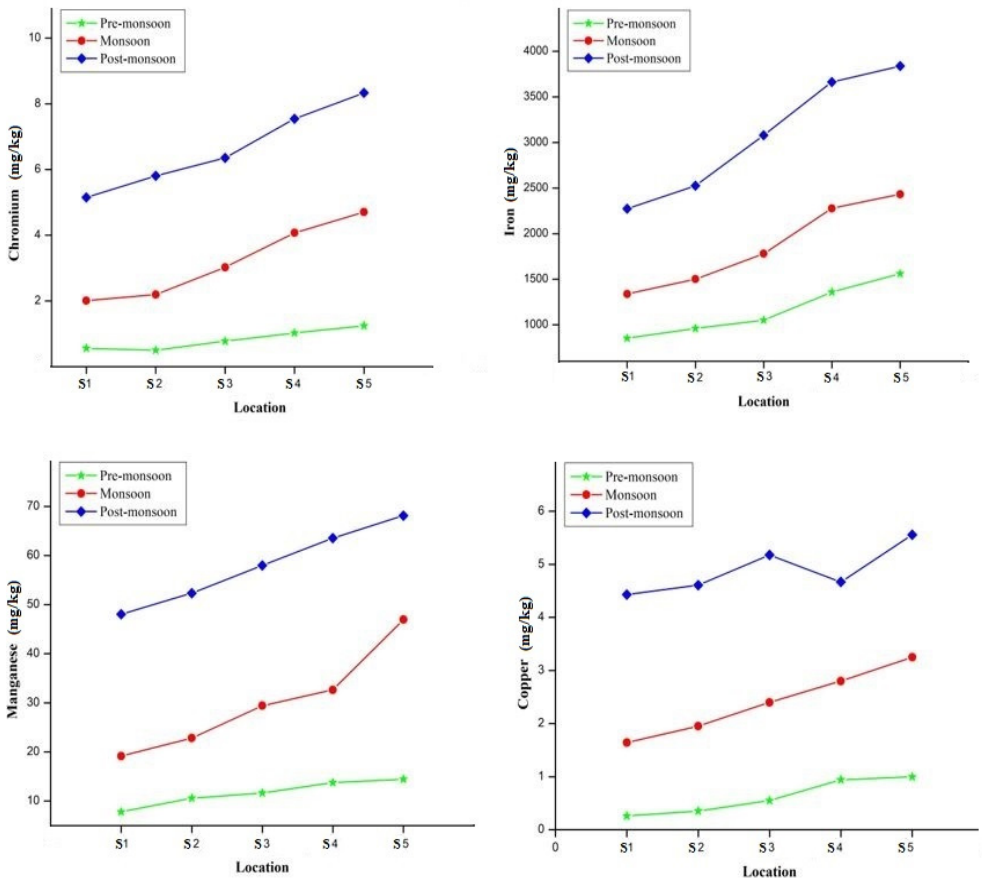

Fig. 2: Seasonal variation of Cr, Fe, Mn, and Cu in sediments

kg) concentration of Cu during post-monsoon and pre-monsoon respectively. Additionally, the highest (8.3 mg/kg) and lowest (5.2 mg/kg) concentrations of Cr were at Stations 5 and 2, respectively. All the heavy metal values are within the acceptable range, in comparison with Indian, European, and American standards.

In terms of the ratio of concentrations between pre-monsoon and post-monsoon, the result shows that Cr has the highest increase rate, which is 6.643, followed by Cu with a rate of 5.636. The other two heavy metals, i.e., Fe and Mn, showed mild increases of 2.456 and 4.696, respectively. The finer sediment deposits in the farthest downstream end and thus have higher adsorbed heavy metals. This becomes the reason for higher concentrations of heavy metals in the downstream and least in the upstream. In this study, Cr, Fe, Mn, and Cu all had significant correlation coefficients, indicating that they have closely associated origins and may be influenced by an exclusive factor. Cu had a strong positive relationship with Cr and Mn and, to a lesser extent, Fe. Heavy metals are present due to anthropogenic sources such as municipal and industrial wastewater, but agricultural wastewaters are the original sources of copper. Table 4 shows comparative concentrations of elements in Tamiraparani River sediments.

Spatial distribution analysis

GIS technology has been used in this study to understand the geospatial variation of heavy metals in sediments. A GIS-based kriging tool has been used to interpolate the heavy metals in sediments for analysing and developing spatial variation maps of the same at the study area. Fig. 3 depicts a spatial variation concentration map for various seasons. It was revealed that the concentrations increase from upstream to downstream and the dry season had

Table 4: Trace metal presence in Tamiraparani river sediment with statistical analysis (Bhaskar *et al*., 2016)

Data	Heavy metals (mg/kg)			
	Cr	Fe	Mn	Cu
Mean	3.6	2033.1	33.3	2.64
Deviation	2.92	970.2	23.3	2.2
Minimum	0.5	853	7.8	0.26
Maximum	8.3	3837	68.1	5.6
IRSA*	87	29000	605	28
WRSA*	100	48000	1050	100

*Indian river sediment average (IRSA); world's river sediment average (WRSA)

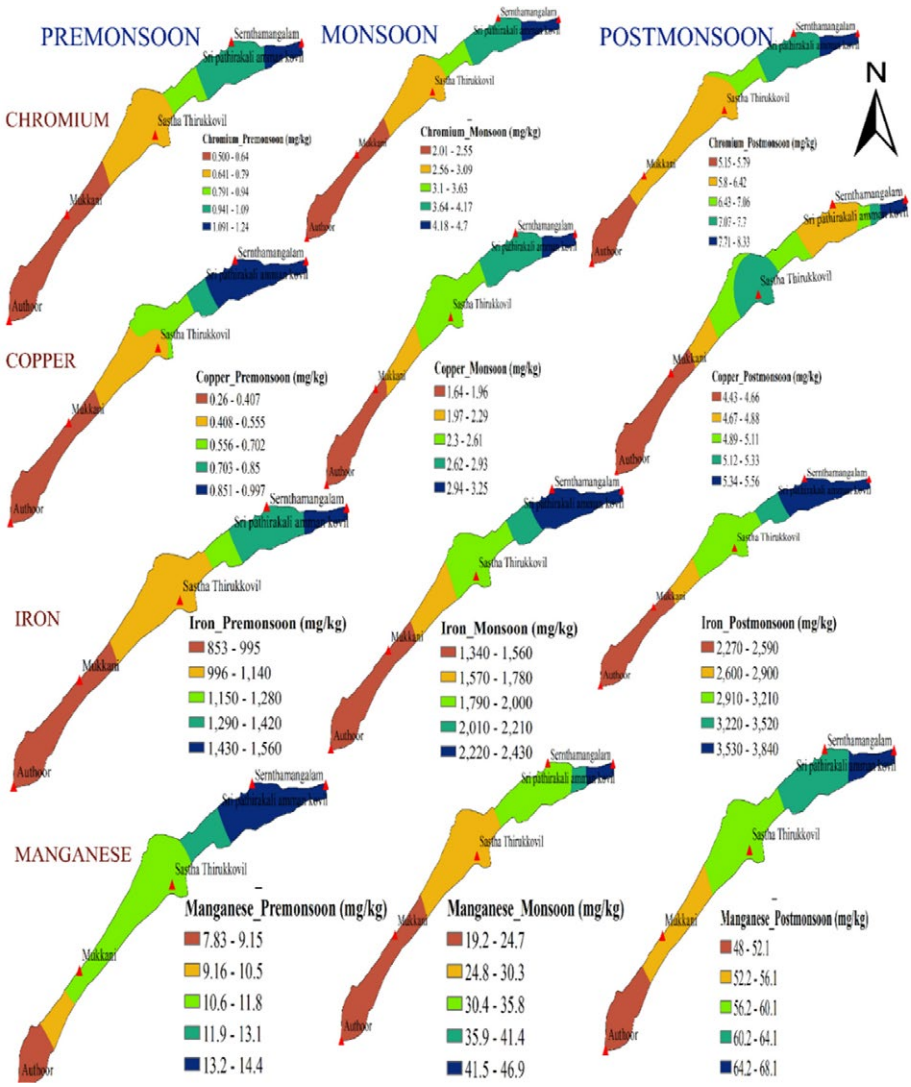

Fig. 3: Seasonal variations of heavy metals in sediments

Table 5: Contamination factor of collected samples during various seasons

Station number	Pre-monsoon				Monsoon				Post-monsoon			
	Cr	Mn	Fe	Cu	Cr	Mn	Fe	Cu	Cr	Mn	Fe	Cu
1	0.006	0.009	0.018	0.006	0.022	0.023	0.028	0.037	0.057	0.057	0.048	0.098
2	0.006	0.012	0.020	0.008	0.024	0.027	0.032	0.043	0.065	0.062	0.054	0.102
3	0.009	0.014	0.022	0.012	0.034	0.035	0.038	0.053	0.071	0.068	0.065	0.115
4	0.011	0.016	0.029	0.021	0.045	0.038	0.048	0.062	0.084	0.075	0.078	0.104
5	0.014	0.017	0.033	0.022	0.052	0.055	0.052	0.072	0.093	0.080	0.081	0.124

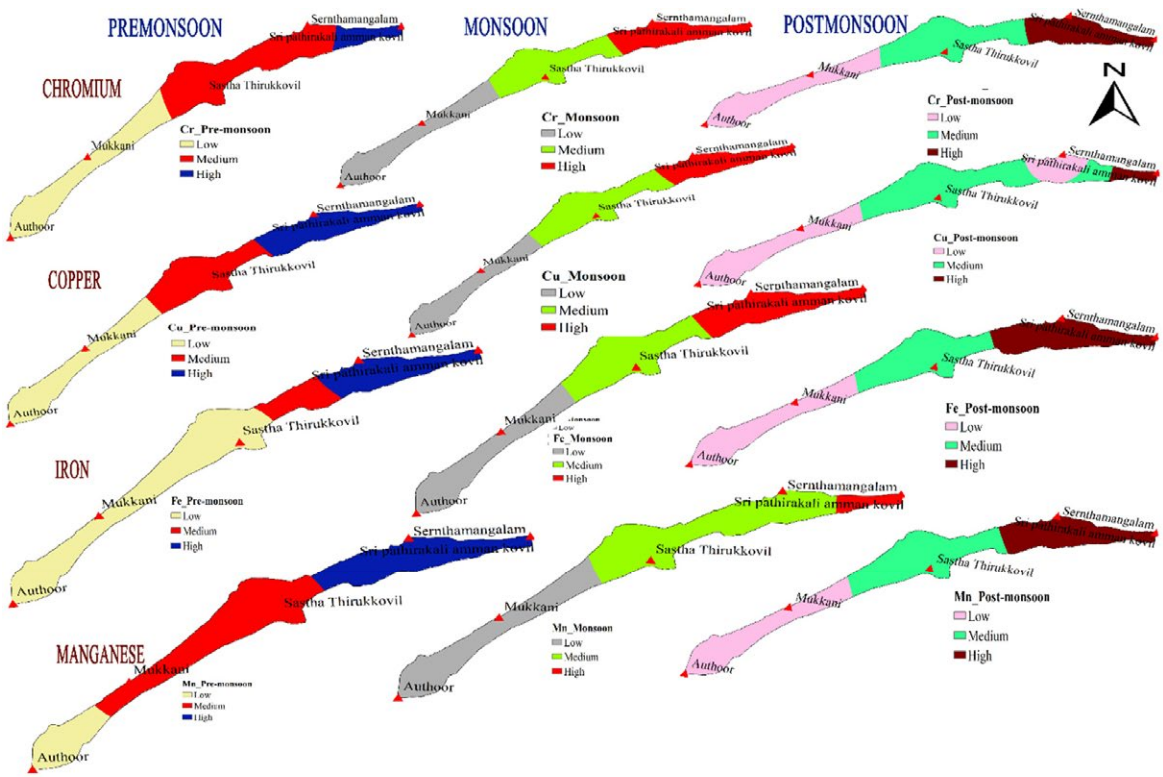

Fig. 4: Contamination factor of Cr, Cu, Fe, and Mn in sediments

the largest concentration, followed by the monsoon and pre-monsoon seasons. Furthermore, the figure revealed that all the heavy metals such as Fe, Cr, Cu, and Mn in the sediments have higher concentrations at the estuary of the river. It was also observed that the patterns are similar for all the metals in all the seasons. The least values are observed at Station 1 and average from Stations 2 to 4 and the maximum at Station 5. Generally, it was observed from the study that hydrodynamic conditions impact the spreading of heavy metals in the sediments downstream of the study area.

Contamination factor

C_f has been used to determine heavy metal concentrations in sediments. With the reference to CF-derived concentrations as shown in Table 5, the concentrations are less than 1. As per the study, C_f < 1 is considered no contamination (Aradpour *et al*., 2020).

The CF values for all the elements in the monsoon season ranged over the interval of 0.022–0.072. The highest value of 0.022 for Cu at Station 5 and the least value of 0.006 for Cr and Cu at Station 1 were detected in the pre-monsoon season. The maximum

value of 0.072 for Cu at Station 5 and the least value of 0.022 for Cr at Station 1 were observed in the monsoon season. The highest value of 0.124 for Cu at Station 5 and the least value of 0.048 for Fe at Station 1 were observed in the post-monsoon season. The CF for Cu is higher than the other elements in all the stations.

Additionally, Fig. 4 presents the CF on different heavy metals for various seasons. It was revealed from the figure that heavy metal concentration is increasing downstream in all three seasons. The post-monsoon season had higher heavy metal concentrations than the other two seasons due to higher deposition of heavy metals. It is also revealed that due to the disintegration of rocks and anthropogenic activities, downstream had higher trace metals accumulation in sediments.

Contamination degree

The contamination degree (C_d) is derived with reference to CF and depicted in Fig. 5. It was understood that the CD values for Cr, Mn, Fe, and Cu in all the studied locations are <6 and fall in the low pollution category. The maximum values of CD for all the heavy metals were observed at Sernthamangalam in the post-monsoon season, and the minimum values were recorded at Authoor in the pre-monsoon seasons.

All the stations in the pre-monsoon season revealed a low contamination degree. The maximum CD was observed in post-monsoon at Station 5. The highest value of 0.378 was observed at Station 5 in the post-monsoon season, and the lowest value of 0.039 at Station 1 was detected in the pre-monsoon season. The resultant was the same as downstream showing higher concentrations of heavy metals in post-monsoon than the rest of the season.

Fig. 6 shows the CD spatial variation map of the study area. This figure shows that the lowest CD was found at Stations 1 and 2, the medium CD was shown at Station 3, and the highest CD was identified at Stations 4 and 5, regardless of the season.

Pollution load index

Fig. 7 displays the PLI results for each sampling station. It was indicated that the heavy metals are increased in sediments during post-monsoon than in other seasons. However, the overall impact is less as per the guideline's values of PLI is less than 1 in sampling locations. The compaction factor, contamination degree, and PLI all show an increasing trend from pre-monsoon to post-monsoon through monsoon seasons. The reason behind this is that the sediments are lowered during pre-monsoon and start to increase in the flood of monsoon. Later in the post-monsoon, all the sediments started to settle down, which arrived freshly from the upstream of the Tamiraparani River.

Interpretation

This study intends to determine the presence of toxic metals in sediment through CF, CD, and PLI from downstream of the Tamiraparani River. As per Magesh *et al*. (2016), due to channel topography

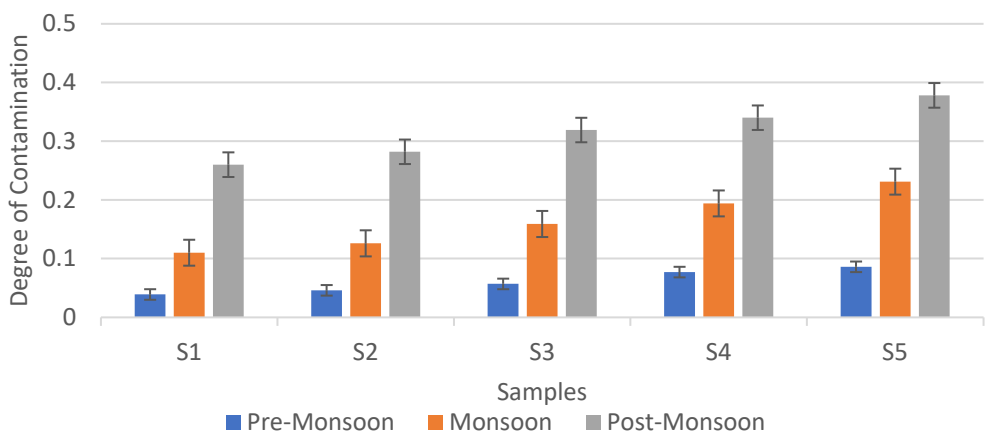

Fig. 5: Contamination degree in various seasons

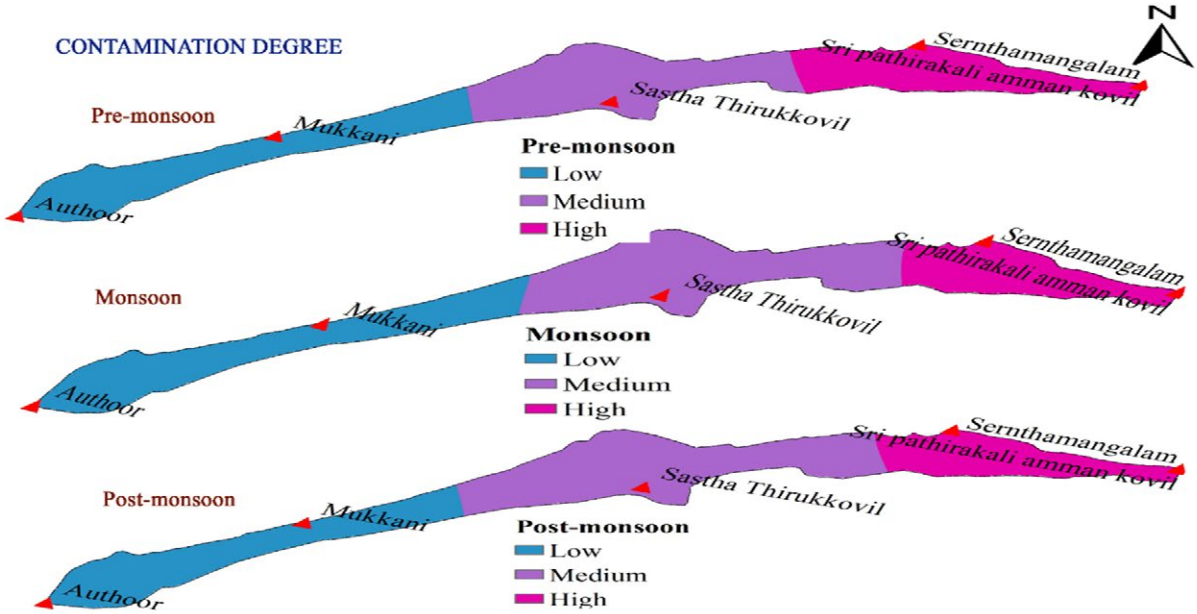

Fig. 6: Contamination degree in sediments during various seasons

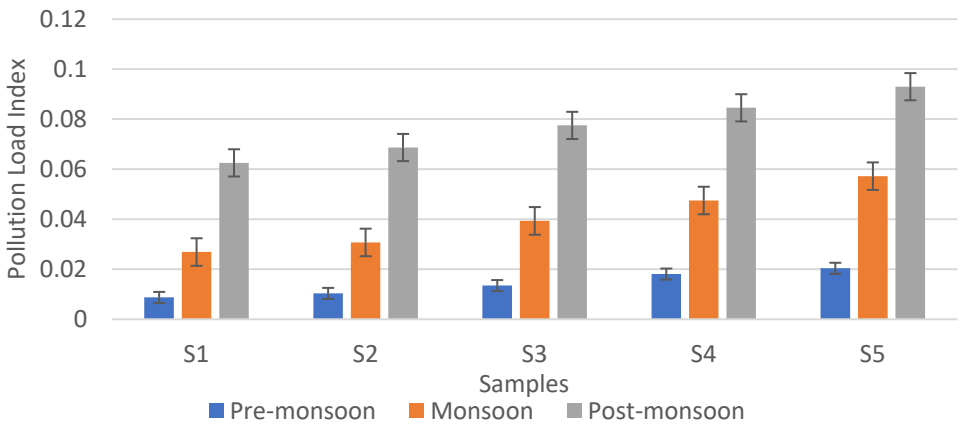

Fig. 7: Pollution load index in various seasons

and soil erodibility, the deposition of sediment is higher downstream of the study site. According to the derived contamination factor, in the study region, the highest index was 0.124 for Cu at Station 5. Magesh *et al*. (2017), in their study carried out in the Tamiraparani River, have identified that Cu concentration is contributed higher because it is rich in calcareous in nature and observed that the elevated lead (Pb) is due to port activities and nearby thermal power plant. Shanbehzadeh *et al*. (2014), in their study carried out in the same area, have determined the contamination factor specified as low to moderately contaminated except for CD at Tamiraparani River. The maximum concentrations of heavy metals such as Fe, Mn, Cu, and Cr were detected in sample areas amassed immediately downstream of the Station 5, where approximately 58% of the industrial activities are located, as well as the lower

portions of the river's Station 4 (Bhuyan *et al*., 2017). However, it was observed from another study, that higher concentrations of Cd and Pb were found in the downstream direction of the Tamiraparani River due to high pH, salinity, and anthropogenic pollution during the winter season (Silva *et al*., 2014). According to the research carried out by Feng *et al*. (2012), the pollution intensity determined using enrichment factor exhibited that Zn, Pb, and cadmium (Cd) were found at the estuary of Tamiraparani River due to unrestricted anthropogenic activities. The analysis revealed that heavy metal concentrations of Fe range from 853 to 3837 mg/kg in the study area, whereas the result obtained from the Benin River in Nigeria showed that the values range from 867.8 to 7195.0 mg/kg (Tao *et al*., 2012). Furthermore, Arisekar *et al*. (2020) from Nigeria completed their analysis of sediments in soil, in which they observed that Fe concentration is higher. Additionally, they revealed that a high quantum of chromium reaches rivers and streams mainly because of wastewater and metal-containing products in the river. The quantity of these metals is predicted to reveal long-term exposure of sediments to several activities, such as organic waste and the surrounding chemical plants. Tuticorin is well known for chemical-, fertilizer-, and mineral-based industries (Zhang *et al*., 2019). The release of industrial wastes from surrounding petrochemical and copper smelting industries into the river has amplified the concentration of these metals in sediments. Fertilizers, pesticides from agricultural activities, municipal sewage, and fly ash from nearby industries have worsened the problem (Ma *et al*., 2015). Heavy metal pollution endangers humans, fish, and vertebrates alike. Contaminants bioaccumulated in water and sediments and then biomagnified in aquatic animals, trying to pose a risk of certain cancers once they enter the food chain (Shafie *et al*., 2013). The above results show that the river sediments fall in the "Class 1—low contamination" zone. The concentration of copper is observed to be high downstream during the post-monsoon season. The values of C_f and C_d were low at Station 1 and high at Station 5. All stations in the present study recorded low CF, CD, and PLI for Cr, Mn, Fe, and Cu.

CONCLUSION

The study evaluated the heavy metal concentration from the sediments at the Tamiraparani River delta with the help of CF, CD, and PLI. The results show that there is the existence of heavy metals such as Cr, Cu, Fe, and Mn at a detectable level. These are the constitutes of various industrial, agricultural, and domestic sewage discharges. Cr concentration ranged from 0.5 to 8.3 mg/kg with a mean of 3.6 mg/kg, Fe concentration ranged from 853 to 3837 mg/kg with a mean of 2033.1 mg/kg, Mn concentration ranged from 7.8 to 68.1 mg/kg with a mean of 33.3 mg/kg, and Cu concentration ranged from 0.26 to 5.6 mg/kg with a mean of 2.64 mg/kg. All four metals are in an increasing trend between pre-monsoon and post-monsoon through monsoon seasons. This is due to the increase in lower sediment deposits in the prior and subsequent increase of sediment deposit in monsoon and post-monsoon. Spatially, the upstream sampling Station S1 experienced a lower concentration, and the downstream station S5 experienced the highest concentration indicating that the sedimentation rate had been increasing from the upstream to the downstream. CF and CD show that the study area lies in the low pollution category. However, there was an increasing trend of pollutants and should be checked in the early stage as a prevention measure. This increase was due to anthropogenic activities, industrial effluent discharge, agricultural discharge, and untreated sewage discharge in the rivers. Moreover, the PLI, which was less than 1, indicates the low impact of pollution in the deltaic region. However, naturally, copper concentration was higher in sediment throughout Tamiraparani River because of the higher deposits in the Agasthiyar hill ranges where the river originates; moreover, because the river is highly calcareous in nature, Fe was high at the estuary of the study area due to lithogenic and anthropogenic activities along the river. With the reference to the field investigation, the major heavy metal pollutants identified were from industries, sand mining activities, agricultural runoff, and untreated sewage wastewater. Aside from the abovementioned reasons, soil erosion and flooding also transport heavy metals from upstream to downstream. To understand the increasing pattern of heavy metal concentration, the study recommended temporal monitoring of the pollution concentrations at the river to refrain from the activities influencing or increasing the concentration level in the study area. The need for the study is to identify the analysis of heavy metals due to their toxicity effect on the ecosystem,

especially due to the impact of industries and urbanization around the river banks. Spatiotemporal analysis downstream is focused due to higher deposits of sediments in the floodplain delta. The study is considered essential as per the Water Act 1974 to prevent and control water pollution at the river. Additionally, the identified higher concentration stations should be observed closely by government authorities such as the District Collectorate Office and municipal corporations to impose legal actions against default polluters to avoid pollution in the study area. Heavy metal controlling and monitoring activities are required in the study region because of metal bioaccumulation characteristics and the potentially harmful effects of long-term exposure to biota and humans. Illegal discharges into the river system should be closely monitored to protect the river ecosystem, and wastewater from industries, municipalities, and households should be treated before being discharged into the river. The findings could serve as a basis for the predictions of human-induced effects, which could be used to examine and define an effective management decision policy to reduce heavy metal contamination.

AUTHOR CONTRIBUTIONS

J.D. Reymond performed the literature review and analysed and interpreted the data. K. Sudalaimuthu prepared the manuscript text and manuscript edition.

ACKNOWLEDGEMENT

The authors thank the head of the Department of Civil Engineering, SRM Institute of Science and Technology (SRMIST), Kattankulathur, Chengalpattu, Tamil Nadu, India, and the Management of SRMIST for providing the opportunity to carry out this extensive research work.

CONFLICT OF INTEREST

The authors declare no potential conflict of interest regarding the publication of this work. Additionally, the ethical issues including plagiarism, informed consent, misconduct, data fabrication and/or falsification, double publication and/or submission, and redundancy have been completely addressed by the authors.

OPEN ACCESS

PUBLISHER'S NOTE

ABBREVIATIONS

°C	Degree Celsius
C_d	Degree of contamination
C_f	Contamination factor
%	Percentage
µm	Micrometre
AAS	Atomic absorption spectrophotometer
ArcGIS	Aeronautical reconnaissance coverage geographic information system
CD	Degree of contamination
Cd	Cadmium
CF	Contamination factor
Cr	Chromium
Cu	Copper
Fe	Iron (Ferrous)
g	Gram
GFAAS	Graphite furnace atomic absorption spectroscopy
GIS	Geographical information system
GPS	Global positioning system
h	Hours

ICP-OES	Inductively coupled plasma - optical emission spectrometry
IRSA	Indian river sediment average
kg	Kilogram
km	Kilometre
km	Kilometre
km^2	Square kilometre
mg	Milligram
mL	Millilitre
mm	Millimetre
Mn	Manganese
Pb	Lead
PLI	Pollution load index
WRSA	Worlds River sediment average
Zn	Zinc

REFERENCES

Annammala, K.V.; Mohamad, N.A.; Sugumaran, D.; Masilamani, L.S.; Liang, Y.Q.; Jamal, M.H.; Yusop, Z.; Yusoff, A.R.M.; Nainar, A., (2021). Sediment clues in flood mitigation: the key to determining the origin, transport, and degree of heavy metal contamination. Hydrol. Res., 52(1): 91–106 **(16 pages).**

Aradpour, S.; Noori, R.; Tang, Q.; Bhattarai, R.; Hooshyaripor, F.; Hosseinzadeh, M.; Haghighi, A.T.; Klove, B., (2020). Metal contamination assessment in water column and surface sediments of a warm monomictic man-made lake: Sabalan dam reservoir, Iran. Hydrol. Res., 51(4): 799–814 **(16 pages).**

Arisekar, U.; Shakila, R.J.; Shalini, R.; Jeyasekaran, G., (2020). Human health risk assessment of heavy metals in aquatic sediments and freshwater fish caught from Thamirabarani River, the western ghats of south Tamil Nadu. Mar. Pollut. Bull., 159(111496): 1-10 **(10 pages).**

Bai, Y.R.; Abbs Fen Reji, T.F., (2015). Sediment quality of Tamiraparani River in Kanyakumari district. J. Saudi Chem. Soc., 19(2): 142–146 **(5 pages).**

Bhaskar, J.; Saikia, G.; Parthasarathy, R.; Borah, R.; Borthakur., (2016). Raman and FTIR spectroscopic evaluation of clay minerals and estimation of metal contaminations in natural deposition of surface sediments from Brahmaputra River. Int. J. Geosci., 7: 873–883 **(11 pages).**

Bhuyan, M.S.; Bakar, M.A., (2017). Seasonal variation of heavy metals in water and sediments in the Halda River, Chittagong, Bangladesh. Environ. Sci. Pollut. Res., 24(35): 27587–27600 **(14 pages)**.

Brady, J.P.; Ayoko, G.A.; Martens, W.N.; Goonetilleke, A., (2015). Development of a hybrid pollution index for heavy metals in marine and estuarine sediments. Environ. Monit. Assess., 187 (5): 1-14 **(14 pages)**.

Chen, B.; Liang, X.; Xu, W.; Huang, X.; Li, X., (2012). The changes in trace metal contamination over the last decade in surface sediments of the Pearl River estuary south China. Sci. Total. Environ., 439: 141–149 **(9 pages).**

Feng, S.; Zhang, N.; Liu, H.; Du, X.; Liu, Y., (2012). Comprehensive analysis of heavy metals in sediments contaminated by different pollutants. J. Environ. Eng., 138(4): 483–489 **(7 pages).**

Guo, Y.; Yang, S., (2016). Heavy metal enrichments in the Changjiang (Yangtze River) catchment and on the inner shelf of the East China Sea over the last 150 years. Sci. Total. Environ., 543: 105–115 **(11 pages).**

Hu, B.; Cui, R.; Li, J.; Wei, H.; Zhao, J.; Bai, F.; Song, W.; Ding, X., (2013). Occurrence and distribution of heavy metals in surface sediments of the Changhua River estuary and adjacent shelf (Hainan Island). Mar. Pollut. Bull., 76 (1–2): 400–405 **(6 pages)**.

Islam, M.S.; Ahmed, M.K.; Raknuzzaman, M.; Habibullah-Al-Mamun, M.; Islam, M.K., (2015). Heavy metal pollution in surface water and sediment: A preliminary assessment of an urban river in a developing country. Ecol. Indic., 48: 282–291 **(10 pages)**.

Jaishankar, M.; Tseten, T.; Anbalagan, N.; Mathew, B.B.; Beeregowda, K.N., (2014). Toxicity, mechanism and health effects of some heavy metals. Interdiscip. Toxicol., 7: 60–72 **(13 pages)**.

Khorasani, N., (2013). Evaluating the metallic pollution of riverine water and sediments: a case study of Aras River. Environ. Monit. Assess., 18(5): 197-203 **(7 pages)**.

Kuchelar, P.; Ramesh, S.B.; Sudhir, S.; Kaliaperumal Sugirthamani, A., (2022). Assessment of groundwater quality around the Pallavaram urban solid waste dumpsite using GIS. Environ. Qual. Manage., 32(1): 265–277 **(13 pages)**.

Kumar, R.N.; Solanki, R.; Kumar, J.I.N., (2013). Seasonal variation in heavy metal contamination in water and sediments of river Sabarmati and Kharicut canal at Ahmedabad, Gujarat. Environ. Monit. Assess., 185(1): 359–368 **(10 pages)**.

Ma, Y.; Qin, Y.; Zheng, B.; Zhang, L.; Zhao, Y., (2015). Seasonal variation of enrichment, accumulation and sources of heavy metals in suspended particulate matter and surface sediments in the Daliao river and Daliao River estuary, Northeast China. Environ. Earth Sci., 73(9): 5107–5117 **(11 pages)**.

Magesh, N.S.; Chandrasekar, N., (2014). GIS model-based morphometric evaluation of Tamiraparani subbasin, Tirunelveli district, Tamil Nadu, India. Arabian J. Geosci., 7(1): 131–141 **(11 pages)**.

Magesh, N.S.; Chandrasekar, N., (2016). Assessment of soil erosion and sediment yield in the Tamiraparani sub-basin, south India, using an automated RUSLE-SY model. Environ. Earth Sci., 75(1208): 1-17 **(17 pages).**

Magesh, N.S.; Chandrasekar, N.; Krishnakumar, S.; Simon Peter, T., (2017). Trace element contamination in the nearshore sediments of the Tamiraparani estuary, Southeast coast of India. Mar. Pollut. Bull., 116(1–2): 508–516 **(9 pages)**.

Michael, M.; Meyyazhagan, A.; Velayudhannair, K.; Pappuswamy, M.; Maria, A.; Xavier, V.; Balasubramanian, B.; Baskaran, R.; Kamyab, H.; Vasseghian, Y.; Chelliapan, S.; Safa, M.; Moradi, Z.; Khadimallah, M.A., (2022). The Content of Heavy Metals in Cigarettes and the Impact of Their Leachates on the Aquatic Ecosystem. Sustainability. 14(8): 4752 **(13 pages)**.

Mukesh, M.V.; Chandrasekaran, A.; Premkumar, R.; Keerthi, B.N., (2018). Metal enrichment and contamination in river and estuary sediments of Tamirabarani, South India. J. Earth Sci. Clim. Change. 9(10): 1–6 **(6 pages)**.

Nayagam, J.; Reymond, J.; Somasundaram, R., (2019).

Environmental assessment of marine and estuarine waters along the coast of Thoothukudi city. Int. J. Eng. Adv. Technol., 8: 934–938 **(5 pages)**.

Okedeyi, O.O.; Dube, S.; Awofolu, O.R.; Nindi, M.M., (2014). Assessing the enrichment of heavy metals in surface soil and plant (Digitaria eriantha) around coal-fired power plants in South Africa. Environ. Sci. Pollut. Res., 21(6): 4686–4696 **(11 pages)**.

Pandey, M.; Pandey, A.K.; Mishra, A.; Tripathi, B.D., (2015). Assessment of metal species in river Ganga sediment at Varanasi, India using sequential extraction procedure and SEM–EDS. Chemo., 134: 466–474 **(9 pages)**.

Perumal, K.; Antony, J.; Muthuramalingam, S., (2021). Heavy metal pollutants and their spatial distribution in surface sediments from Thondi coast, Palk Bay, South India. Environ. Sci. Eur., 33(1): 1–20 **(20 pages)**.

Rakib, R.J.; Hossain, M.B.; Jolly, Y.N.; Akther, S.; Islam, S., (2021). EDXRF detection of trace elements in salt marsh sediment of Bangladesh and probabilistic ecological risk assessment. Soil Sediment Contam., 30(2): 220–239 **(20 pages)**.

Ramesh, S.; Nagalakshmi, R., (2022). Influence of COVID-19 on microplastics pollution in coastal water and sediment of Chennai, India. Lect. Notes Civ. Eng., 191: 547–563 **(17 pages)**.

Reymond, J.; Sudalaimuthu, K., (2021). Water quality during pre-monsoon and post monsoon and modelling of total dissolved solids for Tamiraparani river, Tamilnadu, India. Rasayan. J. Chem., 14(3): 1910–1919 **(10 pages)**.

Said, I.; Salman, S.A.; Elnazer, A.A., (2019). Multivariate statistics and contamination factor to identify trace elements pollution in soil around Gerga City, Egypt. Bull. Natl. Res. Cent., 43: 1–6 **(6 pages)**.

Shafie, N.A.; Aris, A.Z.; Zakaria, M.P.; Haris, H.; Lim, W.Y.; Isa, N.M., (2013). Application of geo-accumulation index and enrichment factors on the assessment of heavy metal pollution in the sediments. J. Environ. Sci. Health. Part A Toxic/Hazard. Subst. Environ. Eng., 48(2): 182–190 **(9 pages)**.

Shanbehzadeh, S.; Vahid Dastjerdi, M.; Hassanzadeh, A.; Kiyanizadeh, T., (2014). Heavy metals in water and sediment: A case study of Tembi River. J. Environ. Public Health. 2014: 1–5 **(5 pages)**.

Silva, J.D.; Srinivasalu, S.; Roy, P.D.; Jonathan, M.P., (2014). Environmental conditions inferred from multi-element concentrations in sediments off Cauvery delta, Southeast India. Environ. Earth Sci., 71(5): 2043–2058 **(16 pages)**.

Singh, H.; Pandey, R.; Sudhir Singh, K.; Shukla, D.N., (2017). Assessment of heavy metal contamination in the sediment of the river Ghaghara, a major tributary of the river Ganga in Northern India. Appl. Water Sci., 7(7): 4133–4149 **(17 pages)**.

Skordas, K.; Kelepertzis, E.; Kosmidis, D.; Panagiotaki, P.; Vafidis, D., (2015). Assessment of nutrients and heavy metals in the surface sediments of the artificially lake water reservoir Karla, Thessaly, Greece. Environ. Earth. Sci., 73: 4483 - 4493 **(11 pages)**.

Sojka, M.; Siepak, M.; Jaskuła, J.; Wicher-Dysarz, J., (2018). Heavy metal transport in a river-reservoir system: A case study from central Poland. Pol. J. Environ. Stud., 27: 1725–1734 **(10 pages)**.

Tao, Y.; Zhang, Y.; Meng, W.; Hu, X., (2012). Characterization of heavy metals in water and sediments in Taihu Lake, China. Environ. Monit. Assess., 184(7): 4367–4382 **(16 pages)**.

Vaezi, A.R.; Karbassi, A.R.; Fakhraee, M.; Valikhani Samani, A.R.; Heidari, M., (2014). Assessment of sources and concentration of metal contaminants in marine sediments of musa estuary of Persian Gulf. J. Environ. Stud., 40(2): 345-360 **(16 pages).**

Vaezi, A.; Karbassi, A.R.; Valavi, S.; Ganjali, M.R., (2015). Ecological risk assessment of metals contamination in the sediment of the Bamdezh wetland, Iran. Int. J. Environ. Sci. Technol., 12(3): 951-958 **(8 pages)**.

Zhang, Q.; Han, G.; Liu, M.; Liang, T., (2019). Spatial distribution and controlling factors of heavy metals in soils from Puding karst critical zone observatory, Southwest China. Environ. Earth Sci., 78(9): 1–13 **(13 pages)**.

AUTHOR (S) BIOSKETCHES

Justus Reymond, D., Ph.D. Candidate, Department of Civil Engineering, SRM Institute of Science and Technology, Kattankulathur, Chengalpattu, Tamil Nadu, India.
- Email: *justusrd@srmist.edu.in*
- ORCID: 0000-0001-7680-8741
- Web of Science ResearcherID: GLR-2138-2022
- Scopus Author ID: 57191254384
- Homepage: https://www.srmist.edu.in/faculty/mr-d-justus-reymond/

Sudalaimuthu, K., Ph.D., Associate Professor, Department of Civil Engineering, SRM Institute of Science and Technology, Kattankulathur, Chengalpattu, Tamil Nadu, India.
- Email *karuppas@srmist.edu.in*
- ORCID: 0000-0001-6612-6763
- Web of Science ResearcherID: AAW-4904-2021
- Scopus Author ID: 57209618364
- Homepage: https://www.srmist.edu.in/faculty/dr-s-karuppasamy/

HOW TO CITE THIS ARTICLE

Justus Reymond, D.; Sudalaimuthu, K., (2023). Geospatial visualization and seasonal variation of heavy metals in river sediments. Global J. Environ. Sci. Manage., 9(2): 309-322.

DOI: 10.22034/gjesm.2023.02.10

url: https://www.gjesm.net/article_696644.html

Global J. Environ. Sci. Manage. 9(2): 323-336, Spring 2023, Serial #34

Global Journal of Environmental Science and Management
(GJESM)

Homepage: https://www.gjesm.net/

ORIGINAL RESEARCH ARTICLE

Heavy metals concentration in the sediment of the aquaticenvironment caused by the leachate discharge from a landfill

L. Sulistyowati[1,*], N. Nurhasanah[1], E. Riani[2], M.R. Cordova[3]

[1] *Environmental Studies Graduate Program, Universitas Terbuka, Jl, Pamulang Tangerang Selatan, Indonesia*

[2] *Department of Aquatic Resources Management, Faculty of Fishery and Marine Science, Bogor Agricultural University, Bogor, Indonesia*

[3] *Research Center for Oceanography, National Research and Innovation Agency Republic of Indonesia, BRIN Kawasan Jakarta Ancol, Jl, Jakarta, Indonesia*

ARTICLE INFO

Article History:
Received 16 June 2022
Revised 24 August 2022
Accepted 29 September 2022

Keywords:
Cadmium (Cd)
Chromium (Cr)
Cisadane River
Lead (Pb)
Sediment
Indonesia

DOI: 10.22034/gjesm.2023.02.11

ABSTRACT

BACKGROUND AND OBJECTIVES: Heavy metals are categorized as hazardous pollutants due to their incapability in decomposing and undergoing bioaccumulation and biomagnification. Heavy metal pollution is a global issue, particularly in emerging nations such as Indonesia. In this case, sediments contribute to pollution dispersion because they can transport, mobilize, and redistribute toxic compounds. The Cisadane river is one of 15 watersheds in Indonesia with the highest restoration priority. Therefore, it is essential to conduct study on the sediment quality of this river. This investigation aimed to evaluate the levels of cadmium, chromium, and lead in the sediments to assess the conditions of the Cisadane River.
METHODS: At eight stations (representing the midstream and downstream region), surface sediment samples were collected using a van Veen sediment grab based on the hypothesis that heavy metal pollution originated from land-based activities and migrated down river estuaries. The Thermo Scientific iCAP 7400 was utilized to assess heavy metals (cadmium, chromium, and lead) by adopting prior research methodologies and method guidelines.
FINDINGS: Except for lead, which surpassed the interim sediment quality standard, the levels of heavy metals observed in the midstream and downstream sections of the Cisadane River were found to be well below the guideline level. In this case, lead was the metal with the highest concentration in the sediments of the Cisadane River, followed by chromium and cadmium. The enrichment of heavy metals in river sediments was most likely caused by soil leaching, municipal and industrial sewage, as well as land waste disposal. After the landfill area, there were two areas with the highest concentration. Therefore, this investigation indicated the existence of landfills as point sources of heavy metals. Regarding specifics, two sites following the landfill constitute the apex of heavy metal amplification.
CONCLUSION: This analysis shows that the sediment's cadmium, chromium, and lead contents are below the standards' threshold and safe for the habitat. Cadmium, chromium and lead exceed sediment quality requirements in sample sites after landfills, assumed to be due to leachate discharge and landfill activities. This study further also reveals that landfills are point sources of heavy metals. In this case, the heavy metals are two to four times higher in one kilometer from the landfill's leachate discharge. Therefore, the Enforcement of the Indonesia Waste Law Number 18 Year 2008 would have replaced unsanitary dumping including implementation of physicochemical, biological, and combination remediation techniques, with a vastly superior waste management system.

NUMBER OF REFERENCES	NUMBER OF FIGURES	NUMBER OF TABLES
96	3	2

*Corresponding Author:
Email: *liliks@ecampus.ut.ac.id*
Phone: +62217490941
ORCID: 0000-0002-2200-1157

Note: Discussion period for this manuscript open until July 1, 2023 on GJESM website at the "Show Article".

INTRODUCTION

The persistence and toxicity of heavy metals in waterways have sparked global alarm (Islam *et al.*, 2015). The rapid global population growth, which has led to a rise in agricultural and industrial activity, is regarded as a significant source of metal pollution in aquatic environment, which may offer deadly health dangers to humans and wildlife (Riani *et al.*, 2014, 2018; Xie *et al.*, 2022). The improper management of industrial and domestic waste contributes to the environmental problem of heavy metals in emerging nations, including Indonesia. Heavy metals are hazardous pollutants because such pollutant cannot be decomposed, accumulates in the body (bioaccumulation), and gradually moves up the food chain to higher concentrations (biomagnification) (Ali and Khan, 2019; Saher and Siddiqui, 2019; Vandecasteele *et al.*, 2004). Environmental pollution occurs when a contaminant, including heavy metals, enters the environment and surpasses the tolerance level to be disruptive to the environment and dangerous to living beings (Mohammed *et al.*, 2011; Rosado *et al.*, 2016). Among the various types of heavy metals, some are toxic, including cadmium (Cd), chromium (Cr) and lead (Pb), which are also classified as harmful heavy metals by the Agency for Toxic Substances and Disease Registry (ATSDR, 2012). People often use Cd, Cr, and Pb as raw materials for making furniture, as coating materials for toolkits, as mixtures of metallic ingredients and antifouling colorants, as well as in agriculture (Ayangbenro and Babalola, 2017; Burton *et al.*, 2005a; Burton *et al.*, 2005b; Li and Ren, 2011; Liu *et al.*, 2016). By measuring the heavy metal concentrations directly and estimating what has accumulated in the environment, specifically in sediments, therefore, it is possible to determine the degree of heavy metal contamination (Kaewtubtim *et al.*, 2016). Sediments have a role in dispersing pollution because they can carry, mobilize, and redistribute harmful substances (Miranda *et al.*, 2021). Although heavy metals can be deposited in sediments after being absorbed by suspended materials and amassing to high concentrations, this retention is not permanent, and the metals may be released if the surrounding environment changes (Custodio *et al.*, 2020). United States Environmental Protection Agency (USEPA, 2005) stated heavy metals' sorption is influenced by several conditions, including pH, alkalinity, and fractions of clay-silicate and exchangeable carbonate. Frequently, heavy metal contamination in the sediments is evaluated by calculating their total metal content; where differences in metal levels along the watershed may indicate distinct metal input sources (Pagnanelli *et al.*, 2004). Measuring the overall concentration of metals in sediments is beneficial for detecting anomalies in the watercourse caused by several conceivable events, exempli gratia (e.g.) leaching from or to groundwater, erosion, sedimentation event; however, it does not reveal the chemical pattern of metals in sediments (Pagnanelli *et al.*, 2004). Understanding heavy metals partitioning among different geochemical phases is crucial to evaluate the potential of bioavailable materials and related ecotoxicity hazards (Dixit *et al.*, 2015; Kalender and Çiçek Uçar, 2013). Previous research has revealed that non-point source pollution (such as scattered residential and industrial activities) and point source pollution in the study area are responsible for various geographical and temporal distributions of hazardous pollutants in sediments (such as landfills in the Cisadane watershed). A landfill is a place where hazardous waste, such as exhaust gas emissions and liquid waste through leachate, is deposited (Roudi *et al.*, 2020). Waste and pollution from landfills can infiltrate the aquatic environment because landfills are typically situated on the banks of river regions. Due to a lack of technological advances and infrastructure, waste disposal and treatment are especially problematic in developing nations (Essien *et al.*, 2022). In Indonesia, the waste management system is poor, and there are almost no landfills with proper liner bottoms. Toxic leachates could contaminate soil and groundwater through non-sanitary landfills, which are the norm in Indonesia (Meidiana and Gamse, 2010; Munawar *et al.*, 2018). Consequently, detecting and characterizing the ecotoxicological profile of heavy metals in the environment affected by landfill leachate and the accompanying health hazards posed by municipal dumpsites is of utmost importance. Rivers are essential to life, serving as potable water sources, transportation routes, recreational spaces, and agricultural irrigation water. Introducing pollutants such as heavy metals into rivers will disturb the river's ecosystem. Indonesia has about 5,500 major rivers and over 65,000 tributaries; however, over 50% of the rivers are contaminated (Statistic Indonesia, 2021). The Cisadane River is one of 15 Indonesian watersheds with the highest restoration priority. Same as other rivers, the Cisadane river provides raw water for drinking water,

food production, sanitation, purification, and coastal stabilization, among other essential uses. Research on heavy metals such as Cd, Cr and Pb in the Cisadane River is crucial, given that the river serves as a source of raw water for the potable water delivery systems in the midstream (South Tangerang, Tangerang) and downstream (Tangerang, and Tangerang Regency) areas. In addition to being surrounded by various anthropogenic activities (settlement, agriculture, and industry), the Cisadane River is a home to three final disposal sites for the inhabitants of this region. Even as recently as May 2020, one of the landfill walls collapsed, resulting in the release of approximately 100 tons of waste into the Cisadane River (The Jakarta Post, 2020). It resulted in an immediate release of waste material, including heavy metals, which ultimately deposited in the sediment of the Cisadane River. Population growth and human activity along the river's flow made it possible for metal pollutants to get into the river. These pollutants then followed the river's flow downstream and into the sea. Therefore, this study was conducted based on the hypothesis that the increase in toxic metals in the Cisadane River was linked to anthropogenic activities in the area, namely non-point sources (scattered household, commercial, and industrial activities) and point sources (two landfills on the edge of Cisadane River). The hypothesis provided was that there was a significant difference between the two types of sources, which made point sources more likely to influence the accumulation of toxic heavy metals in river sediments. The above background shows that enriching the comprehension of toxic heavy metals (Cd, Cr, and Pb) contamination in urban river sediment to build realistic ways and strategies for mitigating the conflicting effects of heavy metals contamination on the aquatic ecosystem is necessary. In this case, the current study aimed to measure Cd, Cr, and Pb levels in the riverine sediments and to evaluate the river conditions based on specific heavy metal concentrations. Furthermore, this study was conducted on the Cisadane River in Indonesia during the dry season (April-May) of 2022.

MATERIALS AND METHODS

Study area

The Cisadane River is 138 miles long and covers an area of 154,652 hectare (ha). Due to its high pace of land change, the Cisadane watershed is among Indonesia's 15 priority watersheds. Between 1995 and 2012, the land cover changed by 63.05%. The most changes happened in bushland, forests, and rice fields by 29.65%, 27.87%, and 13.44%, respectively. The distance between the river and the city's downtown area is primarily responsible for this disparity. The city downtown offers convenient and essential services, enabling the expansion of settlements and the fulfillment of other community demands. The Cisadane River receives water from the Gede-Pangrango and Halimun-Salak mountains upstream and empties into the Teluk Naga coast in the Java Sea. Furthermore, the Cisadane River passes through 44 sub-districts in five cities. These cities are Bogor Regency and Bogor City in the upstream area, South Tangerang and Tangerang City in the midstream, and Tangerang Regency in the downstream area. In this case, more than 15 million people reside in the Cisadane watershed, contributing over 8,400 tons of solid waste daily. In this watershed, however, three landfills are located directly on the Cisadane River: the Galuga Landfill in Bogor Regency, the Cipeucang Landfill in South Tangerang, and the Rawa Kucing Landfill in Tangerang City. The leachate water from the three landfills drains to the Cisadane River via a canal. In addition, the Cisadane River supplies tap water sources for the midstream and downstream regions.

Field sampling

At eight stations sampling (ST), a van Veen sediment grab was used to acquire samples of surface sediment under the assumption that heavy metal pollution originated from land-based activities and migrated down river estuaries into the ocean, such as industry, mining, and agriculture (Koesmawati *et al.*, 2018; Lestari *et al.*, 2018; Riani *et al.*, 2014). The first four stations (ST01-4) represent the midstream region, whereas the subsequent four stations (ST05-ST08) represent the downstream region (Fig. 1). The two stations were situated 1 kilometer (km) before and after the two landfill sites (Cipeucang and Rawa Kucing Landfill) and the leachate disposal sites from the two landfills. The samples were collected from three spots on the river's right, middle, and left sides. Using a clean plastic spoon, the top layer of sediment; ~10 centimeter (cm) from each sediment grab sample was collected, and the sediments were mixed to generate a composite sample. In stainless steel canisters, triplicate sediment samples were

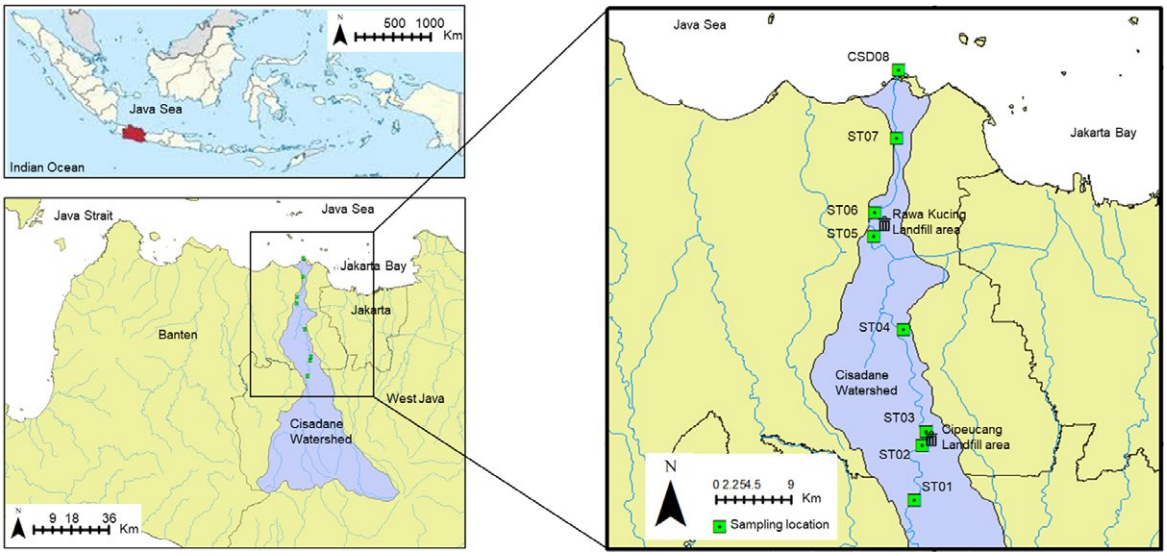

Fig. 1: Geographic location of the study area along with sampling locations at Cisadane River, Indonesia

homogenized. The samples were then scooped using a rinsed plastic scoop and transferred to a 500 milliliter (mL) cleaned and rinsed glass canister. Furthermore, all samples were preserved at 4±2 degree Celsius (°C) in sealed plastic containers to prevent contamination.

Laboratory analysis and quality assurance/quality control

The Thermo Scientific iCAP 7400 Inductively Coupled Plasma – Optical Emission Spectrometry (ICP-OES) was used to analyze heavy metals by accommodating the USEPA (2007) method 3051a from prior research (Cordova *et al.*, 2017; da Silva *et al.*, 2013; Harmesa and Cordova, 2020; Puspitasari *et al.*, 2020; Puspitasari and Lestari, 2018; Riani *et al.*, 2018). Briefly, the river surface sediment samples were dried in an oven at 105°C for twenty-four hours. The objective of the drying process was to eliminate the moisture. A mortar was further used to grind the dried samples. The grinded samples (range 0.49-0.51 gram) were then mixed with 9 mL of nitric acid (HNO_3 or Hydrogen nitrate) and 3 mL of Hydrochloric acid (HCl or Hydrogen chloride). Complex organometallic compounds were converted to inorganic compounds through the treatment of HNO_3 and HCl. The sample was then being placed in a the CEM MARS5 Xpress microwave digestive reactor for 15 minutes at 185°C and kept for 30 minutes. The samples were filtered using Whatman filter paper No. 41 and diluted to 25 mL with DDDW (Double Distilled Deionized Water). The sample was subsequently introduced to the ICP-OES to determine the concentrations of selected heavy metals. The National Research Council of Canada's Certified Reference Material (CRM) PACS-3 for sediments was utilized to verify that the instruments and procedures were reliable and controlled. The sample analysis of CRM was still within the standard range, indicating that the method and ICP-OES utilized in this study were valid and regulated.

Data analysis

The statistical test was conducted using PAST Software Version 4.03, which included examining univariate statistics and assessing statistical significance differences between Cd, Cr, and Pb for each sampling region via the Kruskal-Wallis test for equal medians and Mann-Whitney pairwise post hoc test. Due to the absence of sediment quality guidelines in Indonesia, a descriptive analysis of the mean and standard deviation of Cd, Cr, and Pb concentrations in riverine sediments was performed and compared to sediment quality guidelines from the Australia New Zealand Environment and Conservation Council (ANZECC) and Agriculture and Resource Management Council of Australia and New Zealand (ARMCANZ), as well as Canadian Council of Ministers of the Environment (CCME). Using the

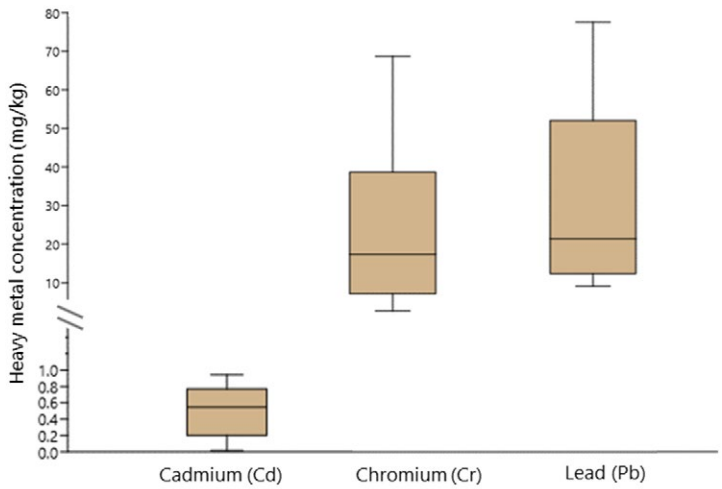

Fig. 2: The concentrations of selected heavy metals in the sediments of Cisadane River.

same software, a Pearson correlation test was done to comprehend the metal's interaction with the sediment. With a higher coefficient value, it was considered that the metals originate from the same place, were interdependent and had an identical flow behavior (Harmesa and Cordova, 2020).

RESULTS AND DISCUSSION

Selected heavy metal concentrations in the Cisadane River sediments

Fig. 2 depicts the distribution of Cd, Cr, and Pb concentrations in riverine sediments. With an average value of 30.3053 ± 23.4339 milligram per kilogram dry weight (mg/kg), Pb had the highest concentration in the Riverine Sediment of the Cisadane River, followed by Cr (23.4672 ± 20.1228 mg/kg). Compared to Pb and Cr, Cd was found to have the lowest concentration (0.5140 ± 0.2983 mg/kg). Furthermore, the Kruskal-Wallis and Mann-Whitney tests revealed a statistically significant difference ($p<0.05$) between Cd - Cr and Cd - Pb. Table 1 further illustrates the spatial distribution of the mean and standard deviation of the Cd, Cr, and Pb concentrations at each location, as well as their comparison to sediment quality standards. On the basis of sediment quality guidelines from ANZECC and ARMCANZ (2000) and CCME (2001), selected heavy metals observed (Table 1) in midstream and downstream Cisadane River were moderately lower than the guideline level, with the exception of Pb, which exceeded the ISQG (Interim Sediment Quality Guideline) from CCME (2001). The selected heavy metal concentrations in this study were below or comparable to those in other well-known major rivers (Gaillardet *et al.*, 2013; Nasrabadi *et al.*, 2018). Selected heavy metals in the Cisadane River sediments were relatively lower than those in Yellow River (W. Li *et al.*, 2022), Han River (X. Li *et al.*, 2022), Nanfei River (Fang *et al.*, 2022) in China, and the Brahmaputra River in India (Saikia *et al.*, 2022); on the same magnitude compared to the Teesta River, India (Chettri *et al.*, 2022) and the Oder river and Vistula river in Poland (Jaskuła and Sojka, 2022). However, heavy metals in the Cisadane River sediments were higher than the Kafue River and Zambezi River in Zambia (Nakayama *et al.*, 2010). Compared to dissolved concentrations discovered in urban runoff, the results of this study showed a stronger link (Pinedo-Gonzalez *et al.*, 2017). Greater urban land use resulted in higher quantities of dissolved metals in watersheds compared to those found in natural areas (Gardner and Carey, 2004; Pinedo-Gonzalez *et al.*, 2017; Yoon and Stein, 2008). In general, heavy metal pollution levels in the Cisadane River sediments were still below the threshold at which they could cause harm to the aquatic organism. Albeit the selected heavy metals concentration in this study was moderately modest compared to the guidelines (Table 1), it must nevertheless be taken into account because Cd and Pb surpass their natural values in the upper continental crust. Wedepohl (1994) specifically

Table 1: The concentrations of selected heavy metals in each sampling station in the Cisadane River

Location	Station code number	Concentration (mg/kg)		
		Cd	Cr	Pb
Midstream (ST01-ST04)	ST01	0.0628 ± 0.0614	5.3425 ± 0.7623	9.8746 ± 1.4921
	ST02	0.1825 ± 0.0139	4.2874 ± 2.1266	9.1596 ± 0.3991
	ST03	0.8000 ± 0.0295	52.1811 ± 8.2727	63.6332 ± 6.3275
	ST04	0.6854 ± 0.0573	15.8714 ± 6.2011	26.4032 ± 8.9145
Downstream (ST05-ST08)	ST05	0.3214 ± 0.1143	13.0176 ± 2.6695	20.5500 ± 10.2734
	ST06	0.9278 ± 0.0126	57.9242 ± 9.3170	72.0347 ± 7.0349
	ST07	0.6196 ± 0.1644	15.7160 ± 6.0428	20.2391 ± 1.3909
	ST08	0.5127 ± 0.0941	23.3976 ± 3.3947	20.5476 ± 0.9902
ANZECC and ARMCANZ Guidelines	Low	1.5	80	50
	High	10	370	220
CCME Guidelines	ISQG	0.7	52.3	30.2
	PEL	4.2	160	112

ISQG: interim sediment quality guidelines; PEL: probable effect levels

stated that the natural concentrations of Cd, Cr, and Pb were 0.102 mg/kg, 35 mg/kg, and 17 mg/kg, respectively.

The largest concentration of heavy metals in the Cisadane River sediments was Pb, followed by Cr and Cd. The enrichment of heavy metals in riverine sediments is caused by natural sources, including volcanic eruption and weathering from soil or rocks, which causes leaching (Fang *et al.*, 2016). In addition to natural sources, anthropogenic activities waste, such as unmanaged waste, is a source of heavy metal pollution (Fang *et al.*, 2016). Pb is emitted through urban runoff, atmospheric deposition, combustion engine automobile and industrial emissions, and craft maintenance activities (Burton *et al.*, 2005a; Hossain *et al.*, 2019; Liu *et al.*, 2016; Sakawi *et al.*, 2013). Meanwhile, Cd pollution is linked to farming activities such as using many phosphate fertilizers with Cd impurities (Liu *et al.*, 2016). Moreover, Cd usually comes from activities that make farming more productive, such as using a lot of fertilizers and pesticides and mining (Ayangbenro and Babalola, 2017; Tang *et al.*, 2010). Furthermore, Cr is often found in antifouling paints used in the screen-printing and textile industries (Costa-Böddeker *et al.*, 2017; Duodu *et al.*, 2017).

The linear correlation matrix of Pearson's correlation coefficients between Cd, Cr, and Pb in Cisadane river sediments is shown in Table 2. According to the Pearson correlation value, the statistical output between Cd - Cr and between Cr - Pb suggested a moderately positive relationship (r between 0.6 and 0.8), although the correlation between Cr - Pb indicated a fairly strong positive relationship (r between 0.8-0.99). In this case, the three correlations had a 99% confidence interval (Table 2). Based on the discovered Pearson's correlation coefficient (Table 2), Cd - Cr and Cr - Pb were shown to have a moderately positive connection. Moreover, the correlation between Cr and Pb was significantly positive. This linkage demonstrated that heavy metals were interdependent, exhibited the same transit behavior, and most likely originated from the same origin, whether natural or manmade (Harmesa *et al.*, 2020; Liu *et al.*, 2016; Suresh *et al.*, 2012).

Spatial distribution of heavy metals in Cisadane River

Table 1 demonstrates that all sampling locations detected heavy metals (Cd, Cr, and Pb), showing that the trend of heavy metals pollution is increasing to the Cisadane River's downstream section. In this investigation, the lowest concentrations of heavy metals were identified at ST01 and ST02, the first and second midstream sites. Nonpoint and point sources were the sources of heavy metals in the sediments of the Cisadane River. Dispersed throughout the Cisadane

Table 2: Pearson's correlation coefficient (r) for selected heavy metals concentration in Cisadane River sediments

Heavy metals	Cd	Cr	Pb
Cd	1		
Cr	0.7916*	1	
Pb	0.7877*	0.9254*	1

watershed were nonpoint sources in the form of effluent from community activities. The household and commercial areas were the densest in the mid-midstream and downstream regions. Similar to households, the majority of industries in the Cisadane watershed were relatively small (those located in the upstream and early midstream), with 143 medium and heavy industries dispersed throughout the mid-midstream and downstream regions (Kementerian Perindustrian, 2020). The landfills on the river's banks were considered to be the point sources of heavy metals in the sediments of the Cisadane River. After landfill leachate disposal, the mean and standard deviation of the examined heavy metals were higher than the data without area (ST03 and ST06). ST03 and ST06, both of which are located after the landfill area, contained the highest concentration. Detail-wise, ST03 and ST06 represented the pinnacle of heavy metal amplification (Table 1). Moreover, at these two stations, Cd, Cr, and Pb concentrations exceeded the ISQG guidelines from CCME (2001). Furthermore, Pb in ST03 and ST06 surpassed the lower limit specified by ANZECC and ARMCANZ (2000). Heavy metals data's mean and standard deviation without a sample point before a landfill were two to four times lower. In addition, a statistically significant difference occurred between the regions before and after landfilling for all examined heavy metals ($p<0.01$). Depending on the type of heavy metal, the increase occurred between 2.89 and 12.17 times. At ST03 and ST06, Cd levels were 4.38 and 2.89 times higher, Cr levels were 12.17 and 4.45 times higher, and Pb levels were 6.95 and 3.50 times higher, respectively. There was a presumption that there was a correlation between the landfill location and landfill leachate and the concentration of heavy metals in the sediments of the Cisadane River. The limitation of this study was that it did not investigate landfill leachate in two dump regions located along the Cisadane River. If a comparative study is undertaken, the heavy metals level in landfill leachate must be analyzed in greater detail. The results of this investigation indicated the existence of landfills as probable point origins of harmful heavy metals (Deng *et al.*, 2018; Houessionon *et al.*, 2021; Hussein *et al.*, 2021; Robinson, 2017). Leachate treatment facilities in Indonesian landfills typically consist of ponds for collection and treatment. Some of the leachate in the pond is disposed of as a result of microbial fermentation and gravity effects (Xu *et al.*, 2018); however, because the leachate treatment is not comparable to a sanitary landfill, the leachate produced and discharged into the watershed has a complex composition and contains toxic heavy metals (Hou *et al.*, 2019; Singh *et al.*, 2015). The leachate carried into the watershed will negatively impact the river's environment. In turn, this will increase the expense of environmental management and may adversely affect human health (Hussein *et al.*, 2019; Ishak *et al.*, 2016). Along the Cisadane River, three unsanitary landfills have direct leachate discharge channels into the river (Nurhasanah *et al.*, 2021; Sulistyowati *et al.*, 2022). After one kilometer from the landfill leachate outlet, the concentration of heavy metals at the sampling station was two to four times greater. In landfill leachate, critical heavy metals are frequently abundant, physiologically complex, and bioaccumulative, rendering them highly accessible to trophic food systems (Atta *et al.*, 2015; Kaschl *et al.*, 2002; Sánchez-Chardi and Nadal, 2007). A transition from an unsanitary (open) dumping system to a properly sanitary landfill system, is essential for improving this situation since it can raise the heavy metals removal rate (Deng *et al.*, 2018; Jaradat *et al.*, 2021; Robinson, 2017). Some levels of heavy metals in natural soil were found to exceed predetermined background values. Despite the fact that the metal content of these soils is considerable, it is significantly lower than that of waste/leachate-affected soils (Hussein *et al.*, 2021). Notably, heavy metals are also natural trace elements that are infrequently harmful (Wuana and Okieimen, 2011). Under typical conditions, it is unlikely that metals are dissolved,

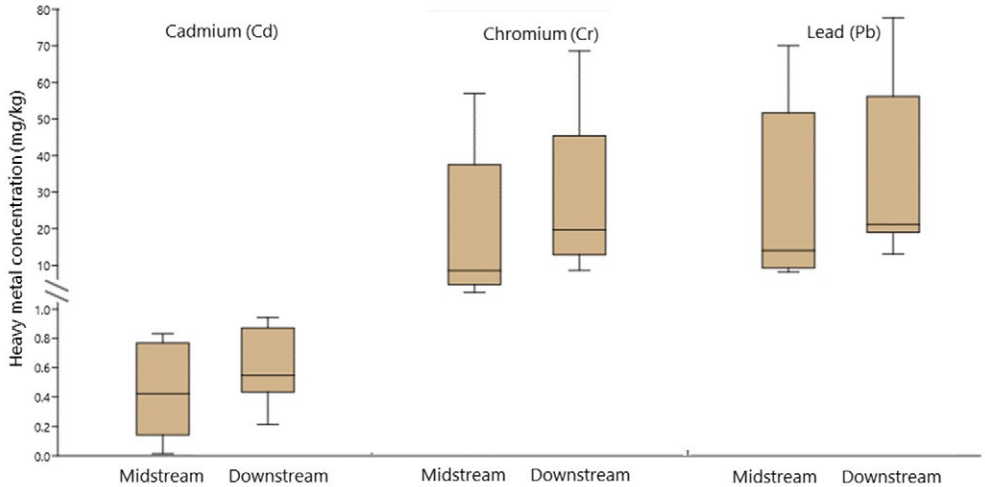

Fig. 3: Comparison of selected heavy metals concentration in midstream and downstream of Cisadane River

leached, and transportable in the environment. However, it can be induced by successive reductive circumstances and anaerobic bio-decompositions (Hussein *et al.*, 2021; Ishchenko, 2019; Li *et al.*, 2009; Thongyuan *et al.*, 2021). These circumstances may result in the leaching of toxic metals deposited in the riverine sediment (Demirbilek *et al.*, 2013). Due to the decrease in oxygen content, methanogenic conditions have led to the dissolution of a reductive metal in the leachate (Demirbilek *et al.*, 2013). Additionally, metal leaching occurs in soil affected by leachate with high organic content (DeLemos *et al.*, 2006; Ford *et al.*, 2011).

Fig. 3 depicts the calculated average concentrations and fluctuations of Cd, Cr, Pb in the midstream and downstream sediments of the Cisadane River. Along the Cisadane Yellow River, all investigated heavy metals in sediments demonstrated an upward trend, with greater average concentrations in downstream than in the midstream. Cr had the most significant increase in the mean concentration of selected heavy metals from midstream to downstream, followed by Cd, while Pb had the smallest increase (Fig. 3). The average concentration of Cr in the midstream (19.4206 ± 20.8090 mg/kg) increased by 41.67% in the downstream (27.5138 ± 19.4402 mg/kg). The mean Cd concentration in the midstream (0.4327 ± 0.3318 mg/kg) increased by 37.60% in the downstream (0.5953 ± 0.2481 mg/kg). The average Pb content in the midstream increased by 22.28% in the downstream (27.2677 ± 23.5577 mg/kg to 33.3429 ± 23.9400 mg/kg). Our findings are consistent with the previous studies on heavy metal contamination of soils in the middle and lower reaches of China's Xiangjiang River (Wang *et al.*, 2008). Heavy metals originating from improperly managed pollution in the Cisadane watershed reached the aquatic ecosystem and were further carried by the water, and were deposited in river sediments. Moreover, the water carried pollutants from the land to the aquatic environment. Although many heavy metals might be predominantly associated with organic material particles or suspended sediment, heavy metals can be shifted into a more bioavailable dissolved form (Bergamaschi *et al.*, 2012; Roussiez *et al.*, 2011). Various hydrological regimes can impact heavy metal mobility. For instance, during a precipitation event following a prolonged period of drought, overland water runoff is frequently the primary transport mechanism for anthropogenic toxic metals (Wijesiri *et al.*, 2018; Yong and Chen, 2002). In this study, landfills were also considered point sources of toxic metals in addition to non-point sources of heavy metals throughout the Cisadane river. Widespread usage of non-engineered and unmanaged landfills without suitable bottom liners, leachate collection, or treatment systems prevented better management of solid waste from municipalities (Ishchenko, 2019). This has resulted in the production of leachates from landfills that include substantial amounts of

organic and inorganic pollutants and are particularly dangerous to the environment (Naveen *et al.*, 2017; Öman and Junestedt, 2008). In this case, 84% of waste management in Indonesia was accomplished through waste disposal sites with open dumping landfill system (Munawar *et al.*, 2018). However, the proportion of landfills with improved systems has not yet met the requirements for a sanitary landfill system (Meidiana and Gamse, 2010), meaning that only a portion of the fundamental conditions for controlled landfills was achieved. This leads in the release of leachates containing harmful substances including toxic heavy metals into the aquatic environment (Hussein *et al.*, 2021). In some landfills, leachate consists of fluids that have reached the open landfill from a variety of external sources, such as wastewater, groundwater, soil erosion, and precipitation generated from the breakdown of organic waste (Ghosh *et al.*, 2017). In certain instances, groundwater flow following flood water subsidence can contribute significantly to metal loading in downstream waterways (Santos *et al.*, 2011). Heavy metal emissions could be deposited within riverine to estuarine sediments and transferred to the marine system (Fernández-Cadena *et al.*, 2014; González-Ortegón *et al.*, 2019). The Indonesian government might have helped alleviate this problem by enforcing the Waste Law Number 18 Year 2008, which mandates the replacement of all open dumping with more regulated landfills or sanitary landfills. The elimination of heavy metals from non-point sources, such as leachate landfills, can be accomplished through various methods, including physicochemical (coagulation/flocculation treatment, membrane application, and adsorption treatment), biological (phytoremediation, bioremediation, and arrangement of aerobic and anaerobic bioreactors), and combination (physicochemical and biological) techniques. The elimination of heavy metals in aquatic environments directly results from the transition to sanitary landfills (Mojiri *et al.*, 2011). Changes should also be made at the regional level, considering available infrastructure, human capacity, and funding.

CONCLUSION

The purpose of this study is to characterize heavy metals in Cisadane River sediments. This investigation leads us to conclude that the Cd, Cr, and Pb concentrations in the sediment are still below the threshold established by the standards and are, therefore, safe for the habitat inside. In this study, concentrations of Cd, Cr, and Pb were found to be lower than or comparable to those in other well-known large rivers. Although the concentrations of heavy metals in this study are relatively modest in comparison to the guidelines, they must still be taken into account because Cd and Pb are higher than they should be in the upper continental crust. However, the concentration of Cd, Cr, and Pb exceeds the sediment quality guidelines in the sampling sites after landfills, which is believed to be the result of leachate discharge and landfill activities. Therefore, it requires special consideration including the implementation of physicochemical, biological, and combination remediation techniques. This study discovers that heavy metals are interdependent, have the same transport patterns, and most likely originate from the same sources. In the Riverine Sediment of the Cisadane River, Pb has the highest concentration, followed by Cr, while Cd that has the lowest concentration. Sources of heavy metals in the Cisadane River sediments comprise nonpoint and point sources. The nonpoint sources in the form of wastewater from community activities are dispersed throughout the Cisadane watershed. In comparison, two riverbank landfills are recognized as the point sources of heavy metals in the sediments of the Cisadane River. Two landfills along the Cisadane River discharge their leachate directly into the waterway. The concentration of heavy metals at the test location is two to four times higher one kilometer from the landfill's leachate discharge. In this case, investigation indicates that heavy metal pollution in the Cisadane River's downstream segment is escalating. Therefore, through the enforcement of the Indonesian Waste Law Number 18 Year 2008 which would have replaced all open dumping with better-controlled landfills or sanitary landfills, would have helped the Indonesian government address this problem. Furthermore, further research is required to determine the levels of harmful heavy metals in leachate landfills, drain sediment in leachate ponds, and groundwater, which can also be contaminated by suboptimal management of leachate landfills.

AUTHOR CONTRIBUTIONS

L. Sulistyowati, the corresponding author, has contributed in interpreted the results, and preparing

the manuscript. Nurhasanah performed data analysis. E. Riani designed the field sampling contributed to the data analysis and interpretation of the results. M.R. Cordova contributed to supervision, study design, laboratory analysis, data analysis and writing with the assistance of L. Sulistyowati, Nurhasanah and E. Riani. M.R. Cordova is the main contributor to this manuscript.

ACKNOWLEDGEMENT

The authors would like to thank waste picker and fishers who have voluntary supported this study. This study is supported by the Universitas Terbuka funding scheme 2022 [Grant No. B/284/UN31.LPPM/PT.01.03/2022 and B/410/UN31.LPPM/PT.01.03/2022] for L. Sulistyowati, Nurhasanah, and M.R. Cordova. All authors discussed the results and provided input and comments on the manuscript. The authors would like to express gratitude to the anonymous reviewers for their insightful and constructive comments, which resulted in a significant improvement of the manuscript. The editor's constructive comments on earlier drafts of the manuscript are greatly appreciated.

CONFLICT OF INTEREST

The author declares that there is no conflict of interests regarding the publication of this manuscript. In addition, the ethical issues, including plagiarism, informed consent, misconduct, data fabrication and/or falsification, double publication and/or submission, and redundancy have been completely observed by the authors.

ABBREVIATIONS

ANZECC	Australia New Zealand Environment and Conservation Council
ARMCANZ	Agriculture and Resource Management Council of Australia and New Zealand
ATSDR	Agency for Toxic Substances and Disease Registry
°C	degree Celsius
CCME	Canadian Council of Ministers of the Environment
Cd	Cadmium
cm	Centimeter
Cr	Chrome
CRM	Certified reference material
DDDW	Double distilled deionized water
e.g.	Exempli gratia (for example)
ha	hectare
HCl	Hydrogen chloride (Hydrochloric acid)
HNO_3	Hydrogen nitrate (nitric acid)
ICP-OES	Inductively coupled plasma – optical emission spectrometry
ISQG	Interim sediment quality guidelines
kg	Kilogram
km	Kilometer
mg/kg	Milligram per kilogram dry weight
mL	Milliliter
PEL	Probable effect levels
Pb	Lead
r	Pearson's correlation coefficient
ST	Station sampling
USEPA	United States Environmental Protection Agency

REFERENCES

Abdullah, M.Z.; Hazwani, N.; Tahir Abas, M., (2016). The use of Ipomoea pes-caprae plant species to monitor metal pollutions of the coastal soil. J. Teknologi., 78(6–6): 1–6 **(6 pages)**.

Ali, H.; Khan, E., (2019). Trophic transfer, bioaccumulation, and biomagnification of non-essential hazardous heavy metals and metalloids in food chains/webs—Concepts and implications for wildlife and human health. Hum. Ecol. Risk Assess., 25(6): 1353–1376 **(24 pages)**.

ANZECC and ARMCANZ, (2000). Volume 1: The Guidelines. In Australian and New Zealand Guidelines for Fresh and Marine Water Quality. Australian and New Zealand Environment and Conservation Council, Agriculture and Resource Management Council of Australia and New Zealand **(314 pages)**.

ATSDR, (2012). Toxicity profile for heavy metals. Agency for Toxic Substances and Disease Registry.

Atta, M.; Yaacob, W.Z.W.; Bin Jaafar, O., (2015). The potential impact of leachate-contaminated groundwater of an ex-landfill site at Taman Beringin Kuala Lumpur, Malaysia. Environ. Earth Sci., 73(7): 3913–3923 **(11 pages)**.

Ayangbenro, A.S.; Babalola, O.O., (2017). A new strategy for heavy metal polluted environments: A review of microbial biosorbents. Int. J. Environ. Health Res., 14(1): 94 **(16 pages)**.

Bergamaschi, B.A.; Krabbenhoft, D.P.; Aiken, G.R.; Patino, E.; Rumbold, D.G.; Orem, W.H., (2012). Tidally driven export of dissolved organic carbon, total mercury, and methylmercury from a mangrove-dominated estuary. Environ. Sci. Technol., 46(3): 1371–1378 **(8 pages)**.

Burton, E.D.; Phillips, I.R.; Hawker, D.W., (2005a). Geochemical partitioning of copper, lead, and zinc in benthic, estuarine sediment profiles. J. Environ. Qual., 34(1): 263–273 **(11 pages)**.

Burton, E.D.; Phillips, I.R.; Hawker, D.W., (2005b). Trace metal distribution and enrichment in benthic, estuarine sediments: Southport Broadwater, Australia. Environ. Geochem. Health, 27: 369–383 **(15 pages)**.

CCME, (2001). Canadian sediment quality guidelines for the protection of aquatic life. in canadian environmental quality guidelines. Canadian Council of Minister of the Environment, Winnipeg.

Chettri, U.; Chakrabarty, T.K.; Joshi, S.R. (2022). Pollution index assessment of surface water and sediment quality with reference to heavy metals in Teesta River in Eastern Himalayan range, India. Environ. Nanotechnol. Monit. Manage., 18: 100742 **(9 pages)**.

Cordova, M.R.; Eftiah, F.D.M.; Zamani, N.P., (2017). Ability of mangrove apple as mercury bioindicator. Omni-Akuatika, 13(2): 137–143 **(7 pages).**

Costa-Böddeker, S.; Hoelzmann, P.; Thuyên, L.X.; Huy, H.D.; Nguyen, H.A.; Richter, O.; Schwalb, A., (2017). Ecological risk assessment of a coastal zone in Southern Vietnam: Spatial distribution and content of heavy metals in water and surface sediments of the Thi Vai Estuary and Can Gio Mangrove Forest. Mar. Pollut. Bull., 114(2): 1141–1151 **(11 pages)**.

Custodio, M.; Orellana-Mendoza, E.; Peñaloza, R.; De la Cruz-Solano, H.; Bulege-Gutiérrez, W.; Quispe-Mendoza, R., (2020). Heavy metal accumulation in sediment and removal efficiency in the stabilization ponds with the hydrocotyle ranunculoides filter. J. Ecol. Eng., 21(5): 72–79 **(8 pages)**.

da Silva, Y.J.A.B.; do Nascimento, C.W.A.; Biondi, C.M., (2013). Comparison of USEPA digestion methods to heavy metals in soil samples comparison of USEPA digestion methods to heavy metals in soil samples. Environ. Monit. Assess., 186: 47–53 **(7 pages)**.

DeLemos, J.L.; Bostick, B.C.; Renshaw, C.E.; Stürup, S.; Feng, X., (2006). Landfill-stimulated iron reduction and arsenic release at the Coakley Superfund Site (NH). Environ. Sci. Technol., 40(1): 67□73 **(7 pages)**.

Demirbilek, D.; Öztüfekçi Önal, A.; Demir, V.; Uslu, G.; Arslanoglu-Isık, H., (2013). Characterization and pollution potential assessment of Tunceli, Turkey municipal solid waste open dumping site leachates. Environ. Monit. Assess., 185(11): 9435–9449 **(15 pages)**.

Deng, M.; Kuo, D.T.F.; Wu, Q.; Zhang, Y.; Liu, X.; Liu, S.; Hu, X.; Mai, B.; Liu, Z.; Zhang, H., (2018). Organophosphorus flame retardants and heavy metals in municipal landfill leachate treatment system in Guangzhou, China. Environ. Pollut., 236: 137–145 **(9 pages)**.

Dixit, R.; Wasiullah, Malaviya, D.; Pandiyan, K.; Singh, U. B.; Sahu, A.; Shukla, R.; Singh, B.P.; Rai, J.P.; Sharma, P.K.; Lade, H.; Paul, D., (2015). Bioremediation of heavy metals from soil and aquatic environment: An overview of principles and criteria of fundamental processes. Sustainability. 7(2): 2189–2212 **(24 pages)**.

Duodu, G.O.; Goonetilleke, A.; Ayoko, G.A., (2017). Potential bioavailability assessment, source apportionment and ecological risk of heavy metals in the sediment of Brisbane River estuary, Australia. Mar. Pollut. Bull., 117(1–2): 523–531 **(9 pages)**.

Essien, J.P.; Ikpe, D.I.; Inam, E.D.; Okon, A.O.; Ebong, G.A.; Benson, N.U., (2022). Occurrence and spatial distribution of heavy metals in landfill leachates and impacted freshwater ecosystem: An environmental and human health threat. PLoS ONE, 17(2) **(18 pages)**.

Fang, W.; Wei, Y.; Liu, J., (2016). Comparative characterization of sewage sludge compost and soil: Heavy metal leaching characteristics. J. Hazard. Mater., 310: 1–10 **(10 pages)**.

Fang, W.; Wei, Y.; Liu, J.; Kosson, D.S.; van der Sloot, H.A.; Zhang, P., (2016). Effects of aerobic and anaerobic biological processes on leaching of heavy metals from soil amended with sewage sludge compost. Waste Manage., 58: 324–334 **(11 pages)**.

Fang, T.; Wang, H.; Liang, Y.; Cui, K.; Yang, K.; Lu, W.; Li, J.; Zhao, X.; Gao, N.; Yu, Q.; Li, H.; Jiang, H. (2022). Source tracing with cadmium isotope and risk assessment of heavy metals in sediment of an urban river, China. Environ. Pollut., 305: 119325 **(8 pages)**.

Fernández-Cadena, J.C.; Andrade, S.; Silva-Coello, C.L.; De la Iglesia, R., (2014). Heavy metal concentration in mangrove surface sediments from the north-west coast of South America. Mar. Pollut. Bull., 82(1–2): 221–226 **(6 pages)**.

Ford, R.G.; Acree, S.D.; Lien, B.K.; Scheckel, K.G.; Luxton, T.P.; Ross, R.R.; Williams, A.G.; Clark, P., (2011). Delineating landfill leachate discharge to an arsenic contaminated waterway. Chemosphere, 85(9): 1525–1537 **(13 pages)**.

Gaillardet, J.; Viers, J.; Dupré, B., (2013). Trace Elements in River Waters. In Treatise on Geochem.: Second Edition. 7: 195–235 **(41 pages)**.

Gardner, C.B.; Carey, A.E., (2004). Trace metal and major ion inputs into the Olentangy River from an urban storm sewer. Environ. Sci. Technol., 38(20): 5319–5326 **(8 pages)**.

Ghosh, P.; Thakur, I.S.; Kaushik, A., (2017). Bioassays for toxicological risk assessment of landfill leachate: A review. Ecotoxicol. Environ. Saf., 141: 259–270 **(12 pages)**.

González-Ortegón, E.; Laiz, I.; Sánchez-Quiles, D.; Cobelo-Garcia, A.; Tovar-Sánchez, A., (2019). Trace metal characterization and fluxes from the Guadiana, Tinto-Odiel and Guadalquivir estuaries to the Gulf of Cadiz. Sci. Total Environ., 650: 2454–2466 **(13 pages)**.

Harmesa, H.; Cordova, M.R., (2020). A preliminary study on heavy metal pollutants chrome (Cr): cadmium (Cd): and lead (Pb) in sediments and beach morning glory vegetation (Ipomoea pes-caprae) from Dasun Estuary, Rembang, Indonesia. Mar. Pollut. Bull., 111819 **(6 pages)**.

Harmesa, H.; Lestari, L.; Budiyanto, F., (2020). Distribusi logam berat dalam air laut dan sedimen di perairan Cimanuk, Jawa Barat, Indonesia. OLDI., 5(1): 19-32 **(14 pages)**.

Hossain, M.B.; Shanta, T.B.; Ahmed, A.S.S.; Hossain, M.K.; Semme, S.A., (2019). Baseline study of heavy metal contamination in the Sangu River estuary, Chattogram, Bangladesh. Mar. Pollut. Bull., 140: 255–261 **(7 pages)**.

Hou, S.; Zheng, N.; Tang, L.; Ji, X.; Li, Y.; Hua, X., (2019). Pollution characteristics, sources, and health risk assessment of human exposure to Cu, Zn, Cd and Pb pollution in urban street dust across China between 2009 and 2018. Environ. Int., 128, 430–437 **(8 pages).**

Houessionon, M.G.K.; Ouendo, E.-M.D.; Bouland, C.; Takyi, S.A.; Kedote, N.M.; Fayomi, B.; Fobil, J. N.; Basu, N., (2021). Environmental heavy metal contamination from electronic waste (e-waste) recycling activities worldwide: a systematic review from 2005 to 2017. Int. J. Environ. Health Res., 18(7) **(16 pages)**.

Hussein, M.; Yoneda, K.; Zaki, Z.M.; Othman, N.; Amir, A. (2019). Leachate characterizations and pollution indices of active and closed unlined landfills in Malaysia. Environ. Nanotechnol. Monit. Manage., 12: 100232 **(9 pages)**.

Hussein, M.; Yoneda, K.; Mohd-Zaki, Z.; Amir, A.; Othman, N., (2021). Heavy metals in leachate, impacted soils and natural soils of different landfills in Malaysia: An alarming threat. Chemosphere, 267 **(19 pages).**

Ishak, A.R.; Mohamad, S.; Soo, T.K.; Hamid, F.S. (2016). Leachate and Surface Water Characterization and Heavy Metal Health Risk on Cockles in Kuala Selangor. Procedia – Soci. Behav. Sci., 222: 263–271 **(9 pages)**.

Ishchenko, V., (2019). Heavy metals in municipal waste: the content and leaching ability by waste fraction. J. Environ. Sci. Health A., 54(14): 1448–1456 **(9 pages)**.

Islam, M.S.; Ahmed, M.K.; Raknuzzaman, M.; Habibullah -Al-Mamun, M.; Islam, M.K., (2015). Heavy metal pollution in surface water and sediment: A preliminary assessment of an urban river in a developing country. Ecol. Indic., 48: 282–291 **(10 pages)**.

Jaradat, A.Q.; Telfah, D.B.; Ismail, R., (2021). Heavy metals removal from landfill leachate by coagulation/flocculation process combined with continuous adsorption using eggshell waste materials. Water Sci. Technol., 84(12): 3817–3832 **(16 pages)**.

Jaskuła, J.; Sojka, M., (2022). Assessment of spatial distribution of sediment contamination with heavy metals in the two biggest rivers in Poland. Catena, 211: 105959 **(13 pages)**.

Kaewtubtim, P.; Meeinkuirt, W.; Seepom, S.; Pichtel, J., (2016). Heavy metal phytoremediation potential of plant species in a mangrove ecosystem in Pattani Bay, Thailand. Appl. Ecol. Environ. Res., 14(1): 367–382 **(16 pages)**.

Kementerian Perindustrian, (2020). Direktori Perusahaan Industri. Perusahaan Jenis Komoditi Di Banten dan Jawa Barat, Indonesia.

Kalender, L.; Çiçek Uçar, S., (2013). Assessment of metal contamination in sediments in the tributaries of the Euphrates River, using pollution indices and the determination of the pollution source, Turkey. J. Geochem. Explor., 134: 73–84 **(12 pages)**.

Kaschl, A.; Römheld, V.; Chen, Y., (2002). The influence of soluble organic matter from municipal solid waste compost on trace metal leaching in calcareous soils. Sci. Total Environ., 291(1–3): 45–57 **(13 pages)**.

Koesmawati, T.A.; Suratno, S.; Cordova, M.R., (2018). Preliminary assessment of mercury, arsenic and selenium content in fish from Batam Island Indonesia. AIP Conf. Proc., 2024 **(10 pages)**.

Lestari, L.; Budiyanto, F.; Puspitasari, R.; Purbonegoro, T.; Cordova, M.R.; Hindarti, D., (2018). Fractionation of metal in surface sediment from Cirebon coastal waters, West Java, Indonesia. AIP Conf. Proc., 2024 **(10 pages)**.

Li, W.; Qian, H.; Xu, P.; Zhang, Q.; Chen, J.; Hou, K.; Ren, W.; Qu, W.; Chen, Y. (2022). Distribution characteristics, source identification and risk assessment of heavy metals in surface sediments of the Yellow River, China. Catena, 216: 106376 **(10 pages)**.

Li, X.; Bing, J.; Zhang, J.; Guo, L.; Deng, Z.; Wang, D.; Liu, L. (2022). Ecological risk assessment and sources identification of heavy metals in surface sediments of a river–reservoir system. Sci. Total Environ., 842: 156683 **(13 pages)**.

Li, Y.; Ren, S., (2011). Metal decorative materials. In Building Decorative Materials. 169–200 **(32 pages)**.

Li, Y.; Richardson, J.B.; Mark Bricka, R.; Niu, X.; Yang, H.; Li, L.; Jimenez, A., (2009). Leaching of heavy metals from E-waste in simulated landfill columns. Waste Manage., 29(7): 2147–2150 **(4 pages)**.

Liu, J.; Yin, P.; Chen, B.; Gao, F.; Song, H.; Li, M., (2016). Distribution and contamination assessment of heavy metals in surface sediments of the Luanhe River Estuary, northwest of the Bohai Sea. Mar. Pollut. Bull., 109(1): 633–639 **(7 pages)**.

Meidiana, C.; Gamse, T., (2010). The new Waste Law: Challenging opportunity for future landfill operation in Indonesia. Waste Manage. Res., 29(1): 20–29 **(10 pages)**.

Miranda, L.S.; Wijesiri, B.; Ayoko, G.A.; Egodawatta, P.; Goonetilleke, A., (2021). Water-sediment interactions and mobility of heavy metals in aquatic environments. Water Res., 202 **(9 pages)**.

Mojiri, A.; Zhou, J.L.; Ratnaweera, H., Ohashi, A.; Ozaki, N.; Kindaichi, T.; Asakura, H. (2021). Treatment of landfill leachate with different techniques: An overview. J. Water Reuse Desalin., 11(1): 66–96 **(11 pages).**

Mohammed, A.S.; Kapri, A.; Goel, R., (2011). Heavy metal pollution: Source, impact, and remedies. 1–28 **(28 pages)**.

Munawar, E.; Yunardi, Y.; Lederer, J.; Fellner, J., (2018). The development of landfill operation and management in Indonesia. J. Mater. Cycles Waste Manage., 20(2): 1128–1142 **(15 pages)**.

Nakayama, S.M.M.; Ikenaka, Y.; Muzandu, K.; Choongo, K.; Oroszlany, B.; Teraoka, H.; Mizuno, N.; Ishizuka, M. (2010). Heavy metal accumulation in lake sediments, fish (Oreochromis niloticus and Serranochromis thumbergi), and crayfish (Cherax

quadricarinatus) in lake itezhi-tezhi and lake Kariba, Zambia. Arch. Environ. Contamin. Toxicol., 59(2): 291–300 **(10 pages)**.

Nasrabadi, T.; Ruegner, H.; Schwientek, M.; Bennett, J.; Valipour, S.F.; Grathwohl, P., (2018). Bulk metal concentrations versus total suspended solids in rivers: Time-invariant and catchment-specific relationships. PLoS ONE. 13(1) **(19 pages)**.

Naveen, B.P.; Mahapatra, D.M.; Sitharam, T.G.; Sivapullaiah, P.V.; Ramachandra, T.V., (2017). Physico-chemical and biological characterization of urban municipal landfill leachate. Environ. Pollut., 220: 1–12 **(12 pages)**.

Nurhasanah, Cordova, M.R.; Riani, E., (2021). Micro- and mesoplastics release from the Indonesian municipal solid waste landfill leachate to the aquatic environment: Case study in Galuga Landfill Area, Indonesia. Mar. Pollut. Bull., 163, 111986 **(9 pages)**.

Öman, C.B.; Junestedt, C., (2008). Chemical characterization of landfill leachates - 400 parameters and compounds. Waste Manage., 28(10): 1876–1891 **(16 pages)**.

Pagnanelli, F.; Moscardini, E.; Giuliano, V.; Toro, L., (2004). Sequential extraction of heavy metals in river sediments of an abandoned pyrite mining area: Pollution detection and affinity series. Environ. Pollut., 132(2): 189–201 **(13 pages)**.

Pinedo-Gonzalez, P.; Hellige, B.; West, A.J.; Sañudo-Wilhelmy, S.A., (2017). Changes in the size partitioning of metals in storm runoff following wildfires: Implications for the transport of bioactive trace metals. Appl. Geochem., 83: 62–71 **(10 pages)**.

Puspitasari, R.; Lestari, L., (2018). Assesment of heavy metal in kramat kebo estuary, west java, indonesia as habitat of Oryzias javanicus. J. Segara, 14(2) **(8 pages)**.

Puspitasari, R.; Suratno; Purbonegoro, T., (2020). Health risk assessment of metal accumulated in marine bivalves from Semarang, Indonesia. AACL Bioflux, 13(2): 993–1002 **(10 pages)**.

Riani, E.; Cordova, M.R.; Arifin, Z., (2018). Heavy metal pollution and its relation to the malformation of green mussels cultured in Muara Kamal waters, Jakarta Bay, Indonesia. Mar. Pollut. Bull., 133: 664–670 **(7 pages)**.

Riani, E.; Sudarso, Y.; Cordova, M.R., (2014). Heavy metals effect on unviable larvae of dicrotendipes simpsoni (diptera: Chironomidae): a case study from Saguling Dam, Indonesia. AACL Bioflux, 7(2): 76–84 **(9 pages)**.

Robinson, T., (2017). Removal of toxic metals during biological treatment of landfill leachates. Waste Manage., 63: 299–309 **(11 pages)**.

Rosado, D.; Usero, J.; Morillo, J., (2016). Assessment of heavy metals bioavailability and toxicity toward Vibrio fischeri in sediment of the Huelva estuary. Chemosphere, 153: 10–17 **(8 pages)**.

Roudi, A.M.; Kamyab, H.; Chelliapan, S.; Ashokkumar, V.; Kumar, A.; Yadav, K.K.; Gupta, N. (2020). Application of response surface method for Total organic carbon reduction in leachate treatment using Fenton process. Environ. Technol. Innovation. 19 **(13 pages)**.

Roussiez, V.; Ludwig, W.; Radakovitch, O.; Probst, J.L.; Monaco, A.; Charrière, B.; Buscail, R., (2011). Fate of metals in coastal sediments of a Mediterranean flood-dominated system: An approach based on total and labile fractions. Estuar. Coast. Shelf Sci., 92(3): 486–495 **(10 pages)**.

Saher, N.U.; Siddiqui, A.S., (2019). Occurrence of heavy metals in sediment and their bioaccumulation in sentinel crab (Macrophthalmus depressus) from highly impacted coastal zone. Chemosphere, 221: 89–98 **(10 pages)**.

Saikia, B.J.; Parthasarathy, G.; Borah, R.R. (2022). Geoenvironment and weathering of silicate minerals in sediments of the Brahmaputra river, India: Implications for heavy metal pollution assessment. Geosyst. Geoenviron., 1(3): 100065 **(6 pages)**.

Sakawi, Z.; Rozaimi Ariffin, M.; Mastura, S.S.A.; Jali, M.F.M., (2013). The analysis of heavy metal concentration per distance and depth around the vicinity of open landfill. Res. J. Appl. Sci. Eng. Technol., 5(24): 8619–8625 **(7 pages)**.

Sánchez-Chardi, A.; Nadal, J., (2007). Bioaccumulation of metals and effects of landfill pollution in small mammals. Part I. The greater white-toothed shrew, Crocidura russula. Chemosphere, 68(4): 703–711 **(9 pages)**.

Santos, I.R.; De Weys, J.; Eyre, B.D., (2011). Groundwater or floodwater? Assessing the pathways of metal exports from a coastal acid sulfate soil catchment. Environ. Sci. Technol., 45(22): 9641–9648 **(8 pages)**.

Singh, R.; Coyne, L.S.; Wallace, L.S. (2015). Brief screening items to identify spanish-speaking adults with limited health literacy and numeracy skills. BMC Health Serv. Res., 15(1) **(7 pages)**.

Statistic Indonesia, (2021). Statistik Lingkungan Hidup Indonesia 2021. Badan Pusat Statistik Indonesia **(318 pages).**

Sulistyowati, L.; Nurhasanah, Riani, E.; Cordova, M.R., (2022). The occurrence and abundance of microplastics in surface water of the midstream and downstream of the Cisadane River, Indonesia. Chemosphere, 291: 133071 **(8 pages)**.

Suresh, G.; Sutharsan, P.; Ramasamy, V.; Venkatachalapathy, R., (2012). Assessment of spatial distribution and potential ecological risk of the heavy metals in relation to granulometric contents of Veeranam Lake sediments, India. Ecotoxicol. Environ. Saf., 84: 117–124 **(8 pages)**.

Tang, W.; Shan, B.; Zhang, H.; Mao, Z., (2010). Heavy metal sources and associated risk in response to agricultural intensification in the estuarine sediments of Chaohu Lake Valley, East China. J. Hazard. Mater., 176(1–3): 945–951 **(7 pages)**.

The Jakarta Post, (2020). South Tangerang landfill wall collapses, spilling 100 tons of waste into Cisadane River.

Thongyuan, S.; Khantamoon, T.; Aendo, P.; Binot, A.; Tulayakul, P., (2021). Ecological and health risk assessment, carcinogenic and non-carcinogenic effects of heavy metals contamination in the soil from municipal solid waste landfill in Central, Thailand. Hum. Ecol. Risk Assess., 27(4): 876–897 **(22 pages)**.

USEPA, (2005). Contaminated sediment remediation guidance for hazardous waste sites. In Office of Solid Waste and Emergency Response. United States of Environmental Protection Agency.

USEPA, (2007). Method 3051A (SW-846): Microwave assisted acid digestion of sediments, sludges, and oils (Revision 1). United States of Environmental Protection Agency.

Vandecasteele, B.; Samyn, J.; Quataert, P.; Muys, B.; Tack, F.M.G., (2004). Earthworm biomass as additional information for risk assessment of heavy metal biomagnification: A case study for dredged sediment-derived soils and polluted floodplain soils. Environ. Pollut., 129(3): 363–375 **(13 pages)**.

Wang, L.; Guo, Z.; Xiao, X.; Chen, T.; Liao, X.; Song, J.; Wu, B. (2008). Heavy metal pollution of soils and vegetables in the midstream and downstream of the Xiangjiang River, Hunan Province. J. Geogr. Sci., 18(3): 353–362 **(10 pages)**.

Wedepohl, K.H., (1994). The Composition of the Continental Crust. Mineralogical Magazine, 58A(2): 959–960 **(2 pages)**.

Wijesiri, B.; Deilami, K.; Goonetilleke, A., (2018). Evaluating the relationship between temporal changes in land use and resulting water quality. Environ. Pollut., 234: 480–486 **(17 pages)**.

Wuana, R.A.; Okieimen, F.E., (2011). Heavy metals in contaminated soils: a review of sources, chemistry, risks and best available strategies for remediation. ISRN Ecology, 2011, 1–20 **(20 pages)**.

Xie, F.; Yu, M.; Yuan, Q.; Meng, Y.; Qie, Y.; Shang, Z.; Luan, F.; Zhang, D., (2022). Spatial distribution, pollution assessment, and source identification of heavy metals in the Yellow River. J. Hazard. Mater., 436: 129309 **(16 pages)**.

Xu, Y.; Xue, X., Dong, L.; Nai, C.; Liu, Y.; Huang, Q. (2018). Long-term dynamics of leachate production, leakage from hazardous waste landfill sites and the impact on groundwater quality and human health. Waste Manage., 82: 156–166 **(11 pages)**.

Yong, S.T.Y.; Chen, W., (2002). Modeling the relationship between land use and surface water quality. J. Environ. Manage., 66(4): 377–393 **(17 pages)**.

Yoon, V.K.; Stein, E.D., (2008). Natural catchments as sources of background levels of storm-water metals, nutrients, and solids. J. Environ. Eng., 134(12): 961–973 **(13 pages)**.

AUTHOR (S) BIOSKETCHES

Sulistyowati, L., Ph.D., Assistant Professor, Environmental Studies Graduate Program, Universitas Terbuka, Jl. Cabe Raya, Pondok Cabe, Pamulang Tangerang Selatan, 15418, Indonesia.
- Email: *liliks@ecampus.ut.ac.id*
- ORCID: 0000-0002-2200-1157
- Web of Science ResearcherID: A-9464-2018
- Scopus Author ID: 57357897800
- Homepage: https://pwk-fst.ut.ac.id/lilik-sulistyowati/

Nurhasanah, Ph.D., Assistant Professor, Environmental Studies Graduate Program, Universitas Terbuka, Jl. Cabe Raya, Pondok Cabe, Pamulang Tangerang Selatan, 15418, Indonesia.
- Email: *nenganah@ecampus.ut.ac.id*
- ORCID: 0000-0001-7234-9111
- Web of Science ResearcherID: A-9600-2018
- Scopus Author ID: 57214684688
- Homepage: https://nurhas.staff.ut.ac.id/

Riani, E., Ph.D., Professor, Department of Aquatic Resources Management, Faculty of Fishery and Marine Science, Bogor Agricultural University, Bogor, Indonesia.
- Email: *etty_riani@apps.ipb.ac.id*
- ORCID: 0000-0003-2080-4236
- Web of Science ResearcherID: AER-8235-2022
- Scopus Author ID: 23398401800
- Homepage: http://psl.ipb.ac.id/teachers/prof-dr-etty-riani-ms/

Cordova, M.R., Ph.D. Senior Researcher, Research Center for Oceanography, National Research and Innovation Agency Republic of Indonesia, BRIN Kawasan Jakarta Ancol, Jl. Pasir Putih 1, Ancol Timur, Jakarta, Indonesia.
- Email: *muhammad.reza.cordova@brin.go.id*
- ORCID: 0000-0002-4756-9646
- Web of Science ResearcherID: AAL-7273-2020
- Scopus Author ID: 56147418700
- Homepage: https://siin.brin.go.id/smi/7F0D69E8-2A0B-4C8E-8E51-69D3734456E0

HOW TO CITE THIS ARTICLE

Sulistyowati, L.; Nurhasanah; Riani, E.; Cordova, M.R., (2022). Heavy metals concentration in the sediment of the aquatic environment caused by the leachate discharge from a landfill. Global J. Environ. Sci. Manage., 9(2): 323-336.

DOI: 10.22034/gjesm.2023.02.11

url: https://www.gjesm.net/article_254984.html

Global J. Environ. Sci. Manage. 9(2): 337-352, Spring 2023, Serial #34

Global Journal of Environmental Science and Management
(GJESM)

Homepage: https://www.gjesm.net/

CASE STUDY

Characterization and quantification of solid waste in rural regions

S. Syafrudin[1], J.M. Masjhoer[2,3*], M. Maryono[4]

[1] *Department of Environmental Engineering, Faculty of Engineering, Diponegoro University, Semarang, Indonesia*

[2] *Environmental Science Doctoral Program, School of Postgraduate Studies, Diponegoro University, Semarang, Indonesia*

[3] *Sekolah Tinggi Pariwisata Ambarrukmo Yogyakarta, S1 Pariwisata, Indonesia*

[4] *Department of Urban and Regional Planning, Faculty of Engineering, Diponegoro University, Semarang, Indonesia*

ARTICLE INFO

Article History:
Received 11 June 2022
Revised 11 September 2022
Accepted 18 October 2022

Keywords:
Rural areas
Solid waste
Waste composition
Waste density
Waste generation
Waste management

DOI: 10.22034/gjesm.2023.02.12

ABSTRACT

BACKGROUND AND OBJECTIVES: Population growth and economic activity in rural areas are factors driving the waste generation rate. Rural waste management generally still applies conventional patterns and has the potential to damage the environment and threaten human health. Challenges and remedial measures for solid waste management in rural areas differ from urban ones. The first step in planning a waste management system is to identify the generation and characteristics of waste. Unfortunately, data on waste generation and characteristics in rural areas in developing countries are still minimal. The problems are mainly caused by the development of the tourism industry, and it certainly requires waste management as the solution. However, due to the unavailability of waste generation data, this study aims to measure and analyze waste characteristics in the southern zone of Gunungkidul Regency.
METHODS: *Primary* data collection was taken from 16 randomly selected villages in six sub-districts in Gunungkidul Regency. A door-to-door survey was carried to 110 residential and 160 non-residential samples for eight consecutive days using the Indonesian National Standard 19-3964-1994 method. The processed data were analyzed using a quantitative descriptive method.
FINDINGS: The results showed that the average waste generation was 0.29 kilograms per person per day. It shows that the waste generation in the study area is categorized in small-town classification. 75 percent of solid waste generated is food waste and leaves. Meanwhile, paper, plastic, glass, wood, other materials, and fabrics were calculated at 11.8 percent, 10.1 percent, 1.7 percent, 0.5 percent, 0.5 percent, and 0.4 percent respectively. Housing produced less recycled waste as indicated by a high density of 110.6 kilograms per cubic meter. Waste generation and composition are influenced by socioeconomic factors such as economic activity and lifestyle, geographic conditions, and downtown attractiveness.
CONCLUSION: The characteristics of the waste produced by the southern zone of Gunungkidul Regency are not much different from most rural areas in developing countries. Rural waste management needs to see organic waste as the main management material. Organic waste processing through composting can be a future solution, but the active role of residents determines its success. In addition, this method can help extend the life of the landfill capacity because the volume of organic waste will be reduced by half.

NUMBER OF REFERENCES	NUMBER OF FIGURES	NUMBER OF TABLES
52	8	2

*Corresponding Author:
Email: *jussac@students.undip.ac.id*
Phone: +6224 8452770
ORCID: 0000-0001-7042-2098

Note: Discussion period for this manuscript open until July 1, 2023 on GJESM website at the “Show Article”.

INTRODUCTION

Population and human activities directly relate to the generation rate and composition of solid waste. The lack of waste services in both urban and rural areas will cause environmental and public health problems. Generally, rural areas in developing countries manage their waste by burning them (de Morais Lima and Paulo, 2018), burying them, or dumping them in backyard pits. Some use the waste from the leftover food as animal feed (Qi *et al*., 2021; Nguyen and Watanabe, 2019). The level of household education, the availability of public waste collection facilities (Liu *et al*., 2020), village spatial planning (Wang *et al*., 2018), social, economic, and natural conditions (Han *et al*., 2018) have influenced these behaviors. Conventional waste management by rural communities can trigger further environmental problems and threaten human health. Small-scale burning of waste in rural China produces emissions of dioxins and dioxin-like pollutants that can be easily exposed to humans through inhalation (Yang *et al*., 2019). Waste incineration increases toxic elements in the air, soil, and water, so it significantly impacts freshwater ecosystems (Lima *et al*., 2021). The decline in environmental quality and public health will ultimately reduce productivity and economic growth (Kubanza and Simatele, 2019). These various risks illustrate that rural areas need waste management. Planning for sustainable waste management can be initiated by understanding the generation and composition of waste. The availability of waste generation and composition data is the basis for appropriate waste management methods and technologies. To date, several studies have quantified the generation and composition of waste. There are differences between rural and urban areas in waste generation rate and composition. Based on some studies, rural waste generation in various developing countries ranges between 0.178-0.9 kilogram per capita per day (kg/capita/day). Romania's rural areas produce an average of 0.4 kilogram per day (kg/day) of waste (Ciuta *et al*., 2015). Villages in Southwest China generated an average of 0.178 kg of waste per day (Han *et al*., 2015). Rural areas in Iran produce waste from 0.293 to 0.588 kg per capita per day (Darban Astane and Hajilo, 2017; Vahidi *et al*., 2017; Taghipour *et al*., 2016). Mae Salong Nok Sub-district in Thailand generates 0.9 kg of waste per day (Suma *et al*., 2019). In contrast to earlier findings, urban areas in 20 countries generated an average of 3.4 kg of solid waste per day (Programme, 2010), which is 70-80 percent (%) greater than rural areas (Hoang *et al*., 2017). Based on the waste composition generated, rural areas in various countries produce 50.5% organic waste on average. Rural areas in Iran such as Khosrowshah District (Taghipour *et al*., 2016), Khodabandeh District (Darban Astane and Hajilo, 2017), Chaharmahal and Bakhtiari Provinces, and Yazd Province (Vahidi *et al*., 2017), on average, produce 49.8% organic waste materials such as food waste, vegetables, fruits, and leaves. The percentage of organic waste produced is quite similar compared to the waste generated in the village of Desoq, Kafr El Sheikh, Egypt, which is 50.1% (Anwar *et al*., 2018). Inorganic waste in the form of plastic is the most commonly found for about 20% of the total waste produced by rural areas (Anwar *et al*., 2018; Darban Astane and Hajilo, 2017). Organic waste is found in all socioeconomic groups, and the proportion will decrease as the family economy increases (Ramachandra *et al*., 2018). Socioeconomic factors such as economic activity and lifestyle influence waste generation and composition (Nguyen *et al*., 2020), rural geographic location (Taghipour *et al*., 2016; Han *et al*., 2015b), downtown attractiveness, and tourism (Medjahed and Brahamia, 2019; Suma *et al*., 2019) influence waste generation and composition. Furthermore, the type of industry in rural areas also greatly influences the characteristics of the waste (Bilgili *et al*., 2019; Han *et al*., 2018). The waste management system implementation in rural areas requires a different approach compared to urban areas (Yukalang *et al*., 2018). However, data on the generation and composition of solid waste in rural areas are still not widely available. It is valuable and prominent to obtain more accurate data on waste characteristics in rural areas (Han *et al*., 2018). Taghipour *et al.* (2016) stated that investigating waste quantity and composition, waste management, and disposal systems in rural areas is still necessary. The lack of accurate information will make the governments difficult to design solid waste management strategies and the right technology (Abdel-Shafy and Mansour, 2018). The Southern Zone of Gunungkidul Regency (SZGR) is a rural area with a coastal area developed as a tourism area and is part of the Gunung Sewu UNESCO Global Geopark. SZGR continues to experience a positive trend of population

and economic growth due to the development of tourism and the improvement of accessibility. These conditions cause an increase in waste generation that needs to be managed properly (Masjhoer *et al*., 2020; Masjhoer, 2018). Challenges and remedial measures for solid waste management vary in every country (Al-Dailami *et al*., 2022). One aspect that needs to be considered in waste management system planning is the precise amount and type of waste produced (Quan *et al*., 2022). Empirical data on waste generation and characteristics by residents in SZGR is not yet available. This condition prompts the research question, how much waste is generated, and what is the composition of the waste produced by SZGR? Is the generation and composition of the waste produced by SZGR different from rural areas in other developing countries? Several previous studies (Abdel-Shafy and Mansour, 2018; Han *et al*., 2018; Taghipour *et al*., 2016) have reviewed the importance of waste generation and composition data as a basic foundation in rural waste management planning. The position of this research will add references and support similar research carried out by previous researchers. This research will enrich the data on the generation and composition of rural waste in developing countries. The data obtained from this study will provide an overview of the quantity and composition of the waste generated by residents in rural areas of SZGR. Interested parties can use this valuable information regarding the potential for waste that can be used commercially or non-commercially, processed into energy sources, converted into fertilizers, and designed solid waste management in rural areas. The current study aims is to provide actual data regarding the generation and composition of waste in rural areas in the southern zone of Gunungkidul regency, Indonesia, in 2021.

MATERIAL AND METHODS

Study area

This study is specifically located in the southern coastal area of Gunungkidul Regency. Administratively located in Purwosari sub-districts, Panggang sub-district, Saptosari sub-district, Tanjungsari sub-district, Tepus sub-district, and Girisubo sub-district (Fig. 1). SZGR is a rural area of 530.5 square kilometer (km^2), or 36 percent (%) of the total area of Gunungkidul Regency (Gunungkidul, 2020). The inhabitant is 182,642 people, with an average population density of 344 people per km^2. The population growth rate continues to increase to 1.11% in 2019 (Gunungkidul, 2020). The geographical location of SZGR is in the karst hills area of *Gunung Sewu*, which topography is mostly hillsides with an average height of 299 meters above sea level and a moderate to steep land slope (Gunungkidul, 2020). SZGR is a barren area due to the high porosity surface of the karst hills where surface water flow is hard to find. Typical karst hill soils are red Mediterranean and nutrient-poor latosols. Nevertheless, the locals in this area mostly work as farmers of secondary crops, rice, coconut, rubber, and coffee. SZGR has a coastal area with white sand beaches decorated with steep karst cliffs. The local government has designated this area as a tourism destination. Access to this area is getting easier with the construction of the southern causeway which triggers the development of commercial facilities such as hotels, restaurants, and shops (Masjhoer *et al*., 2020). This condition causes the emergence of waste that must be managed properly.

Material

This study measures the waste generated by residential, called household waste, and non-residential waste called household-related waste. The unit of measurement for waste generation uses the provisions of the Indonesian National Standard (INS) 19-3964-1994, namely, liter per person per day (L/person/day) for volume and kilogram per person per day (kg/person/day) for weight. The waste characteristics measured in this study are limited to physical characteristics, namely composition and density. The composition of waste is divided into organic and inorganic waste. Organic waste is the residue of organic material originating from human or natural activities and will naturally undergo a decomposition process within a certain time. Organic waste consists of food waste and leaves (Or), paper (Pr), and wood (Wd). Inorganic waste is a material that is not easily biodegraded, comes from minerals, and can be recycled. Based on this definition, inorganic waste consists of fiber (Fb), rubber (Rb), plastic (Pl), metal (Mt), and glass (Gs). Other materials are common waste found in residential and non-residential such as batteries, masks, and electronic devices which are considered as residue. The units used to measure the waste composition are in weight % and the density of the waste in kilogram per meter cubic (kg/m^3).

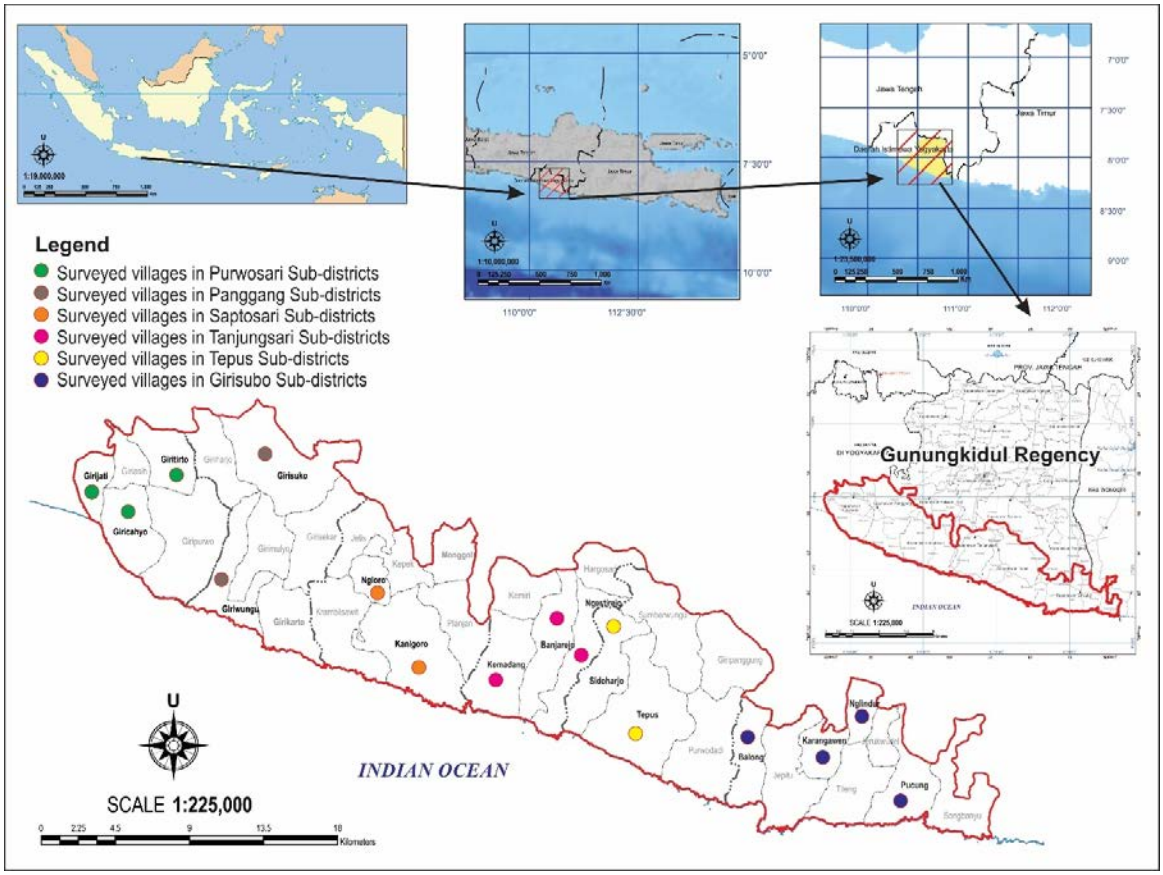

Fig. 1: Geographic location of the study area and surveyed villages in the southern zone of Gunungkidul Regency, in Indonesia

Methods

Primary data collection was held in 16 randomly selected villages, three in the Purwosari sub-district, two in the Panggang sub-district, two in the Saptosari sub-district, three in the Kemadang sub-district, two in the Tepus sub-district, and four in the Girisubo sub-district. These villages were selected from the most populated villages in the sub-district and were willing to be surveyed. Villages that refused due to the Coronavirus Disease 2019 (Covid-19) outbreak were transferred to another village. The village distribution can be seen in Fig. 1. The Secondary data were acquired from the Gunungkidul Regency Central Bureau of Statistics website and the village government. These data are the basis for determining the number of residence and non-residential samples using the stratified random sampling method that INS 19-3964-1994 has specified (Herianto *et al*., 2019; Alfons and Padmi, 2018). Residential is categorized based on the family's economic condition into permanent, semi-permanent, and non-permanent. Non-residential is divided into shops, restaurants, hotels, markets, offices, and public facilities (Table 1). A door-to-door survey was carried out from January to March 2021 to collect data from 270 samples. This process applied strict health procedures regarding the Java-Bali Community Activity Restrictions (JBCAR) policy due to the Covid-19 outbreak. Before the survey, a surveyor team was formed and provided with training and safety equipment such as gloves, hand sanitizer, disinfectant liquid, and masks. Before implementing the measurement, 40-liter garbage bags were given to the residential and non-residential samples. Every day for eight consecutive days, the weight and volume of waste were measured using a 20×20×100 centimeter (cm) measuring box equipped

Table 1: Residential and non-residential samples

Residential	Samples	Non-residential	Samples
Permanent	77	Shops	103
Semi-Permanent	30	Restaurants	21
Non-Permanent	3	Hotels	6
Subtotal	**110**	Markets	8
		Offices	18
		Public facilities	4
		Subtotal	**160**

Table 2: Weight, volume, and waste density in SZGR

No	Samples group	Unit	Weight (kg)	Volume (Liter)	Density (kg/m^3)
I	Residential				
	Permanent	Person/day	0.10	0.51	204.29
	Semi-Permanent	Person/day	0.07	0.46	153.27
	Non-Permanent	Person/day	0.02	0.08	218.04
II	Non-Residential				
	Shops	(m^2/day)	0.02	0.42	54.10
	Restaurants	(m^2/day)	0.06	0.54	105.59
	Hotels	(Room/day)	0.01	0.25	43.70
	Markets	(m^2/day)	0.002	0.03	90.75
	Offices	(m^2/day)	0.0002	0.00	50.27
	Public facilities	(m^2/day)	0.003	0.04	75.64
III	Total residential waste generation		0.19	1.05	
IV	Total non-residential waste generation		0.10	1.29	
V	Total waste generation (III + IV)		0.29	2.34	

with a height scale. After the weighing process, the waste is poured into the ground to sort based on its type. Organic and inorganic waste was weighed separately before each component of the waste type is measured. The survey data was processed and presented in a table using Microsoft Excel 2019 software and graphic using the Origin 2018 software. The processed data were analyzed using a quantitative descriptive method to describe a simple summary of the basic characteristics of the sample in this type of research (Vahidi *et al*., 2017).

RESULTS AND DISCUSSION

Waste generation

The success of developing a rural solid waste management system is determined by the measurement of waste generation as a prerequisite (Taghipour *et al*., 2016). Based on the waste measurements of 16 villages, the total average waste generated by locals in SZGR every day is 0.29 kg/person, or with a population of 182,642, SZGR produces 52.90 tons of solid waste daily (Table 2). It is below the small-town classification according to INS 19-3983-1995, which is 0.625-0.70 kg/person/day. Rural waste generation in SZGR is relatively low compared to rural areas in Romania whose population is 500–15,000 and produces an average of 0.4 kg/person/day (Ciuta *et al*., 2015). It is also lower compared to the rural areas in Iran which generate waste ranging from 0.293 to 0.588 kg/person/day (Darban Astane and Hajilo, 2017; Vahidi *et al*., 2017). However, compared to rural areas in China, especially in the Tibetan Plateau, which generates 0.085 kg of waste per person per day, SZGR generates waste up to triple daily (Han *et al*., 2015a), and it is 38.6% greater compared to Southwest China's rural areas (Han *et al*., 2015b).

Fig. 2 shows that residents in each village produce various amounts of waste. The residents of Banjarejo produce the highest amount of waste at 0.59 kg/day. On the other hand, Giriwungu and Girisuko generate the smallest waste, which is 0.08 kg/person/day. Variations in the amount of waste generated in the SZGR villages show a non-uniformity

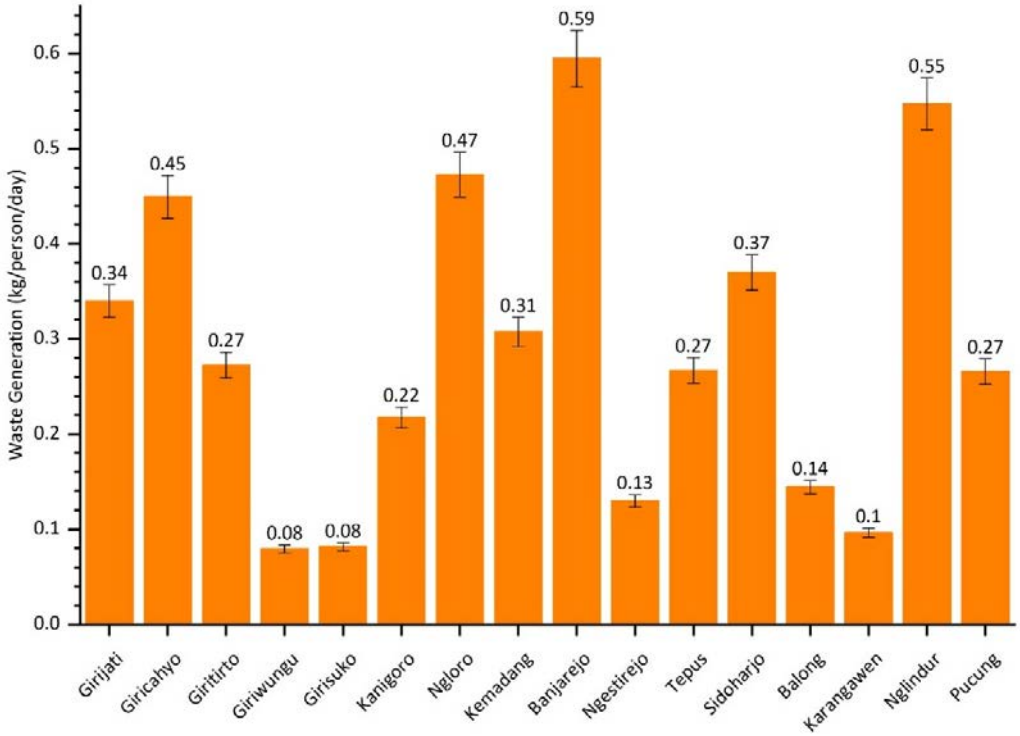

Fig. 2: Waste generation in sample villages

in the community's economic conditions. The change in people's lifestyles is one of the causes of the increasing waste generation. Waste generation and composition are influenced by socioeconomic factors such as economic activity and lifestyle (Nguyen *et al*., 2020), rural geographic location (Han *et al*., 2015b; Taghipour *et al*., 2016), and downtown attractiveness (Medjahed and Brahamia, 2019).

Based on the sample group, the waste generation originating from residential is 0.09 kg/day more than a non-residential waste generation. Permanent residential produce waste 52.63% more than semi-permanent and non-permanent in the residential category, which are only 36.84% and 10.53%, respectively (Fig. 3). The data shows that households with better economic conditions tend to produce more waste. Han *et al.* (2018) stated that an increase in family income in rural areas in developing countries affects food consumption and other necessities of life. This finding was proved by Nguyen *et al.* (2020) who found that household economic conditions and the number of family members correlated with the amount of waste generated. The dominant waste contributors from the non-residential sample are restaurants, shops, and hotels. They produce 93.9% of the total waste generated by non-residential (Fig. 2). The development of the tourism sector in SZGR also triggers the growth of commercial trade along the road to the tourism sites. During the Covid outbreak, the trading activity in SZGR continues to function despite the JBCAR implementation because they provide the essential need of locals. This traditional market in SZGR contributes 2.8% of the total non-residential waste generation. The market operates only twice a week, and the market area becomes a divider that reduces the amount of waste generated. Due to JBCAR implementation to suppress the Covid-19 outbreak, offices and other public facilities operate with a limited number of employees, which causes waste generation to be considerably small. Therefore, it can be clearly stated that local activities and the type of economy in the village determined the waste generation rate. The Mae Salong Nok countryside has waste generation up to 3 times more than SZGR. The tourist who comes to Mae Salong Nok contributes to the amount of waste other than that

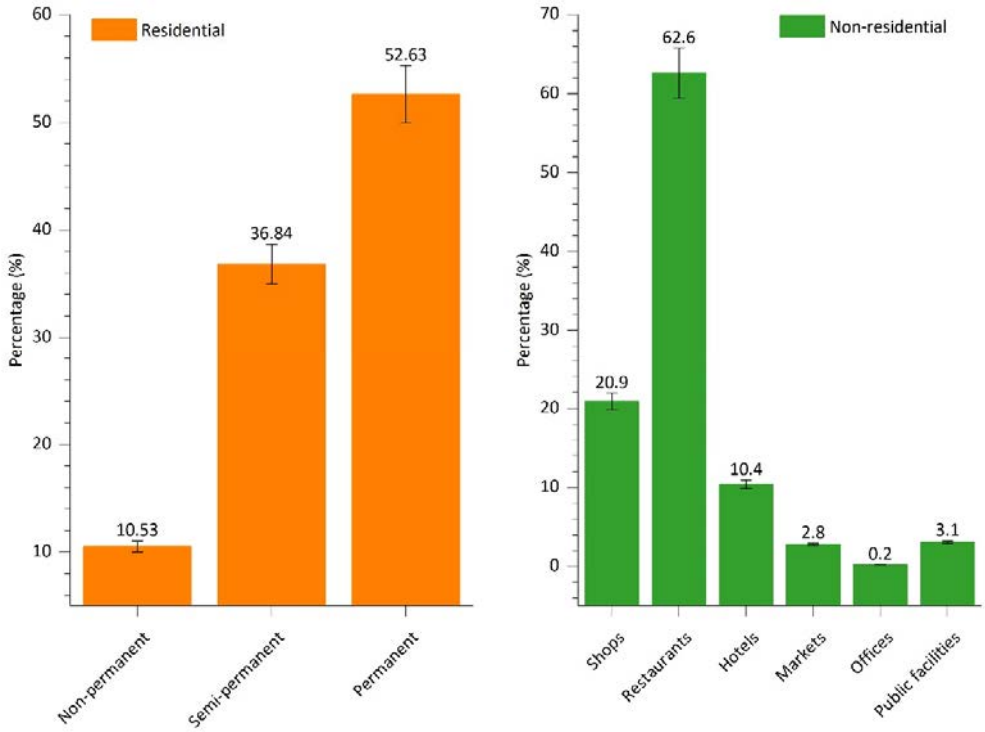

Fig. 3: Waste generation based on samples group

produced by the local community (Suma *et al*., 2019). Han *et al.* (2018) and Bilgili *et al.* (2019) agreed that economic drivers or the type of industry in rural areas affect the waste generation rate.

Waste composition and density

Understanding the composition of rural solid waste will determine the appropriate method and technology in each stage of solid waste management, starting from the storage, collection, transportation, and final processing stages. SZGR produces waste with an average composition of 87.3% organic material and 12.7% inorganic material. This proportion is similar to rural areas in developing countries. Rural areas in various developing countries such as Iran (Darban Astane and Hajilo, 2017; Vahidi *et al*., 2017; Taghipour *et al*., 2016), Egypt (Anwar *et al*., 2018), China (Han *et al*., 2015b), and Ghana (Boateng *et al*., 2016), produce more organic waste materials such as food waste, vegetables, fruits, and leaves than inorganic waste types. The most inorganic waste produced by rural areas in SZGR is plastic, with a proportion of 10.1%, followed by glass waste (1.7%), other materials (0.5%), and fabrics (0.4%). Plastic is the most common inorganic waste type, with less than 20% of the total waste produced by rural areas (Anwar *et al*., 2018; Darban Astane and Hajilo, 2017; Vahidi *et al*., 2017).

All sample villages generally produce waste with a composition of more organic waste than inorganic waste. Organic materials in the form of food waste, leaves, and paper were found in all villages, while inorganic materials produced by all villages were in the form of plastic (Fig. 4). Sidoharjo became the village with the largest organic material whereas the most inorganic material was found in Girijati village. The types of food waste and leaves in Pucung and Girijati villages have a small portion compared to other types of waste. The non-residential sample, which is larger than the residential sample, could be the reason. Various economic activities in an area will affect the waste composition. According to Boateng

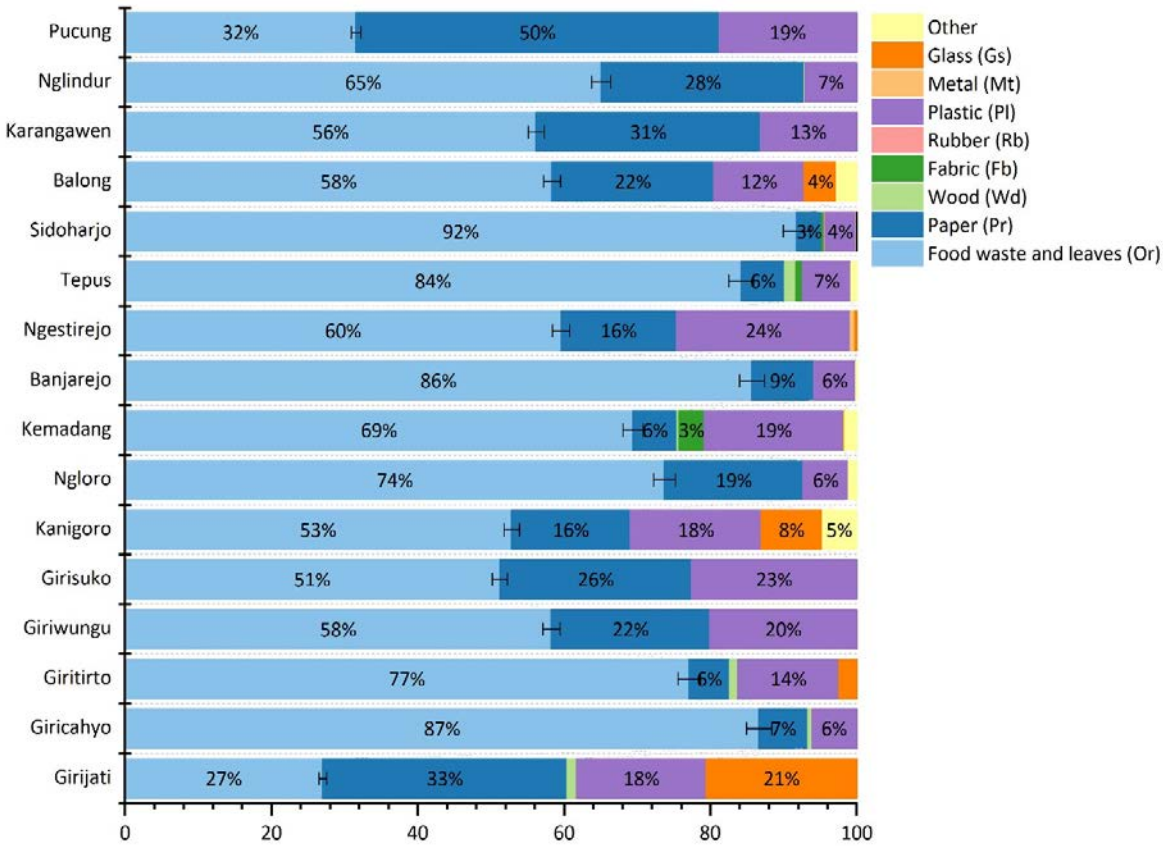

Fig. 4: Waste composition based on sample villages

et al. (2016), rural residents still buy raw materials for fresh food in large portions, thus producing the largest amount of organic waste. Furthermore, different types of industries in rural areas significantly influence the characteristics of waste (Han *et al*., 2018; Bilgili *et al*., 2019). Based on the sample group, the residential sample produces an average of 92.84% organic waste, while the rest is inorganic waste. Plastic, fabric, and other materials are 6.7%, 0.39%, and 0.02%, respectively. Glass, metal, and rubber wastes were not found in the residential samples (Fig. 5). The non-permanent residential produces more organic waste compared to semi-permanent and permanent. It shows that the family's economic condition also encourages the diversity of waste produced. Organic waste is discovered in all social strata, but as the family economy increases, the proportion of inorganic waste types increases (Ramachandra *et al*., 2018). The composition of recycled waste originating from residential in SZGR tends not to vary. The locals have a low level of consumption, and they tend to cook their daily meals using raw materials from around their yards.

The non-residential sample produced an average of 86.33% organic waste; the rest was inorganic waste (Fig. 6). Markets and restaurants generate the most organic waste, while the most inorganic waste comes from shops, hotels, offices, and public facilities. The local markets generate organic waste such as leftover vegetables, fruits, fish, poultry, and other easily rotten or unsold products. Meanwhile, restaurants generally produce raw leftovers and food scraps. Meanwhile, paper is mostly disposed of by offices and shops, while plastic waste is collected from shops, hotels, and other public facilities.

On average, the solid waste density produced by SZGR is 110.6 kg/m^3. The residential area has a higher density value than the non-residential (Fig. 7). High

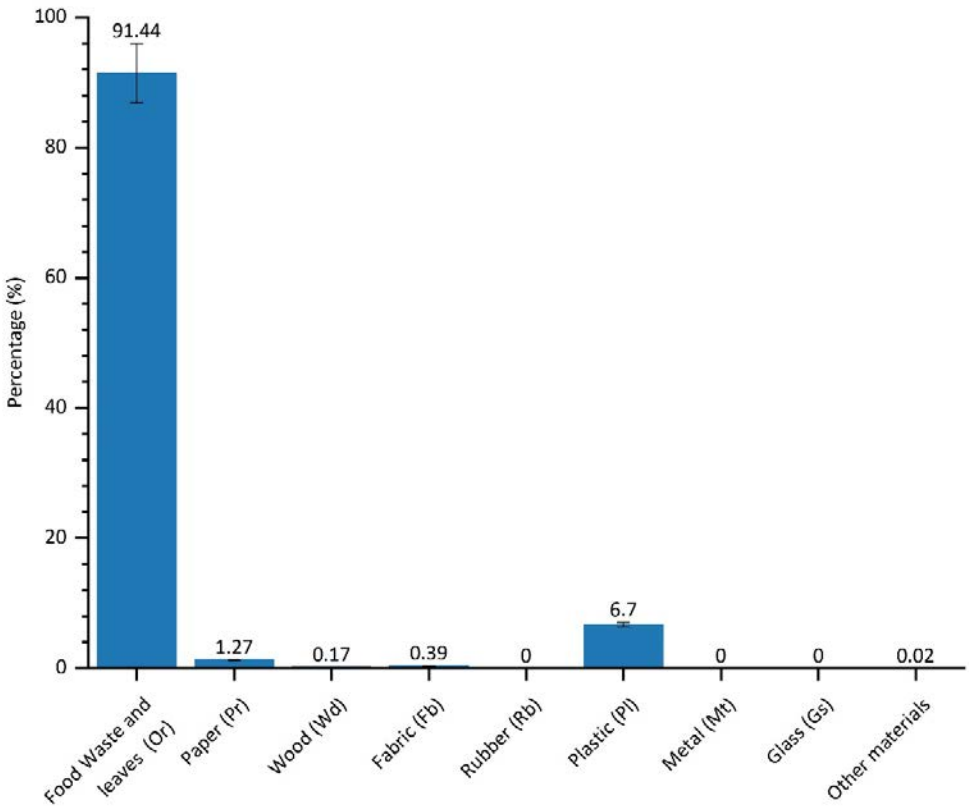

Fig. 5: Residential waste composition

solid waste density indicates that the residential sample produces less recyclable waste. These results align with the variety of inorganic waste discovered in non-residential premises. In a different case, rural areas in Western China, for example, have low solid waste density because they contain large amounts of paper/cardboard and plastic or rubber (Han *et al*., 2019). The solid waste density will determine the type of transportation ideal for transporting waste.

According to the sample villages, the waste density shows that Giricahyo has the highest average waste density, and Giriwungu has the smallest (Fig. 8). The waste density shows differences in organic and inorganic compositions portion in each village. A high-density value indicates that the village produces more waste with high moisture and low calories. The three villages with the highest solid waste density, namely Giricahyo (93.9%), Ngloro (92.7%), and Banjarejo (94.2%), produced a higher portion of organic material than inorganic (Fig. 8). However, there is a compelling finding in Sidoharjo Village. This village has an organic composition of (95.3%), with a solid waste density of 151.16 kg/m^3. Allegedly, the inorganic waste in that village has a larger dimension, thus reducing the waste density. The waste density determines the appropriate treatment, especially for organic waste, which is ideal as a raw material for composting and biogas. According to Syafrudin *et al*. (2018), waste density affects the decomposition rate and the content of methane gas used for biogas.

The generation, composition, and density of waste in SZGR are well known and have similarities with rural areas in other developing countries, including applied waste management. SZGR's rural waste management practices are still conventional. The residents burn and stockpile their generated waste (Masjhoer *et al*., 2022). In Brazil, rural waste is commonly burned or buried without any safeguards (Caiado Couto *et al*., 2021). In rural China, most waste is burned and dumped on roads, rivers, and open dumps (Cao *et al*., 2018). The processing of organic waste requires additional attention compared to inorganic waste.

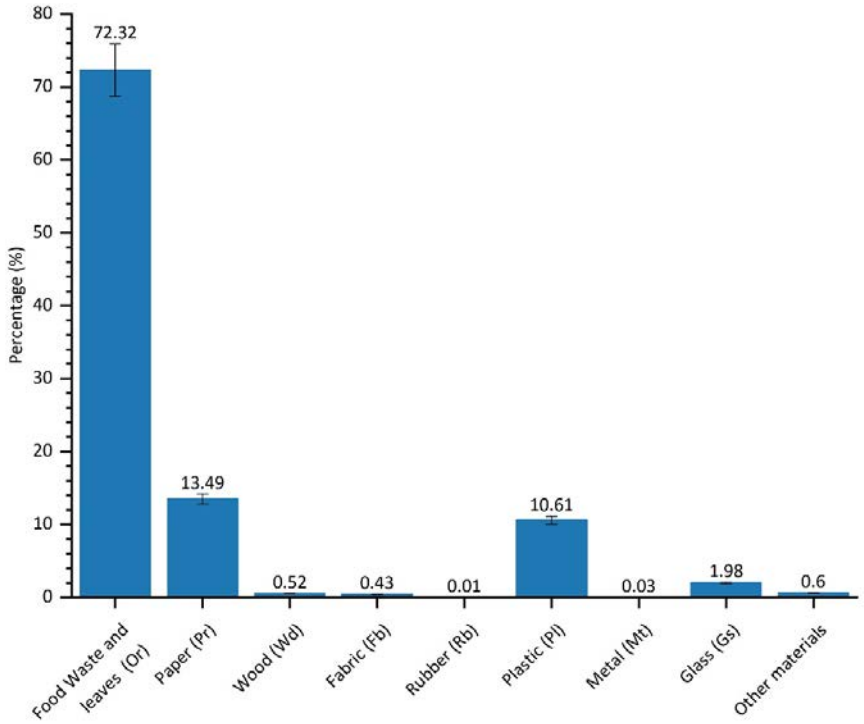

Fig. 6: Non-residential waste composition

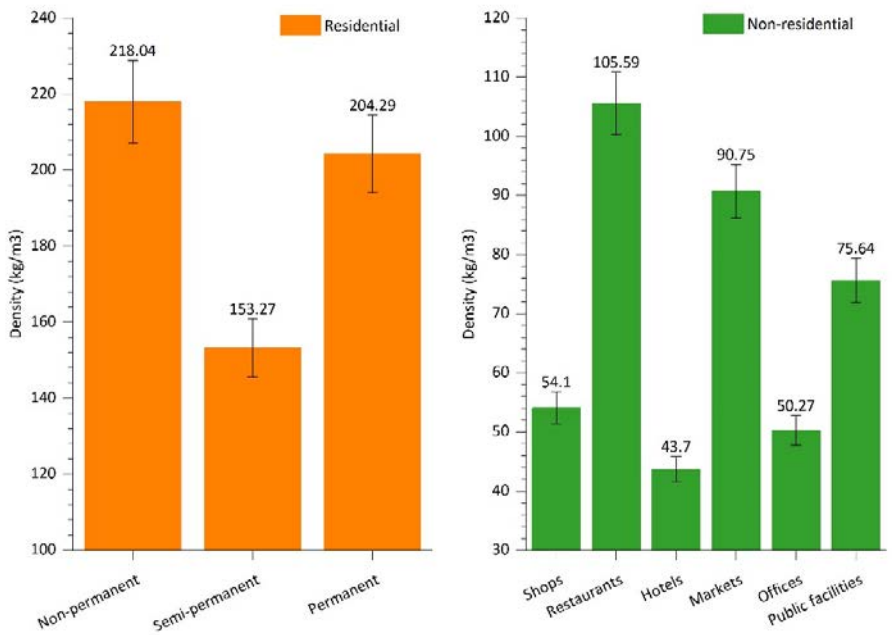

Fig. 7: Waste density in the Southern Zone of Gunungkidul Regency

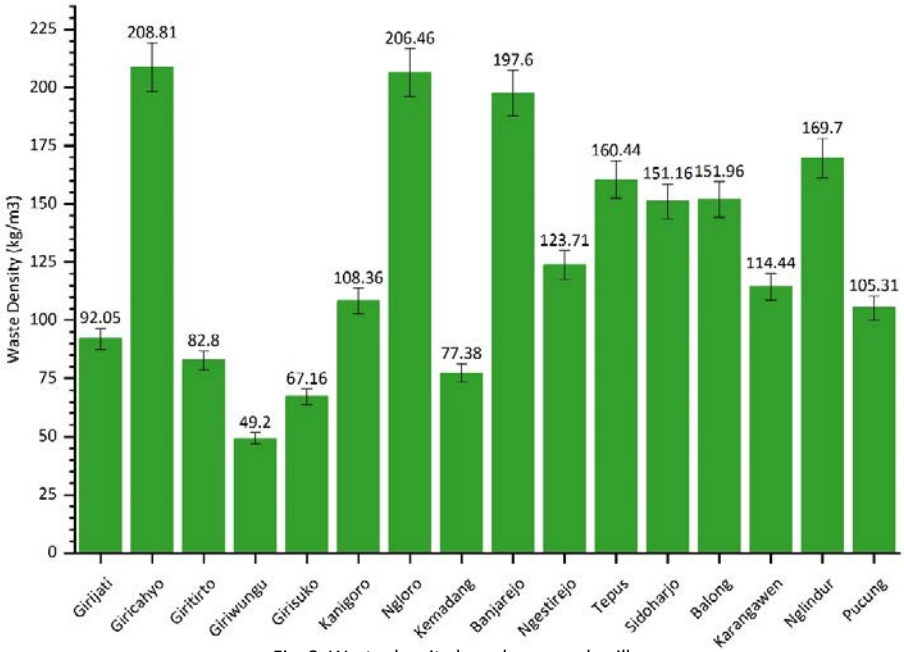

Fig. 8. Waste density based on sample villages

The combustion of organic matter produces harmful and toxic gases because it has a low calorific value (Kim and Kim, 2010). Research by Lima *et al*. (2021) shows that open waste burning threatens the health of rural communities and aquatic ecosystems. The smoke produced from burning waste contains Particulate Matter (PM), carcinogenic dioxins, and various other harmful pollutants such as nitrogen oxides (NOx), sulfur dioxide (SO_2), carbon monoxide (CO), and non-methane volatile organic compounds (NMVOCs) (Das *et al*., 2018). Open burning can trigger a variety of health impacts, such as acute and chronic respiratory disease, cardiovascular disease, and cancer, in addition to impacts on the local climate. Therefore, the burning of organic waste potentially causes environmental hazards. On the other hand, landfilling methods for waste give rise to leachate, groundwater pollution, and toxic emissions (Shahnazari *et al*., 2021). The risks that can arise from improperly-managed landfill include groundwater contamination caused by leachate, methane gas emissions, and combustion fumes containing harmful gases. Unsustainable waste management can impact human health, such as the emergence of cholera, skin infections, and chronic diseases caused by hazardous chemical waste (Al-Dailami *et al*., 2022). In line with the increasing volume of waste generation, waste management that is not environmentally friendly can harm health and disrupt the preservation of environmental functions. The environmental quality needs to be improved to ensure future welfare and quality of life. Human behavior can affect the life and well-being of humans and other living creatures (Abdul and Syafrudin, 2018). Waste management in rural areas is more dependent on citizen participation because of several characteristics, such as a relatively large area, scattered sources of waste, and difficult transportation (Shi *et al*., 2021). Waste generated by the community should be managed at the waste source by sorting it based on the waste composition. Waste sorting will facilitate the handling of waste in the next stage. Segregated waste will facilitate handling in landfills and thermal incinerators (Quan *et al*., 2022). Meanwhile, mixed organic and inorganic waste will be difficult to use as raw materials in composting, biogas, or recycling (Syafrudin *et al*., 2018). Reducing waste at the source of waste is the most effective strategy and solution to overcoming the problem of waste accumulation in rural areas (Shen *et al*., 2020; Mihai and Grozavu, 2019). Al-Dailami *et al*. (2022) stated that the application of Reduce Reuse and Recycle (3R) is considered the

best strategy in solid waste management. The best and most practical method of processing organic waste is by recycling organic waste into fertilizer (Shahnazari *et al*., 2021). Organic waste will go through decomposition by nature into nutrients. However, uncontrolled quantities and conditions in the decomposition process can cause environmental problems. SZGR produces 87.3% of organic waste that needs to be handled by a raw material-oriented method. Chen, Zhang, and Yuan (2020) argue that organic materials must be viewed as raw materials and have value. Organic materials can be used as raw materials to manufacture fertilizers through the composting process. Composting organic waste into fertilizer is a superior technology in rural waste management (Patwa *et al*., 2020; de Morais Lima and Paulo, 2018). This process decomposes organic waste in a faster time and reduces volume significantly, and reduces the amount of waste disposed of in the landfill. The reduction in organic waste volume results from an overhaul of microbial activity (Sayara *et al*., 2022). Composting technique is a method that can reduce the volume of organic waste by half (Ma *et al*., 2017). The waste bank program promoted by the Gunungkidul government to reduce waste at the source (Faradina *et al*., 2020) needs to consider organic waste as a potential raw material that can be transformed into a valuable main product. Organic fertilizers produced from the composting process are considered more effective in reducing waste and do not require expensive technology in processing; thus, people can do it at the household level. Rural organic waste is more biodegradable compared to that of urban areas, and the practice of composting is an alternative that households can do (Báreková *et al*., 2020). The organic waste composting practice is a form of good waste management based on reduction, reuse, and recycling principles (Han *et al*., 2015a). SZGR is a karst area with nutrient-poor soil that can be improved by adding nutrient-rich organic fertilizer. The farmers will also have economic benefits from using organic fertilizers. They can produce and use organic fertilizers to replace chemical ones. However, efforts to apply organic fertilizers to the community in SZGR need to be accompanied by the socialization of the nutrient content and economic value of organic fertilizers (Chen *et al*., 2020).

CONCLUSIONS

Population and economic growth in rural areas lead to waste generation, even at a different level from the urban. Unfortunately, local governments in developing countries do not give more attention to waste services in rural areas. This condition leads rural communities to manage their waste conventionally, such as by piling them up or burning them in the open air. However, this conventional waste management can trigger environmental problems and threaten human health. The initial data on waste generation and composition produced by rural areas will determine the ideal method and technology for designing the solid waste management system. The results showed that the generation and composition of rural waste in SZGR were categorized into the small-town classification. Although the generation of rural waste is not as large as in urban areas, it still requires proper waste management. In SZGR, the composition of organic waste is greater than inorganic waste. Commercial activities generate a more diverse waste composition than residential. The calculation of waste density also supports the domination of organic waste. The waste characteristics produced in the Southern Zone of Gunungkidul are not much different from most rural areas in developing countries. The results of this study certainly add information and serve as a comparison for formulating rural waste management strategies in a wider context. Based on the research result, local governments need to consider the generation and composition of waste as a milestone to improve the waste management system quality. Rural waste management needs to see organic waste as the primary management material. Abundant organic waste should be the primary focus to be handled and seen as raw materials for other valuable products. Composting organic waste will provide many benefits for the residents who work as farmers. In addition, this method can help extend the life of the landfill capacity because the volume of organic waste will be reduced by half. Composting requires the local community's participation in adopting composting as a rational and profitable method. Therefore, further research is needed to provide information on the community's willingness to participate in composting. Moreover, a feasibility study of the fertilizer content

and the economic feasibility of its application may also be required for further research.

AUTHOR CONTRIBUTIONS

J.M. Masjhoer, the corresponding author and second author has contributed in the data analysis, interpreted the results, and preparing the manuscript. S. Syafrudin as the first author supervising the second author, conceptualization, and methodology for the research. M. Maryono participated in supervision-design and revision the manuscript.

ACKNOWLEDGEMENT

The second author would like to thank the Domestic Postgraduate Education Scholarship [No: B/67/D.D3/KD.02.00/2019] from the Ministry of Research, Technology and Higher Education of the Republic of Indonesia. Most importantly, authors would like to thank each participant in this study for their willingness to be surveyed during this Covid-19 pandemic.

CONFLICT OF INTEREST

The author declares that there is no conflict of interests regarding the publication of this manuscript. In addition, the ethical issues, including plagiarism, informed consent, misconduct, data fabrication and/or falsification, double publication and/or submission, and redundancy have been completely observed by the authors.

OPEN ACCESS

PUBLISHER'S NOTE

GJESM Publisher remains neutral with regard to jurisdictional claims in published maps and institutional afflictions.

ABBREVIATIONS

%	Percent
3R	Reduce Reuse and Recycle
CO	Carbon monoxide
Covid-19	Coronavirus Disease 2019
cm	Centimeter
Fig.	Figure
INS	Indonesian National Standard
JBCAR	The Java-Bali Community Activity Restrictions
kg/day	Kilogram per day
kg/capita/day	Kilogram per capita per day
kg/m^3	Kilogram per meter cubic
kg/person/day	Kilogram per person per day
km^2	Square kilometer
L/person/day	Liter per person per day
m^2/day	Square meter per day
NMVOCs	Non-methane volatile organic compounds
NOx	Nitrogen oxides
PM	Particulate matter
SO_2	Sulfur dioxide
SZGR	Southern Zone of Gunungkidul Regency
UNESCO	The United Nations Educational, Scientific and Cultural Organization

REFERENCES

Abdel-Shafy, H.I.; Mansour, M.S.M., (2018). Solid waste issue: Sources, composition, disposal, recycling, and valorization. Egypt. J. Pet., 27(4): 1275–1290 **(16 pages).**

Abdul, M.; Syafrudin, S., (2018). The importance of integration waste management aspects as a system in good and sustainable waste management. E3S Web Conferences., 73(07012): 1-5 **(5 pages)**.

Al-Dailami, A.; Ahmad, I.; Kamyab, H.; Abdullah, N.; Koji, I.; Ashokkumar, V.; Zabara, B., (2022). Sustainable solid

waste management in Yemen: Environmental, social aspects, and challenges. Biomass Convers. Biorefin., 2022: 1-27 **(27 pages)**.

Alfons, A.B.; Padmi, T., (2018). Multi-Criteria Analysis for selecting solid waste management concept case study: Rural areas in Sentani Lake Region, Jayapura. Indones. J. Urban Environ. Technol., 2(1): 88–101 **(14 pages).**

Anwar, S.; Elagroudy, S.; Abdel Razik, M.; Gaber, A.; Bong, C.P.C.; Ho, W.S., (2018). Optimization of solid waste management in rural villages of developing countries. Clean Technol. Environ. Policy., 20(3): 489–502 **(14 pages).**

Báreková, A.; Tátošová, L.; Kišš, V.; Kovácová, M., (2020). Composition of the separated green waste in rural and urban area. J. Ecol. Eng., 21(5): 234–239 **(6 pages).**

Bilgili, M.S.; Adar, E.; Yildiz, S.; Sezer, K., (2019). Characterisation of wastes collected from beaches, coastlines, marine surface cleaning processes and ships: A case study of Istanbul. Waste Manage. Res., 37(6): 621–630 **(10 pages).**

Boateng, S.; Amoako, P.; Appiah, D.O.; Poku, A.A.; Garsonu, E.K., (2016). Comparative Analysis of households solid waste management in rural and urban Ghana. J. Environ. Public Health., 5780258: 1-10 **(10 pages)**.

Caiado Couto, L.; Campos, L.C.; da Fonseca-Zang, W.; Zang, J.; Bleischwitz, R., (2021). Water, waste, energy and food nexus in Brazil: Identifying a resource interlinkage research agenda through a systematic review. Renew. Sustain. Energy Rev. 138: 110554 **(18 pages)**.

Cao, S.; Xu, D.; Liu, S., (2018). A study of the relationships between the characteristics of the village population structure and rural residential solid waste collection services: Evidence from China. Int. J. Environ. Res. Public Health. 15(11): 1–17 **(17 pages)**.

Chen, T.; Zhang, S.; Yuan, Z., (2020). Adoption of solid organic waste composting products: A critical review. J. Cleaner. Prod., 272: 122712 **(10 pages)**.

Ciuta, S.; Apostol, T.; Rusu, V., (2015). Urban and rural MSW stream characterization for separate collection improvement. Sustainability., 7(1): 916–931 **(16 pages)**.

Darban Astane, A.R.; Hajilo, M., (2017). Factors affecting the rural domestic waste generation. Global J. Environ. Sci. Manage., 3(4): 417–426 **(10 pages)**.

Das, B.; Bhave, P.V.; Sapkota, A.; Byanju, R.M., (2018). Estimating emissions from open burning of municipal solid waste in municipalities of Nepal. Waste Manage., 79(2018): 481–490 **(10 pages)**.

de Morais Lima, P.; Paulo, P.L., (2018). Solid-waste management in the rural area of Brazil: A case study in Quilombola communities. J. Mater. Cycles Waste Manage., 20(3): 1583–1593 **(11 pages)**.

Faradina, D.; Maryono, M.; Warsito, B., (2020). The role of waste banks in reducing waste in Gunung Kidul Regency. E3S Web Conferences., 202(18): 1–8 **(8 pages)**.

Gunungkidul, B.P.S.K., (2020). Kabupaten Gunungkidul dalam Angka "Penyediaan Data untuk Perencanaan Pembangunan." BPS Badan Pusat Statistik Kabupaten Gunungkidul.

Han, Z.; Dan, Z.; Shi, G.; Shen, L.; Xu, W.; Xie, Y., (2015a). Characteristics and management of domestic waste in a rural area of the Tibetan Plateau. J. Air Waste Manage. Assoc., 65(11): 1365–1375 **(11 pages)**.

Han, Z.; Liu, D.; Lei, Y.; Wu, J.; Li, S., (2015b). Characteristics and management of domestic waste in the rural area of Southwest China. Waste Manage. Res., 33(1): 39–47 **(9 pages)**.

Han, Z.; Liu, Y.; Zhong, M.; Shi, G.; Li, Q.; Zeng, D.; Zhang, Y.; Fei, Y.; Xie, Y., (2018). Influencing factors of domestic waste characteristics in rural areas of developing countries. Waste Manage., 72(2018): 45–54 **(10 pages)**.

Han, Z.; Ye, C.; Zhang, Y.; Dan, Z.; Zou, Z.; Liu, D.; Shi, G., (2019). Characteristics and management modes of domestic waste in rural areas of developing countries: A case study of China. Environ. Sci. Pollut. Res., 26(9): 8485–8501 **(17 pages)**.

Herianto, H.; Maryono, M.; Budihardjo, M.A., (2019). Factors affecting waste generation: Household study in Palangka Raya City, Central Kalimantan. E3S Web Conferences., 125: 7–11 **(5 pages)**.

Hoang, M.G.; Fujiwara, T.; Pham Phu, S.T.; Nguyen Thi, K.T., (2017). Predicting waste generation using Bayesian model averaging. Global J. Environ. Sci. Manage., 3(4): 385–402 **(18 pages)**.

Kim, M.H.; Kim, J.W., (2010). Comparison through a LCA evaluation analysis of food waste disposal options from the perspective of global warming and resource recovery. Sci. Total Environ., 408(19): 3998–4006 **(9 pages)**.

Lima, P. de M.; Morais, M.F. de; Constantino, M.A.; Paulo, P.L.; Magralhães Filho, F.J.C., (2021). Environmental assessment of waste handling in rural Brazil: Improvements towards circular economy. Clean. Environ. Syst., 2: 100013 **(9 pages)**.

Liu, A.; Osewe, M.; Wang, H.; Xiong, H., (2020). Rural residents' awareness of environmental protection and waste classification behavior in Jiangsu, China: An empirical analysis. Int. J. Environ. Res. Public Health., 17(23): 1–12 **(12 pages)**.

Ma, Y.; Yin, Y.; Liu, Y., (2017). A holistic approach for food waste management towards zero-solid disposal and energy/resource recovery. Bioresour. Technol., 228: 56–61 **(6 pages)**.

Masjhoer, J.M., (2018). Partisipasi pelaku usaha pariwisata dalam pengelolaan sampah di Pantai Pulang Sawal, Kabupaten Gunungkidul, Yogyakarta. J. Pariwisata Terap., 2(2): 122-133 **(12 pages)**.

Masjhoer, J.M.; Retawimbi, A.Y.; Sari, Y.S., (2020).

Participation of local restaurants in solid waste management in south coast of Gunungkidul Regency, Indonesia. J. Commun. Based Environ. Eng. Manage., 4(1): 1–8 **(8 pages)**.

Masjhoer, J.M.; Syafrudin, S.; Maryono, M., (2022). Rural waste management system in southern zone of Gunungkidul Regency. Environ. Res. Eng. Manage., 78(1): 70–82 **(13 pages)**.

Medjahed, H.; Brahamia, K., (2019). Characterization of solid waste from commercial activities and services in the municipality of Annaba, Algeria. J. Air Waste Manage. Assoc., 69(11): 1293–1303 **(11 pages)**.

Mihai, F.C.; Grozavu, A., (2019). Role of waste collection efficiency in providing a cleaner rural environment. Sustainability. 11(23): 6855 **(22 pages)**.

Nguyen, K.L.P.; Chuang, Y.H.; Chen, H.W.; Chang, C.C., (2020). Impacts of socioeconomic changes on municipal solid waste characteristics in Taiwan. Resour. Conserv. Recycl., 161: 104931 **(15 pages)**.

Nguyen, T.T.; Watanabe, T., (2019). Win-win outcomes in waste separation behavior in the rural area: A case study in vietnam. J. Cleaner Prod., 230: 488–498 **(11 pages)**.

Nxumalo, S.M.; Mabaso, S.D.; Mamba, S.F.; Singwane, S.S., (2020). Plastic waste management practices in the rural areas of Eswatini. Social Sci. Humanit. Open., 2(1): 100066 **(11 pages)**.

Patwa, A.; Parde, D.; Dohare, D.; Vijay, R.; Kumar, R., (2020). Solid waste characterization and treatment technologies in rural areas: An Indian and international review. Environ. Technol. Innovation., 20: 101066 **(15 pages)**.

Programme, U.N.H.S., (2010). Solid Waste Management in the World's Cities – Water and Sanitation in the World's Cities 2010, United Nations Human Settlements Programme (UN-HABITAT). Earthscan.

Qi, D.; Lai, W.; Roe, B.E., (2021). Food waste declined more in rural Chinese households with livestock. Food Policy., 98: 101893 **(15 pages)**.

Quan, L.M.; Kamyab, H.; Yuzir, A.; Ashokkumar, V.; Hosseini, S.E.; Balasubramanian, B.; Kirpichnikova, I., (2022). Review of the application of gasification and combustion technology and waste-to-energy technologies in sewage sludge treatment. Fuel., 316: 123199 **(22 pages)**.

Ramachandra, T.V.; Bharath, H.A.; Kulkarni, G.; Han, S.S., (2018). Municipal solid waste: Generation, composition and GHG emissions in Bangalore, India. Renewable Sustainable Energy Rev., 82: 1122–1136 **(15 pages)**.

Sayara, T.; Shadouf, M.; Issa, H.; Obaid, H.; Hanoun, R., (2022). Home composting of food wastes using rotary drum reactor as an alternative treatment option for organic household wastes. J. Ecol. Eng., 23(6): 139–147 **(9 pages)**.

Syafrudin, S.; Prasetyo, S.B.; Wisnu, W.I., (2018). Composition of domestic solid waste on biogas production and characteristic in MSW landfill. E3S Web Conferences., 73: 10–13 **(4 pages)**.

Kubanza, N.S.; Simatele, M.D., (2019). Sustainable solid waste management in developing countries: A study of institutional strengthening for solid waste management in Johannesburg, South Africa. J. Environ. Plann. Manage., 63(2): 1–14 **(14 pages)**.

Shahnazari, A.; Pourdej, H.; Kharage, M.D., (2021). Ranking of organic fertilizer production from solid municipal waste systems using analytic hierarchy process (AHP) and VIKOR models. Biocatal. Agric. Biotechnol., 32: 101946 **(7 pages)**.

Shen, J.; Zheng, D.; Zhang, X.; Qu, M., (2020). Investigating rural domestic waste sorting intentions based on an integrative framework of Planned Behavior Theory and Normative Activation Models: Evidence from Guanzhong Basin, China. Int. J. Environ. Res. Public Health., 17(13): 4887 **(14 pages)**.

Shi, J. gang; Xu, K.; Si, H.; Song, L.; Duan, K., (2021). Investigating intention and behaviour towards sorting household waste in Chinese rural and urban–rural integration areas. J. Cleaner Prod., 298: 126827 **(9 pages)**.

Suma, Y.; Pasukphun, N.; Hongtong, A.; Keawdunglek, V.; Laor, P.; Apidechkul, T., (2019). Waste composition evaluation for solid waste management guideline in highland rural tourist area in Thailand. Appl. Environ. Res., 41(2): 13–26 **(14 pages)**.

Taghipour, H.; Amjad, Z.; Aslani, H.; Armanfar, F.; Dehghanzadeh, R., (2016). Characterizing and quantifying solid waste of rural communities. J. Mater. Cycles Waste Manage., 18(4): 790–797 **(8 pages)**.

Vahidi, H.; Nematollahi, H.; Padash, A.; Sadeghi, B.; RiyaziNejad, M., (2017). Comparison of rural solid waste management in two central provinces of Iran. Environ. Energy Econ. Res., 1(2): 195–206 **(12 pages)**.

Wang, F.; Cheng, Z.; Reisner, A.; Liu, Y., (2018). Compliance with household solid waste management in rural villages in developing countries. J. Cleaner Prod., 202: 293–298 **(6 pages)**.

Yang, L.; Liu, G.; Zhu, Q.; Zheng, M., (2019). Small-scale waste incinerators in rural China: Potential risks of dioxin and polychlorinated naphthalene emissions. Emerging Contam., 5: 31–34 **(4 pages)**.

Yukalang, N.; Clarke, B.; Ross, K., (2018). Solid waste management solutions for a rapidly urbanizing area in Thailand: Recommendations based on stakeholder input. Int. J. Environ. Res. Public Health. 15(7): 1–23 **(23 pages)**.

AUTHOR (S) BIOSKETCHES

Syafrudin, S., Ph.D., Professor, Department of Environmental Engineering, Faculty of Engineering, Diponegoro University, Semarang, Indonesia.
- Email: *udin_syaf@yahoo.com*
- ORCID: 0000-0002-1187-6361
- Web of Science ResearcherID: GVU-6363-2022
- Scopus Author ID: 57216353895
- Homepage: https://ft.undip.ac.id/prof-dr-ir-syafrudinces-m-t/

Masjhoer, J.M., M.Sc., Instructor, Environmental Science Doctoral Program, School of Postgraduate Studies, Diponegoro University, Semarang, Indonesia.
- Email: *jussac@students.undip.ac.id*
- ORCID: 0000-0001-7042-2098
- Web of Science ResearcherID: ACF-4452-2022
- Scopus Author ID: 57576494200
- Homepage: https://pasca.undip.ac.id/

Maryono, M., Ph.D., Associate Professor, Department of Urban and Regional Planning, Faculty of Engineering, Diponegoro University, Semarang, Indonesia.
- Email: *m.maryono@undip.ac.id*
- ORCID: 0000-0003-4626-2068
- Web of Science ResearcherID: GQH-5993-2022
- Scopus Author ID: 57201121365
- Homepage: https://pwk.ft.undip.ac.id/id/dr-eng-maryono-st-mt/

HOW TO CITE THIS ARTICLE

Syafrudin, S.; Masjhoer, J.M.; Maryono, M., (2023). Characterization and quantification of solid waste in rural regions. Global J. Environ. Sci. Manage., 9(2): 337-352.

DOI: 10.22034/gjesm.2023.02.12

url: https://www.gjesm.net/article_696590.html

PUBLICATION ETHICS

The ethical policy of GJESM is based on the Committee on Publication Ethics (COPE) guidelines and complies with International Committee of GJESM Editorial Board codes of conduct. Readers, authors, reviewers and editors should follow these ethical policies once working with GJESM. The ethical policy of GJESM is liable to determine which of the typical research papers or articles submitted to the journal should be published in the concerned issue. For information on this matter in publishing and ethical guidelines please visit http://publicationethics.org

Duties and Responsibilities of Publishers

1. GJESM is committing to ensure that editorial decisions on manuscript submissions are the final.
2. GJESM is promising to ensure that the decision on manuscript submissions is only made based on professional judgment and will not be affected by any commercial interests.
3. GJESM is committing to maintain the integrity of academic and research records.
4. GJESM is monitoring the ethics by Editor-in-Chief, Associate Editors, Editorial Board Members, Reviewers, Authors, and Readers.
5. GJESM is always checking the plagiarism and fraudulent data issues involving in the submitted manuscript.
6. GJESM is always willing to publish corrections, clarifications and retractions involving its publications as and when needed.

Duties and Responsibilities of Editors

1. The Editors of the journal should have the full authority to reject/accept a manuscript.
2. The Editors of the journal should maintain the confidentiality of submitted manuscripts under review or until they are published.
3. The Editor-in-Chief should take a decision on submitted manuscripts, whether to be published or not with other editors and reviewers
4. The Editors of the journal should preserve the anonymity of reviewers.
5. The Editors of the journal should disclose and try to avoid any conflict of interest.
6. The Editors of the journal should maintain academic integrity and strive to meet the needs of readers and authors.
7. The Editors of the journal should be willing to investigate plagiarism and fraudulent data issues and willing to publish corrections, clarifications, retractions, and apologies when needed.
8. The Editors of the journal should have the limit themselves only to the intellectual content.
9. The Editors of the journal must not disclose any information about submitted manuscripts to anyone other than the corresponding author, reviewers, potential reviewers, other editorial advisers, and the publisher, as appropriate.
10. Unpublished materials disclosed in a submitted paper will not be used by the editor or the members of the editorial board for their own research purposes without the author's explicit written consent.

Duties and Responsibilities of Reviewers

1. The Reviewers of the journal should assist the Editors in taking the decision for publishing the submitted manuscripts.
2. The Reviewers should maintain the confidentiality of manuscripts, which they are invited to review.
3. The Reviewers should provide comments in time that will help editors to make decision on the submitted manuscript to be published or not.
4. The Reviewers are bound to treat the manuscript received for peer reviewing as confidential, and must not use the information obtained through peer review for personal advantage.
5. The Reviewers comments against each invited manuscript should be technical, professional and objective.
6. The Reviewers should not review the manuscripts in which they have found conflicts of interest with any of the authors, companies, or institutions.
7. The Reviewers should disclose and try to avoid any conflict of interest.

Duties and Responsibilities of Authors

1. Manuscripts must be submitted only in English and should be written according to sound grammar and proper terminology.
2. Manuscripts must be submitted with the understanding that they have not been published elsewhere (except in the form of an abstract or as part of a published lecture, review, or thesis) and are not currently under consideration by another journal published by or any other publisher.
3. The submitting (corresponding) author is responsible for ensuring that the manuscript article's publication has been approved by all the other coauthors.
4. In order to sustain the peer review system, authors have an obligation to participate in peer review process to evaluate manuscripts from others.
5. It is also the authors' responsibility to ensure that the manuscripts emanating from a particular institution are submitted with the approval of the necessary institution.
6. It is a condition for submission of a manuscript that the authors permit editing of the paper for readability.
7. Authors are requested to clearly identify who provided financial support for the conduct of research and/or preparation of the manuscript and briefly describe the role of the funder/sponsor in any part of the work.
8. A copy right release and conflict of interest disclosure form must be signed by the corresponding author in case of multiple authorships, prior to the acceptation of the

manuscript, by all authors, for publication to be legally responsible towards the Journal ethics and privacy policy.

9. Under open access license, authors retain ownership of the copyright for their content, but allow anyone to download, reuse, reprint, modify, distribute, and/ or copy the content as long as the original authors and source are cited properly.
10. All authors have agreed to allow the corresponding author to serve as the primary correspondent with the editorial office, to review the edited manuscript and proof.
11. When author(s) discovers a significant error or inaccuracy in his/her own published work, it is the author's obligation to promptly notify the journal editor or publisher to retract or correct the manuscript.
12. All authors must know that that the submitted manuscripts under review or published with GJESM are subject to screening using Plagiarism Prevention Software. Plagiarism is a serious violation of publication ethics.

Violation of Publication Ethics

1. **Plagiarism:** Plagiarism is intentionally using someone else's ideas or other original material as if they are one's own. Copying even one sentence from someone else's manuscript, or even one of your own that has previously been published, without proper citation is considered by GJESM Journals as plagiarism. All manuscripts under review or published with GJESM are subject to screening using plagiarism prevention software. Thus, plagiarism is a serious violation of publication ethics. The development of CrossCheck is a service that helps editors to verify the originality of papers. CrossCheck is powered by the Ithenticate software from iParadigms, known in the academic community as providers of Turnitin. For a searchable list of all journals in the CrossCheck database, please visit: www.ithenticate.com/search
2. **Data Fabrication and Falsification:** Data fabrication and falsification means the researcher did not really carry out the study, but made up data or results and had recorded or reported the fabricated information. Data falsification means the researcher did the experiment, but manipulated, changed, or omitted data or results from the research findings.
3. **Simultaneous Submission:** Simultaneous submission occurs when a manuscript (or substantial sections from a manuscript) is submitted to a journal when it is already under consideration by another journal.
4. **Duplicate Publication:** Duplicate publication occurs when two or more papers, without full cross referencing, share essentially the same hypotheses, data, discussion points, and conclusions.
5. **Redundant Publications:** Redundant publications involve the inappropriate division of study outcomes into several articles, most often consequent to the desire to plump academic vitae.
6. **Improper Author Contribution or Attribution:** All listed authors must have made a significant scientific contribution to the research in the manuscript and approved all its claims. Don't forget to list everyone who made a significant scientific contribution, including students and laboratory technicians.
7. **Citation Manipulation:** Citation Manipulation is including excessive citations, in the submitted manuscript, that do not contribute to the scholarly content of the article and have been included solely for the purpose of increasing citations to a given author's work, or to articles published in a particular journal. This leads to misrepresenting the importance of the specific work and journal in which it appears and is thus a form of scientific misconduct.

Handling Cases of Misconduct

Once GJESM confirms a violation against GJESM's publication ethics, GJESM addresses ethical concerns diligently following an issue-specific standard practice as summarized below.

1. The first action of the journal Editor is to inform the Editorial Office of GJESM by supplying copies of the relevant material and a draft letter to the corresponding author asking for an explanation in a nonjudgmental manner.
2. If the author's explanation is unacceptable and it seems that serious unethical conduct has taken place, the matter is referred to the Publication Committee via Editorial Office. After deliberation, the Committee will decide whether the case is sufficiently serious to warrant a ban on future submissions.
3. If the infraction is less severe, the Editor, upon the advice of the Publication Committee, sends the author a letter of reprimand and reminds the author of GJESM publication policies; if the manuscript has been published, the Editor may request the author to publish an apology in the journal to correct the record.
4. Notification will be sent to corresponding author and any work by the author responsible for the violation or any work these persons coauthored that is under review by GJESM journal will be rejected immediately.
5. The authors are prohibited from serving on GJESM editorial board and serving as a reviewer for GJESM Journal. GJESM reserves the right to take more actions.
6. In extreme cases, notifications will be sent to the affiliations of the authors and the authors are prohibited from submitting their work to GJESM for 5 years.
7. In serious cases of fraud that result in retraction of the article, a retraction notice will be published in the journal and will be linked to the article in the online version. The online version will also be marked "retracted" with the retraction date.

GUIDE FOR AUTHORS

"Global Journal of Environmental Science and Management" (GJESM) is a double blind peer reviewed electronic and print quarterly publication concerned with all aspects of environmental science and management. GJESM publishes original research papers, review papers, case reports and short communications, letters to editor and authors' response about letters to editor across the broad field of environment. These include but are not limited to environmental science, environmental management, environmental engineering, environmental planning and design, urban and regional landscape design and industrial ecology. Environmentalist disciplines are invited to contribute their knowledge and experience. The publication appears at regular intervals time quarterly. The Journal database is fully open access and full text of published articles are available for everyone who can get access to the Journal website free of cost. The authors never pay any charges for submission, article processing and publication.

Guide for Authors: More details on guide for authors refer: http://gjesm.net/journal/authors.note

GENERAL

1. Authors should submit their contributions electronically through the GJESM website submission system to the Editorial Office.

2. Manuscripts must be submitted only in English and should be written according to sound grammar and proper terminology. Manuscripts should be typed in Times New Roman of 11 pt. font and in MS-Word format in one column with 2.5 cm margin at each side. Manuscript submission must be applied once in order to obtain only one submission ID number. More than one submission for a single manuscript can lose the chance of the manuscript consideration. Manuscript must be accompanied by a covering letter including title and author(s) name.

3. There are no strict formatting requirements but all manuscripts must contain the essential elements needed to convey your manuscript, for example Abstract, Keywords, Introduction, Materials and Methods, Results, Conclusions, Artwork and Tables with Captions. Please ensure the figures and the tables included in the single file are placed next to the relevant text in the manuscript, rather than at the bottom or the top of the file. There are no strict requirements on reference formatting at submission. References can be in any style or format as long as the style is consistent.

BEFORE YOU BEGIN

1. Peer-Review Process: In order to sustain the peer review system, authors have an obligation to participate in peer review process to evaluate manuscripts from others. When appropriate, authors are obliged to provide retractions and/or corrections of errors to the editors and the Publisher. All papers submitted to GJESM journal will be peer reviewed for at least one round. GJESM journal adopts a double-blinded review policy: authors are blind to reviewers, but reviewers are not blind to authors. After receiving reviewers' comments, the editorial team member makes a decision. Because reviewers sometimes do not agree with each other, the final decision sent to the author may not exactly reflect recommendations by any of the reviewers. The decision after each round of peer review may include (a) Accept without any further changes, (b) Accept with minor revision, (c) Major changes are necessary for resubmission and (d) Decline without encouraging resubmission.

2. Post-Publication Evaluation: In addition to rapid Peer Review Process, the GJESM Journal has Post-Publication Evaluation by the scientific community. Post-Publication Evaluation is concentrated to ensure that the quality of published research, review and case report meets certain standards and the conclusions that are presented are justified. The post-publication evaluation includes online comments and citations on published papers. Authors may respond to the comments of the scientific community and may revise their manuscript. The Post-Publication Evaluation is described in such a way; it is allowing authors to publish quickly about Environmental science, management, engineering and technology concepts.

3. Publication Ethics: The ethical policy of GJESM is based on the Committee on Publication Ethics (COPE) guidelines and complies with International Committee of GJESM Editorial Board codes of conduct. Readers, authors, reviewers and editors should follow these ethical policies once working with GJESM. The ethical policy of GJESM is liable to determine which of the typical research papers or articles submitted to the journal should be published in the concerned issue. The ethical policy insisted the Editor-in-Chief, may confer with other editors or reviewers in making the decision. Visit at: http://publicationethics.org

4. Conflict of Interest: Authors are requested to evident whether impending conflicts do or do not exist. A copyright transfer agreement is signed by the corresponding author, upon the acceptance of the manuscript, on behalf of all authors, for publication to be legally responsible towards the journal ethics and privacy policy. Authors will be notified as soon as possible of decisions concerning the suitability of their manuscripts for publication in the journal. The submitted materials may be considered for inclusion but cannot be returned and Editors of the journal reserve the right to accept or reject any article in any stage, if necessary. Conflict of Interest Disclosure form can be found at: www.gjesm.org/conflict_of_interest_discloure_form.docx

5. Submission Declaration and Verification: While submitting a manuscript to GJESM, all contributing author(s) must verify that the manuscript represents authentic and valid work and that neither this manuscript nor one with significantly similar content under their authorship has been published or is being considered for publication elsewhere including electronically in the same form, in English or in other language, without the written consent the copy right holder.

6. Authorship: All contributing authors should qualify for authorship and corresponding author should sign the authorship form while submitting the manuscript. It can be found at:
(http://www.gjesm.net/data/gjesm/news/authorship_form.docx).

7. Changes to Authorship: After the manuscript is submitted or accepted for publication, the corresponding author is required to send a request to add or remove an author or to rearrange the author names of the submitted/accepted manuscript by sending the change of authorship form to editorial office. No authorship change is allowed after publication of manuscript. More details may be found at:
(http://www.gjesm.net/data/gjesm/news/change_of_authorship_form.docx)

8. Retained Author Rights: As an author, author or authors' employer or institution retains certain rights. For more information on author rights, found at:
www.gjesm.org/retained_authors_right.docx.

9. Copy Right: Journals should make clear the type of copyright under which authors' work will be published. For open access articles the publisher uses an exclusive licensing agreement in which authors retain copyright in their manuscript. More details may be found at: (www.gjesm.org/copyright_form.docx)

10. User license Agreement: GJESM provides access to archived material through GJESM archives. Manuscripts are the parts of an open archive are made freely available from GJESM website after certain period, which begins from the final publication date of the manuscript. All articles published open access will be immediately and permanently free for everyone to read and download. Permitted reuse is defined by Creative Commons user license called ***Creative Commons Attribution***. Visit at: **(**Creative Commons Attribution 4.0 International (CC BY 4.0)**)**

11. Plagiarism Prevention and Violation of Publication Ethics: All manuscripts under review or published with GJESM are subject to screening using Plagiarism Prevention Software. Plagiarism is a serious violation of publication ethics. Other violations include duplicate publication, data fabrication and falsification, and improper credit of author contribution. Thus, the Plagiarism or Fraudulent or knowingly inaccurate statements constitute unethical behavior are unacceptable and submitting the same manuscript to more than one journal concurrently constitutes unethical publishing behavior and is unacceptable. The development of CrossCheck is a service that helps editors to verify the originality of papers. CrossCheck is powered by the Ithenticate software from iParadigms, known in the academic community as providers of Turnitin. For more details visit at: www.ithenticate.com/search

12. Handling Cases of Misconduct: Once GJESM confirms a violation against GJESM's publication ethics, the following actions will be taken.

a. The work is rejected / retracted immediately. Notification will be sent to corresponding authors. In extreme cases, notifications will be sent to the affiliations of the authors.
b. The authors are prohibited from submitting their work to GJESM for 5 years.
c. Any work by the authors responsible for the violation or any work these persons coauthored that is under review by any GJESM journal will be rejected immediately.
d. The authors are prohibited from serving on GJESM editorial board. GJESM reserves the right to take more actions.

MANUSCRIPT PREPARATION

1. Title Page: The title page should include: the name(s) of the author(s), a concise and informative title, the affiliation(s) and address (es) of the author(s), and e-mail address, telephone and fax numbers of the corresponding author.

2. Manuscript Title: Title of up to 17 words should not contain the name of locations, countries or cities of the research as well as abbreviations. The title should be oriented to Environmental issues while not being obscure or meaningless.

3. Abstract: An abstract of 150 to 250 words that sketches the purpose of the study; basic procedures; main findings its novelty; discussions and the principal conclusions, should not contain any undefined abbreviations or references.

4. Keywords: Provide 5 to 7 keywords which can be used for indexing purposes. Keywords should not repeat the words of the manuscript title or contain abbreviations and shall be written in alphabetical order as separated by semicolon.

5. Introduction: The Introduction should state the purpose of the investigation and identify clearly the gap of knowledge that will be filled in the Literature review study. Date and location of the research carried out throughout the study must be mentioned at the end of this section.

6. Materials and methods: The Materials and Methods section should provide enough information to permit repetition of the experimental work. It should include clear descriptions and explanations of sampling procedures, experimental design, and essential sample characteristics and descriptive statistics, hypothesis tested, exact references to literature describing the tests used in the manuscript, number of data involved in statistical tests, etc.

7. Results and Discussion: The Results section should describe the outcome of the study. Data should be presented as concisely as possible - if appropriate in the form of tables or figures, although very large tables should be avoided. The Discussion should be an interpretation of the results and their significance with reference to work by other authors. Please note that the policy of the Journal with respect to units and symbols is that of SI symbols.

8. Tables: Do not submit tables and graphs as photograph. Place explanatory matters in footnotes, not in the heading. Do not use internal horizontal and vertical rules. Tables should be called out in the text and should have a clear and rational structure and consecutive numerical order. All tables should be numbered 1, 2, 3, etc. Give enough information in subtitles so that each table is understandable without reference to the text. Footnotes to tables should be indicated by superscript lower-case letters (or asterisks for significance values and other statistical data) and included beneath the table body.

9. Figures: Figures/ illustrations should be in high quality art work, within 200-300 dpi and separately provided in Excel format. Ensure that figures are clear, labeled, and of a size that can be reproduced legibly in the journal. Each figure should have a concise caption describing accurately what the figure depicts. Figure captions begin with the term Fig. Figures should be with the captions placed below in limited numbers. No punctuation is to be placed at the end of the caption.

10. Conclusion: This section should highlight the major, firm discoveries, and state what the added value of the main finding is, without literature references.

11. Acknowledgements: Acknowledgments of people, grants, funds, etc. should be placed in a separate section before the reference list. The names of funding organizations should be written in full. Financial support affiliation of the study, if exists, must be mentioned in this section. Thereby, the Grant number of financial support must be included.

12. References: All the references should be cited throughout the manuscript text as well as in the Reference section organized in accordance with Harvard system. Groups of references should be listed first alphabetically, then chronologically. The number of references extracted from each journal should not exceed 3 to 5 citations, which is the average acceptable amount. The number of references should not be less than 30 for original paper, less than 100 for review paper. It is substantially recommended to the authors to refer to more recent references rather than old and out of date ones. Volume, issue and pages of the whole references must be specified according to the GJESM format.

Citing and listing of Web references: As a minimum, the full URL should be given. Any further information, if known (Author names, dates, reference to a source publication, etc.), should also be given.

Text: All citations in the text should refer to: 1. Single author: the author's name (without initials, unless there is ambiguity) and the year of publication; 2. Two authors: both authors' names and the year of publication; and 3. Three or more authors: first author's name followed by "et al." and the year of publication. Citations may be made directly (or parenthetically). Groups of references should be listed first alphabetically, then chronologically. Examples: "as demonstrated (Allan, 1996a, 1996b, 1999; Allan and Jones, 1995). Kramer *et al.,* (2000) have recently shown …".

List: References should be arranged first alphabetically and then further sorted chronologically if necessary. More than one reference from the same Author(s) in the same year must be identified by the letters "a", "b", "c", etc., placed after the year of publication.

Journal article: Nouri J.; Lorestani B.; Yousefi N.; Khorasani N.; Hassani A. H.; Seif, F.; Cheraghi M., (2011). Phytoremediation potential of native plants grown in the vicinity of Ahangaran lead-zinc mine. Environ. Earth Sci., 62(3): 639-644.

Book: Davis, M. L., (2005). Introduction to Environmental Engineering, 3rd. Ed. McGraw Hill Inc.

Book chapter: Mettam, G. R.; Adams, L. B., (1999). How to prepare an electronic version of your article, in: Jones, B. S., Smith, R. Z. (Eds.), Introduction to the electronic age. E-Publishing Inc., New York.

Conference paper: Brown, J., (2005). Evaluating surveys of transparent governance. In UNDESA, 6th. Global forum on reinventing government: towards participatory and transparent governance. Seoul, Republic of Korea 24-27 May. United Nations: New York.

Dissertation: Trent, J. W., (1975). Experimental acute renal failure. Ph.D. Dissertation, University of California. USA.

Online document: Cartwright, J., (2007). Big stars have weather too. IOP Publishing Physics Web.
http://physicsworld.com/cws/article/news/2007/jun/26/big-stars-have-weather-too

AFTER ACCEPTANCE

1. Online Proof Correction: Corresponding authors will receive an e-mail with a link to our online proofing system, allowing annotation and correction of proofs online. Use this proof only for checking the typesetting, editing, completeness and correctness of the text, tables and figures. Significant changes to the article as accepted for publication will only be considered at this stage with permission from the Editor-in-Chief. It is important to ensure that all corrections are sent back to us in one communication. Please check carefully before replying, as inclusion of any subsequent corrections cannot be guaranteed. Proofreading is solely the corresponding author responsibility.

2. Offprints: The offprints can be downloading from the GJESM website once the final corrected manuscripts are disseminated.

AUTHORS INQUIRIES

Authors can track their submitted article through GJESM website on author's login section at: http://gjesm.net/contacts?_action=login

Global Journal of Environmental Science and Management (GJESM)

Copyright Transfer Agreement

1. Parties of the agreement

Author (s):

Manuscript Title:

Manuscript ID:

(Herewith referred to as the "materials"),

Journal Title: Global Journal of Environmental Science and Management (GJESM)

2. Subject of the agreement

A) Copyright
1- The Author and each co-authors shall transfer and sell to the Publisher for the length of the copyright starting from the moment the present agreement comes into force the exclusive rights to the materials, including the rights to translate, reproduce, transfer, distribute or otherwise use the materials or parts (fragments) contained therein, for publication in scientific, academic, technical or professional journals or other periodicals and in derivative works thereof, worldwide, in English, in print or in electronic editions of such journals, periodicals and derivative works in all media or formats now existing or that may exist in future, as well as the right to license (or give permission to) third parties to use the materials for publication in such journals, periodicals and derivative works worldwide. The transfer under this agreement includes the right to adapt the presentation of the materials for use in conjunction with computer systems and programs, reproduction or publication in machine-readable format and incorporation into retrieval systems.
2- Reproduction, placement, transfer or any other distribution or use of the materials, or any parts of the materials contained therein, in any way permitted under this Agreement, shall be accompanied by reference to the Journal and mentioning of the Publisher, namely: the title of the article, the name of the Author (Co-authors), the name of the Journal, volume/number, copyright of the publisher.

B) Reserved Rights
The Author (Co-authors) or the employer of the Author (Co-authors) of the materials shall retain all proprietary rights (with the exception of the rights transferred to the Publisher under the present Agreement).

C) Author Guarantee
The Author (Co-authors) guarantees that the materials are an original work, submitted only to GJESM, and have not been published previously.
In case the materials were written jointly with co-authors, the Author guarantees that he/she has informed them of the terms of this Agreement and obtained their signatures or written permission to singe on their behalf.
The Author guarantees as well that:
The materials do not contain libelous statements.
The materials do not infringe on other persons' rights (including without limitation copyrights, patent rights and the trademark right).
The materials do not contain facts or instructions that can cause damage or injury to third parties and their publication does not cause the disclosure of any secret or confidential information

Author (Corresponding Author):

Correspondence Address:

Phone:

Fax:

Email:

Corresponding Author Name: Signature Date

On Behalf of the Publisher:

Iran Solid Waste Association,
Faculty of Environment, University of Tehran,
Postal Code: 1417854511, Tehran,
Iran

Telefax: (+9821) 2610 5110

Email: *editor@gjesm.net*
Gjesm.publication@gmail.com

Website: www.gjesm.net

Accepted for publication ☑ Signature Date

PLEASE NOTE: The accepted manuscript cannot be processed for publication until the publisher has received this signed form. The form MUST be signed by the Corresponding Author and then scanned and sent through the system or email. If the manuscript is not published in the Journal, this release will not take effect.

The sole responsibility for the whole content (s) of the article remains only with the corresponding author. However, Editor would reserve the right to adjust the style to certain standards of uniformity before publication.

CONFLICT OF INTEREST DISCLOSURE FORM

Conflict of Interest is defined as a set of conditions in which professional judgment concerning a primary interest, such as the validity of research, may be influenced by a secondary interest, such as financial gain. A Conflict of Interest Disclosure is an agreement or notification from the authors that they have not been paid for the work, or if they have, stating the source of their payment. The purpose of Conflict of Interest Disclosure form is to provide readers of authors' manuscript with information about authors' interests that could influence how the authors receive the work. The corresponding author (on behalf of all co-authors) should submit a conflict of interest disclosure form and is responsible for the accuracy and completeness of the submitted manuscript. Conflict of Interest Disclosure form can be signed by the corresponding author on behalf of all co-authors and stating that the submitted manuscript is the authors' original work, has not received prior publication and is not under consideration for publication elsewhere, permission has been received to use any material in the manuscript much as tables, figures etc. or no permissions have necessary to publish the authors' work.

1. Name of the corresponding author

2. Affiliation including e-mail and phone number

3. Manuscript Title

4. Do the authors or authors' institution at any time receive payment or services from a third party (government, commercial, private foundation, etc.) for any aspect of the submitted manuscript (including but not limited to grants, data monitoring board, study design, manuscript preparation, statistical analysis, etc.)?

   Are there any relevant conflicts of interest? Yes / No

5. Do the authors have any patents, whether planned, pending or issued, broadly relevant to the work?

   Are there any relevant conflicts of interest? Yes / No

6. Are there other relationships or activities that readers could perceive to have influenced, or that give the appearance of potentially influencing, what the authors' information in the submitted manuscript?

   Are there any relevant conflicts of interest? Yes / No

7. Are there any aspect of the work covered in this manuscript that has involved either experimental animals or human patients has been conducted with the ethical approval of all relevant bodies or not.

   Are there any relevant conflicts of interest? Yes / No

Corresponding Author Signature | Print Name | Date

AUTHORSHIP FORM

By completing and signing the following statements, the corresponding author acknowledges and accepts the responsibility on behalf of all contributing authors, if any, concerning Authorship Responsibility.

Manuscript title:

Corresponding author:

Affiliation:

Email:

Phone No:

By signing and filling this form, the corresponding author certifies that each author has met all criteria below (A, B, C, and D) and indicates each author general and specific contributions by listing his or her name next to the relevant section.

A. I certify that

- The manuscript is authentic and valid and that neither this manuscript nor one with considerably similar content under my authorship has been published or is being considered for publication elsewhere, except as described in an attachment, nor copies of closely related manuscripts are provided.
- I will provide the data or will contribute fully in providing and obtaining the data on which the manuscript is based for examination by the editors or their assignees, if requested.
- Every author has agreed to allow the corresponding author to serve as the primary correspondent with the editorial office, to review the edited manuscript and proof.

B. Each author has given final approval of the submitted manuscript.

C. Each author has participated sufficiently in the work to take public responsibility for the whole content.

D. Each author qualifies for authorship by listing his or her name on the appropriate line of the categories of contributions listed below. List appropriate author next to each section – each author must be listed in at least 1 field. More than 1 author can be listed in each field.

- conception and design
- acquisition of data
- analysis and interpretation of data
- drafting of the manuscript
- critical revision of the manuscript for important intellectual content
- statistical analysis
- obtaining funding
- administrative, technical, or material support
- supervision
- no additional contributions
- other (specify)

Corresponding Author Signature **Print Name** **Date**

CHANGE OF AUTHORSHIP FORM

Manuscript Title:

Corresponding Author:

Please check all that apply.

☐ New author(s) have been added.

☐ There is a change in the order of authorship.

☐ An author wishes to remove his/her name. An author's name may only be removed at his/her own request in writing.

ORIGINAL AUTHORSHIP

List ALL AUTHORS in the same order as the original (first) submission.

Print Name	Print Name
Name (1)	Name (6)
Name (2)	Name (7)
Name (3)	Name (8)
Name (4)	Name (9)
Name (5)	Name (10)

NEW AUTHORSHIP

List the ALL AUTHORS in same order as the new version.

Print Name	Print Name
Name (1)	Name (6)
Name (2)	Name (7)
Name (3)	Name (8)
Name (4)	Name (9)
Name (5)	Name (10)

I attest that:

1. The manuscript is not currently under consideration, in press, or published elsewhere, and the research reported will not be submitted for publication elsewhere until a final decision has been made as to its acceptability by the journal (posting of submitted material on a web site may be considered prior publication-note this in your cover letter).
2. The manuscript is truthfully original work without fabrication, fraud, or plagiarism.
3. I have made an important scientific contribution to the study and am thoroughly familiar with the primary data.
4. I have read the complete manuscript and take responsibility for the content and completeness of the manuscript and understand that I share responsibility if the paper, or part of the paper, is found to be faulty or fraudulent.

Corresponding Author Signature Name Date

SUBSCRIPTION FORM

Subscription form

Global Journal of Environmental Science and Management

Please enter my annual subscription to the Global Journal of Environmental Science and Management (GJESM), including 4 quarterly issues for the Year ..... Vol. ..... Nos.....

	Domestic (Rials)	International (USD)
▪ Institutional	3,000,000	150
▪ Individual	2,000,000	100
▪ Student	1,000,000	80
▪ Single Copy	500,000	50

Name: **Tel.:** **Email:**

Mailing Address:

Payment method: Check or money order must be made in order of:
Account #. 0101834143005, Account name: J. Nouri
Bank Melli Iran, IAU Branch, Code 1017, Tehran, Iran

□ Bank receipt enclosed

** Please allow 3 to 5 weeks for delivery*

Please send this filled in order form along with the Bank receipt payment to:

Global Journal of Environmental Science
and Management
No. 2, Kouhestan Deadend, Janpour Street,
Darabad, Tehran 1956934461 Iran

Global

Journal of Environmental Science and Management

CONTENTS

Volume 9, Number 2, Spring 2023

(Serial # 34)

173 - 192
Sediment organic carbon stocks in tropical lakes and its implication for sustainable lake management

T.R. Soeprobowati, N.D. Takarina, P.S. Komala, L. Subehi, M. Wojewódka-Przybył, J. Jumari, R. Nastuti (INDONESIA/ POLAND)

193 - 210
Application of microbially induced calcite precipitation to mitigate soil frost heave

M.F. Nikshoar, M.A. Rowshanzamir, S.M. Abtahi, S. Soleimanian-Zad (IRAN)

211 - 226
Environmental vulnerability characteristics in an active swarm region

A.V.H. Simanjuntak, U. Muksin, A. Arifullah, K. Lythgoe, Y. Asnawi, M. Sinambela, S. Rizal, S. Wei (INDONESIA/ SINGAPORE)

227 - 240
Municipal solid wastes quantification and model forecasting

Y.M. Teshome, N.G.Habtu, M.B. Molla, M.D. Ulsido (ETHIOPEA)

241 - 260
Components and predictability of pollutants emission intensity

Z. Farajzadeh , M.A. Nematollahi (IRAN)

261 - 274
Ecological and human health implications of mercury contamination in the coastal water

A. Mallongi, A.U. Rauf, R.D.P. Astuti, S. Palutturi, H. Ishak (INDONESIA)

275 - 286
Environmental assessment of river water quality near oil and gas fields

A.S. Patimah, A. Prasetya, S.H.M.B. Santosa (INDONESIA)

287 - 298
Drought stress tolerance based on selection indices of resistant crops variety

R. Daneshvar Rad, H. Heidari Sharifabad, M. Torabi, R. Azizinejad, H. Salemi, M. Heidari Soltanabadi (IRAN)

299- 308
Microplastics contamination in two peripheral fish species harvested from a downstream river

M.R. Maulana, S. Saiful, Z.A. Muchlisin (INDONESIA)

309 - 322
Geospatial visualization and seasonal variation of heavy metals in river sediments

D. Justus Reymond, K. Sudalaimuthu (INDIA)

323 - 336
Heavy metals concentration in the sediment of the aquatic environment caused by the leachate discharge from a landfill

L. Sulistyowati, N. Nurhasanah, E. Riani, M.R. Cordova (INDONESIA)

337 - 338
Characterization and quantification of solid waste in rural regions
S. Syafrudin, J.M. Masjhoer, M. Maryono (INDONESIA)